EXPRESSION OF σ^S-DEPENDENT GENES OF *ESCHERICHIA COLI*

EXPRESSION OF STATIONARY PHASE-SPECIFIC, σ^s-DEPENDENT GENES OF *ESCHERICHIA COLI*

By

LINDA I. C. WEI, B.Sc.

A Thesis

Submitted to the School of Graduate Studies

in Partial Fulfilment of the Requirements

for the Degree

Master of Science

McMaster University

MASTER OF SCIENCE (1996)
(Biology)

McMaster University
Hamilton, Ontario

TITLE: Expression of stationary phase-specific, σ^s-dependent genes of *Escherichia coli*

AUTHOR: Linda I. C. Wei, B. Sc. (McMaster University)

SUPERVISOR: Herb E. Schellhorn

NUMBER OF PAGES: xi, 179

ABSTRACT

In the natural environment, bacteria spend the majority of their existence in periods of starvation. While some Gram positive bacteria, such as *Bacillus subtilis* respond to this stress by forming highly heat-resistant spores, others, such as *E. coli*, enter a senescent state known as stationary phase. The stationary phase response is characterized by an increased cellular resistance to stresses associated with dormancy such as heat-shock, oxidative stress and osmotic challenge. These confer the cells the ability to survive prolonged periods of nutrient deprivation. The expression of these genes is regulated in part by σ^s, the stationary phase-specific, alternative sigma factor, encoded by the gene *rpoS*. Several methods have been used to identify these genes including two-dimensional gel electrophoresis (the expression of more than 30 proteins is absent in a *rpoS* mutant) and the identification of mutants possessing *lacZ* fusions that respond to a given related stimulus, such as carbon starvation. On the basis of these methods, the σ^s-regulon is predicted to be quite large. However, only fifteen or so genes have been characterized to date. To identify other σ^s-regulated functions, we have introduced a *rpoS*::Tn10 null allele into a library of 5000 random *lacZ* fusion mutants and determined the effects of the null allele upon *lacZ* expression. One-hundred and five mutants were isolated and the σ^s-dependent phenotype confirmed by complementing the *rpoS* function. Seventy-three strains were complemented, four were not and complementation results were not obtained for twenty-eight strains. Growth-phase-expression assays performed on the strains demonstrated induction of fusions at the onset of stationary phase, and this induction was reduced or abolished in an isogenic *rpoS* mutant. Furthermore, each mutant exhibited its own characteristic pattern of induction, consistent with the diversity of factors regulated by σ^s. Identification of selected σ^s-dependent functions was accomplished by sequencing the fusion junctions and comparing the sequence obtained with published *E. coli* sequence databanks. Results show that six fusions map to open reading frames

encoding proteins of unknown function and two do not map to any known region in the *E. coli* chromosome. One fusion maps to a gene encoding a putative lysine decarboxylase. This enzyme is implicated in the maintenance of medium pH and generation of carbon dioxide for cellular growth. The other maps to a recently identified *talB* gene. *talB* encodes a transaldolase protein involved in the pentose phosphate cycle, which generates precursors of nucleic acids, aromatic amino acids, and vitamins.

ACKNOWLEDGEMENTS

First and foremost, I extend my appreciation to my supervisor and friend, Dr. Herb E. Schellhorn, whose encouragement, patience, constructive criticisms, and confidence in my abilities has made this thesis possible. I thank Dr. T. Finan for his helpful suggestions in committee meetings and to Dr. Finan and Dr. R. Morton for taking the time to read this manuscript. I thank Suman Mukhopadyhay and David Smith their helpful suggestions and time investment in reading portions of this thesis, and Fariboroz Yazdani for last-minute crash-courses on sequence analysis and surfing the Internet. Thanks to Suman again, for three years of patience in helping me with "lab stuff" -- techniques and theory, and Suzana Gligorijevic for generating data for the expression studies.

To the "fifth-floor gang" and notable members of the "fish lab," much appreciation for the fond memories of music, pot-lucks, sports and other social events that have made graduate studies a pleasurable experience. Last, I thank my family for their support, love and encouragement during my overextended stay at McMaster University. And because of her unwavering belief in me, I dedicate this thesis to Mom.

TABLE OF CONTENTS

METHODS

RESULTS

DISCUSSION

LIST OF FIGURES

LIST OF TABLES

LIST OF ABBREVIATIONS

cm	centimetre
CFU	colony forming unit
°C	degrees Celsius
J/m^2	joules per meter squared (fluence)
kDa	kilodalton
kPa	kilopascals
µg	microgram
µl	microliter
µM	micromolar
mg	milligram
mm	millimetre
mM	millimolar
min	minutes
mwt	molecular weight
ng	nanogram
nm	nanometer
OD (600 nm)	optical density at 600 nm
OD (420 nm)	optical density at 420 nm
OD (280 nm)	optical density at 280 nm
OD (260 nm)	optical density at 260 nm
ORF	open reading frame
PFU	plaque forming unit
rpm	revolutions per minute
s	seconds
UV	ultraviolet

INTRODUCTION

In natural environments, bacteria often encounter temporal variations in nutrient availability and must endure prolonged periods of starvation. While some Gram positive bacteria such as *Bacillus subtilis* respond to this stress by forming highly stress resistant spores, non-differentiating bacteria such as the Gram negative *Escherichia coli* enter a period of reduced cell growth or stationary phase (reviewed in Hengge-Aronis, 1993b; Kolter *et al.*, 1993). The study of stationary phase gene regulation gained interest when it was discovered that the regulatory mechanisms that function during stationary phase are considerably different from those that function in exponential phase. Transition from growth to stationary phase requires a highly ordered process involving changes in physiology and morphology, which allows the cell to retain viability for long periods. Transition into stationary phase involves changes in the composition of the cellular membrane, morphology and in DNA supercoiling (reviewed in Siegele and Kolter, 1992). *E. coli* cells assume a smaller, more spherical shape compared with the larger rod shape, characteristic of exponential phase cells. The synthesis of enzymes begins such as acid phosphatase, storage compounds (eg. glycogen) and protective substances (eg. trehalose). Stationary phase is characterized by the development of a general resistance to several stresses associated with dormancy. This general resistance confers a greater protection than the development of resistance conferred by the adaptive response in exponentially growing cells (Jenkins *et al.*, 1988). Furthermore, this protection develops in cells that have never been previously exposed to the specific stress. Some examples include heat shock, oxidative stress, osmotic challenge (Jenkins *et al.*, 1988; Jenkins *et al.*, 1990), and near-UV exposure (Sammartano *et al.*, 1986). Although bulk protein synthesis is turned off due to the lowered cellular metabolism in stationary phase, approximately 30-50 proteins are induced

during this transition (Groat *et al.*, 1986). A core subset of 15 proteins is induced despite the limiting nutrient (Groat *et al.*, 1986; Matin, 1991). Some stationary phase proteins are probably not immediately required, but their expression upon the cessation of growth may help the cell survive acute exposure to stress conditions that may arise when the cell has a reduced capacity for *de novo* protein synthesis.

Several factors have been implicated in the involvement of the global regulatory switch in gene expression and protein synthesis that occurs as cells enter stationary phase. Dimers of ribosomal monomers can form, affecting protein translation (Wada *et al.*, 1990). Structural changes occur in core RNA polymerase that may also contribute to the selective binding of the sigma subunit (Ozaki *et al.*, 1991). Switching between different sigma factors for core RNA polymerase occurs, resulting in modifications of expression from different promoters. Sigma factors are protein subunits that bind to core RNA polymerase, conferring specificity for certain promoters. The main sigma factors for *E. coli* and *Bacillus subtilis* (σ^{70} and σ^{43}, respectively) are involved in the transcription of many genes, alone or with additional transcriptional factors. Interchanging between different sigma factors in response to an environmental stimulus or changes in growth conditions is a common mechanism for the global switching of gene expression specific to a signal. The sporulation process of *Bacillus subtilis*, for example, requires the involvement of several alternative sigma factors acting in sequence to mediate spore formation (reviewed in Errington, 1993). Physiological similarities between sporulation and the stationary phase response suggested the involvement of alternative sigma factors in gene regulation. To date, one stationary phase sigma factor has been identified and designated σ^{s} (for starvation), encoded by the *rpoS* gene.

Several allelic forms of *rpoS* have been identified. As a stationary-phase specific, alternative sigma factor, it is observed to be involved in the regulation of a large subset of genes with very diverse functions. Although not an essential factor, since *rpoS* mutants are viable up several days into stationary phase, it plays a primary role in the development of general stress resistance encountered by cells in dormancy.

IDENTIFICATION OF σ^S AS A CENTRAL REGULATOR

The regulatory nature of σ^s was identified in several contexts by independent investigators over a period of 15 years. Consequently, σ^s has also been called *katF*, *nur*, *appR*, *csi-2*, and *abrD*. It was initially reported in 1979 when a gene, *nur* (Tuveson and Jonas, 1979) in *Escherichia coli* was found to confer increased near-UV (NUV) (wavelengths of 300-400 nm) resistance to cells upon entry into stationary phase. A mutation in this gene renders cells sensitive to NUV but does not sensitize cells against far-UV (Tuveson and Jonas, 1979).

The *katF* gene was first reported to be involved in the synthesis of one of two catalases or hydroperoxidases in *Escherichia coli* (Loewen and Triggs, 1984). Mapped to 59 min on the chromosome, *katF* was observed to affect the expression of *katE*-encoding hydroperoxidase II (HPII) but was not required for *katG*-encoding hydroperoxidase I (HPI) (Loewen and Triggs, 1984). Further analysis regarding the relationship between *katE* and *katF* revealed that *katF* is the regulator of *katE* (Sak *et al.*, 1989, Schellhorn and Stones, 1992), the structural gene for HPII, and both are required for HPII expression (Loewen *et al.*, 1985a). Pretreatment of *E. coli* or *S. typhimurium* cells with sublethal concentrations of hydrogen peroxide results in protection against subsequent lethal doses of hydrogen peroxide and NUV (Christman *et al.*, 1985). Based on this observation, the possibility of a relationship between the catalase and *nur* genes was suggested. Subsequent mapping of the *nur* gene confirmed it to be an allele of *katF* (Sammartano *et al.*, 1986). Further confirmation of *katF* as a positive regulator of *xthA*-encoded exonuclease III provided the link to the involvement of *katF* to NUV resistance (Sak *et al.*, 1989).

Concurrently, mutants of a gene called *appR*, identified as a positive regulator for *appA*-encoded acid phosphatase (Touati *et al.*, 1986), exhibited phenotypes similar to *katF*::Tn10 mutants, such as sensitivity to hydrogen peroxide and reduced levels of acid phosphatase (Touati *et al.*, 1991). *appR* and *katF* were later found to be alleles (Touati *et al.*, 1991). Analysis of the *katF* DNA sequence revealed a significant homology with *rpoD*, the gene encoding the RNA polymerase sigma factor, σ^{70}. Homology of *rpoS* was also found at the protein level to several other sigma factors, providing strong evidence of KatF as a novel sigma factor involved in cellular protection

and repair (Mulvey and Loewen, 1989). However, its role as a sigma factor was later confirmed using footprinting binding studies and *in vitro* transcription assays (Tanaka *et al.*, 1993; Nguyen *et al.*, 1993).

A search for carbon-starvation-inducible (*csi*) genes using *lacZ* fusions have identified several genes induced during transition into stationary phase. One operon fusion, *csi2*::*lacZ* that confers a pleiotrophic phenotype was studied in detail. Exhibiting growth-phase-dependence, the *csi2*::*lacZ* strain is sensitive to hydrogen peroxide, impaired in stationary phase thermotolerance, incapable of long term survival, and exhibits reduced glycogen and acid phosphatase synthesis (Lange and Hengge-Aronis, 1991a). Furthermore, using two-dimensional gels, 16 proteins that were normally expressed in a wild-type strain were absent in the *csi2*::*lacZ* mutant. *csi2* is an allele of *katF* and the apparent role of KatF as sigma factor led the suggestion that the gene be renamed *rpoS* and the gene product, σ^s, with "s" for starvation (Lange and Hengge-Aronis, 1991a).

Finally, the study of *aidB* as one of several genes induced in response to DNA alkylation damage identified two different factors involved in its induction. One was Ada-dependent and the systematic search for the other identified a suppressor mutation designated *abrD1*, which was an allele of *rpoS* (Volkert *et al.*, 1994).

CHARACTERIZATION OF *rpoS*

Genetic and Biochemical Characterization

The cloning and characterization of the *rpoS* gene reveal an open reading frame of 1086 base pairs encoding a protein of 362 amino acids (Mulvey *et al.*, 1988). The molecular weight of this protein is approximately 41.5 kDa (Mulvey and Loewen, 1989). Subsequent analysis identified differences in the published *rpoS* sequence (Ivanova *et al.*, 1992), shortening the open reading frame of 1026 bp to encode a protein, 342 amino acids in length, with an estimated molecular weight of 38 kDa. Hence σ^s is now also referred to as σ^{38} (Ivanova *et al.*, 1992; Tanaka *et al.*, 1993).

Extensive analysis of 31 sigma factors from various bacteria identified three groups on the basis of evolutionary relationships. Group one contains the primary sigma factors including the *E.*

coli σ^{70}; group two contains the alternative sigma factors that diverged slightly from group one, of which σ^s is a member; and group three contains alternative sigma factors that diverged more extensively from σ^{70}. Sequences of group one and group two sigma factors are highly similar, suggesting similar recognition of promoter consensus sequences (Lonetto *et al.*, 1992).

The examination of the DNA and protein sequence of *rpoS* show homology to σ^{70}, but direct evidence of sigma factor activity for the *rpoS* gene product was not established until 1993. Free σ^s was observed to bind core RNA polymerase using a glycerol density gradient (Nguyen *et al.*, 1993). Experiments with the reconstituted holoenzyme, $E\sigma^s$, showed the production of run-off transcripts of predicted sizes using two known σ^s-dependent genes, *xthA* (Saporito *et al.*, 1988) and *bolAp1* (Aldea *et al.*, 1989). Both promoters were also shown to be recognized by $E\sigma^{70}$. However, with the *bolAp1* promoter, the size of transcripts and relative amounts varies between $E\sigma^{70}$ and $E\sigma^s$ mediated transcription as observed on agarose gels, suggesting different promoter specificities between the two holoenzymes (Nguyen *et al.*, 1993). Additional promoters examined by other researchers led to the classification of promoters into three groups based on preferential selectivity of $E\sigma^{70}$ and $E\sigma^s$ holoenzymes. Type I consist of promoters effectively transcribed by both holoenzymes, while Type II and Type III promoters are transcribed exclusively by $E\sigma^{70}$ and $E\sigma^s$, respectively. The promoter of the *fic-pabA* operon (Kawamukai *et al.*, 1989) is the only promoter yet identified to be transcribed exclusively by $E\sigma^s$ (Tanaka *et al.*, 1993). The ability of $E\sigma^s$ to discriminate among the three types of promoters suggests the presence of additional factors that may affect promoter recognition by $E\sigma^s$.

Variability of the *rpoS* sequence

Sequence variability of the *rpoS* gene has been reported independently by several labs. For example, an *appR* mutant, identified based on its reduced acid phosphatase levels does not exhibit reduced catalase activity, contrary to the *katF*::Tn10 fusion mutant, although *appR* and *rpoS* are alleles. (Touati *et al.*, 1989). Expression levels of *lacZ* fusion mutants differ between a laboratory collection of wild-type strains (Wang and Cronan, 1994; Chang and Cronan, 1994).

These allelic differences, however, may not be manifested in all expected phenotypes given the diversity of the *rpoS* regulon, the requirement of additional factors involved in their expression, and the apparent overlap between promoters recognized by both $E\sigma^{70}$ and $E\sigma^{s}$.

The most significant variation in the *rpoS* sequence, other than single point mutation is a mutation that arises spontaneously in stationary phase cells (Ivanova *et al.*, 1992: Zambrano *et al.*, 1993). Analysis of the sequence reveals that the mutant strains carry a 46 base pair duplication at the 3' end of the coding region, resulting in an elongated *rpoS* gene. The phenotype of stationary phase cells exhibited by this genetic variation is manifested in morphology changes, levels of HPII synthesis, and increased sensitivity to acid and heat (Ivanova *et al.*, 1992). In addition, these strains exhibit a competitive advantage in their ability to survive prolonged periods in starvation, an unexpected observation since a 10-day exposure in these starvation conditions is generally required for the development of a stationary phase growth advantage (Zambrano *et al.*, 1993). This property of competitive advantage is restricted to stationary-phase cells, and was shown by incubating a mixed population of young (1-day-old) and aged (10-day-old) cultures. Despite the initial population ratio, mutants from the aged cells can take over the culture resulting in the subsequent death of the young cells (Zambrano *et al.*, 1993). The nature of this mutation has not been further characterized. It has been suggested, however, that the additional residues lie close to the helix-turn-helix motif common to all sigma factors known to recognize the -35 region of promoters (Loewen and Hengge-Aronis, 1994). Thus, the variability of phenotypes observed in cells containing the mutation may be due to changes in the recognition of promoters of the σ^{s}-regulon.

REGULATORY CONTROL OF *rpoS*

Transcriptional control:

Transcription from the *rpoS* promoter using *lacZ* fusions is observed to be low in exponential phase, but increases substantially as cells entered stationary phase (Mulvey *et al.*, 1990; Lange and Hengge-Aronis, 1991a; Schellhorn and Stones, 1992). Levels and time-course of *rpoS* induction differ between laboratories. For example, using rich media, induction occurs in early

exponential phase and increases across growth into stationary phase (Mulvey *et al.*, 1990), whereas other researchers report no significant induction until the transition into stationary phase (Schellhorn and Stones, 1992). Similarly, suspension of cells in nutrient limiting (minimal) media containing a carbon source results in the immediate induction of *rpoS* early in exponential phase (Mulvey *et al.*, 1990). In contrast, others report *rpoS* induction in minimal media only upon entry into stationary phase. Such contrasting results may be attributed to differences in growth conditions, media composition, strain variations, and the nature of *lacZ* fusions, encoded on multicopy plasmids (Mulvey *et al.*, 1990) or on single-copy chromosomes (Schellhorn and Stones, 1992).

The *rpoS* promoter and upstream sequences:

The promoter sequence of the *rpoS* gene spans the region 1400 bp upstream from the putative transcriptional start site containing four promoters, P1, P2, P3, and P4 (Takayanagi *et al.*, 1994). Using primer extension analysis, P2 is shown to account for 75% of transcripts and is assumed to be the major promoter for *rpoS* expression. The four promoters exhibit similar patterns of growth-phase induction, and their combined activity contribute to the full level of *rpoS* expression (Takayanagi *et al.*, 1994). Recently, however, an independent study detected only two mRNA transcripts originating from the *rpoS* promoter, the stronger upstream *rpoS*p1, previously identified as P2, and the second weaker start site further downstream. Both are within the *nlpD* gene (Lange *et al.*, 1995).

The *nlpD* gene, upstream of *rpoS*, is transcribed in the same counterclockwise direction as *rpoS* (Ichikawa *et al.*, 1994; Lange *et al.*, 1994b) and encodes a lipoprotein involved in morphological changes (Lange and Hengge-Aronis, 1994b). *nlpD* is not stationary phase-induced and no putative termination sequence is located between *nlpD* and *rpoS*, suggesting the possibility of a single mRNA transcript arising from a polycistronic operon (Lange and Hengge-Aronis, 1994b). Deletion of the *nlpD* promoter region (eliminating two *nlpD* promoters) results in a 40% reduction in *rpoS* expression during exponential-phase but does not have an effect in stationary-phase expression. In contrast, 5' deletion analysis, encompassing *rpoS*p1 results in the reduction of

rpoS expression by 20-fold during stationary phase, confirming that *rpoS*p1 is the major promoter (Lange *et al.*, 1995). Taken together, the *nlpD* promoters are responsible for basal level expression of *rpoS*, and the major *rpoS*p1 promoter, found within the *nlpD* gene, controls stationary-phase induction of *rpoS* (Lange and Hengge-Aronis, 1994b).

Post-transcriptional control

Inconsistent results obtained from *katE* and *rpoS lacZ* fusion studies led to the proposal of other regulatory mechanisms besides *rpoS* transcriptional control. For example, expression studies of *katE* and *rpoS* transcriptional fusions reveal that, though transcriptional induction of *rpoS* precedes *katE*, it only accounts for one-third the level of *katE* expression (Mulvey *et al.*, 1990). This could be explained by the presence of other regulators involved in *katE* expression, or the effect of post-transcriptional control mechanisms of *rpoS* expression, which in turn, affect the expression of *katE*. Several other observations support this proposal. Using translation and transcriptional *lacZ* fusions to *rpoS*, it was shown that induction occurs during growth and during glucose starvation (McCann *et al.*, 1993). A two-fold increase of both fusions occurs during exponential phase, but upon entry into stationary phase, induction from the protein fusion continues for an additional three hours resulting in an 8-fold increase in *rpoS* expression (McCann *et al.*, 1993). Others report a similar pattern of *rpoS* induction (Loewen *et al.*, 1993). These phenomena concerning *katE* expression were resolved when it was observed that *rpoS* translation closely parallel *katE* transcription (Loewen *et al.*, 1993). Similarly, a *rpoS* transcriptional fusion is not induced during osmotic challenge, though a subset of *rpoS*-dependent genes is activated under the similar conditions (Hengge-Aronis *et al.*, 1993). Subsequent experiments resolved this issue by demonstrating that *rpoS* translation is osmotically regulated (Lange and Hengge-Aronis, 1994a). Furthermore, the addition of benzoic acid into the media results in full induction of the *rpoS* transcriptional fusion, contrary to the partial induction of the translational fusion (Loewen *et al.*, 1993). These results suggest the possibility of differential control of certain stages of *rpoS* regulation in response to specific environmental or nutrient conditions. Levels of the σ^s protein

increase during entry into stationary phase, an observation confirmed using Western analysis (Gentry *et al.*, 1993).

The stabilization of the protein product, demonstrated by pulse-chase experiments, can also account for increased levels of σ^s detected upon entry into stationary phase. The σ^s protein of exponentially growing cells is unstable, having a half-life of 1.4 minutes. At the onset of glucose starvation, however, this half-life increases to more than 7-fold (Lange and Hengge-Aronis, 1994a). In summary, *rpoS* is regulated at the level of transcription, translation, and protein stability during entry into stationary phase. The combinations of these regulatory mechanisms account for the increased levels of σ^s seen during entry into stationary phase, consistent with previous reports that σ^s is responsible for the expression of approximately 32 genes during carbon starvation (McCann *et al.*, 1991). This complex system of regulation permits the fine tuning of levels of the σ^s protein in the cell.

SIGNALS OF *rpoS* INDUCTION

σ^s is required for the transcriptional initiation of a large subset of stationary phase specific genes (McCann *et al.*, 1991; Lange and Hengge-Aronis, 1991a). Apart from σ^s induction in response to stress conditions (Lange and Hengge-Aronis, 1994a), the expression of *rpoS* is itself induced upon entry into stationary phase under normal growth conditions (Mulvey *et al.*, 1990; Lange and Hengge-Aronis, 1991a; Schellhorn and Stones, 1992). Although the intracellular signal giving rise *rpoS* induction is still unknown, several possible inducers have been identified.

Acetate, intracellular pH, metabolic component in spent medium

The induction of a *rpoS* transcriptional fusion at the beginning of growth in minimal media and during transition into stationary phase in rich media suggests a link with the starvation response (Mulvey *et al.*, 1990). A metabolic component of carbon starvation, perhaps accumulating during entry into stationary phase, was suggested to be a possible signal for *rpoS* induction (Mulvey *et al.*, 1990). Early exponential phase cells resuspended in spent media from stationary phase cultures

results in the immediate induction of *rpoS* (Schellhorn and Stones, 1992). Dialysis of the stationary phase spent medium before the addition of cells results in little expression, suggesting the possibility of the diffusion of the active component out of the dialysis bag (Mulvey *et al.*, 1990). Several compounds known to accumulate in stationary phase cells have been tested for the ability to induce *rpoS* expression. Compounds associated with the induction of *katE*, such as lactate, acetate and succinate are ineffective inducers of *rpoS* (Mulvey *et al.*, 1990). Other investigators, however, found acetate to be an effective inducer of both *katE* and *rpoS* transcriptional fusions (Schellhorn and Stones, 1992), suggesting a possibility that the inducing effect of weak acids is linked to the intracellular pH of the cell. *E. coli* is permeable to protonated forms of low molecular weight weak acids, therefore weak acids such as acetate may lower the intracellular pH of the cell via proton accumulation (Schellhorn and Stones, 1992). Generally, weak acids that are proto-ionophores (Slonczewski *et al.*, 1987) are effective inducers of *rpoS* (Schellhorn and Stones, 1992). Such a suggestion comes considering the discovery of a pH-sensitive regulon induced by the presence of weak acids (Slonczewski *et al.*, 1987). Apart from the possibility of pH-dependent induction of *rpoS* by the presence of the acetate, its function as an inducer is suggested to account for stationary phase induction of *rpoS*. Secreted into the medium as a metabolic by-product at the end of exponential growth, acetate can also be taken up and used as a sole carbon source in stationary phase (reviewed in Tempest and Neijssel, 1987). In the form of acetyl-CoA, acetate is an entrance molecule to the tricarboxylic acid (TCA) cycle that generates CO_2 and supplies the cell with energy and amino acid precursors (Nimmo, 1987).

cAMP/Crp complex

Synthesized by a *cya*-encoded adenylate cyclase, cAMP levels are regulated by glucose metabolism in the bacterial cell. In the presence of glucose, cAMP levels are low, yet upon its depletion, for example when starved for energy sources, concentrations increase. The regulatory property of cAMP requires the binding to a cAMP receptor protein (CRP), encoded by *crp*, forming a complex shown to activate several operons. Thus when the preferred carbon source (glucose) is

limiting, levels of cAMP rises, which activate operons, including the lactose operon, to replenish intracellular glucose levels.

cAMP is a negative regulator of *rpoS* expression (Lange and Hengge-Aronis, 1991a). Studies in minimal media show that a strain carrying a deletion in the adenylate cyclase gene (*Δcya*) exhibit increased levels of *rpoS*. The addition of exogenous cAMP to the media represses *rpoS* expression. cAMP is also a repressor for several *rpoS*-dependent genes, including *bolA* (Lange and Hengge-Aronis, 1991a), *osmY* (*csi5*) (Weichart *et al.*, 1993), and *glgS* (Hengge-Aronis and Fischer, 1992). The mechanism of action in each case is not explicitly known but repression may occur by direct binding of the cAMP/CRPcomplex to the σ^s-dependent gene promoter, or indirectly by effects on *rpoS* itself. Contrary to these reports, other labs do not observe a significant cAMP effect. A decrease in *rpoS* expression during growth and a lack of induction at the onset of glucose starvation occurs in a Δ*cya* background (McCann *et al.*, 1993). Furthermore, the σ^s-dependent gene, *poxB* exhibits a decrease in expression in a Δ*cya* background (Chang *et al.*, 1994). A possible explanation for divergent results seen in *crp* and *cya* mutants may, however, be due to differences between strains used, and the composition of media in expression studies.

Guanosine tetraphosphate (ppGpp)

Guanosine 3', 5'-bispyrophosphate (ppGpp) is a positive and negative regulator of many stringently controlled genes (reviewed in Cashel and Rudd, 1987; Gentry *et al.*, 1993). Its cellular levels increase in response to bacterial carbon, nitrogen, phosphorus and amino acid. The accumulation of ppGpp is dependent upon the expression of two genes, *relA* and *spoT*. The ppGpp synthetic activity of the RelA protein during amino acid starvation is activated by uncharged tRNA's, and the accumulation of ppGpp in response to carbon starvation occurs by blocking its degradation catalysed by the *spoT* gene. Deletion of the *relA* and *spoT* genes result in the complete absence of ppGpp. Such mutants exhibit, to a lesser degree, pleiotrophic phenotypes similar to that of a *rpoS* mutant, thus providing a possible link between ppGpp and σ^s (Gentry *et al.*, 1993). Examples of such phenotypes include the ability to synthesize acid phosphatase (Gentry *et al.*, 1993),

morphological alterations, and salt sensitivity (reviewed in Hengge-Aronis, 1993). Analysis of the *csi* genes isolated by Lange and Hengge-Aronis reveal that a *csi2*::*lacZ* (*rpoS*::*lacZ*) in a *relA*$^-$ background exhibit reduced levels of β-galactosidase activity, which suggests that ppGpp is necessary for normal *rpoS* expression during stationary phase. Using Western blot analysis, σ^s levels in a *relAspoT* mutant are reduced during transition into stationary phase. Artificial elevation of ppGpp levels obtained by a mutation in *spoT* results in parallel increases in σ^s levels and transcription initiation from the major *rpoS*p1 promoter is not altered in a *relAspoT* mutant (Lange *et al.*, 1995). It was suggested that ppGpp may act at *rpoS* transcription elongation or mRNA stability, resulting in reduced levels of mRNA seen (Lange *et al.*, 1995).

Homoserine lactone

Homoserine lactone (HSL) was first implicated as a positive regulator of *rpoS* expression when screening a chromosomal library (cloned into high-copy plasmids) for genes involved in the repression of expression from the σ^s-dependent *bolA*::*lacZ* fusion (Huisman and Kolter, 1994). Strains harboring one recombinant plasmid failed to induce *rpoS* expression during transition into stationary phase. This gene, designated *rspA*, is mapped to 35.6 min on the *E. coli* chromosome. The gene product is homologous to a catabolic enzyme (chloromuconate cycloisomerase) consistent with the idea that a metabolic component is a potential inducer of *rpoS* expression (Mulvey *et al.*, 1990; Schellhorn and Stones, 1992). The RspA amino acid sequence exhibits homology to a lactonizing enzyme suggesting that the metabolite could be a lactone, thus the implication of homoserine lactone (HSL) as positive regulator of σ^s expression. Since precursors of HSL, possibly homoserine (HS) and homoserine phosphate (HSP) are intermediates in the threonine biosynthetic pathway, mutations in the enzymes blocking the synthesis of HSL results in reduced levels of *rpoS* (assayed by catalase activity). Expression is restored by the addition of HSL into the medium. Similar results were obtained when detecting for σ^s levels using immunoblot analysis (Huisman and Kolter, 1994).

UDP-Glucose

To identify additional factors involved in *rpoS*-dependent genes, transposon insertional mutations affecting the expression of the osmotically-inducible *osmY* gene, were isolated (Bohringer *et al.*, 1995). One mutation increases the *osmY* basal level expression in exponential phase and during entry into stationary phase (Bohringer *et al.*, 1995). Furthermore, strains carrying this transposon insertion mutation are unable to grow on glucose minimal media, a common indicator of a possible defect in the synthesis of glycolytic enzymes. A defect in growth on glucose minimal media is due to the build up of toxic phosphorylated metabolic intermediates in the presence of glucose (Bohringer *et al.*, 1995). The mutation maps to the *pgi*-encoding phosphoglucose isomerase (PGI) which, along with *pgm* and *galU*, encode glycolytic enzymes catalyzing the reactions of precursor substrates to UDP-glucose. Since mutations in *pgm* and *galU* also exhibit the same phenotype as a *pgi* mutant, a role for UDP-glucose as a negative repressor for σ^s-dependent genes was suggested. Furthermore, immunoblot assays of σ^s levels in *pgi*, *pgm*, and *galU* mutants reveal an approximate four-fold increase in levels during growth, suggesting that the effects on σ^s-dependent genes occur through the influence of the synthesis of σ^s itself (Bohringer *et al.*, 1995).

SprE

The screening of components involved in *rpoS* regulation was based on the repression of *ompF* by σ^s (McCann *et al.*, 1991; Pratt and Silhavy, in press). OmpF is a major membrane porin protein regulated by the two component regulatory system, EnvZ-OmpR (reviewed in Csonka, 1989). The screening was based on the identification of genes that regulate *ompF*, independent of σ^s and the EnvZ-OmpR system. One mutation was mapped to a previously reported, uncharacterized open reading frame at 27 min on the *E. coli* chromosome. It was subsequently designated *sprE* for stationary phase regulatory element. Mutations in *sprE* confer pleiotrophic phenotypes similar to *rpoS* mutants, though not as severe. These include defects in glycogen synthesis, catalase activity, and morphology changes during entry into stationary phase (Pratt and

Silhavy, in press). Immunoblot assays show that *sprE* interferes with the accumulation of σ^s at the translational level. Transposon IS (insertion sequence) insertions into *sprE* results in the up-regulation of *rpoS* expression suggesting SprE functions as a negative regulator. This negative regulation was also observed at the translational level (Pratt and Silhavy, in press). SprE is suggested to relay the stationary phase trigger signal from the environment to *rpoS* since it exhibits DNA sequence similarity to a response regulator protein (Pratt and Silhavy, in press).

H-NS

H-NS is a DNA-binding protein involved in the compact organization of the chromosome and the direct or indirect negative regulation of the expression of genes (Ueguchi and Mizuno, 1993). As a regulator of *rpoS* expression, using studies on the σ^s-dependent *cbpA* gene (Yamashino *et al.*, 1994), H-NS is also implicated in the repression of other σ^s-dependent *csgAB* and *hdeAB* promoters (Arnqvist *et al.*, 1994). Expression from the *cbpA::lacZ* fusion in an *hns* mutant is largely dependent on the function of σ^s (Yamashino *et al.*, 1995). Cellular levels of σ^s are substantially elevated in an *hns* mutant, particularly during exponential phase. This elevation is independent of the accumulation of ppGpp. An *hns*$^-$ mutant exposed to heat shock (55°C) exhibits stationary phase thermotolerance, even in exponentially growing cells, suggesting that the accumulation of σ^s in the *hns*$^-$ background plays a physiological role. The effects of H-NS on *rpoS* expression are at the post-transcriptional level. The *hns* mutation enhances both translation of *rpoS* mRNA and stabilization of the σ^s protein, accounting for increased levels in growing and stationary phase cells. An interesting observation was the lack of induction from the *cbpA* promoter during exponential phase (in *hns*$^-$ background) even with σ^s at levels sufficient to cause an induction. These results show that σ^s alone is not the primary factor involved in the induction members of its regulon, but rather the state of σ^s under certain physiological conditions (Yamashino *et al.*, 1995).

MEMBERS OF THE σ^S REGULON

Genes involved in DNA protection and repair: *katE, katG, dps, xthA, aidB*

A variety of stresses that exert deleterious effects on bacterial cells occur through the generation of active oxygen species which causes direct DNA damage (Storz *et al.*, 1990). Oxidative respiration and near-UV irradiation, which are implicated in the production of hydrogen peroxide (McCormick *et. al.*, 1976), have been shown to cause single-strand breaks in DNA (Anathaswamy and Eisenstark, 1976). Some of these protective and repair mechanisms are regulated by σ^s.

Catalases and peroxidases break down hydrogen peroxide into water and oxygen before it can inflict cellular damage or lead to more reactive oxygen radicals. Two species of catalase exist in *E. coli*, hydroperoxidase I (HPI) and hydroperoxidase II (HPII), which differ in structure, subcellular location, biochemical properties, responses to metabolic changes, and regulatory mechanisms. HPII, encoded by *katE*, is at 37.8 min on the chromosome (Loewen, 1984), and is capable of catalase activity only (Loewen and Switala, 1985a). HPI, encoded by *katG*, is chromosomally mapped to 89.2 min (Loewen *et al.*, 1985b). It is bifunctional, having both catalase and peroxidase activities (Clairborne *et al.*, 1979). *katG* is regulated at the transcriptional level by OxyR (Morgan *et. al.*, 1989), a member of the LysR family of bacterial regulator proteins (Christman *et al.*, 1986), which is responsible for the expression of a subset of proteins induced in the presence of hydrogen peroxide (Christman *et al.*, 1985). *katG* expression is induced when the cell is exposed to hydrogen peroxide via the OxyR-dependent mechanism (Christman *et al.*, 1985). In contrast, *katE* expression does not respond to fluctuations of the oxidant (Schellhorn and Hassan, 1988). HPI induction is understood as a protective response given the function of catalases, however, the unresponsiveness of *katE* is unclear. It has been proposed that *katE* induction during entry into stationary phase may reflect the need for catalase protective responses that may arise during dormancy when *de novo* protein synthesis is not possible. It has also been suggested that catalases do not protect individual cells from oxidative stress but is only advantageous to the survival of a dense population or colony (Ma and Eaton, 1992). Compartmentalization of the two catalases also differs. HPI is located in the periplasmic and cytoplasmic membrane, probably involved in the defense against exogenous oxidative stress

whereas HPII is found in the cytoplasm (Heimberger and Eisenstark, 1988).

σ^s is involved in the transcriptional regulation of both *katE* (Sak *et al.*, 1989; Schellhorn and Stones, 1992) and *katG* (Mukhopadhyay and Schellhorn, 1994; Ivanova *et al.*, 1994) providing a common regulatory link between the two catalases. Using *lacZ* reporter fusions, *katE* transcription is demonstrated to increase approximately 30-fold upon entry into stationary phase (Schellhorn and Hassan, 1988), whereas only a 6-fold increase was observed for *katG* transcription (Mukhopadhyay and Schellhorn, 1994; Ivanova *et al.*, 1994). σ^s is required for both basal expression and stationary phase induction of *katE* (Mulvey *et al.*, 1990; Schellhorn and Stones, 1992), but is only involved in the stationary phase induction of *katG* (Mukhopadhyay and Schellhorn, 1994). An increase of HPII synthesis is correlated to the accumulation of tricarboxylic acid cycle (TCA) intermediates (Loewen *et. al.*, 1985a) which may arise because of higher respiratory activity as cells experience metabolic changes during entry into stationary phase. Resuspending exponentially growing cells in stationary phase culture supernatant, which induces *rpoS* expression, is also an effective inducer of both *katE* (Schellhorn and Hassan, 1988) and *katG* expression (Mukhopadhyay and Schellhorn, 1994). This is consistent with the notion that an extracellular metabolite(s), possibly produced during growth is responsible for growth phase-dependent expression of HPII and HPI after accumulating to high enough levels. Weak acids such as acetate, produced during growth, and subsequently taken up as a carbon source, also induce *katE* (Schellhorn and Hassan, 1988; Schellhorn and Stones, 1992) and *katG* expression (Mukhopadhyay and Schellhorn, 1994). Intracellular pH is a suggested signal for inducing *katE* expression (Schellhorn and Hassan, 1988), but aerobic or anaerobic conditions have no effect (Mulvey *et al.*, 1990).

The *dps* gene (DNA-binding protein from starved cells) is regulated by three independent factors, σ^s (Almiron *et. al.*, 1992), OxyR and IHF, a small DNA-binding protein involved in gene expression (Altuvia *et al.*, 1994; reviewed in Friedman, 1988). OxyR-dependent induction only occurs during exponential phase but σ^s and IHF control is exerted during stationary phase (Altuvia *et al.*, 1994). Both σ^s and IHF function as positive regulators of *dps* expression. Also known as PexB (Lomovskaya *et al.*, 1994), the *dps* gene product is a histone-like protein with a molecular mass of

18 kDa that forms highly structured complexes with DNA *in vitro* (Almiron *et. al.*, 1992). *dps* maps to 18 minutes on the *E. coli* chromosome and is induced under osmotic and oxidative stress (Lomovskaya *et al.*, 1994). As a major protein synthesized in late stationary phase (Almiron *et al.*, 1992), its production starts after growth ceases and continues for several days. Dps is transcriptionally regulated by σ^s during entry into stationary phase, and is slightly induced by the addition of 0.009% acetate (Lomovskaya *et al.*, 1994). Apart from its role in starvation-mediated protection against exposure to oxidative stress via the OxyR mechanism (Altuvia *et al.*, 1994), it is also a global regulator of gene expression after prolonged periods of starvation (Almiron *et al.*, 1992). Dps induction during oxidative stress is independent of σ^s but induction during osmotic stress requires σ^s (Lomovskaya *et al.*, 1994). The *dps* -10 promoter region resembles the -10 consensus for σ^{70}-dependent promoters, but its -35 region does not exhibit homology to any known promoters. It does, however, resemble the corresponding region in the *fic* and *osmY* promoters, also observed to be under σ^s control (Altuvia *et al.*, 1994).

xthA encodes the major apurinic/apyrimidinic (AP) endonuclease of *E. coli*, exonuclease III, removing nucleoside 5'-monosphosphates near apurinic and apyrimidinic sites in damaged DNA (Saporito *et al.*, 1988). *xthA* mutants are sensitive to inactivation by hydrogen peroxide (Demple *et al.*, 1983) and broad spectrum UV (Sammartano *et al.*, 1986). Its expression is completely dependent on σ^s function (since exonuclease III activity is not detected in *rpoS*$^-$ cells) but its expression pattern differs from that of most σ^s-dependent genes (Sak *et al.*, 1989). *xthA* expression begins early in exponential phase and declines shortly after reaching stationary phase (Sak *et al.*, 1989). This observation may suggest a physiological role for σ^s in exponential phase (Lange and Hengge-Aronis, 1994a), or more likely, dual regulation by σ^{70} during exponential phase since the *xthA* promoter is recognized by both $E\sigma^{70}$ and $E\sigma^s$ (Nguyen *et al.*, 1993). The -10 and -35 regions upstream of the transcriptional start sites for *xthA* (Saporito *et al.*, 1988) are similar to that of *katE* (von Ossowski *et al.*, 1991)

The *E. coli aidB* gene is one of several genes induced in response to DNA alkylation damage caused by exposure to a methylating agent (Landini *et al.*, 1994). Encoding an enzyme

with a high degree of homology to several enzymes involved in leucine metabolism in mammalian cells (Ikeda *et al.*, 1983) the *aidB* gene is regulated by two independent mechanisms. The Ada protein in *E. coli* is known to mediate the response to alkylation damage, and is activated by methylation to become a regulator for *aidB* promoter transcription (Landini *et al.*, 1994). The second pathway for *aidB* induction occurs during growth under anaerobic conditions and requires σ^s (Volkert *et al.*, 1994). *aidB* expression responds only to the aeration state of the cell and not to growth-rate reduction, since induction can be blocked throughout stationary phase by aeration (Volkert *et al.*, 1994). The function of *aidB* under σ^s regulation is unknown. Evidence suggests other regulators are involved in *aidB* expression during oxygen limitation since its gene product is detectable in a rpoS$^-$ background.

Genes involved in cellular morphology: *bolA, pbp-6, pbp-3, fic*

E. coli morphology alters as the cell enters stationary phase. Unlike exponential phase cells that are rod-shaped and elongated, stationary-phase cells are spherical (Lange and Hengge-Aronis, 1991b). The *bolA* gene is involved in this morphological change. Mapped to 10 min on the *E. coli* chromosome (Aldea *et al.*, 1988), *bolA* encodes a regulatory protein with a molecular weight of 13.5 kDa, containing a potential helix-turn-helix motif. *bolA* expression is induced 12-fold during entry into stationary phase and is completely abolished in an isogenic *rpoS*$^-$ strain suggesting a high dependency on the presence of σ^s (Lange and Hengge-Aronis, 1991b). Overexpression of the *bolA* gene product results in a spherical phenotype for exponentially-growing cells, if a wild-type *ftsZ* allele is present (Aldea *et al.*, 1988). The *ftsZ* gene product plays a central role in septum formation during cell division, and although growth-phase controlled, the gene is not σ^s-dependent (Aldea *et al.*, 1990). The phenotype of *bolA*$^-$ mutants have not been explicitly determined, but *rpoS* mutants exhibit heterogeneous cell lengths ranging from coccobacillary to rod-shaped forms in stationary-phase cultures (Lange and Hengge-Aronis, 1991b). The *bolAp1* promoter contains a "gearbox sequence," but this promoter element is not recognized by σ^s (Lange and Hengge-Aronis, 1991b).

bolA is also required for the stationary phase induction of the penicillin-binding protein (PBP) 6, a carboxypeptidase involved in septum formation resulting in coccobaciliary cell shapes in stationary phase (Buchanan *et al.*, 1982; Aldea *et al.*, 1989). Strains mutated in *rpoS* exhibit decreased expression of the PBP6 protein, probably due to a decrease in *bolA* expression. Thus, σ^s is involved in determining both cell shape and size. In addition, the decline in PBP3 compared with the decline of other PBPs in stationary phase is much less in a *rpoS*$^-$ background, suggesting that σ^s functions to downregulate the expression of PBP3 (Dougherty and Pucci, 1994). Despite the dependence of PBP6 and PBP3 expression on σ^s, a disruption of *rpoS* does not appear to cause a specific phenotype associated with their function (Dougherty and Pucci, 1994).

The *fic* gene is located at 75 min of the *E. coli* chromosome and has been identified as a regulatory factor involved in cell division (Kawamukai *et al.*, 1989). The *fic* reading frame lies 30 bp upstream from the *pabA* gene, and the two genes comprise an operon. The *fic-pabA* operon is the only type III promoter known to date that is recognized preferentially by Eσ^s (Tanaka *et al.*, 1993). *lacZ* fusions to the *fic* promoter exhibit growth-phase-dependent expression that is totally abolished in a *rpoS* mutant (Utsumi *et al.*, 1993). Mutants of *fic* require para-aminobenzoic acid (PABA) or folate for growth (Komano *et al.*, 1991), exhibit the morphology of short rods in contrast to the longer rod-shapes of wild-type strains (Kawamukai *et al.*, 1988) and cannot grow at 43°C (Utsumi *et al.*, 1993). The p*fic* promoter sequence reveals a conserved -10 region to the σ^{70} consensus, while the -35 does not exhibit a similar recognition sequence (Utsumi *et al.*, 1993).

Glycogen Synthesis: *glgS*

σ^s is involved in the control of *glgS*, a gene involved in glycogen synthesis (Hengge-Aronis and Fischer, 1992). Although glycogen is also synthesized by enzymes encoded by the *glgCAP* operon, which is not under σ^s control, *rpoS*$^-$ mutants are as strongly defective in glycogen synthesis as *glgC* and *glgA* mutants (Lange and Hengge-Aronis, 1991a). *glgS* maps to 66.6 min on the *E. coli* chromosome and encodes a 7.9 kDa protein. A *lacZ* fusion to the *glgS* gene demonstrates growth-phase-dependent expression positively regulated by σ^s and cAMP (Hengge-Aronis and

Fischer, 1992). Induced 30 to 50-fold in stationary phase, it is the most highly expressed gene in the σ^s-regulon. *glgS* is also slightly induced by increased medium osmolarity (Hengge-Aronis *et al.*, 1993) and expression during entry into stationary phase is reduced by 60% in a *rpoS* mutant (Hengge-Aronis and Fischer, 1992). Two transcriptional start sites are identified in the *glgS* promoter region, one transcribed by σ^s, and the other by cAMP. The combined activity of the two differentially regulated promoters is suggested to ensure maximal *glgS* expression.

Genes involved in the control of Acid Phosphatase: *appY*, *appA*
and a Third Cytochrome Oxidase: *cyxAB*

appA, the structural gene for a periplasmic acid phosphatase, has an optimum enzyme activity at pH 2.5 (Touati *et al.*, 1987). Mapped to 22 min on the *E. coli* chromosome, *appA* expression is induced under several conditions. In rich media, cells accumulate the enzyme during entry into stationary phase that is maintained for more than two to three days. Expression is also induced under conditions of oxygen and P_i (inorganic phosphate) limitation, the latter being the most effective stimulus (Touati *et al.*, 1987). *appA* expression is positively regulated by σ^s (Touati *et al.*, 1986) and negatively regulated by cAMP (Touati *et al.*, 1987). Overproduction of a protein, AppY from multicopy plasmids also stimulates *appA* production (Atlung *et al.*, 1989). Two genes called *appC* and *appB*, located upstream from *appA* are regulated by the same factors as *appA* and the three comprise the *appCBA* operon. *appC* and *appB* (also known as *cyxA* and *cyxB*, respectively) encode one of three cytochrome oxidases in *E. coli* (Dassa *et al.*, 1992).

The *appY* gene is mapped to 13 min on the *E.coli* chromosome. Besides its positive regulatory effect on *appA* expression, overproduction of AppY affects the rate of synthesis of more than 30 cellular proteins as a function of growth-phase (Atlung *et al.*, 1989). *lacZ* fusions to *appY* are reduced in *rpoS* mutants (Atlung *et al.*, 1989). Thus the regulation of the *appCBA* operon by σ^s may be indirect, mediated through AppY (Hengge-Aronis, 1993a).

Osmotically Regulated Genes: *osmB, osmY (csi5), ompF, otsBA, proP, treA*

rpoS mutants are more sensitive to increased medium osmolarity than wild-type cells (McCann *et al.*, 1991). Two-dimensional gel analysis of proteins induced during osmotic upshift (>300 mM NaCl) revealed 18 proteins that are under σ^s control (Hengge-Aronis *et al.*, 1993). Some of these are probably important in stationary phase osmoprotection.

The expression of the *osmY* (*csi5*) gene is strongly induced in cells during entry into stationary phase (Lange and Hengge-Aronis, 1991a) and is also regulated by medium osmolarity (Yim and Villarejo, 1992). Mapped to 99.3 min on the *E. coli* chromosome (Yim and Villarejo, 1992), it encodes a periplasmic protein of unknown function (Lange *et al.*, 1993), but has been suggested to be involved in capsule formation (Yim and Villarejo, 1992). *osmY* is transiently expressed, transcribed to maximum levels in osmotically stressed cultures and returning to pre-induction states within two hours (Yim and Villarejo, 1992). Growth-phase expression of *osmY* in a *rpoS* strain is almost completely abolished compared with an isogenic *rpoS*$^+$ strain (Hengge-Aronis *et al.*, 1993). In contrast, osmotic induction of *csi5::lacZ* is still observed in a *rpoS* mutant, suggesting that additional factors other than σ^s are involved in osmotic induction (Lange *et al.*, 1993). *osmY* mutants do not exhibit a specific phenotype apart from a slight sensitivity to hyperosmotic stress (Yim and Villarejo, 1992). Besides σ^s, at least three other regulators are involved in the control of *osmY* transcription. These are Lrp, a regulator protein involved in the induction of genes required after nutritional downshift (eg. amino acid biosynthetic genes), IHF, and cAMP. In contrast to σ^s, Lrp, IHF, and cAMP act as negative regulators and are not required for *osmY* expression during osmotic induction. All repressing regulators are suggested to act independently of one another (Lange *et al.*, 1993). Molecular characterization of the *osmY* promoter suggests that σ^s is the principal regulator of *osmY* expression during osmotic stress and entry into stationary phase (Yim *et al.*, 1994). The -10 region of the *osmY* promoter reveals similarity to the σ^{70} consensus, but the -35 region does not exhibit homology to the σ^{70} consensus (Yim *et al.*, 1994).

The *osmB* gene encodes a lipoprotein located in the outer membrane of *E. coli* (Jung *et*

al., 1990). Under σ^s control (Hengge-Aronis *et al.*, 1991), *osmB* expression is growth-phase-dependent and responds to increases in medium osmolarity (Jung *et al.*, 1990). Levels of OsmB are reduced in a *rpoS* mutant (Hengge-Aronis *et al.*, 1991). The addition of sodium chloride to actively growing cultures results in an induction pattern that can be divided into two phases. The first phase of induction begins at the onset of osmotic upshift and the second induction during entry into stationary phase. *osmB* expression does not appear to respond to factors associated with stationary phase such as starvation for carbon, nitrogen, phosphorus, or sulfur, oxygen tension, and pH decreases (Jung *et al.*, 1990). The only phenotypic change for an *osmB* mutant is the lack of cell aggregation normally seen with stationary phase cells under osmotic stress (Jung *et al.*, 1990). *osmB* is transcribed from two promoters, P1 and P2. Transcription is initiated from the downstream P2 promoter at the onset of stationary phase when cells are grown under low osmolarity conditions. Transcripts initiate at both P1 and P2 during high osmolarity at stationary phase, P2 being the more active. The -10 and -35 consensus sequences for σ^{70} promoters are present in P2 but the corresponding regions are less prominent in P1 (Jung *et al.*, 1990).

E. coli contains two major outer membrane protein channels, OmpF and OmpC that permit the passive diffusion of molecules into the periplasm (reviewed in Csonka, 1989). The productions of these porins are regulated by several environmental factors such as osmolarity, carbon sources and temperature. Cellular levels of the two porins remain constant but their relative proportions are inversely regulated. For example, factors that promote the production of OmpF such as low osmolarity, poor carbon sources and low temperature diminish the production of OmpC, and vise-versa. The transcription of *ompF* and *ompC* are dependent on the OmpR and EnvZ proteins that comprise a two-component regulatory pathway, EnvZ as the cytoplasmic membrane sensor of environmental signals and OmpR as the transcriptional activator of the porin-encoding genes. OmpF porin levels are also regulated by an antisense mRNA, designated *micF*. Highly complementary to the 5' region of the *ompF* mRNA, *micF* is involved in the negative regulation of *ompF* at the translational level by binding to the 5' region of the *ompF* mRNA, preventing ribosome binding (reviewed in Csonka, 1989). Although the nature of σ^s control over *ompF* is not extensively

documented, two-dimensional gels reveal increased levels of the OmpF protein in a *rpoS* mutant (McCann *et al.*, 1991).

E. coli accumulates endogenously synthesized trehalose, a compatible solute that serves as an osmoprotectant when cells are exposed to conditions of high osmolarity (reviewed in Csonka, 1989). Mutants defective in trehalose accumulation can grow as well as the parental strain when exposed to 0.2 M NaCl, but cannot grow on high media osmolarity (0.5 M NaCl). This sensitivity can be alleviated by the addition of other osmoprotectants such as glycine betaine (Giaever *et al.*, 1988). The synthesis of trehalose is dependent upon the expression of two genes, *otsA* and *otsB*, located at 41.6 min on the *E. coli* chromosome (Kaasen *et al.*, 1992). Exposure to high medium osmolarity results in expression from the *otsBA* regulon, encoding trehalose-6-phosphate phosphatase and trehalose-6-phosphate synthase, respectively (Giaever *et al.*, 1988; Kaasen *et al.*, 1992). Trehalose is also used as a sole carbon source for *E. coli*. Broken down by a periplasmic trehalase encoded by the gene *treA*, the glucose component of trehalose is transported to the cytoplasm and used as an energy source. *treA* maps to 26 min on the *E. coli* chromosome (Boos *et al.*, 1987) and is osmotically induced (reviewed in Csonka, 1989). Using *lacZ* fusions to *otsA*, *otsB* and *treA*, the genes are growth-phase-dependent and osmotically induced in a σ^s-dependent manner. A Tn10 insertion into *rpoS* completely abolish *otsA* and *otsB* expression and reduces *treA* expression. *otsA*::*lacZ* and *otsB*::*lacZ* fusions are induced when osmotically challenged even in exponential phase cells, indicating that σ^s may be important in growing as well as stationary phase cells (Hengge-Aronis *et al.*, 1991; Hengge-Aronis *et al.*, 1993).

The gene *proP* encodes a transporter of proline and glycine betaine, compatible solutes that play important roles in protecting cells during osmotic stress (reviewed in Csonka, 1989). *proP* is located at 94 min on the *E. coli* chromosome and is positively regulated by σ^s, cAMP and Fis, a DNA-binding protein and regulator of gene expression (Xu and Johnson, 1995b). *proP* expression is reduced eight to 10-fold in a *rpoS*$^-$ mutant. Transcribed from two independently controlled promoters, P1 and P2, *proP* exhibits a two-phased expression pattern. *proP1* is transiently induced during exponential phase (phase I) which quickly declines after two hours while *proP2* expression

(phase II) begins during entry into stationary phase. Expression from both promoters is up-regluated in cells exposed to increases in medium osmolarity but only the osmotic induction of P2 is dependent on Fis and σ^s. The -10 region of the P2 promoter displays similarity to those of the σ^{70} promoters but no resemblance in the corresponding -35 region (Xu and Johnson, 1995c).

Of all the osmotically inducible genes mentioned (*osmY, osmB*, *ompF*, *treA*, *proP*) only lesions in *otsAB* results in a sensitive phenotype. This may suggest that although they are induced under osmotic upshift not all are essential for osmoprotection but may serve other vital functions in the cell (Giaever *et al.*, 1988).

Genes Involved in Thermotolerance: *otsBA, htrE*

Sensitivity to heat-shock (>50°C) has been previously observed with *rpoS* mutant strains, a phenotype that is independent of the σ^{32}-family of heat shock proteins (Lange and Hengge-Aronis, 1991a; McCann *et al.*, 1991). Fourteen polypeptides are absent in a *rpoS* mutant after exposure to 42°C (McCann *et al.*, 1991), but only a few genes have been identified to be involved in stationary phase thermotolerance under σ^s regulatory control.

Besides its role in osmoprotection, trehalose is also involved in stationary phase thermotolerance at 55°C and is suggested to contribute to the increased thermal stability of proteins (Back *et al.*, 1979). Trehalose is not required for adaptive thermotolerance in growing cells (Hengge-Aronis *et al.*, 1991), but is not the only factor involved in σ^s-dependent thermotolerance, since *otsAB* mutants are more viable than *rpoS* mutants (Hengge-Aronis *et al.*, 1991).

The product of the *htrE* gene encodes a 95 kDa protein highly homologous to the pilin porin, PapC, involved in pilin transport and assembly (Raina *et al.*, 1993). Mapped to 3.3 min on the *E. coli* chromosome, transcription of the *htrE* operon requires σ^s and IHF. Transcription is initiated from the *htrE* following a temperature shift from 22°C to 42°C, and is independent of the σ^{32}-heat shock regulon. A Tn10 insertion into *rpoS* results in a substantial reduction of *htrE* transcription, suggesting a positive regulatory function for σ^s. *htrE* mutants exhibit three phenotypes (i) the inability to form colonies above 43.5°C, (ii) reduced colony formation on media containing more than 0.7 M

of sodium chloride, (iii) and lethality when exposed to normally sublethal heat-shock at 50°C (Raina *et al.*, 1993).

CFA (Cyclopropane Fatty Acid) synthase: *cfa*

In *E. coli*, a unique post-synthetic modification of the preexisting phospholipid bilayer results in the formation of cyclopropane fatty acids (CFA) that occurs predominantly during entry into stationary phase. The reaction is catalysed by CFA synthase, a soluble enzyme found in the cytoplasm encoded by the *cfa* gene (Wang *et al.*, 1992). Under σ^s regulatory control, CFA synthase activity rapidly increases during late exponential phase but rapidly declines as stationary phase progresses, due to the short half-life and instability of the CFA protein (Wang and Cronan, 1994). CFA synthase is not completely dependent on σ^s since its synthesis reaches half the wild-type levels in a *rpoS* mutant (Wang and Cronan, 1994). Northern analysis of CFA synthase mRNA levels in *rpoS*$^+$ and *rpoS*$^-$, exponential and stationary phase cultures identify two promoters. The upstream promoter, P1, responsible for the longer transcript is active throughout growth-phase. The downstream promoter, P2 is active only upon entry into stationary phase and is under σ^s regulatory control (Wang and Cronan, 1994). Analysis of both promoter sequences reveals a good match to the σ^{70} consensus for the -10 and - 35 region of P1. However, only a reasonable match to the σ^{70} consensus is observed for the P2 -10 region.

Pyruvate Oxidase: *poxB*

The *E. coli* pyruvate oxidase (PoxB) is a flavoprotein dehydrogenase that catalyzes the decarboxylation of pyruvate to acetate and CO_2 (Gennis and Hager, 1976). *poxB* expression is induced during entry into stationary phase and is highly dependent on σ^s control. Pyruvate oxidase activity is completely abolished in a *rpoS* mutant. *lacZ* fusions to *poxB* reveal a 14-fold induction in a wild-type strain and almost no activity from a *rpoS*$^-$ derivative. Cultures exposed to anaerobiosis exhibit a 40-50% decrease in *poxB* transcriptional activity (Chang *et al.*, 1994). Since *E. coli* possesses two other genes involved in the production of acetate, the metabolic role of PoxB

remains unclear (Chang *et al.*, 1994).

Microcin C7: *mccC7*

Microcin C7 (MccC7) is a 1 kDa peptide antibiotic known to inhibit protein synthesis in *E. coli* cells (Garcia-Bustos *et al.*, 1985). It is produced by *E. coli* strains that contain a 43 kb conjugative plasmid (pMccC7) carrying the *mcc* genes (Novoa *et al.*, 1986). The plasmid genes responsible for the production of MccC7 have been mapped to a segment of the plasmid that is induced 100-fold during transition into stationary phase. Mutations isolated by screening for the loss of MccC7 production were mapped to *rpoS*. Screening for MccC7 activity in *rpoS*$^+$ and *rpoS*$^-$ derivatives (Diaz-Guerra *et al.*, 1989) confirmed the role of σ^s as a positive regulator of microcin C7 production. The production of microcins is suggested to be a method of competing against microcin-sensitive strains during nutrient limitations (Hengge-Aronis, 1993).

Genes Involved in Virulence and Pathogenesis: *spvABCD, csgAB*

The *Salmonella* plasmid virulence (*spv*) genes are required by a number of *Salmonella* species to confer lethal disease (Krause *et al.*, 1991). Encoded on large plasmids 50 to 100 kb in size, the regulatory gene *spvR* and structural genes, *spvABCD* form a single operon which exhibit induction during entry into stationary phase (Krause *et al.*, 1992). Transcription from the *spvA*p is σ^s-dependent, both in *S. typhimurium* (Fang *et al.*, 1992) and *E. coli* (Norel *et al.*, 1992) and is modulated by SpvR, a member of the LysR family of transcriptional activators (Henikoff *et al.*, 1988). Using *S. dublin*, increases in the concentration of σ^s during entry into stationary phase leads to the σ^s-dependent induction of *spvR*. SpvR and σ^s then act in concert to induce the *spvABCD* regulon (Chen *et al.*, 1995). Strains of *S. typhimurium* harboring a defect in *rpoS* are more susceptible to oxidative challenge, acid stress, DNA damage and inability to survive prolonged periods in starvation (Fang *et al.*, 1992), conditions to which the bacterium is exposed within phagosomes of host phagocytic cells. Using *lacZ* fusions to the *spvB* gene, it is demonstrated that a mutation in *rpoS* decreases the expression of *spvB* by 86% (Fang *et al.*, 1992).

The expression of thin, aggregated, surface fibers called curlin confer some *E. coli* strains the ability to bind fibronectin and laminin in eukaryotic tissue (Olsen *et al.*, 1989). The formation of these fibers confer a selective advantage in the colonization of organic matter in the extra-intestinal environment and in the gastrointestinal tract. Curlin fibers are formed in response to low temperatures (26°C), low osmolarity, and stationary phase growth conditions (Olsen *et al.*, 1989). Subunits of these curlin fibers are encoded by *csgA* and *csgB*, and the two comprise an operon expressed during stationary phase (Arnqvist *et al.*, 1994). *lacZ* fusions to the *csgBA* promoter reveal increased expression during stationary phase and almost no activity in a *rpoS*$^-$ background (Arnqvist *et al.*, 1994). Similarly, the cell is unable to produce curlin or bind fibronectin in a *rpoS* mutant (Olsen *et al.*, 1993). Expression from the *csgA* gene is repressed by H-NS, since the production of curlin fibers from *E. coli* K-12 curlin-deficient strains occurs in a *hns*$^-$ background. Furthermore, a mutation in *hns* relieves the dependence of curlin production on σ^s since a *rpoShns* double mutant can express curlin fibers under low temperature and low osmolarity (Olsen *et al.*, 1993). The *csgBA* promoter can be recognized by $E\sigma^{70}$ (Arnqvist *et al.*, 1994).

Chaperonin analogue; *cbpA*

The product of the *cbpA* gene is a DNA-binding protein that preferentially recognizes curved DNA sequences. *cbpA* is an analogue of the *E. coli*, heat-shock inducible, chaperone protein, DnaJ (Ueguchi *et al.*, 1994) and the protein is suggested to function as a molecular chaperone to proteins expressed during an environmental stress other than heat-shock manner (Yamashino *et al.*, 1994). *cbpA* expression is not induced upon heat-shock but is induced upon entry into stationary phase in a σ^s-dependent. Expression of *cbpA* in response to phosphate starvation (but not of carbon or nitrogen) is also σ^s-dependent. Studies of the promoter region reveals a curved DNA structure (Yamashino *et al.*, 1994), suggested to be a structural determinant for the recognition or binding of σ^s (Espinosa-Urgel and Tormo, 1993). The *cbpA* promoter reveals similarity to the consensus sequences for the σ^{70}-type promoter (Yamashino *et al.*, 1994).

Integration Host Factor (IHF): *himA, himD/hip*

IHF is a small DNA-binding protein composed of two different subunits, α and β, encoded by the genes *himA* and *himD/hip*, respectively. Involved in a number of cellular processes including the positive and negative regulation of many functions (reviewed in Friedman, 1988), IHF is a known regulator of two σ^s-dependent genes, *dps* (Altuvia *et al.*, 1994) and *osmY* (Lange *et al.*, 1993). Expression from both *himA* and *himD/hip* is growth-phase induced and σ^s-dependent. Transcription from both genes is not completely abolished in a *rpoS* mutant and the two do not have the same level of σ^s-dependence since the *himA* promoter shows a greater reduction in expression (Aviv *et al.*, 1994). The *himA* promoter is positively regulated by ppGpp, a control mediated through *rpoS*. Both *himA* and *himD/hip* transcription is autoregulated. The *himA* -35 promoter region is homologous to the *fic-pabA* promoter but both promoter sequences deviate from the σ^{70} consensus (Aviv *et al.*, 1994).

Members of Fis regulated genes: *aldB, glnQ, mglA, sdhA, xylF, frg-502, frg-541, frg-734*

Fis is a small DNA-binding protein containing a helix-turn-helix motif known to bind to various promoter regions of the *E. coli* chromosome (Finkel and Johnson, 1992). As a member of the general nucleoid-associated proteins that include IHF, H-NS, LRP, and Dps, Fis functions as a regulator of gene expression. The identification of members of the *fis* regulon using *lacZ* fusion insertions reveal a subset of genes within the regulon that is negatively and positively regulated by σ^s (Xu and Johnson, 1995a). Some have been mapped to known regions of the *E. coli* chromosome. Eight protein fusions observed to be negatively repressed by Fis have been analyzed. Five have been mapped to known genes and the remainder designated *frg* for "Fis regulated gene". These are summarized below.

Gene	Map Location	Expression	Effect of σ^s
frg-502	65	stationary	activates
frg-541	31-33	stationary	inhibits slightly
frg-734	43-45	stationary	activates
aldB-731	80-83	stationary	activates
glnQ-732	18	mid log	inhibits slightly
mglA-543	45-47	mid log	inhibits
sdhA-133	16	mid log	inhibits
xylF-103	80	late log	inhibits

Modified from Xu and Johnson, 1995a.

xylF and *mglA* encodes for D-xylose-binding protein and β-methyl-galactoside transporter, respectively. *glnQ* encodes a glutamine permease and *sdhA* encodes a succinate dehydrogenase. Each of these genes encode proteins that are components associated with the cell membrane or periplasm (Xu and Johnson, 1995a). The *sdhA*-encoding succinate dehydrogenase is an important component of the TCA cycle. Its expression is also negatively regulated by other regulators such as Fnr and ArcA (Iuchi *et al.*, 1994).

The *aldB* gene is negatively regulated by Fis but is positively regulated by σ^s at the post-transcriptional level (Xu and Johnson, 1995b). *aldB* is growth-phase-dependent and exhibits a 28-fold decrease in a *rpoS* mutant background. It is also positively regulated by cAMP. Mapped to 80.8 to 80.9 min on the *E. coli* chromosome (Xu and Johnson, 1995a), the *aldB* gene encodes an enzyme, aldehyde dehydrogenase (56.3 kDa), that functions to oxidize aldehydes to their corresponding acid forms (Xu and Johnson, 1995b). *aldB* expression is not affected by medium osmolarity and exhibits only slight induction in the presence of ethanol, suggesting a potential role for AldB in the detoxification of alcohols and aldehydes present in stationary phase cells. The promoter sequences of the *aldB* gene reveal similarity to the -10 σ^{70}-consensus but no reasonable similarity to a σ^{70} -35 consensus (Xu and Johnson, 1995b).

The *Salmonella* Multiple-Nutrient Starvation-Inducible Genes: *stiA, stiB, stiC*

The *sti* genes encode factors involved in the multiple-nutrient starvation-inducible loci in *Salmonella typhimurium* (O'Neal *et al.*, 1994). Three genes identified as *stiA*, *stiB*, and *stiC* are essential for bacterial survival during simultaneous phosphate, carbon and nitrogen starvation conditions. Mutations in any of these loci result in 50 to 75-fold reduction in survival of cells under multiple-nutrient starvation conditions (Spector and Cubitt, 1992). *lacZ* fusions to *stiA* and *stiC* demonstrate that the normal induction observed during carbon, nitrogen and phosphorus starvation is abolished a *rpoS* mutant. In contrast, the *stiB* locus is induced two to three-fold in the absence of *rpoS* during phosphate and carbon starvation (O'Neal *et al.*, 1994).

Genes of Unknown Function: *csiD, csiE, csiF, hdeAB*

The *csi12*::*lacZ*, *csi16*::*lacZ* and *csi32*::*lacZ* genes, initially isolated as carbon-starvation-inducible (Lange and Hengge-Aronis, 1991a), are σ^s-dependent whose functions are unknown (Weichart *et al.*, 1993). Located at 57.6 min, 54.8 min, and 8.8 min on the *E. coli* chromosome, respectively, these genes were subsequently designated *csiD*, *csiE* and *csiF*. Slightly higher levels of β-galactosidase activity is detected for *csiE*, and *csiF* in a Δ*cya* mutant. *csiF* expression is positively regulated by cAMP and is tested to be partially impaired for glycogen synthesis, but does not map to the glycogen producing *glgA* gene (Weichart *et al.*, 1993).

The search for other promoters with regulatory features similar to the promoter of *csgAB* led to the identification of a 12 kDa periplasmic protein expressed with the fibronectin-binding curli protein. The 12 kDa protein is missing from a curli-deficient strain and a *rpoS* mutant and is highly expressed in a *hns*$^-$ mutant (Arnqvist *et al.*, 1994). The 12 kDa protein is encoded by *hdeA*, which, along with *hdeB*, comprise the *hdeAB* operon (Yoshida *et al.*, 1993). The HdeA and HdeB proteins are not involved in curli synthesis. Similar to p*csgBA*, the *hdeAB* operon is completely dependent on σ^s, and this dependency is relieved in a *hns*$^-$ mutant. The *hdeAB* operon is also expressed in exponentially growing cells, but at lower levels. The *hdeAB* promoter sequence exhibits high homology to the σ^{70} promoter consensus sequence (Arnqvist *et al.*, 1994).

σ^s PROMOTER RECOGNITION

The exchange of sigma factors for core RNA polymerase is one primary mechanism of the global switching of gene regulation. Alternative sigma factors synthesized or activated in response to an environmental or growth stimulus can temporarily displace the main sigma subunit as the transcriptional activator. Since σ^s shares considerable homology to σ^{70}, it suggests a common consensus sequence for the promoters they recognize. Confirmation of promoter similarity is provided by evidence that σ^s can initiate transcription from σ^{70} -dependent promoters such as the *lac*UV5 (mutated for lactose metabolism), *trp* (tryptophan biosynthesis), and *dna*Qp2 (subunit of DNA polymerase III) promoters (Tanaka *et al.*, 1993). Some promoters are transcribed exclusively by σ^{70} (*mcbA*) or σ^s (*fic-pabA*). However, analysis of the available promoters does not reveal a likely consensus sequence for σ^s recognition (Tanaka *et al.*, 1993). Sequence comparisons of the first few σ^s-dependent genes identified revealed a potential consensus in the *xthA* and *katE* promoters (Saporito *et al.*, 1988; von Ossowski *et al.*, 1991). However, analysis of promoter regions of additional members of the σ^s-regulon revealed deviations from the previous consensus.

"Gearbox promoter" is a term designated for a subset of promoters which exhibit expression rates inversely proportional to the growth rate and contain distinctive sequences around their -10 and -35 regions (Aldea *et al.*, 1990). Initially thought to be the recognition sequences for σ^s, the suggestion was unlikely based on observations that most σ^s-dependent genes do not contain the gearbox promoter sequence. Furthermore, the gearbox-containing *mcbA* promoter is not recognized by σ^s but is recognized by σ^{70} (Tanaka *et al.*, 1993).

More than 30 *rpoS*-dependent genes or operons have been identified to date. Many of these exhibit differential regulation, or are involved in a multilayered, cascade-regulation mechanism within the *rpoS*-regulon. Some genes are highly dependent on σ^s, and some exhibit induction (although at a lower level), in a *rpoS*$^-$ background. Consequently, a subset of promoters may not be directly recognized by σ^s. With the similarity to σ^{70} promoters, and the involvement of additional regulatory factors such as IHF, Fis, cAMP, H-NS, and OxyR, the derivation of the *rpoS* consensus sequence has become more difficult. The failure to identify a common consensus has

led to the search for other structural features specific to σ^s-dependent promoters. It has been suggested that DNA bending may help in the recognition or binding of σ^s to its promoters. Computer prediction analysis has revealed four σ^s-dependent promoters located in curved DNA regions, a structural feature absent in the σ^{70} -dependent *mcbA* promoter (Espinosa-Urgel and Tormo, 1993). In addition, the p*csgBA* and p*hdeAB* promoters are speculated to contain a bend in the DNA structure. Furthermore, the binding of H-NS is suggested to promote specific bending of the promoter region, orienting DNA topology better to accommodate the binding of either $E\sigma^s$ or $E\sigma^{70}$, perhaps in response to growth phase signals (Arnqvist *et al.*, 1994). Many σ^s-dependent promoters have a σ^{70} consensus at the -10 region, but lack a σ^{70} consensus at the -35 element. Recent evidence has shown using reconstituted promoter elements that the -10 promoter region is the determinant in $E\sigma^s$ recognition (Tanaka *et al.*, 1995). However, *in vitro* experiments may be an imperfect model of *in vivo* conditions, since additional regulatory factors involved in the regulation of the gene, and a possible requirement for DNA-bending as a recognition factor, are not accounted for. Furthermore, due to the diversity of regulatory features of members of the σ^s regulon, the observation of trends using several promoters may not be applicable to the entire regulon as a whole.

SUBFAMILIES AND CASCADE REGULATION WITHIN THE σ^s-REGULON

The identification of σ^s-dependent genes exhibiting a specific phenotype set the basis for the systematic screening for additional members of the regulon. As the number of genes under σ^s control increased, subfamilies apparently exist within the regulon that responds to additional regulatory or environmental factors. This is the case with the *otsBA*, *treA*, and *osmB* genes (Boos *et al.*, 1987; Giaever *et al.*, 1988, Jung *et al.*, 1990), first identified as osmotically inducible genes, and later, as members of the σ^s-regulon. Two-dimensional gel analysis of proteins induced under osmotic upshift revealed a subset of which required σ^s for expression. Within this subset of osmotically-inducible genes, expression is characteristic of each. For example, *glgS* is induced at least 30 to 50-fold during entry into stationary phase but is only induced 2-fold by osmotic upshift. In

contrast, growth-phase expression and expression during osmotic induction is approximately the same for *osmY* and *bolA*, (Hengge-Aronis *et al.*, 1993). Furthermore, at least one gene (*csgA*) is expressed under low osmolarity (Olsen *et al.*,1993). However, not all members of the σ^s-regulon are induced under these conditions (Hengge-Aronis *et al.*, 1993). Several lines of evidence suggest that *rpoS* alone may not be sufficient for the induction of several members of the osmotically-inducible genes. For example, osmotic induction of *osmY* expression is still observed (although at a reduced level) in a *rpoS*$^-$ mutant (Lange *et al.*, 1993). Gene expression from the two promoters of *proP* (P1 and P2) is osmotically inducible though σ^s can only initiate transcription from P2 (Xu and Johnson, 1995c).

A few σ^s-dependent genes encode regulatory proteins that are responsible for the expression of several genes. The *bolA* gene, when overexpressed is involved in the regulation of *pbp6* (Aldea *et al.*, 1989). AppY, a positive regulator of the *appA*-encoding acid phosphatase and *cyxAB* is also required for the expression of approximately 30 other polypeptides (Atlung *et al.*, 1989). Dps, an abundant protein still synthesized in late (3-day-old) stationary phase cells form highly structured complexes with DNA in vitro, and is a global regulator of gene expression after long periods in starvation (Almiron *et al.*, 1992). Genes regulated by these secondary regulators are under indirect control by σ^s, leading to the suggestion that σ^s exerts its influence in stationary phase gene expression by a branched regulatory cascade (reviewed in Hengge-Aronis, 1993b).

Additional global regulators are involved in the control of members of the σ^s-regulon, thus, σ^s is a component in a larger regulatory network in gene expression throughout growth-phase as suggested by Loewen and Hengge-Aronis (Loewen and Hengge-Aronis, 1994). OxyR is involved in the oxidative induction of *katG* (Christman *et al.*, 1989) and *dps* (Altuvia *et al.*, 1994). The cAMP-CRP complex is a positive and negative regulator of a large subset of σ^s-dependent genes and Fis has recently been implicated in the regulation of nine genes (Xu and Johnson, 1995a, 1995c). Even within these subfamilies, several members can be categorized into others. The *proP* gene regulated by Fis is also partially osmotically induced (Xu and Johnson, 1995c). The osmotically induced genes, *otsB* and *otsA*, are also involved in stationary phase thermotolerance (Hengge-

Aronis *et al.*, 1993). These cases clearly define the complexity of regulatory control in the σ^s regulon.

PURPOSE OF CURRENT STUDY

Several approaches have been used to enumerate and identify members of the σ^s regulon. Two-dimensional gel electrophoresis studies of proteins expressed in *rpoS*$^+$ and *rpoS* mutants suggest that expression of a large number of proteins requires a functional *rpoS* gene. Though the numbers obtained is likely an underestimation since proteins of genes expressed at low levels may not be detected. Furthermore, another limitation of this method is the complicated process of identifying the gene from a protein product, particularly when dealing with large numbers. Mutagenesis techniques using random *lacZ* insertions coupled with the screening for *rpoS*-associated phenotypes have also been employed. However, due to the diversity of unrelated functions of members of the σ^s-regulon, no unifying characteristic or differentiating common phenotype can be easily exploited in such mutation strategies. At most, only subfamilies within the σ^s regulon can be identified using these phenotypic screening methods.

To avoid the problems associated with the above methods, we have employed a genetic screen to identify members of the σ^s regulon. The introduction of a *rpoS* null allele into a library of *rpoS*$^+$ stains containing random *lacZ* fusions should, in theory, allow the ready identification of σ^s-dependent functions. Expression from the reporter gene relies solely on the dependency of the target gene promoter on a functional *rpoS*. This procedure does not rely on a single differentiating phenotype, and can be easily conducted on a large scale.

Table 1. Summary of members of the σ^s-regulon.

Gene	Function/phenotype	Map (min)	Mechanism of Regulation/ Additional Regulators	Environmental Inducers	Promoter
aidB	-involved in leucine metabolism -defence against DNA methylated damage	95.1*	-induced by σ^s during limiting O_2 -Ada-dependent during alkylation damage	-acetate-pH inducible -not induced by benzoate or starvation -induced during oxygen limitation	
aldB	-encodes aldehyde dehydrogenase which oxidizes aldehydes to acid forms	80-83	-regulated by σ^s at posttranscriptional level -negatively regulated by Fis -positively regulated by cAMP -expressed during stationary phase	-slight induction in presence of ethanol	
appBCA (cyxBA)	-*appA* encodes periplasmic acid phosphatase, optimum activity at pH 2.5 -*appBC* encodes one of three cytochrome oxidases in *E. coli*	22	-stimulated by *appY* -negatively regulated by cAMP	-induced during oxygen limitation, starvation for Pi, entry into stationary phase	
appY	-involved in synthesis of polypeptides -reduction in growth rate on poor carbon sources	13	-stimulated 100-fold in exponential phase -stimulated 10 to 40-fold in stationary phase		
bolA	-morphogene -confers round morphology -regulator of *pbp6*	10	-negatively regulated by cAMP	-expressed in stationary phase	
cbpA	-encodes an analogue of *E. coli* chaperonin, DnaJ			-induced during phosphate limitation (but not carbon or nitrogen) in a σ^s-dependent manner	-has σ^{70} consensus for -10 and -35 region
cfa	-encodes CFA (cyclopropane fatty acid) synthase -modifies phospholipid bilayer	22.8*		-stationary phase induced -transient expression, activity quickly lost after progession into stationary phase	-P1 σ^{70}-dependent -P2 σ^s-dependent and growth-phase dependent
csgBA	-encodes curlin fibres -involved in pathogenesis -mutants are not pathogenic		-completely dependent on σ^s, relieved by mutation in H-NS -negatively regulated by H-NS -*hnsrpoS* mutant can express curlin fibres	-expressed at low temp (26°C), low osmolarity, stationary phase	-can be recognized by σ^{70}

Gene	Function/phenotype	Map (min)	Mechanism of Regulation/ Additional Regulators	Environmental Inducers	Promoter
csi-12 (csiD)	-slight heat sensitive phenotype -mutation results in changes of protein synthesis patterns	57.6		-carbon starvation inducible	
csi-16 (csiE)	-function unknown	54.8	-negatively regulated by cAMP	-carbon starvation inducible	
csi-32 (csiF)	-slightly impaired for glycogen synthesis	8.8		-carbon starvation inducible	
dps (pexB)	-encodes DNA-binding protein -protection against oxidative stress -regulator of gene expression	18	-expressed up to 3 days in stationary phase	-induced in the presence of acetate, carbon and nitrogen starvation, osmotic and oxidative stress	-similar to σ^{70} consensus for -10, not for -35 region -resemble *fic-pabA* and *osmY* promoters
fic-pabA	-involved in cell division -involved in PABA synthesis -temperature-sensitive phenotype past 43°C	75	-expression completely abolished in *rpoS* mutant		-has σ^{70} consensus for -10, not for -35 region -type III promoter
frg-502	-function unknown	65	-negatively regulated by Fis		
frg-541	-function unknown	31-33	-slight negative regulation by σ^{s} and Fis		
frg-734	-function unknown	43-45	-negatively regulated by Fis		
glgS	-involved in glycogen synthesis -no glycogen produced in mutant	66.6	-30 to 50-fold induction by σ^{s} -positively regulated by cAMP	-induced 2-fold by osmotic upshift	-transcribed from 2 overlapping promoters, one for σ^{s}, one for cAMP
glnQ	-encodes glutamine permease	18	-slightly inhibited by σ^{s} -negatively regulated by Fis -expressed at mid-log phase		
hdeAB	-function unknown	78.8*	-same mechanism of expression as *csgBA* operon		

Gene	Function/phenotype	Map (min)	Mechanism of Regulation/ Additional Regulators	Environmental Inducers	Promoter
himA/ himD-hip	-encodes subunits of IHF which functions as a regulator of gene expression -mutation results in absence of IHF production	38.6 (*himA*) 20.7 (*himD*) *	-positively regulated by ppGpp mediated through σ^s -negatively regulated by IHF (autoregulation)		
htrE	-confers thermotolerance -mutants sensitive to heat-shock and high osmolarity	3.3	-positively regulated by IHF -highly dependent on σ^s		
katE	-encodes cytoplasmic HPII -mutants sensitive to exposure to hydrogen peroxide	37	-highly dependent on σ^s	-induced by presence of TCA cycle intermediates and acetate	-similar *xthA* promoter
katG	-encodes periplasmic HPI -mutants sensitive to growth on media containing hydrogen peroxide	89.2	-positively regulated by OxyR -σ^s involved in stationary phase expression	-induced by hydrogen peroxide via OxyR-dependent manner	
mcc7	-encodes microcin C7 -inhibits protein synthesis -suggested to give competitive advantage over microcin$^-$ strains during nutrient limitation	p	-not completely abolished in *rpoS*$^-$ mutant		
mglA	-encodes β-methyl-galactoside transporter	45-47	-negatively regulated by σ^s and Fis -expressed at mid-log phase		
ompF	-membrane porin protein	21.2*	-negatively regulated by σ^s and *micF*-encoding anitsense RNA -regulated by EnvZ and OmpR	-induced by low osmolarity, low temperature, poor carbon sources	
osmB	-outer membrane lipoprotein -mutants do not form aggregates in elevated medium osmolarity	28.9*	-biphasic expression in high media osmolarity	-osmotically inducible	-P1 & P2 osmotically inducible but more transcripts originate from P2
osmY (csi-5)	-encodes periplasmic protein	99.3	-transient expression -negatively regulated by cAMP, LRP, IHF	-osmotically inducible	-σ^{70} consensus for -10, not for -35 region

Gene	Function/phenotype	Map (min)	Mechanism of Regulation/ Additional Regulators	Environmental Inducers	Promoter
otsBA	-encodes trehalose -involved in osmoprotection and thermoprotection	42		-osmotically inducible	
pbp6	-encodes carboxypeptidase -involved in septum formation -confers coccobacillary shapes		-regulated indirectly by σ^s through *bolA*		
pbp3	-involved in cell division (septum formation)		-slight positive regulation by σ^s		
poxB	-encodes pyruvate oxidase which produces free acetate		-highly dependent on σ^s -minimal effects with cAMP	-decreased expression under anaerobic conditions	
proP	-encodes transporter of proline and glycine betaine -involved in osmoprotection	94	-positively regulated by Fis (50-fold) -negatively regulated by cAMP	-osmotically inducible	-P1 osmotically inducible -P2 transcribed by σ^s and Fis -P2 osmotically and growth-phase induced
sdhA	-encodes succinate dehydrogenase, a component of the TCA cycle	16	-negatively regulated by σ^s, Fis, Fnr, ArcA -expressed at mid-log phase		
spvRA BCD	-confers virulence in *Salmonella* sp. -mutants are non-pathogenic	p		-stationary phase induced	
stiABC	-multiple-nutrient starvation-inducible genes of *Salmonella typhimurium* -required for survivial during combined C, N, P starvation		-*stiA*, *stiC* positively regulated by σ^s -*stiB* negatively regulated by σ^s	-induced during starvation for carbon, nitrogen or phosphorus	
treA	-encodes trehalase which functions to hydrolyse trehalose extracellularly	26		-osmotically inducible	
xthA	-encodes exonuclease III -confers NUV resistance -mutants are sensitive to NUV	38	-induction begins in exponential phase -levels decrease in stationary phase	-NUV inducible	-similar to *katE* promoter
xylF	-encodes D-xylose-binding protein	80	-negatively regulated by σ^s and Fis		

Unless otherwise stated, genes and/or operons are positively regulated by σ^s.
"p" represent genes encoded on plasmids.
Astericks represent map locations obtained from the *Escherichia coli* databank. All other map locations are collected from the literature.

Figure 1. Chromosomal locations of members of the σ^s-regulon. Black dots represent 5 minute intervals of the *E. coli* map. The genes *cfa*, *csgBA*, *pbp6*, *pbp3*, and *poxB* were omitted from the map since their general locations were not available in the literature and the *E. coli* databases. Plasmid encoded genes, *spvRABCD*, *mccC7*, and the *Salmonella stiABC* genes are also not included. The figure is modified and updated from previous literature (Hengge-Aronis, 1993).

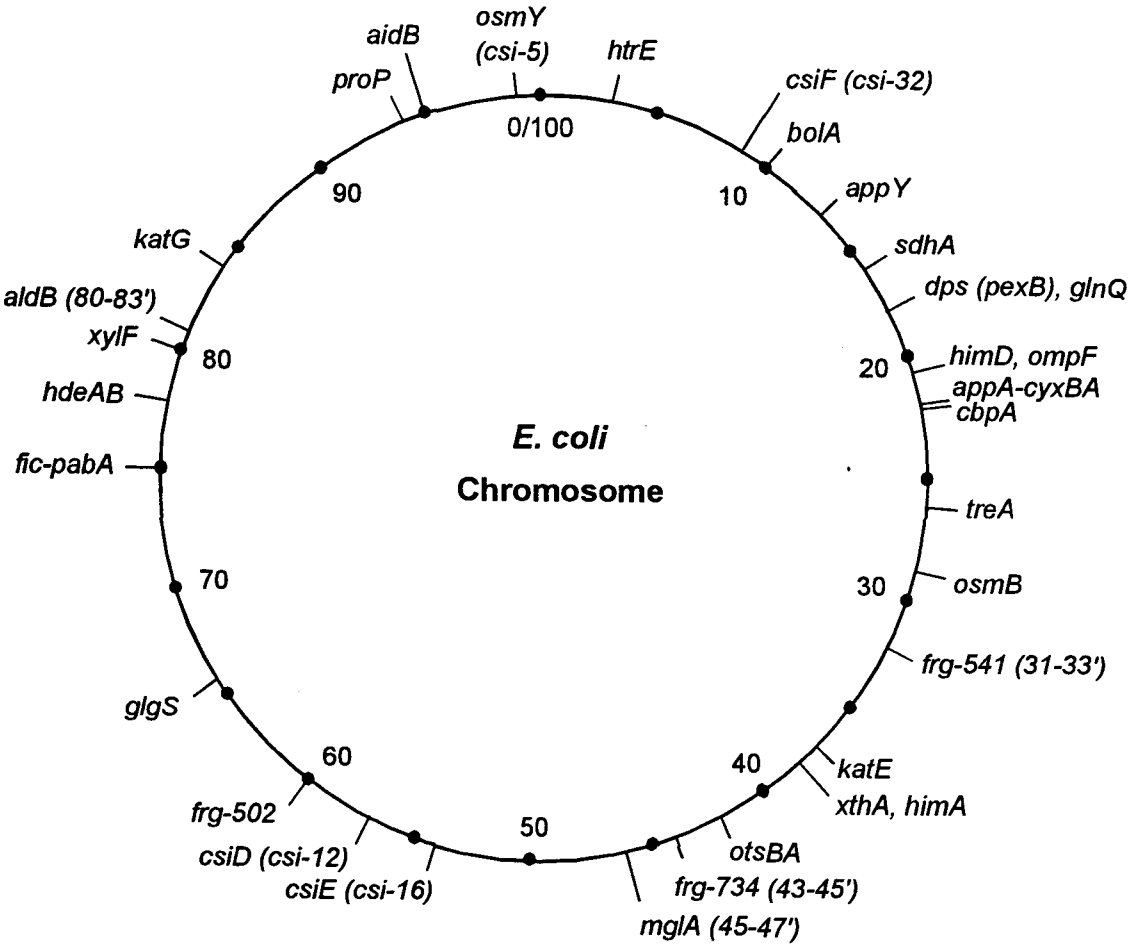
E. coli
Chromosome
0/100
10
20
30
40
50
60
70
80
90
osmY
(csi-5)
htrE
csiF (csi-32)
bolA
appY
sdhA
dps (pexB), glnQ
himD, ompF
appA-cyxBA
cbpA
treA
osmB
frg-541 (31-33')
katE
xthA, himA
otsBA
frg-734 (43-45')
mglA (45-47')
csiE (csi-16)
csiD (csi-12)
frg-502
glgS
fic-pabA
hdeAB
aldB (80-83')
xylF
katG
proP
aidB

MATERIAL AND METHODS

Chemicals. All chemicals were supplied by either Fisher Scientific Ltd. (Toronto, On., Canada), Sigma Chemical Co. (St. Louis, Mo, USA), or Gibco BRL (Burlington, On., Canada). Antibiotics and other non-autoclavable stock solutions were filter sterilized using Gelman Sciences (Ann Arbor, MI, USA) "Acrodisc" sterile filters, pore size 0.45 µm.

Media. Liquid and solid media used were prepared as previously described (Miller, 1992) with modifications. Cultures were grown in Luria-Bertani (LB) rich media (10 g tryptone, 5 g yeast extract, and 10 g NaCl per liter) and adjusted to pH 7.0. Solid media was prepared by adding 15 g of agar per liter to liquid media. Minimal media used was M9 containing per liter, 6 g Na_2HPO_4 (sodium phosphate, dibasic) 3 g KH_2PO_4 (potassium phosphate, monobasic) 1 g NH_4Cl (ammonium chloride), 0.5 g NaCl; 0.2 mM $CaCl_2$, 1 mM $MgSO_4$ and 0.4% glucose (added after autoclaving). R-plates, used for the propagation of P1 phage, contained per liter, 10 g tryptone, 1 g of yeast extract, 8 g of NaCl, 15 g of agar, 2 mM of $CaCl_2$ and 0.1% glucose (added after autoclaving). R-top agar contained per liter, 8 g of agar as opposed to the 15 g in R-plates. The concentrations of antibiotics used were as follows, kanamycin (50 µg/ml), streptomycin (50 µg/ml), tetracycline (12.5 µg/ml), ampicillin (100 µg/ml). X-gal (5-bromo-4-chloro-3-indolyl-β-D-galactoside) was used at a concentration of 50 µg/ml.

Bacterial strains, phage, plasmid. The bacterial strains, plasmids and λ phage constructs are listed in Table 2.

Growth conditions. Cultures were grown overnight in LB media containing appropriate antibiotics on a shaker bed (Gyrotory shaker-model G2, New Brunswick Scientific Co. Inc., Edison, NJ, USA) or in test tubes on a rotator (Rollordrum, model-TC7, New Brunswick Scientific Co., Edison, NJ, USA). Cell growth was monitored spectrophotometrically (UV-VIS Spectrophotometer, model UV-

Table 2. *E. coli* strains and plasmids.

Strains	Genotype	Source/Reference
A) Strains		
MC4100	*Δ(argF-lacZ)205 araD139 flbB5301 relA1 rpsL150 thi flbB5301 ptsF25*	G. Weinstock
GC4468	*ΔlacU169 rpsL*	D. Touati
K-12	wild-type	B. N. Ames
KL16	Hfr(PO45) *relA1 spoT1 thi-1*	K. B. Low
HS180	Like KL16 but *rpoS*::Tn10	P1(NC122) x tet^R
NC4468	As GC4468 but ϕ(*katE::lacZ*$^+$)131	lab collection
HS143	As GC4468 but ϕ(*katF::lacZ*$^+$)143	lab collection
GC202	As GC4468 but ϕ(*katG*::Tn10)131	lab collection
13C10	As MC4100 except lysogenized with λp*lac*Mu53	lab collection
B) Phage		
λp*lac*Mu53	*imm*^{λ}*'trp'lacZ+lacY+lacA"uvrD" Xho::kan* Mu c/ts62 ner + A + 'S	G. Weinstock
λpMu507	c/ ts857 Sam7 Mu c/ts62*ner*+A+B+	G. Weinstock
C) Plasmids		
pMM*katF3*	carries *rpoS* (*katF*)	P. Loewen

1201, Shimadzu Corporation, Kyoto, Japan) at 600 nm.

Bacterial mating. Hfr-mediated bacterial mating was performed as previously described (Miller, 1992). Both donor and recipient strains were grown overnight in LB containing appropriate antibiotics and subcultured the next morning into fresh LB (without antibiotics). Cultures were grown to a cell density between OD(600 nm) of 0.2 to 0.3. Donor cultures were aerated on a rotator or shaker bed at 37°C and the recipient cultures were not aerated. An equal volume of donor and recipients were mixed in a test tube and incubated at 37°C for 30 min. The mating was interrupted by vortexing for 10 s and a 100 µl aliquot spread onto LB-agar containing the appropriate antibiotics for the selection of transconjugants.

β-galactosidase assay. β-galactosidase activity was assayed in duplicate as described previously (Miller, 1992). Aliquots from a culture were transferred in duplicate to 2 ml microtubes containing Z-buffer (the assay medium). For cells predicted to have high levels of enzyme activity, 100 µl of the culture was added to 900 µl of Z-buffer. For samples possessing low β-galactosidase activity, 500 µl of both culture and Z-buffer was added to the microtube. OD(600 nm) was taken for each sample assayed. Two drops of chloroform (100 µl) and one drop of 0.1% SDS (sodium-dodecyl-sulfate) were added and vortexed vigorously for 10 s to disrupt cells. Tubes were prewarmed in a 28°C water bath. An aliquot of 200 µl of ONPG (*o*-nitrophenyl-β-D-galactoside, in 100 mM phosphate buffer, pH 7.0, stock concentration of 4 mg/ml) was added and the tubes gently shaken. The reaction was stopped by the addition of 500 µl of a 1 M Na_2CO_3 solution. Microtubes were centrifuged (10 000 rpm, 10 min) and the absorbance measured at OD(420 nm). Units of activity was calculated as [1000 x OD_{420}] / [time (min) x volume (ml) x OD_{600}]. Activity was expressed in Miller units (Miller, 1992).

Transformation. Transformation was performed using the TSS (transformation and storage solution) method of preparing competent cells (Chung *et al.*, 1989). TSS consists of LB broth containing 10% (wt/vol) polyethylene glycol (PEG, m.wt. 8000), 50 mM $MgSO_4$, and 5% (vol/vol) dimethyl sulfoxide (DMSO), adjusted to pH 6.5. DMSO was added after autoclaving (20 min, 15 kPa, 121°C). For the preparation of competent cells, the TSS solution and empty tubes were pre-

cooled on ice. Two different approaches were used. Cultures were grown in LB broth (5 ml) to mid-exponential phase (OD600 nm 0.3-0.4). Bacterial cells were pelleted by centrifugation (3500 rpm, 15 min, 4°C) and resuspended in 500 µl of 1xTSS. The second approach did not require the centrifugation procedure. An aliquot of 250 µl of the bacteria culture was directly added to an equal volume of 2xTSS. An aliquot of 100 µl of cells of 1xTSS or 2xTSS was transferred to cold polypropylene tubes, mixed with a 1 µl volume of 6.6 ng/µl of pMM*katF3* and left on ice (30 min, 4°C). LB broth containing 20 mM glucose was added to cells to a final volume of 1 ml. Tubes were incubated (37°C, with shaking at 200 rpm, 1 h) to allow expression of the plasmid-borne ampicillin resistance gene. A 100 µl aliquot was plated onto LB-agar plates and incubated overnight at 37°C. For the selection of *rpoS*$^+$ recipients transformed with the plasmid, LB-agar plates containing kanamycin, streptomycin, and ampicillin were used. Transformed *rpoS*$^-$ transconjugants were selected on the same media supplemented with tetracycline.

Transformation efficiency using TSS (Chung *et al.*, 1989) was reported to be between 10^8 and 10^7 transformants/µg DNA. Although our frequencies were not as high, TSS was a simple and quick method that produced enough transformants for our purposes. Given that approximately 50 transformants on average appeared using 6.6 ng of plasmid DNA, the transformation efficiency was calculated to be approximately 7.6×10^3 transformants per µg of plasmid DNA.

Preparation of P1 lysate, titering and transduction. Preparation of lysates, titering of lysate and transduction procedures were followed as previously documented (Miller, 1992) with some modifications.

Preparation of P1 lysate. An overnight culture of the donor strain was subcultured into LB media containing 5 mM $CaCl_2$ and grown to a density of 1×10^8 cells/ml. One ml of the bacterial culture was incubated with 10 µl of a P1 lysate (greater than 10^8 PFU [plaque forming units] /ml) in a glass tube in a water bath (37°C, 20 min) to allow adsorption of the phage. Modified R-top agar (2.5 ml) containing 4 g of agar per liter and an additional 5 mM of $CaCl_2$ (as opposed to 8 g and 2 mM $CaCl_2$, as specified in Miller) was added to the test tube, vortexed, and poured onto R-plates (containing 5 mM $CaCl_2$). Plates were incubated face-up for 5 h, after which 1 ml of MC buffer (100

mM $MgSO_4$, 5 mM $CaCl_2$) was spread onto the surface. We found that decreasing the amount of agar (allowing more diffusion of phage into the surrounding media) and adding MC buffer onto the plates before harvesting (allowing for the diffusion of phage into liquid media) increased the yield of total number of PFU's. Plates were incubated for an additional 3 h. To prevent the growth of resistant bacteria, P1 lysates were harvested after 8 h. R-top agar was scraped into 15 ml polypropylene tubes, 100 µl of chloroform added, vortexed for 30 s and cellular debris centrifuged (3500 rpm, 4°C, 15 min). The supernatant containing lysates were transferred to 2 ml cryogenic tubes and stored at 4°C over 100 µl of chloroform.

Titering of lysate. P1 lysates were titered on overnight cultures of CSH109 grown in LB media containing 5 mM $CaCl_2$. Serial dilutions were made of the phage lysate in MC buffer (100 mM $MgSO_4$, 5 mM $CaCl_2$). An aliquot of 100 µl from at least two dilution series was added to 100 µl of the overnight bacterial culture and incubated (37°C, 20 min) to allow adsorption of the phage. R-top agar (2-3 ml) was added, poured on R-plates, and incubated overnight at 37°C. An aliquot of 100 µl of the bacterial culture was plated simultaneously to allow comparison with plates containing P1 plaques. Plaques were counted the following morning. Titers obtained on average was between 10^8 and 10^{10}. Lysates with titers more than 10^8 PFU/ml were used for transduction.

Transduction with P1 lysate. An overnight culture of the bacterial strain to be transduced was centrifuged and resuspended in the same volume of MC buffer. An aliquot of 100 µl of bacteria (with 10^{10} CFU [colony forming units] /ml) was added to an equal volume of P1 lysate (at least 10^8 PFU/ml). The bacterial strain to be transduced was incubated in parallel to serve as controls for revertants. P1 lysates were also incubated to ensure no contamination with strains capable of growing under the same conditions as the transductants. Tubes were incubated (37°C, 20 min) after which 200 µl of 100 mM citrate buffer (9.6 g of citric acid, 4.4 g of NaOH or 14.69 g of sodium citrate salt per 500 ml of ddH_2O; adjusted to pH 5.5 with 10 N NaOH, autoclaved). Citrate buffer inhibits readsorption of the phage to bacteria by chelating with Ca^{2+}, reducing bacterial killing by virulent phage (Miller, 1992). For the selection of the tet^R marker, (in the construction of HS180), 100 µl of the lysate-citrate buffer mix was plated directly onto LB media containing tetracycline. For

the selection of the kan^R marker (when σ^s-dependent *lacZ* fusions were transduced into a new background), the lysate-citrate buffer mix was incubated at 37°C for an additional hour to allow expression of the marker before plating onto LB-kanamycin plates.

Bacterial conjugation using Hfr-mediated transfer. Bacterial conjugation is a mechanism of DNA transfer from a donor to a recipient cell that involves cell-to-cell contact (reviewed in Willetts and Skurray, 1987). The best known example of genetic transfer is the F-mediated process in *E. coli*. F is a small circular plasmid (94.5 kb) that can replicate autonomously in the cell or integrate into the host chromosome. Encoded on the F plasmid, a series of genes is involved in its conjugative transfer to neighboring cells that begin at a fixed point in a process similar to the rolling circle replication system of λ phage (reviewed in Furth and Wickner, 1983). Cell-to-cell contact is mediated through sex pili, threadlike structures present on the donor in numbers of 2-3 per cell. Single-stranded DNA from the F plasmid is transferred through the pili that enters the recipient through a pore in the cell membrane in the 5' to 3' direction. The replication system of both the donor and recipient synthesizes the second strand completing the conjugation process (reviewed in Willetts and Skurray, 1987).

When the F plasmid integrates into the host chromosome, it retains its conjugative abilities and allows the transfer of host chromosomal markers into the recipient (Miller, 1992). Purification of this recombinant results in the generation of a population of cells capable of transferring host genetic markers into a recipient in at a high frequency, thus the designation of Hfr for "high frequency of recombination." Each Hfr generated will begin the conjugation process at a specific point in the circular chromosome (depending on the point of integration into the host) and DNA transfer will continue at a fixed order. A collection of Hfr's (with points of transfer at different locations in the *E. coli* chromosome) have been generated and are used extensively for transferring genes from one strain to another. Overall, host chromosomal markers closer to the point of integration will be transferred at a higher frequency than more distally located markers (Miller, 1992). We have employed the use of Hfr KL16 for the transfer of the *rpoS*::Tn10 mutation into F^-

Figure 2. Schematic representation of transcriptional and translational *lacZ* gene fusions to Gene X. (A) A translational fusion is created when the promoterless *lacZ* gene is expressed from the exogenous promoter (Px). Since the *lacZ* gene does not contain its own Shine-Dalgarno sequence (represented by a black circle), expression of the protein product is dependent on the translational machinery of the target gene, resulting in a hybrid mRNA and hybrid protein. (B) A transcriptional (operon) fusion is created when a promoterless *lacZ* gene, containing its own Shine-Dalgarno sequence (black circle) is fused in frame to a target gene. Two protein products are produced, a protein from Gene X that may be functional or non-functional, and a functional β-galactosidase protein.

A Translational Fusion

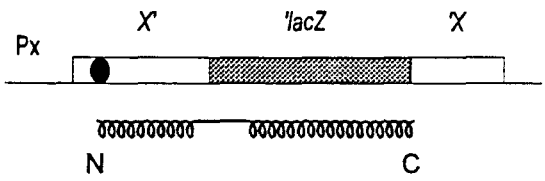

B Transcriptional Fusion

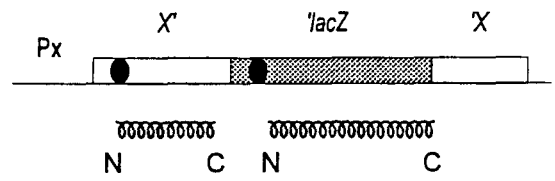

recipient strains. DNA transfer for KL16 initiates at approximately 62' on the *E. coli* chromosome and transfer continues in a counterclockwise direction.

Thus, the *rpoS*::Tn10 mutation is introduced shortly after mating.

Construction of HS180. The phenotypic screen for *rpoS* was based on the dependence of the *katE* gene on σ^s expression. *E. coli* colonies evolve gas bubbles when flooded with hydrogen peroxide due to the activity of catalase HPII. Catalases break down hydrogen peroxide to water and oxygen, thus cells mutated in HPII activity do not evolve oxygen. Since HPII, encoded by *katE* is largely σ^s-dependent, and since a mutation in *rpoS* results in reduced *katE* expression, the presence of *rpoS* was detected by testing for catalase activity. The *rpoS13*::Tn10 mutation (provided by P. Loewen) was introduced into Hfr KL16 from NC122 (*rpoS13*::Tn10; *katE*::*lacZ*) by P1-mediated transduction. Transductants were selected on media containing tetracycline. Transductant colonies were flooded with 30% hydrogen peroxide to determine if the *rpoS13*::Tn10 mutation was transduced successfully. The strain was designated HS180 and is catalase negative. Hfr transfer capabilities of the *rpoS*::Tn10 construct in HS180 was tested on control strains, NC4468 (*katE*::*lacZ*) and MC4100 (wt, *lac*$^-$). A time-dependent mating (0, 5, 10, 20, 30, 60, 120 min) was performed to determine the optimal time of incubation required for null allele transfer. Since KL16 begins chromosomal transfer approximately 61 min and *rpoS* is located at 59 min, transfer of the Tn10 construct was observed to be very efficient. Transconjugants were obtained as early as 1 to 5 min and no changes were seen at subsequent incubation time points past 10 min. The incubation period for transfer of the *rpoS* null allele was 15 min. All transconjugants, as expected, were catalase negative. The transconjugant of NC4468 also showed reduced β-galactosidase activity as predicted.

Gene Regulation using *lacZ* fusions, and the λp*lac*Mu system. Fusion of promoterless *lacZ* to bacterial promoters provides a useful tool for studying the regulatory mechanisms of gene expression. The *lac* operon can be fused to a target promoter in two different ways. Transcriptional (operon) fusions are constructs in which a promoterless *lacZ* gene, containing its own translational

Figure 3. The λp*lac*Mu53 system for creating transcriptional *lacZ* fusions. (A) Mature λp*lac*Mu53 phage. Mu S and c ends are represented as black boxes. Bacterial DNA is represented by a wavy line, λ sequences by a thin line and *lac* genes by stripped boxes. When λp*lac*Mu53 (A) enters the bacterial cell, it circularizes (B) and inserts into the correct orientation and reading frame of target Gene X (represented by a thick line) creating a transcriptional fusion (C). *lacZ* is expressed from the promoter, Px. The *kan* gene (stippled box) serves as a selectable marker, conferring kanamycin resistance to the bacterial cell when expressed from Px. (Figure is adapted from Bremer *et al.*, 1984.)

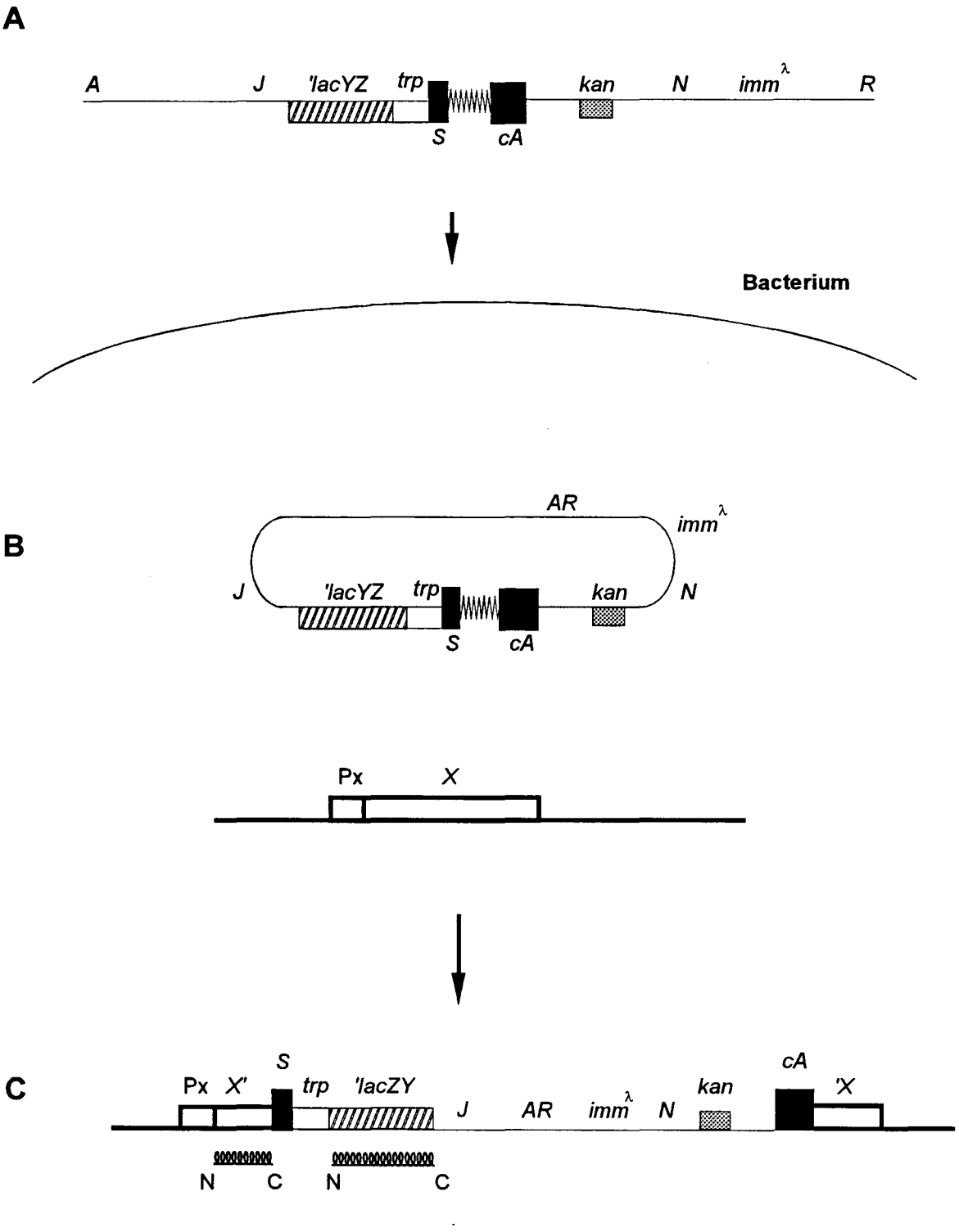
A
A
J
'lacYZ
trp
S
cA
kan
N
imm λ
R
Bacterium
B
AR
imm λ
J
'lacYZ
trp
S
cA
kan
N
Px
X
C
S
Px
X'
trp
'lacZY
J
AR
imm λ
N
kan
cA
'X
N
C
N
C

start site, is fused to the open reading frame of the target gene. Expression from the *lacZ* gene becomes dependent on the proximal promoter, and the level of expression is a proportional measure of the target gene's transcriptional activity. Two protein products result from transcriptional fusions. The truncated target gene product can be either functional or nonfunctional depending on where the *lacZ* construct is fused (near the 5' end of the reading frame or the 3' end). The second protein product is the functional β-galactosidase protein, encoded by the *lacZ* gene (Figure 2B). The second type of fusion is translational (protein) fusions, constructs in which *lacZ*, lacking both its transcriptional and translational initiation signals, is fused in frame to the coding region of a target gene. Expression of the *lacZ* gene is a direct measure of the proximal transcriptional and translational signals. The result is a hybrid protein where the N-terminus of the target gene is fused to the enzymatically active β-galactosidase (Figure 2A).

Although several mechanisms have been previously employed, we have used the λp*lac*Mu system for generating *lacZ* fusions into target genes. λp*lac*Mu, a plaque-forming *lac*$^-$ phage hybrid, is capable of creating transcriptional (Bremer *et al.*, 1985) and translational fusions (Bremer *et al.*, 1984) in a single step. The λ phage is flanked by the Mu attachment sites, 117 bp from the Mu *S* end (Casadaban and Chou, 1984) and approximately 2.8 kb from the Mu *c* end (Leathers *et al.*, 1979). These attachment sites allow λp*lac*Mu, the *recA*-independent transposition properties characteristic of Mu bacteriophage, provided that the MuA and B genes are present. The MuA and B genes are required for Mu transposition (Toussaint and Resibois, 1983) and are carried on a helper phage that is coinfected with the *lacZ* fusion generating phage. Insertion of the λp*lac*Mu into the bacterial chromosome by the Mu transposition mechanism simultaneously generates *lacZ* fusions to the target gene. Since Mu transposition is generally nonspecific, *lacZ* fusions to any part of the chromosome can be created. λp*lac*Mu is temperature resistant and stable, having a transposition frequency of approximately 10^{-8}/CFU as opposed to 10^{-5}/CFU for its predecessor, MudII301(Ap *lac*), in the absence of the helper phage (Bremer *et al.*, 1985). It may be noted that *lacZ* fusion studies use *lac*$^-$ host strains so the appearance of *lac*$^+$ colonies is the result of correct insertion of the *lacZ* containing vehicle.

When mature λp*lac*Mu is introduced into the bacterial cell, it circularizes and inserts into the bacterial chromosome. If insertion occurs in the correct reading frame and orientation, the *lacZ* gene will be expressed by the proximal promoter. In this work, we have screened a library of MC4100 *lacZ* operon fusion mutants created by λp*lac*Mu53 (a derivative containing a kanamycin marker) and λpMu507 (helper phage) for σ^s-dependency (Figure 3).

Insertion of the *rpoS*::Tn10 into F⁻ recipients. Five thousand independent transcriptional *lacZ* mutants were picked and stored in microtiter wells containing 200 µl of LB broth and 15% glycerol (-80°C) (Schellhorn and Stones, 1992). These frozen library stocks were slightly thawed and replica-plated into microtiter plates containing fresh LB media supplemented with kanamycin and streptomycin and grown overnight without shaking at 37°C. Cultures were replica-plated into fresh media (without antibiotics) in microtiter plates the next day and grown to an OD(600 nm) of 0.2 on a shaker bed at 200 rpm. An overnight culture of HS180 in LB with tetracycline was grown in parallel and subcultured the next morning into fresh LB (without antibiotics). For bacterial mating, 100 µl of HS180 was inoculated directly into each microtiter well and incubated (37°C, 30 min). Cells were then replica-plated onto media containing kanamycin, streptomycin, tetracycline and X-gal for the selection of *rpoS*::Tn10 transconjugants only. Since transfer of HS180 begins at approximately 62 min in a clockwise direction, there was a possibility that the *lacZ*⁺ gene (located at 8 min on the *E. coli* chromosome) from HS180 could be transferred into the *lacZ* recipient strains. This would not normally be a concern using standard mating procedures since conjugation is interrupted by vortexing. However, the likelihood of conjugal transfer continuing for 50 min is low since conjugal pairs are naturally disrupted over time. This was tested by mating 18 clones of MC4100 with HS180 in microtiter wells. Conjugal transfer was allowed to proceed for 2 h, and without vortexing, cultures were replica-plated onto media selecting for transconjugants. None of the transconjugants received the *lacZ*⁺ allele from the donor strain. Colonies were flooded with 30% hydrogen peroxide to test for the inactivation of *rpoS* in the transconjugant.

Figure 4. UV induction of the λ prophage. (A) From Figure 3C, the λ prophage. Upon UV induction (B), a variable number of target gene base pairs from either side of the Mu sequences are excised and the ends recircularized. (C) A thick arrow represents the primer constructed for the Mu c end and direction of primer extension. Thin opposing arrows represent the 48 bp inverted sequences of the Mu S end. The 5'--AATACA--3' sequence of the Mu c end was used as a marker to confirm the beginning of the target gene sequences when sequencing the fusion junctions. (Figure is adapted from Roy *et al.*, 1985.)

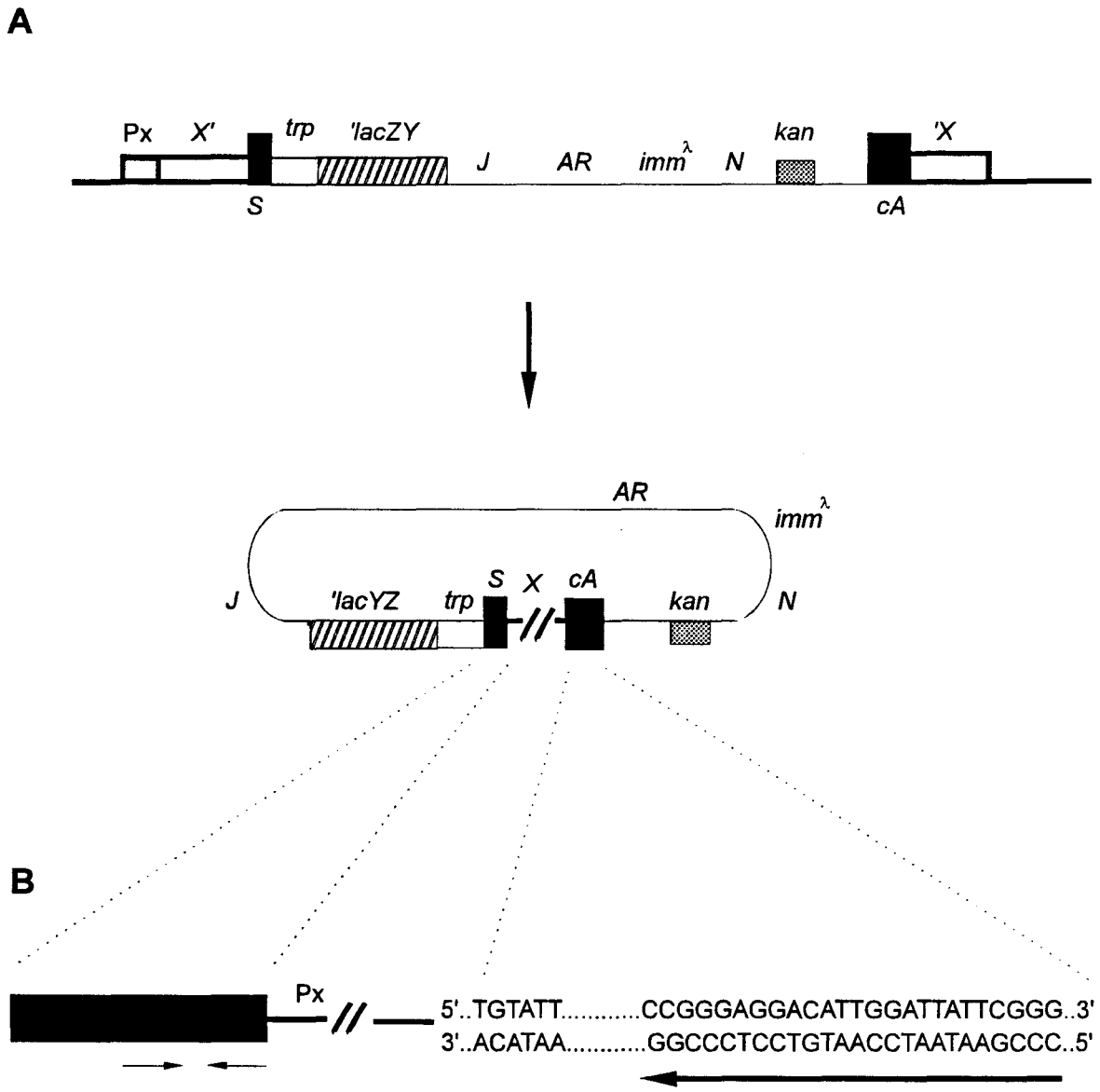
A
Px
X'
trp
'lacZY
J
AR
imm λ
N
kan
'X
S
cA
AR
imm λ
J
'lacYZ
trp
S
X
cA
kan
N
B
Px
5'..TGTATT.....CCGGGAGGACATTGGATTATTCGGG..3'
3'..ACATAA.....GGCCCTCCTGTAACCTAATAAGCCC..5'

Identification of σ^s-dependent *lacZ* fusion promoters. Excision of the wild-type λ prophage by UV induction occurs by inactivation of the repressor of λ lytic functions encoded by the *cI* gene. This inactivation is indirect since it is dependent upon the bacterial *recA* gene, which, in an irradiated cell, cleaves the λ repressor and destroys its ability to bind to the operators. As a result, repression of the prophage is lost and lytic growth begins (Hendrix, 1983). This involves excision from the host chromosome, replication of DNA and the production of phage progeny followed by cell lysis.

UV excision of the λp*lac*Mu prophage occurs by the same method as wild-type λ prophage. An illegitimate recombination event at variable endpoints takes place, resulting in the recircularization of the phage with a variable length of insert DNA from the target gene attached to the Mu ends (Bremer *et al.*, 1984). Although the size of proximal DNA excised is not known, UV induced λp*lac*Mu can carry entire genes (Bremer *et al.*, 1984). The number of base pairs excised are also dependent on the packaging of the λ head, allowing for the isolation of specialized transducing phages using the λp*lac*Mu system (Bremer *et al.*, 1984). We used this property for the identification of σ^s-dependent genes by constructing primers to the Mu *c* end, and sequencing the fusion junctions as described previously (Roy *et al.*, 1995). We have not obtained primers for the Mu S end due to a 48 bp inverted repeat preventing efficient primer extension (Roy *et al.*, 1985). A diagrammatic representation of the mechanism of UV induction is seen in Figure 4.

Isolation of λ DNA. Isolation of λ DNA and sequencing of the fusion junction was performed as previously described with some modifications (Sambrook, 1989).

Preparation of λ lysates. Cultures were incubated overnight in 3 ml LB media containing kanamycin and streptomycin. Cells were subcultured the next morning into 50 ml of fresh LB (no antibiotics) at 1/10 dilution and grown to an OD (600 nm) of 0.5. Cultures were transferred into 200 ml polypropylene bottles, centrifuged (5000 rpm, 20 min, 4°C), and resuspended in 10 ml of 10 mM $MgSO_4$. Cultures were evenly distributed in large Petri dishes (150 x 15 mm) and irradiated (under two 15 W germicidal bulbs, 50 cm distance, 7 s, 31 J/m^2 total fluence, covers off) (Roy *et al.*, 1995). Following irradiation, 5 ml 3xLL broth (containing per liter, 90 g tryptone, 45 g yeast extract, 45 g NaCl, 60 mg of adenine, cytosine, guanine, thymine, adjusted to pH 7.25) was added. Irradiated

cultures were incubated with vigorous shaking (37°C, 3-5 hours or until cell lysis, 200 rpm). Lysed cultures were transferred to 100 ml polypropylene tubes, vortexed for 30 s with a few drops of chloroform to lyse the remainder of cells and centrifuged (5 000 rpm, 20 min) to get rid of cellular debris. Supernates were then transferred to 30 ml Corex tubes and recentrifuged (10 000 rpm, 20 min). The supernatants were titered and the average sample was calculated to be between 10^5 to 10^6 PFU/ml.

Isolation of λ phage. The isolation of phage particles was done using two methods, (I) pelleting phage by ultracentrifugation (35 000 rpm, 30 min, using a Beckman SW41Ti rotor) as previously described (Roy *et al.*, 1995) or (ii) polyethylene glycol (PEG) precipitation (working concentration 10% PEG [m.wt. 8000]; 1 M NaCl) as described in Sambrook. PEG was added to supernatants, mixed by inversion, and allowed to equilibrate on ice for 30 min. The PEG-phage suspension was centrifuged (13 000 rpm, 20 min) leaving a white precipitate on the bottom of the tube. Supernatants were discarded and phage pellets gently washed with distilled deionized water (ddH_2O)and resuspended in 400 µl of 10 mM $MgSO_4$. Mg^{2+} is required for maintaining the structural integrity of the phage head and is recommended to be present when working with, and storing λ phage (Arber *et al.*, 1983). RNase was added at a concentration of 5 µg/ml and incubated in a water bath (37°C, at least 1 h) to degrade bacterial RNA.

Isolation of λ DNA. Standard phenol-chloroform methods were used for the isolation of λ DNA as described (Sambrook). Due to its large size (approximately 50 kb), precautionary measures were taken to prevent its shearing. Microtubes were gently rocked to mix solvents, not vortexed. Tips of pipet tips were removed to prevent shearing and to reduce excessive suction of protein debris separated by the phenol layer. Samples were kept at 4°C and never frozen. An equal volume of Tris-HCl-equilibrated phenol (pH>8.0) was added to the resuspended lysate and gently rocked to digest the phage coat proteins. The sample was centrifuged (13 000 rpm, 5 min) and the top aqueous layer transferred to a new microtube, leaving the protein debris on the surface of the phenol phase undisturbed. Additional drops of 10 mm $MgSO_4$ was added to the phenol and the procedure repeated. This was done to retrieve as much λ DNA remaining in the aqueous layer. A

second extraction was done using an equal volume of phenol-chloroform (24:1 ratio of chloroform and isoamyl alcohol) followed by an equal volume of chloroform to remove trace amounts of phenol. Precipitation of DNA was done using 100 µl of ammonium acetate (7.5 M; pH 6.5) and 2x volume of ice-cold absolute ethanol (Grossberger, 1987). The microtube was kept at -80°C for 1 h, and the DNA pelleted (13 000 rpm, 20 min). Pellets were washed twice with 70% ethanol, dried and resuspended in 40 µl ddH_2O.

λ DNA was visualized on 0.6% agarose gel in electrophoresis buffer, TBE (0.5 x: 0.045 M Tris-borate, 0.001 M EDTA) and stained with 0.5 µg/ml ethydium bromide. A sample from a purified λ DNA stock (0.25 µg per run), served as a control. Visualizing the λ DNA on gel was necessary since we have experienced constant problems with the presence of excessive amounts of RNA that the RNase digestion procedure could not eliminate. Quantification of DNA and sample purity was measured spectrophotometrically. Readings were taken at OD(260 nm) to measure nucleic acid. Calculation of DNA concentration was performed, assuming an OD(260 nm) of 1.0 corresponding to 50 µl/ml for double-stranded DNA (Sambrook, 1989). An estimate of the purity of nucleic acid was determined by taking the ratio of readings at OD(260 nm) (nucleic acid) over OD(280 nm) (protein). Acceptable parameters of the 260 nm / 280 nm ratio is between $1.8<x<2.0$. Contamination with protein or phenol resulted in values significantly less than 1.8. (Sambrook, 1989). An example of the calculation of DNA concentration is as follows:

$$\frac{50\ \mu g\ /\ DNA}{OD(260\ nm)\ 1.0} = \frac{x\ \mu g\ /\ DNA}{OD(260\ nm)\ 0.0526}$$

x = 2.63 µg x 1000-fold dilution
= 2630 µg in 1000 µl

$$\frac{2630\ \mu g}{1000\ \mu l} = \frac{x\ \mu g}{40\ \mu l\ ddH_2O}$$

x = 105 µg in 40 µl of ddH_2O
therefore, DNA concentration = 105 µg/40 µl = 2.63 µg/µl

Sequencing of the fusion junction. Sequencing of the fusion junction was performed by automatic

sequencer (Applied Biosystems Automatic Sequencer), and manually, using the Perkin Elmer Amplicycle, CS' sequencing kit (Roche Molecular Systems, Branchburg, NJ, USA) as specified by the manufacturer. DNA synthesis was primed using a Mu c end primer (5'-CCCGAATAATCCATGTCCTCCCGG-3') (Roy *et al.*, 1985) 5' end-labelled with [α-^{35}S]dATP (1000 Ci/mmol). Cycle sequencing was performed in 25 cycles: 95°C, 30 s; 65°C, 30 s; 72°C, 60 s using a Techne GeneE thermal cycler with heated lid (Techne Incorporated, Princeton, NJ). Approximately 1-2 µg of DNA was sequenced directly.

Screening for *rpoS*-associated phenotypes.

Apart from sequences obtained from the fusion junctions, phenotypic screening of the recipient *lacZ* fusion strains were done as a general method to identify mutants that exhibit a known *rpoS*-associated phenotype. For replica-plate screenings, three clones of each σ^s-dependent *lacZ* fusions transduced into a new GC4468 background were inoculated into microtiter wells containing LB, kanamycin and streptomycin. Cultures were replica-plated onto plates containing several known inducers of putative σ^s-dependent genes, such as in NaCl and acetate, which is known to induce *katE* (Schellhorn and Stones, 1992), and under conditions in which *rpoS* mutants are known to be sensitive.

Starvation induction. Cells were replica-plated onto M9 minimal plates containing 0.4% glucose (non-starved conditions) and 0.04% glucose (starvation conditions). Plates were supplemented with streptomycin and X-gal and incubated overnight at 37°C. Strain HS143 (*rpoS*::Tn10) was used as a positive control for starvation induction. GC4468 was used to monitor growth under both starved and non-starved conditions. No appropriate negative control was available.

Acetate induction. Cells were replica-plated onto M9 media (plus 0.4% glucose) containing 25 mM, 50 mM and 75 mM of acetate supplemented with streptomycin, X-gal and 0.4% glucose. Plates were incubated overnight at 37°C. NC4468 and HS143 were used as positive controls. No appropriate negative controls were used and GC4468 was used to compare growth patterns.

NaCl induction. Cells were replica-plated onto M9 media (plus 0.4% glucose) containing

streptomycin, X-gal and increasing amounts of NaCl. Concentrations used were 250 mM, 500 mM and 750 mM. One set of control plates contained no NaCl, and another contained the regular requirement of NaCl in M9 minimal media (8.6 mM NaCl or 0.5 g per liter). Plates were incubated overnight at 37°C. NC4468 was use as a positive control and HS143 as a negative control (Schellhorn, unpublished results). GC4468 served as a control to compare growth patterns.

Hydrogen peroxide sensitivity. Cells were replica-plated onto LB media containing 0.6 mM and 1.0 mM of hydrogen peroxide. Plates were incubated at 37°C overnight along with a set of control LB plates containing no hydrogen peroxide. GC202 (*katG*::Tn10), which is known to be sensitive, served as a positive control and GC4468 (wild-type) as a negative control.

Screening for the survival deficient phenotype. Methods were followed as previously described to identify mutants incapable of surviving prolonged periods in starvation (Tormo *et al.*, 1990). For the preliminary screening of all 105 strains in GC4468 background, each mutant was inoculated into 3 ml LB media supplemented with kanamycin and streptomycin in test tubes for long term incubation. Cultures were kept aerated at 37°C on a wheel at 60 rotations per min. After 7 days, 10 µl was spread on LB-agar containing the above antibiotics plus X-gal. Strains that exhibited a general decrease in colony counts were selected for dilution studies. Colony counts for the selected strains were obtained for overnight cultures (at 10^{-8} and 10^{-7} dilutions), and compared with values obtained from 7-day-old cultures (at 10^{-6} and 10^{-7} dilutions). HS143 and GC4468 were inoculated during both times as positive and negative controls.

Growth-phase-dependent expression of fusion mutants. Growth-phase expression was determined for all 105 recipient (*rpoS*$^{+}$) and transconjugant (*rpoS*$^{-}$) strains in GC4468 background. For the recipients, overnight cultures grown in LB containing kanamycin and streptomycin were subcultured into LB media the next day (1/500 dilution) and grown to an OD(600 nm) no greater than 0.3. The starting OD(600 nm) was 0.03 at the beginning of the experiment. Duplicate samples were taken for β-galactosidase assay every half-hour for three hours followed by samples every hour for an additional 3 hours, in addition to an overnight sample. The "induction ratio" value was calculated for each as the highest activity in stationary phase divided by the lowest observed in

exponential phase. All mutants exhibited from a two-fold to over 400-fold induction. Since we did not expect growth-phase-dependent expression of the transconjugants, only two time points were taken, one at OD(600 nm) 0.3 (exponential phase) and the second reading at OD(600 nm) 1.5 (stationary phase). Several exhibited a more than five-fold induction ratio during entry into stationary phase, a result not completely unexpected since some σ^s-dependent genes are known to require additional factors for their expression. These were further investigated to determine whether they exhibit growth-phase-induction in the absence of σ^s. Additional time points were performed on these *rpoS* mutants (as for the *rpoS*$^+$ recipients) to determine if this was the case.

RESULTS

ISOLATION OF σ^s-DEPENDENT FUSION MUTANTS.

To identify σ^s-dependent genes in a random transcriptional fusion library, we compared the levels of β-galactosidase expression of the fusions in a *rpoS*$^+$ background and isogenic *rpoS*$^-$ strains. A diagrammatic representation of the screening procedure for the isolation of σ^s-dependent *lacZ* fusions is depicted in Figure 5. Five thousand F$^-$ independent transcriptional *lacZ* fusion mutants were previously generated and stored in microtiter wells (Schellhorn and Stones, 1992). F$^-$ strains were replica-plated onto media containing streptomycin, kanamycin, and X-gal as a control for β-galactosidase comparison. To introduce the *rpoS* null mutation, strain HS180 was mated with F$^-$ recipients in microtiter wells for 30 min and replica-plated onto plates containing the above antibiotics with added tetracycline. To select for the *rpoS*::Tn10 mutation, transfer of the *rpoS* null allele was confirmed by testing the resulting *rpoS*$^-$ transconjugants for catalase activity. Putative σ^s-dependent fusions were identified by comparing the level of β-galactosidase expression of the fusion between *rpoS*$^+$ recipients and *rpoS*$^-$ transconjugants on LB plates containing X-gal. From this preliminary screen, 479 *rpoS*$^-$ transconjugants exhibited reduced levels of β-galactosidase activity compared with the *rpoS*$^+$ recipients. Recipients were streaked out to check for purity and one colony from each retested for σ^s-dependency. A σ^s-dependent *katE*::*lacZ* fusion strain, NC4468, served as a positive control, and a randomly selected σ^s-independent strain, 13C08 was used as a negative control in subsequent mating procedures. Two-hundred and forty strains were selected as presumptive σ^s-dependent strains after the second mating. Since factors such as plate thickness and media composition made β-galactosidase activity comparisons difficult for strains not showing significant σ^s-dependency, both recipients and transconjugants were streaked on the same plate to facilitate comparison. One-hundred and forty σ^s-dependent fusion mutants

Figure 5. Schematic representation of the screening for σ^s-dependent genes. Recipients (R) were selected on LB-agar containing streptomycin, kanamycin and X-gal (SKX). Transconjugants (TCJ) were selected on the same media as the above with the addition of tetracycline (SKTX). TCJ(F3) represents transconjugants transformed with the pMM*katF3* plasmid (p). OD(600 nm) of growth in microtiter wells was not explicitly measured. Density of the cultures was visually approximated.

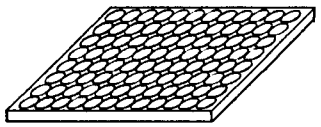

5000 λplacMu53 operon fusions were replica-plated into fresh microtiter wells and grown to an OD (600 nm) of 0.2.

An overnight culture of HS180 (Hfr rpoS::Tn10) was subcultured into fresh LB and grown to OD (600 nm) of 0.2.

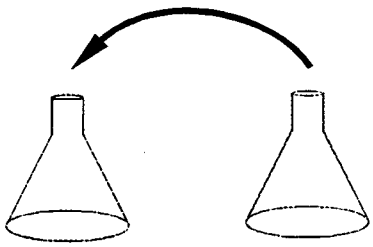

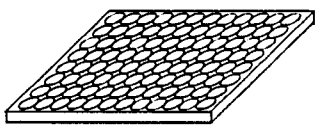

Bacterial Conjugation

100ul of HS180 was inoculated directly into the microtiter wells and incubated for 30 min. The resulting transconjugants were replica-plated onto selective media.

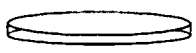

β-galactosidase comparison

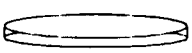

Recipient (controls) (LB: SKX)

Transconjugants (LB: SKTX)

479 transconjugants exhibited reduced levels of β-galactosidase expression relative to the original recipient strains.

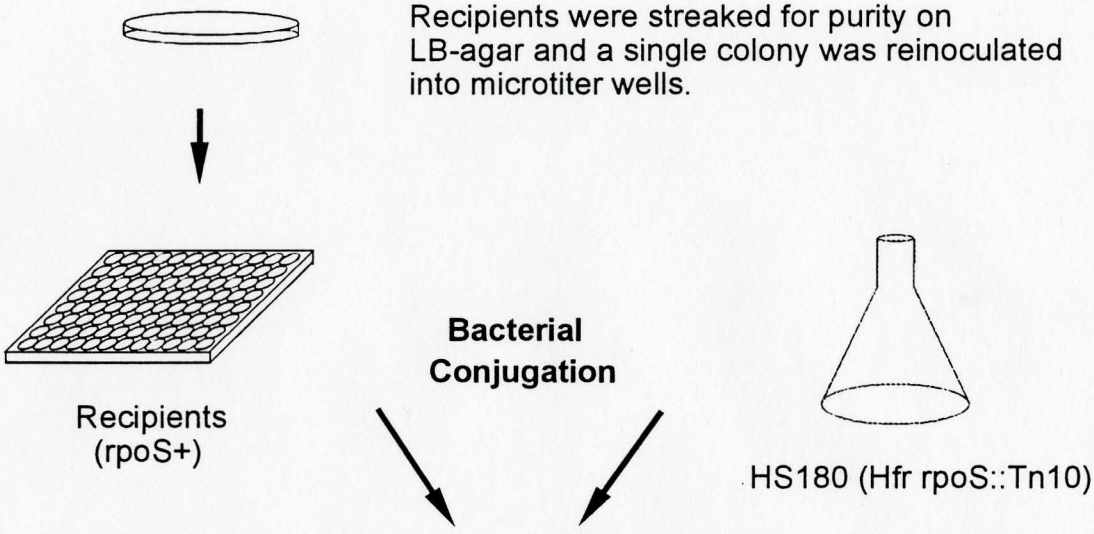
Recipients were streaked for purity on LB-agar and a single colony was reinoculated into microtiter wells.
Recipients (rpoS+)
Bacterial Conjugation
HS180 (Hfr rpoS::Tn10)
140 putative RpoS-dependent fusions were identified.
To facilitate comparison, both recipients and transconjugants were streaked on the same plate. (LB: SKX)
Recipient (rpoS+)
Transconjugant (rpoS-)
p
Transconjugants and recipients (control) were transformed in parallel with pMMkatF3 containing an rpoS+ gene.
R
TCJ(F3)
TCJ
Complementation was detected by scoring for the restoration of β-galactosidase and RpoS-dependent HPII activity.

remained after β-galactosidase comparisons on the same plate, many of which exhibited varying degrees of dependency (consistent with the published literature). Four *rpoS*$^+$ strains and their *rpoS*$^-$ derivatives did not evolve oxygen upon the addition of hydrogen peroxide, suggesting that the *lacZ* fusion may be located within the *katE* coding region.

To confirm that the decrease in β-galactosidase activity of transconjugants was due to the *rpoS* mutation, transconjugants were transformed with pMM*katF3* to test for complementation (Figure 6). Recipients were transformed in parallel, serving as controls for any variation in β-galactosidase levels due to the presence of the vector. In many cases, the transformed *rpoS*$^+$ and *rpoS*$^-$ strains exhibited higher levels of β-galactosidase activity than the non transformed derivatives. This may be due to the increased levels of *rpoS* expression on multicopy plasmids, an observation reported by other investigators (Sak *et al.*, 1989). Complementation of the *rpoS*$^-$ phenotype was determined by observing for the restoration of β-galactosidase activity and catalase activity (Table 3).

Although the λp*lac*Mu53 library was generated using a low MOI (0.1), each putative σ^s-dependent *lacZ* fusion was P1 transduced into GC4468 background to ensure the likelihood that each cell contained only one fusion. Six independent (non-purified) transductants of each of the above 132 strains (excluding the eight omitted) were inoculated into microtiter wells and retested for σ^s-dependency in the new background. Strains that exhibited a σ^s-dependent phenotype for all six isolates were restreaked for purity, and three independent colonies inoculated into microtiter wells and retested.

Of the eighty-two mutants in MC4100 background complemented with respect to β-galactosidase activity and catalase function, only nine were excluded from further studies after transduction into the new background. Many non-complemented mutants, or others that were difficult to handle (eg. did not grow well, could not be complemented or transduced for unknown reasons) were not σ^s-dependent in the new background, suggesting some problems with the *lacZ* insertion. One-hundred and five mutants showed a distinct σ^s-dependent phenotype after the transduction experiment (Figure 7, Table 3). These strains were studied further (sequencing of

Table 3. Results of transformation with pMM*katF3* in MC4100 background and transduction into GC4468 background.

Status of Strains	Number of Strains		
	MC4100[a]	GC4468[b]	omitted[c]
Complemented with respect to β-galactosidase and HPII activity. These include the four catalase negative recipients.	82	73	9
Not complemented with respect to β-galactosidase or HPII activity. The majority of these strains were difficult to handle in terms of aberrant growth patterns and/or difficulties in transforming. Transformations were repeated at least twice.	11	4	7
Exhibited 2 transconjugant phenotypes originating from a purified recipient. Each mating was done at least twice. The basis of this is unknown.	18	11	7
Inconclusive due to poor growth of transconjugants or failure to transform.	21	17	4
Difficult to determine whether their transconjugants were complemented. Although there were apparent differences between recipient and transconjugant in terms of β-galactosidase levels, they were too similar for our purposes. These were not considered to be σ^s-dependent and were omitted from further studies.	8	ND	-----
Total number of strains remaining	140	105	27

(ND) represent strains not transduced into GC4468 background. (a) Complementation results of strains in MC4100 background. (b) Number of strains tested to be σ^s-dependent after transduction of *lacZ* fusions into GC4468 background. (c) Total number of strains omitted after transduction results. These were not tested to be σ^s-dependent in GC4468 background.

Figure 6. Representative complementation of a mutant containing a σ^s-dependent fusion. (A) Three derivatives from strain HS1033 [12A10] are shown here on a LB-agar plate supplemented with streptomycin, kanamycin, and X-gal. The recipient (R), transconjugant (TCJ), and transconjugant transformed with the pMM*katF*3 plasmid (TCJ[F3]) were streaked side-by-side to facilitate comparison of β-galactosidase activity on plate. (B) An enzymatic assay of β-galactosidase activity was performed on a single overnight colony of the strains, R, TCJ, TCJ[F3], and the recipient strain transformed with the pMMkatF3 plasmid (R[F3]). The enzymatic assay verified the results seen on plates.

A

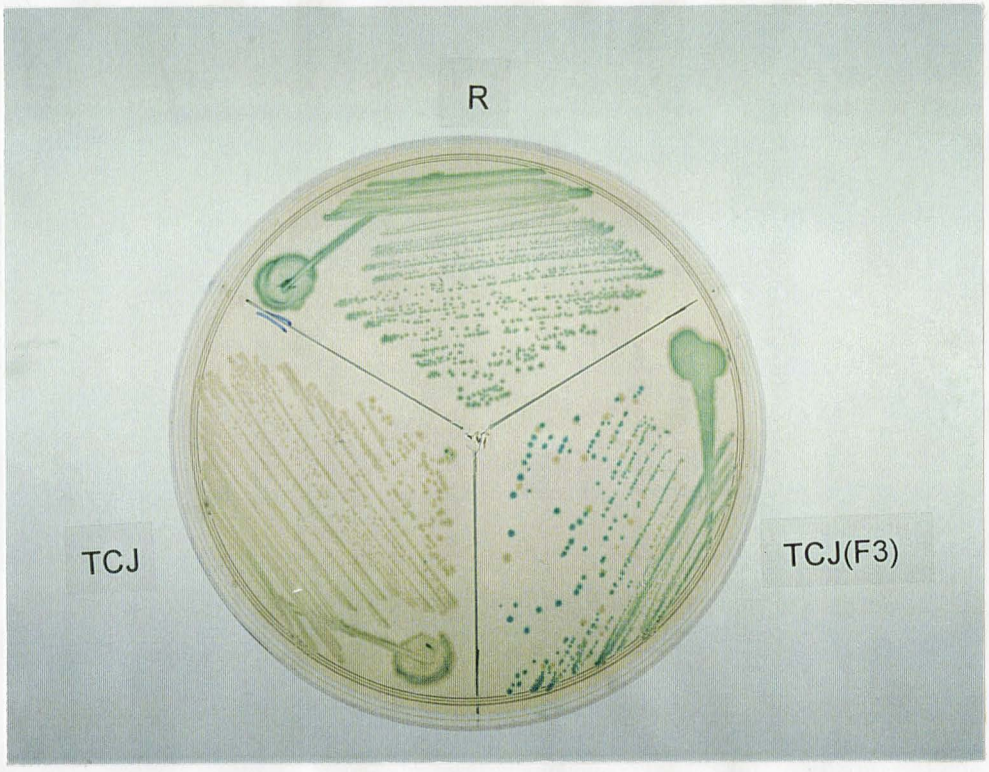
R
TCJ
TCJ(F3)

B

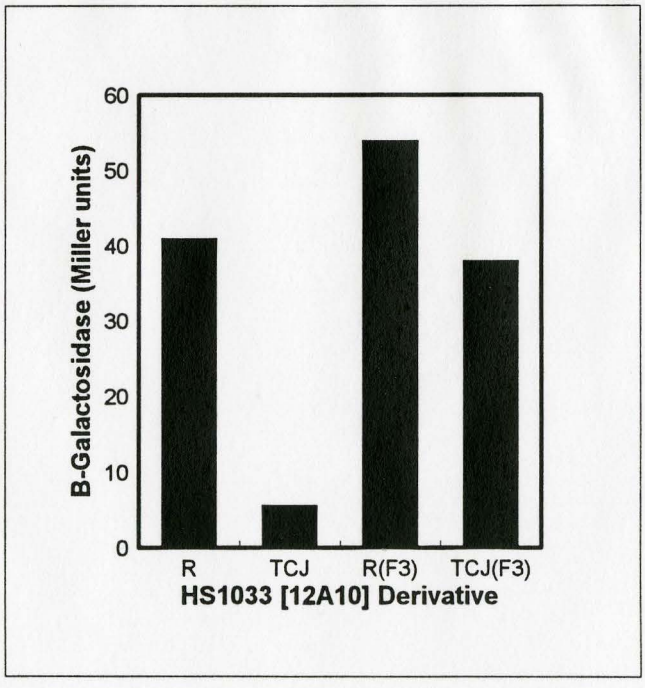
B-Galactosidase (Miller units)
60
50
40
30
20
10
0
R
TCJ
R(F3)
TCJ(F3)
HS1033 [12A10] Derivative

Figure 7. The collection of 105 recipient (*rpoS*$^+$) and transconjugant (*rpoS*$^-$) pairs in GC4468 background. Strains were plated on M9 minimal media supplemented with 0.4% glucose, 0.05% thiamine-HCl, X-gal and the antibiotics streptomycin and kanamycin. σ^s-dependent and independent control strains, NC4468 (*katE*::*lacZ*) and 13C10, respectively, are on the top row with their *rpoS*$^-$ derivatives adjacent. *rpoS*$^+$ and *rpoS*$^-$ derivative pairs are adjacent to one another in rows, starting from the top left. The *rpoS* status of each column is shown on the top as + (*rpoS*$^+$) and - (*rpoS*$^-$). Strain designations are listed on the left and right sides.

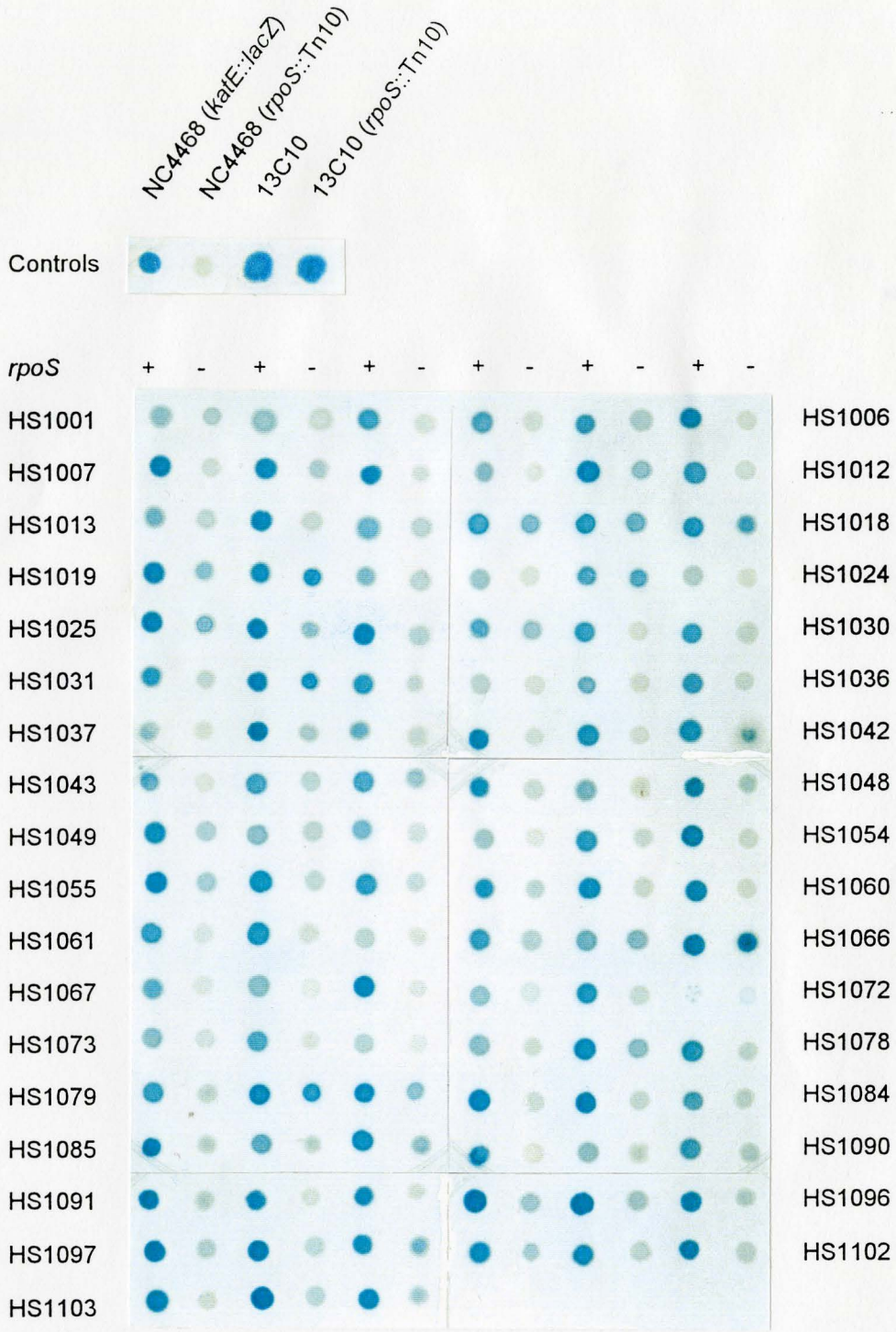
NC4468 (katE::lacZ)
NC4468 (rpoS::Tn10)
13C10
13C10 (rpoS::Tn10)
Controls
rpoS
+ - + - + - + - + - + -
HS1001
HS1006
HS1007
HS1012
HS1013
HS1018
HS1019
HS1024
HS1025
HS1030
HS1031
HS1036
HS1037
HS1042
HS1043
HS1048
HS1049
HS1054
HS1055
HS1060
HS1061
HS1066
HS1067
HS1072
HS1073
HS1078
HS1079
HS1084
HS1085
HS1090
HS1091
HS1096
HS1097
HS1102
HS1103

fusion junctions and growth expression studies).

IDENTIFICATION OF *rpoS*-ASSOCIATED PHENOTYPES.

Replica-plate screenings of the recipients were done as a general method in an attempt to identify qualitatively *rpoS*-associated phenotypes exhibited by mutants as a result of the interrupted genes. Three isolates of each fusion mutant was replica-plated onto several known inducers and grown under conditions to which *rpoS* mutants are known to be sensitive.

Amino Acid requirements.

Most of these plate assays used M9 minimal media containing a carbon source with no supplemented amino acids. All mutants grew under these conditions except strain HS1072 that did not grow in minimal media containing only 0.4% glucose and 0.05% thiamine-hydrochloride. Growth was observed on LB-agar indicating that a component(s) in LB media is required for viability. Induction of the fusion in HS1072 during carbon starvation and osmotic challenge could not be tested as a result.

Catalase Activity and Hydrogen Peroxide Sensitivity.

The two genes encoding catalases, *katE* and *katG*, both regulated by σ^s, are very different in other respects. The *katG* gene is induced by an OxyR-dependent mechanism in response to hydrogen peroxide (Christman *et al.*, 1985) and is the most important factor for cellular hydrogen peroxide resistance. The gene *katE*, on the other hand, is not induced by the presence of hydrogen peroxide but is expressed during entry into stationary phase (Loewen, 1984). HPII was shown to contribute more to catalase levels on agar plates than HPI (Loewen and Triggs, 1984). Thus the screening for catalase deficient mutants are based on either their sensitivity to mutation to hydrogen peroxide (for the isolation of HPI-encoded *katG* mutants), or reduced gas evolution in colonies flooded with hydrogen peroxide (for the isolation of HPII-encoded *katE* deficient mutants).

Since σ^s is known to regulate *katE* expression at the transcriptional level (Schellhorn and

Hassan, 1988), *katG* (Mukhopadhyay and Schellhorn, 1994; Ivanova *et al.*, 1994), and *dps* (*pexB*) (Almiron *et al.*, 1992) we tested whether any of the fusion mutants were deficient in catalase production or sensitive to hydrogen peroxide. Four fusion mutants (HS1006, HS1007, HS1014, and HS1062) were catalase deficient when flooded with 30% hydrogen peroxide and thus are presumptive catalase mutants. The controls, NC4468 (*katE::lacZ*) and HS143 (*rpoS::lacZ*) failed to evolve gas in relation to the catalase positive wild-type, MC4100. Transformation of the recipient with the plasmid pMM*katF3* did not restore catalase activity but did restore β-galactosidase expression. Furthermore, transduction of the *lacZ* fusion into a new background (GC4468) also did not restore catalase activity suggesting that the fusion junction probably lies within the coding region of *katE*, or an unidentified σ^s-dependent gene affecting catalase activity (Table 5). It should be noted that Dps has only been documented to confer cells resistance to hydrogen peroxide (Almiron *et al.*, 1992). Its role in catalase expression is unknown.

None of the mutants exhibited sensitivity to 0.6 mM hydrogen peroxide. However, six mutants were sensitive to higher concentrations of hydrogen peroxide, including the four that is catalase deficient (Table 5). Strain GC202 (*katG::lacZ*) was sensitive to both 0.6 and 1.0 mM hydrogen peroxide, a likely indication that none of the fusions lie in *katG*. Resistance of NC4468 and HS143 to hydrogen peroxide is consistent with the idea that *katG* is more important for cellular protection against hydrogen peroxide than *katE*. Although σ^s is required for the stationary phase expression of *katG* and *dps*, HPI and Dps-inducible protection against hydrogen peroxide is dependent on OxyR and not on σ^s. Therefore, HS143 (*rpoS*$^-$) and NC4468 (*katE*$^-$) are not hydrogen peroxide sensitive. Since the four catalase deficient strains, initially thought to be *katE*, are sensitive to 1.0 mM hydrogen peroxide, it may suggest other σ^s-dependent factor(s) contribute a role in both catalase activity and resistance to growth on hydrogen peroxide. It is difficult to determine from these results whether one fusion resides in *dps* since its sensitivity to 1 mM hydrogen peroxide has not been documented. Previous investigators have used concentrations as high as 15 mM. These differences in growth conditions between investigators complicate data comparisons.

Osmotic Induction.

For the understanding of the osmotic regulation of σ^s-dependent genes, the regulation of *rpoS* itself in response to osmotic upshift was of considerable interest. The slight induction of *rpoS* expression from a transcriptional fusion was not enough to account for the rapid increase of a subset of its regulon (Hengge-Aronis *et al.*, 1993), some of which include the *otsAB* regulon (Hengge-Aronis *et al.*, 1991), *bolA* and *osmY* (*csi-5*) (Hengge-Aronis *et al.*, 1993). This was later resolved when observed that osmotic upshift results in the post-transcriptional induction of *rpoS* (Lange and Hengge-Aronis, 1994a). Furthermore, using two-dimensional gels, an additional 18 proteins induced under osmotic stress require σ^s (Hengge-Aronis *et al.*, 1993). To identify fusion mutants induced by osmotic upshift, the strains were replica-plated onto M9 minimal media with increasing sodium chloride concentrations. β-galactosidase expression was compared with two sets of controls on M9 media, one containing no sodium chloride, and the other containing the regular requirements as specified in Miller (8.56 mM). No differences in β-galactosidase expression and growth were observed with the two sets of controls. As sodium chloride concentrations increased to 500 mM, growth was compromised. No growth occurred in the presence of 750 mM. Hengge-Aronis and colleagues also observed this trend, reporting that maximal induction of the *otsBA* and *treA* genes occurred between salt concentrations of 200 to 400 mM. Concentrations exceeding this amount resulted in a growth reduction and decreased expression (Hengge-Aronis *et al.*, 1991). Induction characteristics were noted after overnight incubation and after another day at room temperature. Strain NC4468 was previously observed to be induced four-fold in the presence of 500 mM sodium chloride (Schellhorn, unpublished results) and was used as a positive control. Induction, however, was not observed during osmotic upshift, which may imply that four-fold induction was not enough to be observed qualitatively on plate assays. Strain HS143 (transcriptional fusion) served as a negative control and was not induced as expected (Hengge-Aronis *et al.*, 1993), while GC4468 was used to observe for variations in growth patterns. Results in Table 4 show that 43 mutants were repressed by 250 mM NaCl and 13 were induced. One was severely repressed and one exhibited very high levels of induction to the point where the agar

surrounding the colonies was deeply stained. This was observed independently three times.

Carbon Starvation.

A subset of genes induced during carbon starvation was previously isolated using random *lacZ* mutagenesis, during which, an allele of *rpoS* (*csi2*::*lacZ*) was identified (Lange and Hengge-Aronis, 1991a). Further analysis of several *csi* fusion mutants resulted in a subset identified to be members of the σ^s-regulon (Watchword *et al.*, 1993). To identify members from our σ^s-dependent gene collection that are carbon-starved-inducible, cells were plated onto media containing limiting glucose and compared with plates containing the normal concentration. All the fusion mutants were slightly induced, but 13 exhibited very apparent induction (Table 4). HS143, which served as a positive control, was induced. Strain NC4468 was not induced (since *katE* is not known to be induced under carbon starvation) and GC4468 served as a control for variations in growth patterns.

Acetate Induction.

As a by-product of cellular metabolism, acetate has been implicated as a signal for the stationary phase response (reviewed in Tempest, 1987). Reported to accumulate during growth in minimal and LB media (Mukhopadhyay and Schellhorn, 1994), acetate is an inducer of some σ^s-dependent genes, such as *katE* (Schellhorn and Stones, 1992), *katG* (Mukhopadhyay and Schellhorn, 1994), and *aidB* (Volkert *et al.*, 1994). Its involvement in the induction of *rpoS* itself is still controversial. Some report no apparent induction (Mulvey *et al.*, 1990) while others observe induction (Schellhorn and Stones, 1992). Based on the observation that acetate does induce *rpoS* expression, we tested its effect on the levels of β-galactosidase on σ^s-dependent fusion mutants. Cells were replica-plated onto media containing increasing concentrations of acetate. The growth of all mutants was compromised as acetate concentrations increased to 100 mM. Plates containing 50 mM of acetate produced the most reliable results. The expression of the fusions in three mutants was induced while nine were repressed, three of which showed significant decrease in β-galactosidase activity (Table 4). Both HS143 and NC4468 were not induced, contrary to previously

Table 4. Phenotypic screening of RpoS-dependent lacZ gene fusions in GC4468 background.

Strain	[location]	Catalase	H2O2 Sensitivity		Carbon	Acetate	Salt Induction		Comments
		Activity	0.6 mM	1.0 mM	Starvation	Induction	250 mM	500 mM	
HS1001	01D04	+			+		-	--	
HS1002	01E04	+			+		-	--	
HS1003	01H01	+			+		-	--	
HS1004	02C08	+			+		--	--	
HS1005	02D11	+			+	-	-	---	
HS1006	02E11	-	+	-	+				Sensitive to 1mM hydrogen peroxide
HS1007	02E12	-	+	-	+				Sensitive to 1mM hydrogen peroxide
HS1008	02H06	+			+	-	-	---	
HS1009	03C06	+			+			-	
HS1010	03F05	+			++			--	
HS1011	04C07	+			+				
HS1012	04D09	+			+		-	--	
HS1013	04F08	+			++	-		--	
HS1014	05A10	-	+	-	+				Sensitive to 1mM hydrogen peroxide
HS1015	05C08	+			++		-	--	
HS1016	06A12	+			+				
HS1017	06C03	+			+				
HS1018	06E01-d	+			+		-		
HS1019	06E01-l	+			+		-		
HS1020	07A08	+			+		-		
HS1021	07B07	+			++		-	--	
HS1022	07B09	+			++		-	--	
HS1023	07D07	+			+		-		
HS1024	07E04	+			++				
HS1025	07F09	+			+	+	+(NC)	(NC)	2 TCJ morphologies
HS1026	07F10	+			+	+	+(NC)	(NC)	2 TCJ morphologies
HS1027	07F11	+			+	+	+(NC)	(NC)	
HS1028	08H08	+			++	-	-	--	
HS1029	09B11	+			+	-	-		
HS1030	09C07	+			+		-		

Strain	[location]	Catalase Activity	H2O2 Sensitivity		Carbon Starvation	Acetate Induction	Salt Induction		Comments
			0.6 mM	1.0 mM			250 mM	500 mM	
HS1031	09E10	+			+				
HS1032	09H12	+			+		+		
HS1033	12A10	+			+		-	--	
HS1034	12C09	+			+		-		
HS1035	13B08	+			+	---	-	--	
HS1036	13C08	+			+		-	-	
HS1037	14C03	+			+		-		
HS1038	14D08	+			+				
HS1039	15G03	+			++				
HS1040	16E03	+			+	---			
HS1041	16F07	+			+				2 TCJ morphologies
HS1042	21B04	+			+		----		
HS1043	21F08	+			+	--	--		
HS1044	22E03	+			+				2 TCJ morphologies
HS1045	22F08	+			+				
HS1046	22F09	+			+				
HS1047	22G10	+			+				
HS1048	23E01	+			+		-		
HS1049	24B12	+		+/-	+		-		2/3 colonies sensitive to 1 mM hydrogen peroxide
HS1050	24C07	+			+		-		
HS1051	25A11	+			+++		++	(NC)	
HS1052	25B04	+			+++		-	--	
HS1053	26A06	+			+		-	--	
HS1054	26E05	+			+		+(NC)	(NC)	
HS1055	28F07	+			+		+(NC)	(NC)	
HS1056	29G11	+			+				2/3 colonies sensitive to 1 mM hydrogen peroxide
HS1057	31B04	+			+				
HS1058	31B09	+			+				
HS1059	31D07-d	+			+				
HS1060	31D07-l	+			+				
HS1061	31F08-n	+			+	-	-	----	

Strain	[location]	Catalase Activity	H2O2 Sensitivity		Carbon Starvation	Acetate Induction	Salt Induction		Comments
			0.6 mM	1.0 mM			250 mM	500 mM	
HS1062	31F09	-	+	-	+				Sensitive to 1mM hydrogen peroxide
HS1063	32D07	+			+++		-		
HS1064	32D11	+			+		-	--	
HS1065	33B07	+			+		+++	(NC)	
HS1066	33C09	+			+			-	
HS1067	34C08-n	+			+		-		
HS1068	34C08-m	+			+		-		
HS1069	34E11	+			+				
HS1070	35B06	+			+		--	--	
HS1071	35B09	+			+				
HS1072	35C12	+			+				no growth on M9 minimal media
HS1073	35F12	+			++			--	
HS1074	35G05	+			+		-	---	
HS1075	35G11	+			++		--		
HS1076	35G12	+			++				
HS1077	36A05	+			+			---	
HS1078	36A11	+			+				
HS1079	36B03	+			+				
HS1080	36B07	+			+		-		
HS1081	36G06	+			+				
HS1082	39C08	+			+				
HS1083	39E02	+			+		+	(NC)	2 TCJ morphologies
HS1084	39E12	+			+		-		
HS1085	39F11	+			+				
HS1086	39H08	+			+		-		
HS1087	41F10	+			+				
HS1088	42B07	+			+				
HS1089	42H10	+			+		-		
HS1090	43E02	+			+		-		
HS1091	43G05-d	+			+				
HS1092	43G05-l	+			+		-		
HS1093	43G11	+			+				

Strain	[location]	Catalase Activity	H2O2 Sensitivity		Carbon Starvation	Acetate Induction	Salt Induction		Comments
			0.6 mM	1.0 mM			250 mM	500 mM	
HS1094	44A08	+			+		++		
HS1095	44C09	+			+				
HS1096	45B11	+			+		++++		very dark blue ring around colony on NaCl plates
HS1097	45F04	+			+				
HS1098	46A08	+			+		++		
HS1099	46D12	+			+				
HS1100	47B12	+			+				
HS1101	47D08	+			+				
HS1102	48B01-n	+			+				
HS1103	48B01-m	+			+				
HS1104	48E04	+			+		+		
HS1105	49F03	+			+				2 TCJ morphologies

(TCJ) represents transconjugants. (NC) represents no observable change. [location] is the strain designation identifying the location of the strain in the lacZ fusion library. Observations for osmotic induction at 500 mM was taken after a two-day incubation. Cells were incubated overnight at 37°C after which plates were allowed to sit at room temperature for an additional 24 hours. Colonies replica-plated onto plates limited for carbon exhibited a bluish-tint relative to control plates containing the regular requirement of carbon. This made comparison relatively difficult since all fusions appeared to be induced.

published data (Schellhorn and Stones, 1992). Several reasons may account for this. The two-fold induction documented for *rpoS* may not be detected qualitatively, however, a six-fold induction of the *katE* reporter fusion (Schellhorn and Stones, 1992) should be observed. Secondly, the plate assay for acetate induction is not the same method used previously (Schellhorn and Stones, 1992), which may account for the lack of observable induction for the *katE* gene fusion. As with other experiments involving qualitative fusion induction on plates, not all cells may be exposed to the same concentrations of the inducer, and the method can only detect several magnitudes of induction.

Screening for the *sur* phenotype.

The *sur* (*A-D*) genes, initially identified by random *lacZ* mutagenesis, are not required for growth at logarithmic phase but are essential for long-term stationary phase survival (Tormo *et al.*, 1990). Little is known about the physiological function of *surC* and *surD*, but *surA* and *surB* have been studied in detail. The *surB* mutation results in a phenotype similar to a temperature-sensitive strain; cells fail to form colonies at 37°C after prolonged incubation but can grow at 30°C (Siegele *et al.*, 1993). In contrast, cells that carry a mutation in *surA* are incapable of surviving prolonged periods in starvation, since lethality is observed within four to five days of incubation (Tormo *et al.*, 1990). Other than their stationary phase-specific function, the relationship between *rpoS* and *sur* became apparent when demonstrated that *rpoS*$^-$ mutants exhibit the *sur* phenotype (Lange and Hengge-Aronis, 1991a). Their screening procedure involved incubating 20 000 random insertion mutants at 37°C and testing for viability over several days by spot plating 10 µl of culture onto LB medium containing the appropriate antibiotics. Since this initial screening does not use serial dilutions, only mutations leading to a decrease of several orders of magnitude can be detected. Our initial screening for the *sur* phenotype followed a similar procedure except 10 µl of a seven-day-old culture was spread onto the surface of the plate. Twenty-three cultures showed a slight decrease in colony counts. However, using the criteria of selection of Tormo and colleagues, none of the mutants would be considered a *sur* mutant. Their results from quantitative serial dilutions of

Figure 8. Screening of the *sur* phenotype. Twenty-three strains observed to be reduced in their ability to survive long-term starvation were selected for serial dilution studies. GC4468 and HS143, along with two strains that did not exhibit defects in long-term growth (HS1019 and HS1103) were assayed as controls. A subset of the results is graphed as an example of the trend seen throughout.

GC4468
HS143
HS1005 02D11
HS1006 02E11
HS1007 02E12
HS1009 03C06

HS1014 05A10
HS1015 05C08
HS1016 06A12
HS1018 06E1-d
HS1019 06E1-l
HS1023 07D07
HS1035 13B08
HS1036 13C08
HS1037 14C03
HS1038 14D08
HS1046 22F09
HS1066 33C09
HS1082 39C08
HS1087 41F10
HS1090 43E02
HS1094 44A08
HS1096 45B11
HS1099 46D12
HS1102 48B01-n
HS1103 48B01-m
HS1105 49F03

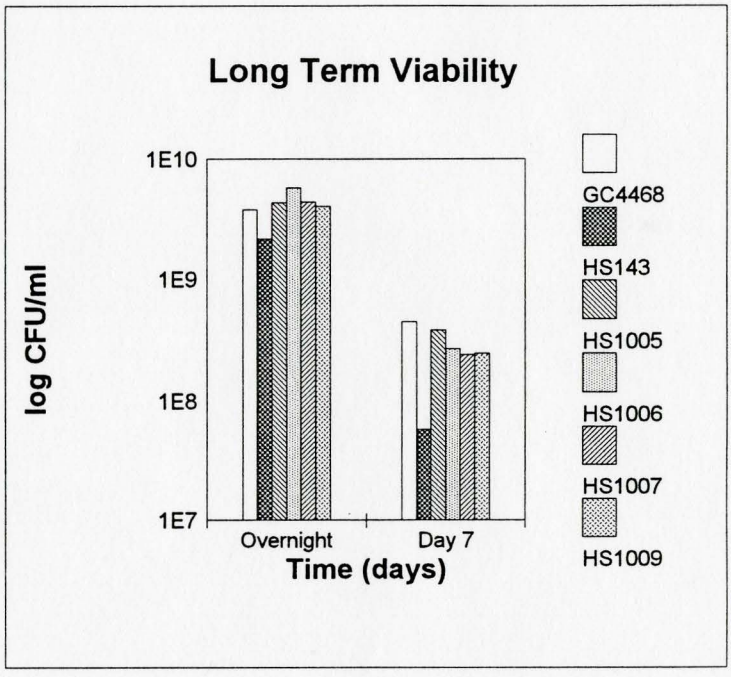

sur mutants show that only a few hundreds of cells remained per ml after five days of incubation, a number that is easily counted on a single plate. Nonetheless, to confirm our results, the twenty-four recipients that appeared to show a reduction in growth were retested using quantitative serial dilutions. Duplicate counts of cells of overnight cultures were compared with 7-day-old cultures (Figure 8). All the strains, including a GC4468 control showed a 10-fold decrease from 10^{-8} cells in overnight cultures to 10^{-7} after seven days of incubation. HS143, however, exhibited a 100-fold decrease, from 10^{-8} to 10^{-6}, a viability loss that is consistent with published data (Lange and Hengge-Aronis, 1991a).

Growth-phase expression curves of *lacZ* isogenic *rpoS*$^+$ and *rpoS*$^-$ strains.

Since *rpoS* is a stationary phase sigma factor known to be responsible for the growth phase induction of many members of its regulon, the growth-phase-expression curves of the *rpoS*$^+$ and *rpoS*$^-$ fusion mutants were determined. Results showed that although the pattern of induction varied between strains (consistent with the diversity of expression within members of the regulon) a general trend was observed. The majority of strains exhibited induction at approximately OD(600 nm) 0.3 and increased steadily to differing maximum levels in stationary phase. The range of the induction ratio (calculated as the ratio of the maximum levels of β-galactosidase attained in stationary phase and the minimum levels in exponential phase) varied between two-fold to over 400-fold, as determined from results of 101 recipients. The plot of induction ratios on a scale in ascending order did not reveal any particular subset to which growth-phase-dependent expression of *rpoS*$^+$ strains can be categorized (Figure 9B).

rpoS$^-$ strains also exhibited varying induction ratios, ranging from less than one-fold to over 5-fold. From the 101 transconjugants assayed, 64 exhibited less than two-fold induction, 19 of which showed higher levels of β-galactosidase activity in exponential phase than in stationary phase, suggesting that the *rpoS* mutation completely abolished expression from the fusion. An induction ratio of less than one may suggest that during exponential phase, basal levels of the gene may be sustained by another regulator (eg. σ^{70}) and the decrease into stationary phase is a result

Figure 9. σ^s-dependency and induction ratios. (A) Values of σ^s-dependency of the *lacZ* fusion mutants over the number of strains are plotted in ascending order. (B) The induction ratios of both *rpoS*$^+$ (recipients) and *rpoS*$^-$ (transconjugants) are plotted similarly to identify any subsets or categories of gene expression.

A

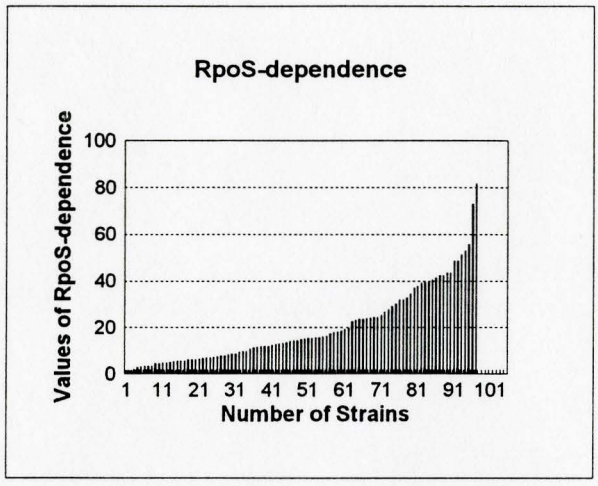
RpoS-dependence
Values of RpoS-dependence
100
80
60
40
20
0
1 11 21 31 41 51 61 71 81 91 101
Number of Strains

B

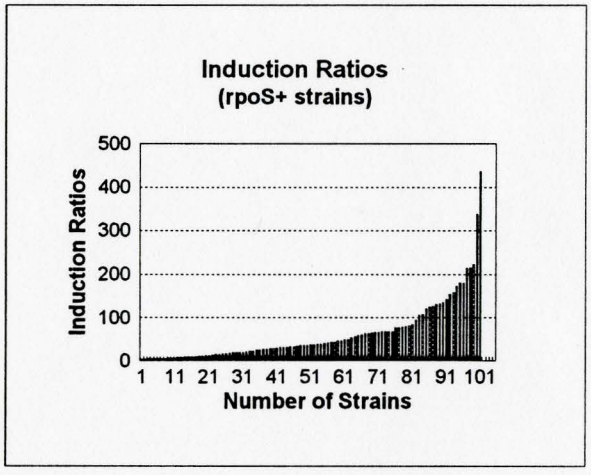
Induction Ratios
(rpoS+ strains)
Induction Ratios
500
400
300
200
100
0
1 11 21 31 41 51 61 71 81 91 101
Number of Strains

C

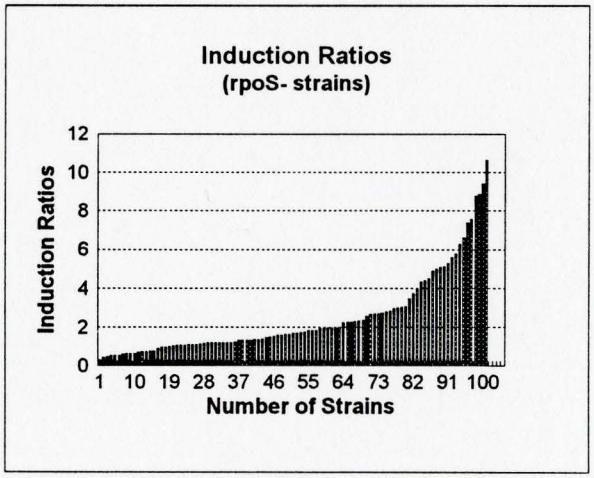
Induction Ratios
(rpoS- strains)
Induction Ratios
12
10
8
6
4
2
0
1 10 19 28 37 46 55 64 73 82 91 100
Number of Strains

of the degradation of preexisting protein due to the absence of σ^s that is responsible for stationary phase induction of the gene. More likely, lower β-galactosidase levels in stationary phase are due to the diluting out of residual activity during the start of the experiment. Nonetheless, these results suggest that the *rpoS* mutation completely abolished expression from the fusion junction. Twenty-three strains had induction ratios between two and five-fold and 15 strains exhibited over five-fold induction (Table 5). As with the *rpoS*$^+$ strains, the induction ratios of *rpoS*$^-$ derivatives when plotted in ascending order did not reveal any observable categories (Figure 9C).

For *rpoS*$^-$ derivatives that were significantly induced, the question was addressed whether their expression was growth-phase-dependent without σ^s. Strains that exhibited over five-fold induction in a *rpoS*$^-$ background were reassayed with the complete range of time points as used for the recipients. Recipients were also reassayed as a control. Results obtained for 12 of the 15 strains showed growth-phase-dependence of the gene fusions in a *rpoS*$^-$ background, implicating other factors involved in growth-phase expression other than σ^s (Figure 10). Curiously, the quantitative induction ratio values of both the reassayed recipients and transconjugants were different from the values of the results obtained in the first induction study (Appendix D). The reasons for these discrepancies are unknown but several possibilities are outlined in the Discussion. It should be noted that although numerical values may appear very different, nine of the 12 recipients reassayed showed similar patterns of induction when observed graphically.

To determine the σ^s-dependency of the fusions, the maximum level of β-galactosidase activity attained by *rpoS*$^+$ strains was divided by the maximum level achieved by the *rpoS*$^-$ strains [$R_{max}(s)$ / $TCJ_{max}(s)$]. Values obtained correlated well with qualitative values observed on plates, but only for *rpoS*$^+$ and *rpoS*$^-$ pairs that were very similar in activity levels, and *rpoS*$^-$ strains which appeared to have a high level of β-galactosidase activity (Compare values in Table 6 with observations in Appendix B). The σ^s-dependency values for 96 of the 105 strains varied between 1.5 to 55.8 units (Figure 6), but no apparent categories exist (Figure 9A). β-galactosidase activity assayed on LB plates is a quantitative assay. Though the variation in color difference between *rpoS*$^-$ strains are more obvious, the levels between *rpoS*$^+$ strains are not. This is because the range

Table 5. Summary of induction ratios of rpoS+ and isogenic rpoS- strains and values of RpoS-dependency.

		Recipients (rpoS+)			Transconjugants (rpoS-)			
		B-galactosidase		Ind	B-galactosidase		Ind	RpoS
Strain	[Location]	[min]	[max]	Ratio	[min]	[max]	Ratio	Dep
HS1001	01D04	36.7	168.0	4.6	5.7	4.3	0.8	39.34
HS1002	01E04	35.1	187.0	5.3	8.1	5.1	0.6	36.90
HS1003	01H01	15.1	67.2	4.5	5.4	9.7	1.8	6.90
HS1004	02C08	15.2	62.4	4.1	3.5	9.4	2.7	6.61
HS1005	02D11	14.9	101.3	6.8	1.9	14.4	7.4 *	7.04
HS1006	02E11	0.8	178.9	223.6	1.9	4.4	2.3	40.35
HS1007	02E12	0.9	112.9	125.4	0.8	3.3	4.0	34.44
HS1008	02H06	0.8	144.0	180.0	1.7	9.2	5.6 *	15.62
HS1009	03C06	1.5	203.1	135.4	2.3	8.7	3.7	23.44
HS1010	03F05	0.9	393.0	436.7	1.4	12.3	8.9 *	31.97
HS1011	04C07	15.9	241.9	15.2	16.8	20.5	1.2	11.83
HS1012	04D09	4.4	85.5	19.4	6.8	9.9	1.5	8.63
HS1013	04F08	1.1	45.6	41.5	1.1	5.5	5.0 *	8.28
HS1014	05A10	1.9	130.0	68.4	0.7	3.1	4.3	42.41
HS1015	05C08	0.6	56.2	93.7	1.8	5.0	2.8	11.31
HS1016	06A12	15.4	135.0	8.8	51.8	24.6	0.5	5.49
HS1017	06C03	23.9	123.4	5.2	49.6	26.3	0.5	4.69
HS1018	06E01-d	9.1	143.5	15.8	13.5	18.5	1.4	7.77
HS1019	06E01-l	8.7	101.8	11.7	10.6	13.0	1.2	7.81
HS1020	07A08	32.3	94.9	2.9	59.5	64.7	1.1	1.47
HS1021	07B07	ND	ND	ND	1.6	4.1	2.6	ND
HS1022	07B09	0.7	47.3	67.6	1.7	3.0	1.7	15.96
HS1023	07D07	33.8	152.2	4.5	60.5	45.4	0.7	3.36
HS1024	07E04	0.6	95.0	158.3	1.0	11.1	10.6 *	8.53
HS1025	07F09	9.9	337.4	34.1	ND	ND	ND	ND
HS1026	07F10	10.2	400.2	39.2	ND	ND	ND	ND
HS1027	07F11	12.5	241.9	19.4	ND	ND	ND	ND
HS1028	08H08	7.1	85.6	12.1	13.1	25.5	2.0	3.35
HS1029	09B11	1.2	158.2	131.8	2.0	7.0	3.5	22.53
HS1030	09C07	3.5	137.2	39.2	2.7	3.3	1.2	42.21
HS1031	09E10	1.1	170.5	155.0	1.5	11.4	7.6 *	14.90
HS1032	09H12	8.7	140.0	16.1	14.6	14.6	1.0	9.58
HS1033	12A10	0.8	48.3	60.4	1.5	2.0	1.4	24.21
HS1034	12C09	1.5	73.9	49.3	1.1	10.2	9.4 *	7.27
HS1035	13B08	0.7	121.5	173.6	1.0	2.3	2.4	52.92
HS1036	13C08	3.0	93.1	31.0	3.3	7.6	2.3	12.23
HS1037	14C03	0.3	64.3	214.3	0.4	2.7	6.6 *	23.66
HS1038	14D08	0.3	64.7	215.7	7.1	13.0	1.8	4.97
HS1039	15G03	3.2	89.0	27.8	4.6	13.7	3.0	6.51
HS1040	16E03	0.7	127.0	181.4	18.3	7.9	0.4	16.14
HS1041	16F07	1.7	110.8	65.2	4.0	12.0	3.0	9.25
HS1042	21B04	2.3	106.2	46.2	6.6	7.9	1.2	13.44
HS1043	21F08	0.9	59.9	66.6	1.0	5.0	5.1 *	11.90

		Recipients (rpoS+)			Transconjugants (rpoS-)			
		B-galactosidase		Ind	B-galactosidase		Ind	RpoS
Strain	[Location]	[min]	[max]	Ratio	[min]	[max]	Ratio	Dep
HS1044	22E03	4.5	86.4	19.2	16.5	18.4	1.1	4.69
HS1045	22F08	8.9	88.7	10.0	15.1	15.9	1.1	5.59
HS1046	22F09	7.6	171.8	22.6	6.8	7.5	1.1	23.00
HS1047	22G10	1.4	61.3	43.8	0.9	1.3	1.3	48.73
HS1048	23E01	2.6	79.8	30.7	1.0	1.9	1.9	41.35
HS1049	24B12	2.4	87.6	36.5	0.9	2.7	3.0	32.93
HS1050	24C07	3.7	37.7	10.2	5.5	6.2	1.1	6.13
HS1051	25A11	2.4	96.2	40.1	7.5	9.0	1.2	10.75
HS1052	25B04	2.9	103.4	35.7	3.0	8.0	2.7	12.94
HS1053	26A06	1.0	79.5	79.5	2.3	5.2	2.2	15.22
HS1054	26E05	11.3	305.2	27.0	6.1	7.0	1.1	43.52
HS1055	28F07	14.2	253.8	17.9	11.9	19.4	1.6	13.07
HS1056	29G11	3.7	217.4	58.8	6.8	9.1	1.3	24.02
HS1057	31B04	4.3	349.1	81.2	3.6	18.3	5.1 *	19.06
HS1058	31B09	4.6	487.9	106.1	4.2	20.7	4.9 *	23.62
HS1059	31D07-d	5.1	163.4	32.0	2.3	6.5	2.8	25.10
HS1060	31D07-l	5.7	127.3	22.3	1.7	10.1	5.8 *	12.65
HS1061	31F08-n	1.0	142.7	142.7	1.1	9.9	8.8 *	14.41
HS1062	31F09	0.7	89.2	127.4	1.2	2.4	2.0	37.73
HS1063	32D07	1.2	37.9	31.3	1.1	7.1	6.3 *	5.38
HS1064	32D11	10.1	64.3	6.4	8.9	14.3	1.6	4.49
HS1065	33B07	2.9	17.6	6.1	7.3	11.2	1.5	1.57
HS1066	33C09	13.8	59.0	4.3	13.5	20.1	1.5	2.94
HS1067	34C08-n	1.4	42.1	30.1	1.4	2.3	1.6	18.41
HS1068	34C08-m	1.1	36.0	32.7	1.6	2.1	1.3	17.23
HS1069	34E11	6.1	402.4	66.0	5.1	5.5	1.1	73.03
HS1070	35B06	6.7	54.7	8.2	26.6	16.7	0.6	3.29
HS1071	35B09	4.7	97.2	20.7	4.0	7.0	1.7	13.97
HS1072	35C12	ND	ND	ND	28.1	21.4	0.8	ND
HS1073	35F12	1.2	58.0	48.3	3.3	6.0	1.8	9.68
HS1074	35G05	2.4	65.4	27.3	3.5	4.2	1.2	15.66
HS1075	35G11	2.3	64.5	28.0	2.0	10.6	5.3 *	6.09
HS1076	35G12	1.9	146.0	76.8	2.3	5.3	2.3	27.68
HS1077	36A05	1.0	338.2	338.2	2.9	12.7	4.4	26.55
HS1078	36A11	8.4	83.5	9.9	10.5	13.9	1.3	6.01
HS1079	36B03	4.9	69.5	14.2	6.8	15.8	2.3	4.40
HS1080	36B07	1.4	61.3	43.8	92.6	29.2	0.3	2.10
HS1081	36G06	1.4	110.4	78.9	0.7	2.0	3.0	55.76
HS1082	39C08	2.5	170.0	68.0	9.0	8.7	1.0	19.65
HS1083	39E02	16.6	429.1	25.8	10.7	28.3	2.7	15.16
HS1084	39E12	1.7	108.2	63.6	5.1	6.0	1.2	18.06
HS1085	39F11	2.7	326.3	120.9	8.9	10.9	1.2	30.01
HS1086	39H08	1.7	61.7	36.3	9.3	8.4	0.9	7.31
HS1087	41F10	1.3	109.9	84.5	2.8	7.6	2.7	14.42
HS1088	42B07	1.0	64.0	64.0	1.6	2.6	1.7	24.24
HS1089	42H10	2.3	248.2	107.9	3.3	6.3	1.9	39.21

		Recipients (rpoS+)			Transconjugants (rpoS-)			
		B-galactosidase		Ind	B-galactosidase		Ind	RpoS
Strain	[Location]	[min]	[max]	Ratio	[min]	[max]	Ratio	Dep
HS1090	43E02	5.8	114.9	19.8	7.8	7.4	1.0	15.47
HS1091	43G05-d	14.5	775.8	53.5	6.8	9.5	1.4	81.75
HS1092	43G05-l	0.8	104.7	130.9	2.2	2.4	1.1	43.38
HS1093	43G11	2.2	123.3	56.0	1.2	2.4	2.0	51.29
HS1094	44A08	2.8	191.3	68.3	ND	ND	ND	ND
HS1095	44C09	19.5	206.8	10.6	12.9	7.1	0.5	29.12
HS1096	45B11	11.4	423.4	37.1	7.2	8.7	1.2	48.61
HS1097	45F04	ND	ND	ND	6.5	10.6	1.6	ND
HS1098	46A08	3.4	259.2	76.2	1.8	8.1	4.5	31.84
HS1099	46D12	27.0	236.1	8.7	37.7	20.6	0.5	11.47
HS1100	47B12	9.7	78.5	8.1	11.9	23.7	2.0	3.31
HS1101	47D08	3.2	115.1	36.0	4.6	3.0	0.6	38.90
HS1102	48B01-n	ND	ND	ND	6.6	4.6	0.7	ND
HS1103	48B01-m	4.4	57.6	13.1	7.4	4.8	0.7	11.90
HS1104	48E04	17.1	442.6	25.9	34.7	24.9	0.7	17.76
HS1105	49F03	4.3	200.7	46.7	20.6	36.1	1.8	5.55

ND Assays not done.

* Identifies the rpoS- mutants with induction ratios of more than 5.0.

90

Figure 10. Growth-phase-dependent expression of *lacZ* fusion mutants in a *rpoS*$^-$ background. Graphs were constructed for 12 of 15 *rpoS*$^-$ strains with an induction ratio greater than 5.0. Raw data of graphs are in Appendix C.

HS1008t
[02H06t]

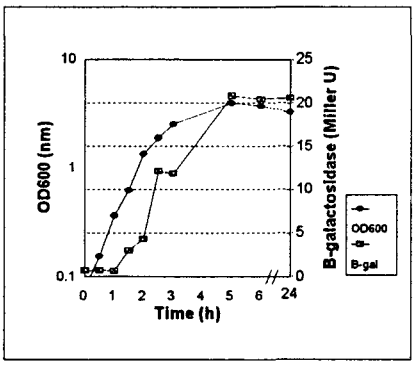

HS1034t
[12C09t]

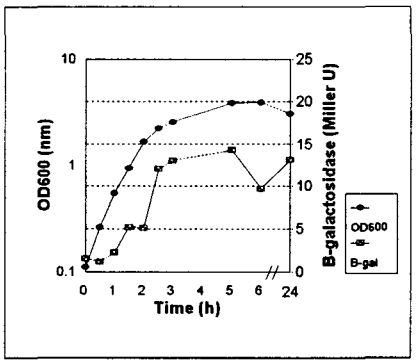

HS1010t
[03F05t]

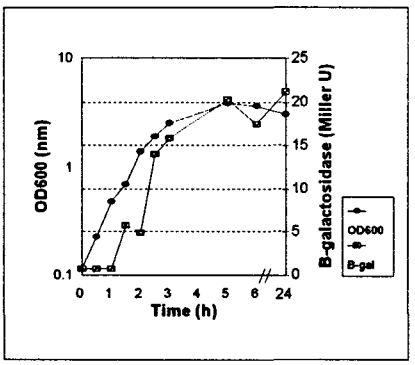

HS1037t
[14C03t]

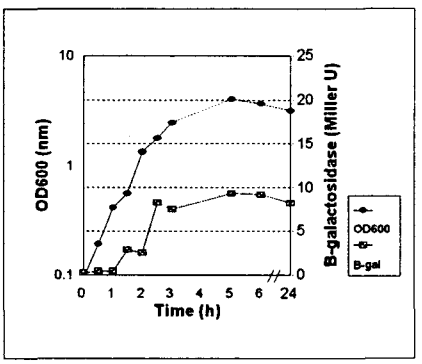

HS1024t
[07E04t]

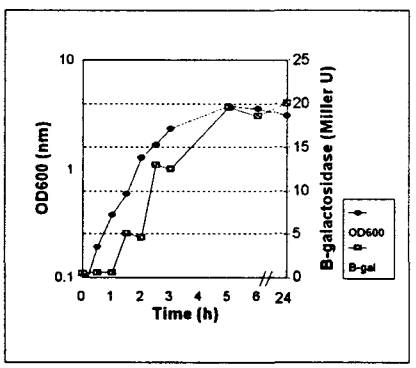

HS1043t
[21F08t]

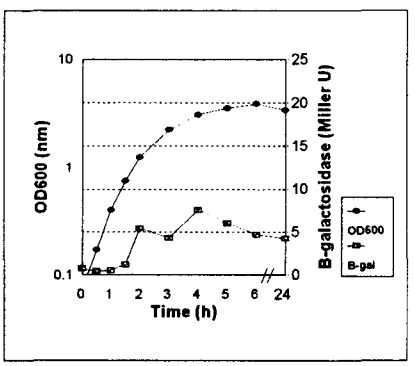

HS1031t
[09E10t]

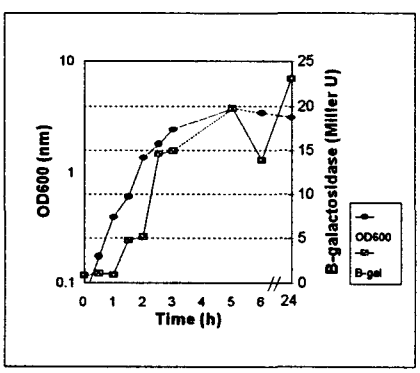

HS1057t
[31B04t]

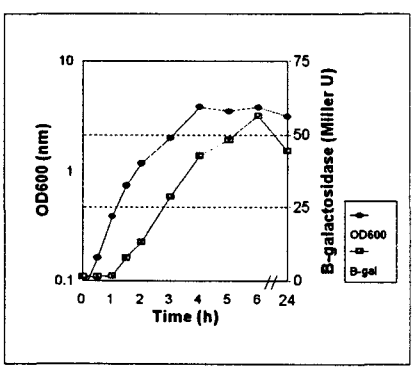

HS1058t
[31B09t]

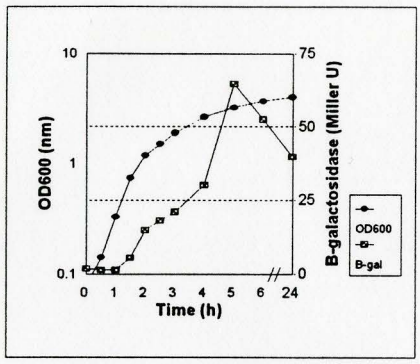

HS1063t
[32D07t]

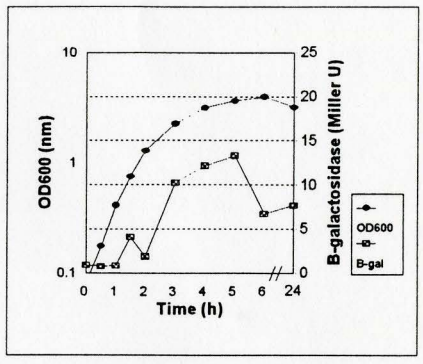

HS1061t
[31F08t]

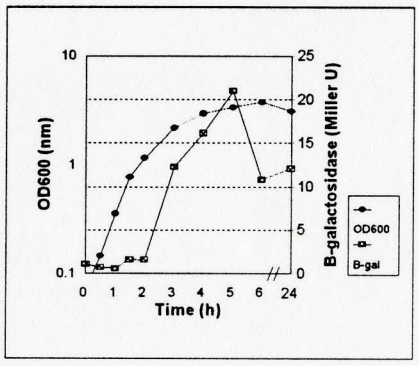

HS1075t
[35G11t]

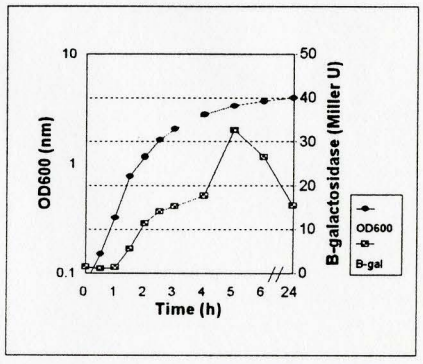

of activity versus color change is near the saturation point. In other words, two *rpoS*$^+$ strains may appear to have the same level of β-galactosidase activity on plates but may be several fractions off when measured enzymatically. Dark blue versus blue is harder to detect than distinguishing the difference between white and light blue. This may account for the reason for a higher correlation between low σ^s-dependence with *rpoS*$^-$ that has a high level of β-galactosidase activity. Varying the concentrations of X-gal in the media might aid in distinguishing between the levels of seen β-galactosidase.

IDENTIFICATION OF FUSION JUNCTIONS BY SEQUENCING.

The preparation of λ DNA was done as described in Materials and Methods. λ DNA was first visualized on an agarose gel to check for bacterial RNA contamination, cut by restriction endonuclease and quantified spectrophotometrically. Ten fusion junctions were sequenced, seven manually and three (HS1028, HS1038, and HS1001) by automatic sequencer. The Mu c end vector sequences, 5'-AATACA-3' (Figure 4) was confirmed for all sequences and the data compared with published *E. coli* sequences (Genbank). Six mapped to open reading frames coding for proteins of unknown function and two did not map to any known region in the *E. coli* genome. Two fusion junctions map to recently identified genes, *ldcC*, coding for a constitutively expressed lysine decarboxylase, and *talB*, encoding a transaldolase homologue. A summary of the results is listed in Table 6 and a diagrammatic representation of the location of the fusion junctions in the *E. coli* chromosome is reproduced from published literature in Figure 11. Alignment of sequences from the Genbank searches showed that submitted sequences were not perfectly matched to the corresponding regions in the *E. coli* chromosome. Although some matches were adequate, some would require resequencing of the fusion junction. Submitted sequences and alignment to their corresponding region in the *E. coli* chromosome are in Appendix E.

The *lacZ* fusion constructs were designated "rsd" for *rpoS*-dependent fusions and parallels the name of the strain from which it originated. Of the ten sequenced, seven were mapped to putative open reading frames (ORF's) coding for proteins whose functions are currently unknown.

Strains HS1001 and HS1002 are mapped to the same ORF in the chromosome. ORF-o69 codes for a protein of 69 amino acids of unknown function. Residing downstream from the *dinF* and *lexA* genes, it is located at approximately 92 min. A putative promoter sequence is found 209 bp upstream of the translational start site within the 3' end of the *dinF* coding region. rsd038 (from strain HS1038) is mapped to ORF-o394, a region similar to an unidentified open reading frame near 47 min on the *E. coli* chromosome. A putative promoter is located 123 bp upstream from the translational start site.

rsd028 from strain HS1028 is mapped to a region spanning two open reading frames and a repetitive DNA sequence is located between. ORF-o361 is the upstream open reading frame and ORF-f500 resides further downstream. Since the sequenced fusion junction reads from the opposite orientation, the σ^s-dependent function is probably the downstream ORF-f500.

rsd042 maps to an open reading frame ORF-f234, oriented in the reverse direction, residing 229 bp downstream of a putative promoter region. Another 476 bp upstream of this promoter is a predicted bend in the DNA structure, a possible determinant for σ^s recognition (Espinosa-Urgel and Tormo, 1993). The *lacZ* fusion of strain HS1077 is mapped to ORF-o394, and is under control of its own promoter.

rsd009 (from strain HS1009) is mapped to a gene *talB* located at 0.2 min, encoding a recently isolated transaldolase homolog of the yeast *talA* gene (Horecker and Smyrniotis, 1955). The protein is 317 amino acids long, and possibly forms a dimer with identical subunits of molecular mass 35 kDa (Sprenger *et al.*, 1995). Little information is known of this newly characterized gene and protein product in *E. coli*. The gene resides upstream of *dnaK* and downstream of the *thrC* gene.

Strain rsd004 (from strain HS1004) mapped to a recently identified *ldcC* gene encoding a lysine decarboxylase. *ldcC* resides downstream from the *accA* gene that encodes a subunit of acetyl-CoA carboxylase (Li and Cronan, 1993). A rho-independent transcriptional terminator is located between the two genes and no putative *ldcC* promoter region was identified. Expression from the *ldcC* gene is thought to be constitutively expressed. This proposal is inconsistent with our

current observations since results from growth-phase expression curves (Appendix A) suggests that rsd004 in HS1004 is growth-phase induced, with an induction ratio of 4.1 in a *rpoS*$^{+}$ background (Table 5). Thus we propose that since *accA* is growth-phase induced (Li and Cronan, 1993), the transcriptional terminator between the two adjacent genes may be leaky, resulting in the growth-phase expression of *ldcC*.

Table 6. Summary of results from the sequencing of selected fusion junctions.

Fusion[a]	Strain[b]	P(N)[c] Probability	Map location (min)	NT[d]	Sequence Description
rsd001	HS1001 (01D04)	6.9×10^{-8}	92	124461	orf o69 downstream from *lex*A, *dinF* genes
rsd002	HS1002 (01E04)	1.0×10^{-15}	92	124482	orf o69 downstream from *lex*A, *dinF* genes
rsd004	HS1004 (02C08)	1.2×10^{-15}	4.3	2985	gene *ldcC*-encoding a lysine decarboxylase similar to lysine decarboxylase *cadA* gene
rsd009	HS1009 (03C06)	6.4×10^{-20}	0.2	8244	*talB* gene encoding a transaldolase
rsd028	HS1028 (08H08)	1.2×10^{-108}	96.8	179509	spanning 3' of orf o361, 5' of orf f500 (opposite orientation)
rsd038	HS1038 (14D08)	4.6×10^{-6}	82	26214	o394, similar to orf near 47 min
rsd042	HS1042 (21B04)	6.7×10^{-15}	78.8	127066	f234 (opposite orientation)
rsd077	HS1077 (36A05)	3.6×10^{-23}	77.6	74895	orf o1037
rsd007	HS1011 (04C07)	no match	---------	---------	---------
rsd073	HS1073 (35F12)	no match	---------	---------	---------

(a) represent designations given to the "*rpoS*-dependent" gene fusions, which correspond to the strain names. Designations in parentheses (b) represent the location of the strain in the library strain collection for laboratory purposes. P(N) is a statistical value obtained from the *E. coli* Genbank searches (c) and is the probability of the submitted sequence matching an unrelated sequence in the database by chance. (NT) represents the position of the first nucleotide of the fusion junction sequenced within the ORF.

Figure 11. Diagrammatic representation of the location of fusion junctions in the *E. coli* chromosome. Approximately two kilobases of flanking regions of seven of the mapped fusion junctions are shown. Putative ORF's and genes are represented by thick black arrows indicating their transcriptional orientation. Thin arrows with open tip and tail are predicted promoter sequences also oriented in the direction of transcription. Stippled thick arrows represent the gene or ORF of the mapped fusion junction. Thin broken arrows indicate the direction of the sequenced fusion junction. Orientation of flanking sequences for HS1004 (whose fusion junction resides in a gene encoding a putative lysine decarboxylase) is currently unavailable.

Calculations of map locations were made based on the reports that 45 kb approximates 1min on the *E. coli* genome. Diagrams were modified from published sources involved in the *E. coli* genome project.

HS1001 (01D04), HS1002 (01E04)
Map Location: 92 min
(modified from Blattner et al., 1993)

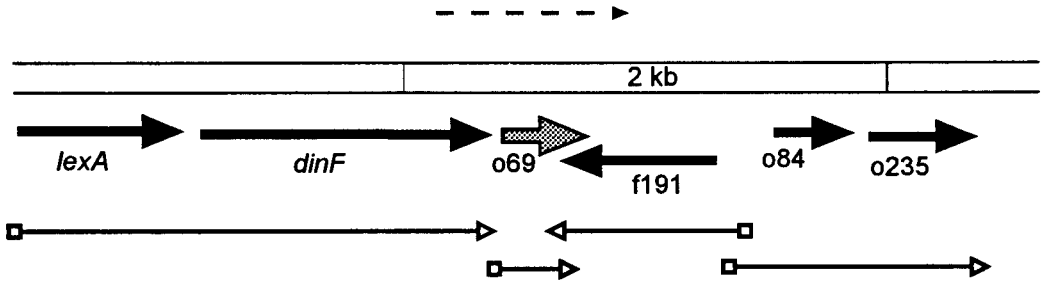

HS1009 (03C06)
Map Location: 0.2 min
(modified from Yura et al., 1992)

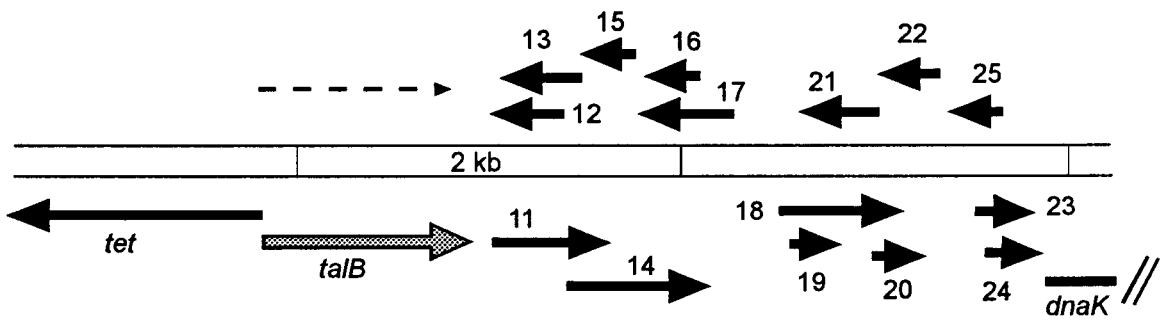

HS1024 (08H08)
Map Location: 96.8 min
(modified from Burland et al., 1995)

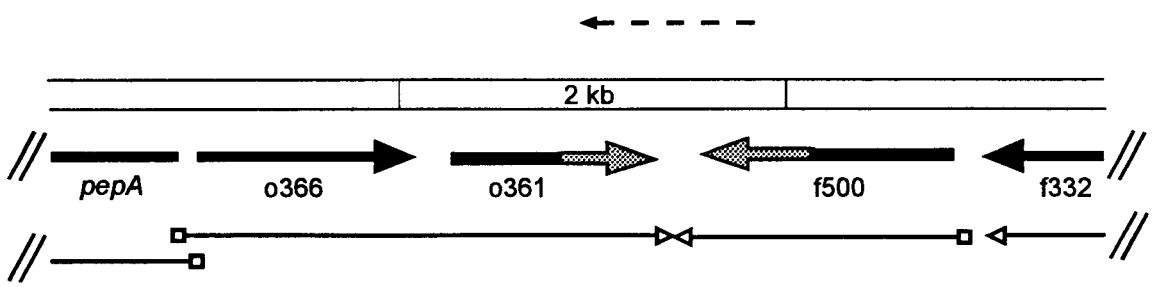

HS1038 (14D08)
Map Location: 82 min
(modified from Burland et al., 1993)

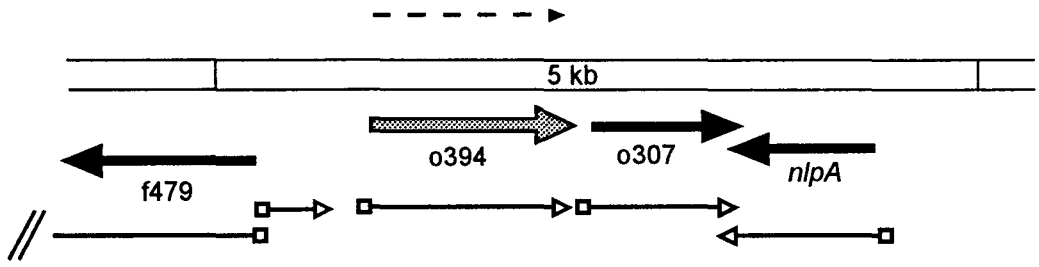

HS1042 (21B04)
Map Location: 78.8 min
(modified from Sofia et al., 1994)

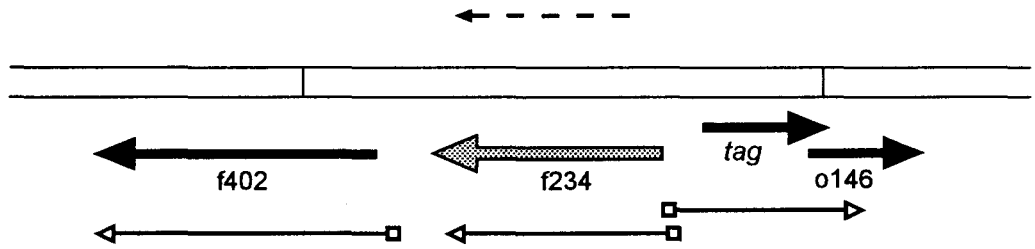

HS1077 (36A05)
Map Location: 77.6 min
(modified from Sofia et al., 1994)

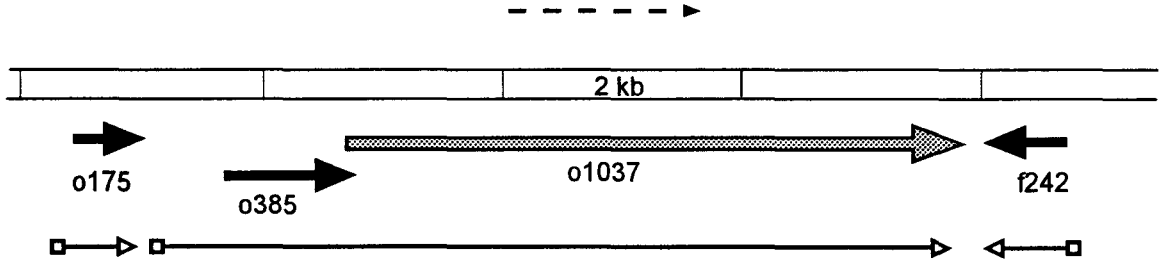

DISCUSSION

Implications of the screening for σ^s-dependent genes

The large-scale isolation of σ^s-dependent genes was accomplished by introducing a *rpoS* null allele into a random library of transcriptional *lacZ* fusion strains and observing for changes in β-galactosidase activity in *rpoS*$^+$ and isogenic *rpoS* mutants. The *rpoS*::Tn10 mutation was introduced into a Hfr strain and subsequently mated into F$^-$ strains. *rpoS*$^+$ and isogenic *rpoS*$^-$ derivatives were replica-plated onto plates containing X-gal and observed for differences in β-galactosidase expression.

Previous methods used to identify σ^s-dependent functions included two-dimensional gel analysis of *rpoS*$^+$ and isogenic *rpoS*$^-$ derivatives, which showed changes in the pattern of protein expression of approximately 30 polypeptides affected in a *rpoS*$^-$ background (McCann *et al.*, 1991). Identification of the regulon using this procedure has several disadvantages. Analysis using this method may underestimate the actual numbers for two reasons. Proteins not highly expressed would be missed under these conditions, and several σ^s-dependent genes may encode subunits to one protein, the latter of which has already been documented. σ^s is required for the expression of the *himA* and *himD/hip* genes that encode subunits of the IHF protein (Aviv *et al.*, 1994). Furthermore, the identification of the gene from the protein product is a laborious procedure and is not a logical method to use, particularly when dealing with large numbers. Two-dimensional gel analysis, however, serves an advantage over other methods, such that it does not mutate genes of interest, contrary to the use of *lacZ* fusions. This would not allow the identification of essential genes, or genes required for viability that is (are) under partial σ^s-control. Although *rpoS* mutants are viable, it does not eliminate the possibility of a role for σ^s in the regulation of an essential gene. Considering the regulatory control of some σ^s-dependent functions in the literature, other global

regulators (possibly including the ones already known, such as LRP, IHF, cAMP and H-NS) may contribute to the regulation of the essential factor.

Random mutagenesis techniques using *lacZ* fusions coupled with the screening for a specific phenotype is an alternative method used for the identification of members of the σ^s-regulon. Although the method has not, in the past, been solely used for the large scale identification of σ^s-dependent genes, it has been useful in the identification of subsets of genes induced under specific growth and environmental conditions. For example, the screening for genes induced under elevated osmolarity (300mM of sodium chloride) reveals that of the many proteins expressed, a subset of these (approximately 18) requires *rpoS* for osmotic induction (Hengge-Aronis *et al.*, 1993). Although this method has the potential to identify large or small subsets using other *rpoS*-associated phenotypes (eg. stationary phase specific heat-shock response, induction under nutrient starvation, and catalase activity), the complexity, diversity and particularly the unrelated function of members of the regulon does not make it a satisfactory method for the large-scale elucidation σ^s-dependent functions. Furthermore, mutations in genes that do not exhibit a specific phenotype and/or respond to a specific environmental or growth condition would be overlooked, such as *osmB* (Jung *et al.*, 1990).

The method we have employed is a novel procedure that does not require any single phenotypic characteristic of *rpoS* mutants. Although a limitation of this procedure is its inability to detect essential functions due to a *lacZ* mutagenesis of the gene of interest, observing for changes in β-galactosidase activity on plates was a simple procedure for our purpose in the large-scale isolation of σ^s-dependent *lacZ* fusions. Visual comparison of maximum levels of β-galactosidase expression in *rpoS*$^+$ and isogenic *rpoS*$^-$ strains can detect as low as two to three-fold reduction in a *rpoS*$^-$ background as confirmed with enzymatic assays (Table 5, see strains HS1020, HS1028 and HS1066). One hundred and five strains bearing σ^s-dependent *lacZ* fusions were isolated after a series of purifications, steps including remating, complementation with pMM*katF3* and transduction into a new GC4468 background as described in Materials and Methods and Results.

Hfr mating is widely used for the transfer of genetic markers between strains. The closer

the marker to the origin of transfer, the more likely of early gene transfer and recombination of the marker into the host DNA. Transfer of genetic material is efficient during the first 30 min of incubation, and interrupting the mating procedure (generally by vortexing) is unnecessary since mating pairs naturally disrupt over time (Miller, 1992). Since our method of introducing the *rpoS*::Tn10 mutation cannot use a mating interruptor, we anticipated a potential problem in the transfer of the *lac*$^+$ allele from Hfr HS180 into the F$^-$ strains. Deletion of the *lac*$^+$ gene, particularly, when dealing with *lac* expression studies of recipient strains should have been done. However, we do not anticipate a serious problem from this oversight. The reasons are that at most, a σ^s-dependent strain may not be detected since the reduction of β-galactosidase expression from the σ^s-dependent *lacZ* fusion would be masked by the expression transferred from the *lac*$^+$ from HS180. Furthermore, we have checked for the frequency of transfer into 24 independent matings by allowing the incubation period to continue for more than two hours. No *lac*$^-$ strains were observed to be *lac*$^+$. A better method for the transfer of the *rpoS*::Tn10 mutation would be the use P1-mediated transduction. P1 transducing particles can carry up to 80 kb of bacterial DNA, equal to approximately 2 min considering 1 min is proportional to 45 kb. This is much less than the amount of donor bacterial DNA introduced into the recipient cell during the conjugation procedure. In addition, *lacZ* fusions may have been transduced into a cell harboring a *rpoS* mutation, thus eliminating the additional step of introducing the *rpoS*::Tn10.

An observation in the mating procedure that warrants mention is the appearance of two β-galactosidase phenotypes arising from a purified, recipient (*rpoS*$^+$) colony. Reproducibly consistent with 18 strains in MC4100 background, it was suspected to be the result of two or more *lacZ* fusions in the *E. coli* chromosome (see Table 3). To decide if this were the case and as a general practice when using *lacZ* expression studies, the *lacZ* fusions were transduced into a GC4468 background and retested for σ^s-dependency. We proposed that if this phenomena is the result of double lysogens, different levels of β-galactosidase expression of transductants would be seen. However, only three strains exhibited this trend (results not shown), suggesting the involvement of other factors. Furthermore, several strains in the new genetic background exhibited two

tranconjugant phenotypes that were not immediately noticed after an overnight incubation, but appeared over several days of expression at room temperature (Appendix B). Due to the slight differences in expression levels, I am convinced that this observation is the result of variations within parental and daughter strains. No other explanations can be proposed at this time, but it can be noted that the characteristics seen were reproducible and limited only to certain strains. Thus, we suggest that the cause of the results be not a random event but once characteristic to only several genotypes.

Since the mating procedure involves the possible introduction of other factors from the Hfr strain genotype (KL16), and since 30 min of incubation time was allowed for gene transfer, then any function within the 30 min of the donor DNA, approximating 1350 kb (1 min equivalent to 45 kb) can be recombined into the host chromosome. One possible explanation for the variation in phenotypes seen after mating in the *rpoS::*Tn10 mutation is the transfer of a specific factor(s) from donor to host DNA affecting the level expression of the reporter fusion. Ideally, the best method for gene transfer would be to exclude all other factors except the marker of interest. Thus, the maximum time of incubation for the introduction of the *rpoS*::Tn10 should have been reduced to 5 to 10 min since a sufficient number of transconjugants were seen at this time. Although this factor(s) is currently unknown, it may influence either expression of the target gene itself or act through *rpoS.*

ppGpp regulates the expression of *rpoS* (Gentry *et al.*, 1993). Synthesized in response to amino acid starvation, the accumulation of ppGpp depends on the expression of the *relA* and *spoT* gene products. The presence of uncharged tRNA's stimulates ppGpp synthesis and its degradation is blocked by the *spoT* gene product (Cashel and Rudd, 1983). The *relA* gene maps to 62.7 min on the *E. coli* chromosome, and is transferred to the recipient strain from the donor. However, this is not a significant cause for concern in the conjugation process since the Hfr parental strain of HS180 (KL16) is *relA*$^-$. The *lacZ* fusions, however, were transduced from a *relA*$^-$ (MC4100) into a *relA*$^+$ (GC4468) background. The effect of ppGpp on *rpoS* expression is debatable considering two factors. The MC4100 (*relA*$^-$)has been used by several laboratories in *rpoS* expression studies

before the implication of ppGpp as a positive regulator (Lange and Hengge-Aronis, 1991a; Diaz-Guerra *et al.*, 1989; Hengge-Aronis and Fischer, 1992) and has not been observed to cause a reduction in *rpoS* as significant as claimed by Gentry and colleagues. The activity of σ^s, measured by the σ^s-dependent *appA* (acid phosphatase) is completely abolished in a *relAspoT* mutant strain (Gentry *et al.*, 1993). Furthermore, catalase activity in both MC4100 and GC4468 visualized on plates is not significantly different (Schellhorn, unpublished data). This is consistent with observations that *relA*$^-$ mutants do not necessarily exhibit a defect in its ability to accumulate ppGpp since lowered levels have been detected, and *relA*-independent ppGpp synthesis is known to occur in *E. coli* (Cashel and Rudd, 1983). Transduction of the *lacZ* fusions into the new background resulted in the subsequent elimination of twenty-seven strains. Though *relA* is not suspected to be the main factor responsible for this result, it does suggest the likely possibility that an unknown factor(s) absent in the new background is required for σ^s-dependent expression. This can be tested by transducing the σ^s-dependent *lacZ* fusions into a new MC4100 strain and testing for σ^s-dependency. Since the elimination of twenty-seven strains from the transduction procedure is still unexplained, it may be noted that complementation of *rpoS*$^-$ derivatives should have been done in GC4468 background.

Overall, despite the problems documented above, we have shown that our method for screening for σ^s-dependent genes in a library of *lacZ* insertion mutants can generate useful information. This procedure can be applied as a general method in the identification of nonessential functions under regulatory control of a regulator for which selectable null alleles can be obtained.

Qualitative screening of σ^s-dependent genes and growth-phase expression curves.

The quantitative screening for σ^s-associated phenotypes using replica-plating was used as a general method to determine the phenotypes exhibited by the interrupted gene. Although this section of the thesis, apart from the isolation of σ^s-dependent *lacZ* fusion mutants and identification of the target gene is not the primary focus, the phenotypic screening does provide a valuable

informative search for characteristics exhibited by the fusion mutants.

Screening for catalase activity and sensitivity to hydrogen peroxide was done by conventional methods. Four catalase negative strains (putative *katE* mutants) were identified by flooding plates with 30% hydrogen peroxide and can be further investigated using a quantitative catalase assay where the breakdown of hydrogen peroxide by a culture of the strain is measured spectrophotometrically. Observing for β-galactosidase expression on plates, is a qualitative screening, the limitations being the ability to detect only mutants exhibiting over a certain magnitude of induction, during carbon starvation, osmotic up-shift, or in the presence of acetate. Carbon starvation inducible genes were previously identified by random *lacZ* mutagenesis (Lange and Hengge-Aronis, 1991a), the method employed in our screening. It may be noted that colonies growing on plates under starvation conditions showed a different color tint compared with plates containing the regular carbon requirements making β-galactosidase activity comparisons difficult. Colonies on starvation plates were blue compared with non-starved colonies that were greenish-blue in tint. All fusions appeared to be induced during these starvation conditions. However, on a conservative note, fourteen strains exhibited a significant level of induction (Table 4).

Observing for osmotic induction of *lacZ* fusion mutants by replica-plating onto media containing increasing levels of sodium chloride has not been the conventional method used. Instead, strains are challenged with an increase in media osmolarity in liquid assays, a more sensitive procedure. Nonetheless, several of our fusions were significantly induced on plates in the presence of 250 mM of sodium chloride. Although this amount may appear close to the specified concentrations in LB media (approximately 243 mM), LB is known to contain compatible solutes such as glycine betaine and proline (reviewed in Csonka, 1989) which is known to inhibit the expression of osmotically-inducible genes, such as *osmY*, when challenged with hyperosmotic stress (Yim and Villarejo, 1992).

Although several fusions were significantly induced and repressed in the presence of elevated acetate concentrations, the mutant containing the *katE::lacZ* fusion (control) was not induced, as previously described in enzymatic assays (Schellhorn and Stones, 1992). Induction on

plates may not be visible due to the limitation in the qualitative screen in that the level of β-galactosidase induction or repression may not be detectable. Furthermore, not all cells are exposed to the same concentrations of the inducing agent, particularly applicable for acetate since the compound can be used by cells as a carbon source (reviewed in Tempest, 1987).

The observation of a deficiency in the production of glycogen of *rpoS* mutants (Hengge-Aronis, 1991a), led to the subsequent identification of a glycogen producing gene, *glgS*, found to be regulated by σ^s (Hengge-Aronis and Fischer, 1992). The screen for mutants deficient in glycogen production was previously performed and is a simple procedure (Lange and Hengge-Aronis, 1991a). Strains replica-plated onto LB-agar are exposed to fumes from iodine crystals for several minutes, and colonies stained brown shows glycogen production (since glycogen binds iodine vapors). Our initial attempts at this procedure were inconclusive due to uneven exposure of the plate to iodine vapors. Furthermore, the procedure did not seem sensitive since a *rpoS*::Tn10 control (HS143) did not look deficient in glycogen accumulation than other control strains capable of producing its production (eg. MC4100, GC4468).

Near-UV and far-UV exposure to identify genes involved in cellular repair mechanisms cannot be performed directly. This is because the λp*lac*Mu53 construct can be excised using UV irradiation, the method employed for the isolation of λ DNA.

The stationary phase response protects cells against exposure to heat shock, a thermotolerance that increases the further cells progress into stationary phase (Jenkins *et al.*, 1988). *rpoS*$^-$ mutants are sensitive to heat challenge at 55-57°C (Lange and Hengge-Aronis, 1991a; McCann *et al.*, 1991). Though not performed on the isolated σ^s-dependent *lacZ* fusion mutants, I have tested several control strains including MC4100 (wt), GC4468 (wt), NC4468 (*katE::lacZ*) and HS143 (*katF::lacZ*). Aliquots of an overnight culture were resuspended in M9 liquid media and exposed to 55°C for 5 min. Viability was determined by colony counts the next day. As expected, HS143 (*katF::lacZ*) exhibited a decrease in viability, consistent with previous publications (Lange and Hengge-Aronis, 1991a; McCann *et al.*, 1991). Future work may include the screening of heat-shock sensitive strains of the σ^s-dependent *lacZ* fusion mutants.

The growth-phase expression data of fusion mutants in GC4468 background (Appendix A) provided an informative screen of the general pattern of gene expression. Results showed that all mutants showed a strain-specific induction during entry into stationary phase, consistent with what is known of members of the σ^s-regulon. A possible concern regarding the data is the difference in expression when certain strains were reassayed. It can be suggested that the different spectrophotometers used accounts for some fraction of the error besides the fact that the assays were done by independent technicians. However, if this were the case, the maximum and minimum values should be proportionally different and the induction ratios and σ^s dependence should be similar. Since the induction ratio is calculated by the maximum level obtained in the β-galactosidase assay divided by the minimum value or basal level at the onset of the experiment, if basal levels are not reached, the value of the induction ratio will be less than the expected. Since β-galactosidase levels are lower in exponential phase than in stationary phase, slight fluctuations will have a greater effect on induction ratio levels than fluctuations in starvation. In addition, the maximum and minimum values were determined by a single point on the growth induction curve, thus increasing the impact of possible incorrect readings. A better estimation of the induction ratio and σ^s-dependence would be to designate exponential and stationary phase OD(600 nm) parameters and take the minimum and maximum values as the average of 3 or 4 points. This will decrease the likelihood of spurious results having a great impact on values. A problem with this method is, for the sake of keeping consistency, the rigid parameters set do not provide the flexibility required considering the diversity of the σ^s regulon, as seen in the induction pattern of the mutants. These growth curve experiments were only assayed once, thus the experiments would have to be duplicated to resolve present discrepancies. Nonetheless, the data provides valuable information regarding the general expression of fusion mutants. The precise growth-curve expression data, for example, the point of induction into stationary phase or maximum levels attained can be examined later when dealing with individual fusion mutants.

Sequencing of the fusion junctions.

Subsequent sequencing of the fusion junctions have shown σ^s-dependent functions mapping to putative open reading frames coding for yet unknown proteins. These results confirm the general proposal that the several members of the σ^s-regulon have yet to be identified. Although our sequencing results have not been mapped to a known σ^s-dependent gene, the reliability of our procedure has been shown by mapping our phenotypically screened laboratory *katE* and *rpoS* mutant strains to their respective regions as previously described (Roy *et al.*, 1995). Two fusions have mapped to putative genes in the *E. coli* chromosome encoding proteins with predicted functions and six others have mapped to ORF's encoding proteins of unknown function. It may be noted that there were no direct matches with sequences from the database. While some showed good a sequence match to a specific locus in the *E. coli* genome, others were questionable to the extent that resequencing of the fusion junction may be required (Appendix E).

The transaldolase (TAL) enzyme is involved in the catabolism of pentose sugars (D-xylose, D-ribose, and L-arabinose) in the pentose phosphate cycle. As one of the central metabolic pathways, the pentose phosphate cycle produces the pentose phosphates that are precursors to ribose and deoxyribose in the formation of nucleic acids (reviewed in White, 1995). Furthermore the catabolic production of erythrose phosphate is the precursor to aromatic amino acids (phenylalanine, tyrosine, and tryptophan), and NADPH is a source of electrons for biosynthetic reduction (reviewed in White, 1995). Our *lacZ* fusion, rsd009 from strain HS1009, maps to the recently identified *talB* gene located at 0.2 min on the *E. coli* chromosome (Sprenger *et al.*, 1995). The *talB* gene encodes an enzyme TAL B of molecular weight 70 kD, and is the second transaldolase protein identified in *E. coli*. The first isolated transaldolase, TAL A, was initially identified by reacting *E. coli* with TAL antibodies raised against the TAL A yeast enzyme (Sprenger, *et al.*, 1995), but the gene responsible for its production has not been identified. Little is known about the transaldolase enzymes or the mechanism of gene expression in *E coli*. Furthermore, mutants that lack TAL have not yet been reported, thus a phenotype(s) for TAL-deficient mutants is unknown. Given the function of transaldolase in the pentose phosphate cycle, however, we suspect

that TAL-deficient mutants are incapable of growing on the pentose sugars (D-xylose, D-ribose, L-arabinose). The issue is complicated by the fact that the TAL A gene has not been identified, and mutations in each transaldolase-encoding gene will be required to study the relative contributions of each to the pentose phosphate pathway in *E. coli*.

The mutant HS1004 carrying the *lacZ* fusion, rsd1004, maps to 4 min on the *E. coli* chromosome to a presumptive, constitutively expressed gene designated *ldcC*, which encodes a presumptive lysine decarboxylase. Located downstream from the *accA*-encoding acetyl-CoA carboxylase (Li and Cronan, 1993), information obtained from the nucleotide databases (Genbank) report the presence of a rho-independent transcriptional termination site located between *accA* and *ldcC* and similarities of the uncharacterized *ldcC* gene to the *cadA* gene, which encodes a lysine decarboxylase. Little is known about the *ldcC* gene itself, but by homology to the *cadA* gene, its gene product may suggest a possible function(s) of the σ^s-dependent *ldcC* gene.

The *cadA* gene maps to 93.5 min on the *E. coli* chromosome (Auger *et al.*, 1989), upstream from the *cadB* gene-encoding a lysine/cadaverine transporter, and the two genes comprise an operon (Meng and Bennett, 1992a). The product of *cadA* is lysine decarboxylase, 715 amino acids in length (Meng and Bennett, 1992a) which converts L-lysine into cadaverine and carbon dioxide. The expression of the *cad* operon is induced under several conditions including low external pH, aerobiosis, presence of lysine (Meng and Bennett, 1992a,b), and low carbon dioxide or is derivatives (Takayama *et al.*, 1994). The *cadA* gene is suggested to play a physiological role of increasing the pH of the medium by converting lysine from the medium into cadaverine. This process involves the shuttling of H^+ ions and lysine from the medium by the *cadB*-encoding lysine/cadaverine transporter to be converted to cadaverine and carbon dioxide by the cell. The excess cadaverine is removed from the cell into the environment by the transporter (Meng and Bennett, 1992a). Stimulation of expression from the *cad* operon during anaerobiosis and low carbon dioxide levels may help fulfill a metabolic need for carbon dioxide that, under aerobic conditions, is supplied by the TCA cycle. Given that the TCA cycle is tightly linked to the respiratory chain, it is reasonable that a metabolite is a regulator of the metabolic pathway involved in its

production (Takayama *et al.*, 1994). As a result, the *cadA* gene product is also suggested to be involved in the control of intracellular carbon dioxide required for bacterial growth (Boeker and Snell, 1972).

Two enzyme forms of lysine decarboxylase is suggested to exist in *E. coli*, an inducible, thermostable protein (documented above) and a constitutively expressed, thermosensitive protein (Goldemberg, 1980). Only the inducible form has been isolated and characterized. Information obtained from genomic databases (Genbank) suggests that *ldcC* is constitutively expressed based on previous reports that a constitutively expressed gene does exist. Results from our growth-phase expression assays of the σ^s-dependent fusion mutants, however, shows a clear induction of the *ldcC::lacZ* fusion during entry into stationary phase, characteristic of genes regulated by σ^s (Appendix A). This may suggest that the information concerning constitutive expression of *ldcC* is incorrect, or that our results may be explained in terms of a leaky transcriptional terminator, and induction of expression during entry into stationary phase is the result of read-through transcription from the upstream growth-phase induced *accA* gene (Li and Cronan, 1993). The latter suggest that growth-phase induction of HS1004 is not the result of σ^s, an unlikely possibility given that a mutation in *rpoS* resulted in a decrease in expression from the reporter fusion (Table 6). Unfortunately, the phenotype associated with a mutated *cadA* gene is not precisely known since more than one lysine decarboxylase-encoding gene is presumed to exist in *E. coli* (Goldemberg, 1980), thus a phenotypic screen for the mutation caused by the fusion insertion is not currently possible. Expression of the fusion, however, in conditions to which the inducible form of lysine decarboxylase is induced may serve as a preliminary screen. Nonetheless, future work is required to confirm the σ^s-dependent functions.

Although it appears to be a systematic approach, we have encountered problems during this final stage of sequencing. λ DNA has been isolated, purified, visualized on gels and cut with restriction endonucleases as described in Materials and Methods. However, clean sequence has been difficult to obtain on a systematic basis. Other than problems encountered with technical

work, we have not been able to effectively employ the primer obtained from the Mu S end based on a 48 bp duplication during the initial construction of the λp*lac*Mu53 phage (Roy *et al.*, 1995). Use of this primer might simplify the procedure since PCR amplification would be a possibility, as opposed to cycle sequencing using only the Mu c end primer. Furthermore, upstream sequences would identify the σ^s-dependent function just as well as our method currently employed, and provide additional information of potential upstream elements affecting expression and promoter sequences directing the *lacZ* fusions. Identifying the gene or open reading frame of the fusion insertion, however, may not explicitly imply that it is the σ^s-dependent function of interest. For the purpose of our general analysis, the immediate upstream promoter is the taken to be the most likely transcriptional activator of the target gene. Nevertheless, the possibility does exist where a σ^s-dependent promoter of an upstream gene is responsible for the expression of the downstream *lacZ* target gene. Consequently, the σ^s-dependent gene in which the reporter phage resides may not be the gene of interest. Further analysis, such as screening for a known phenotype associated with a mutant of the particular target gene, or a direct mutagenesis study using a Tn10, would be required. The work presented thus far sets the initial purpose of the project that is far from completion. Undoubtedly, the main bulk of future work involves the sequencing of the remaining σ^s-dependent genes and subsequent verification of σ^s-dependency on a more specific basis.

CONCLUSION

- The isolation of σ^s-dependent genes from a random library of *lacZ* fusion mutants was done by mating a *rpoS*::Tn10 mutation into F^- recipients and observing for changes in expression in *rpoS*$^+$ and isogenic *rpoS*$^-$ derivates.
- 105 mutants were isolated after a series of purifications, rematings and transduction into a new GC4468 background.
- σ^s-dependency was confirmed by complementing the *rpoS* mutation with a plasmid bearing a functional *rpoS* gene. Results show that 73 were complemented with respect to β-galactosidase expression and catalase activity, and 4 were not complemented with either one or the other. Complementation results were not done for 28 strains.
- Growth-phase expression experiments reveal that all strains assayed exhibit induction during entry into stationary phase, and this induction is reduced in a *rpoS*$^-$ derivative. Twelve *rpoS*$^-$ strains assayed exhibited induction into stationary phase in the absence of *rpoS* suggesting other factors involved in stationary-phase induction.
- Sequencing of selected fusion junctions showed that two do not map to any known region in the *E. coli* chromosome, and six map to open reading frames encoding proteins of unknown function.
- One fusion maps to a putative *ldcC* gene that is located at 4 min, and shows similarity to the *cadA* gene. By sequence homology, *ldcC* is suggested to encode a lysine decarboxylase suggested to function as a regulator of medium pH and levels of cellular carbon dioxide
- Another fusion maps to a recently identified *talB* gene encoding a transaldolase. Located at 0.2 min on the *E. coli* chromosome, the gene product is involved in the pentose phosphate cycle. Substrates in this cycle are precursors to nucleic acids, vitamins and aromatic amino acids
- The method we have employed in the large-scale identification of the σ^s-regulon is phenotype-

independent and can be applied to the identification of other regulon members providing that null alleles of the regulator is available.

- The work presented currently sets the foundation for future work in sequencing the remainder of the σ^s-regulon and specific characterization of the function.

APPENDICES

Appendix A. Raw data of growth-phase expression curves of 102 *rpoS*$^{+}$ recipients in GC4468 background. Three strains (HS1021, HS1097, HS1102) were not assayed.

[1000 x OD(420 nm)] / [Rxn Time (min) x Volume Assayed (ml) x OD(600 nm)]

Calculation for Total Activity:

[Specific Activity x OD(600 nm)]

Time 7 h represents an overnight cultured assayed. All data in Appendix A was generated by Suzana Gligorijevic.

Strain	Time [h]	OD600 [nm]	Rxn Time [min]	Cell Vol [ml]	OD420 [nm] sample1	OD420 [nm] sample2	Avg.	Specific Activity [Miller U]	Total Activity [Miller U]
HS1001	0	0.059	6	2	0.049	0.052	0.045	62.9	3.7
[01D04]	0.5	0.092	6	2	0.071	0.076	0.068	61.1	5.6
	1	0.181	6	2	0.097	0.091	0.088	40.5	7.3
	1.5	0.294	6	2	0.130	0.141	0.130	36.7	10.8
	2	0.480	6	2	0.305	0.291	0.292	50.7	24.3
	2.5	0.940	6	1	0.494	0.568	0.525	93.1	87.5
	3	1.200	6	1	0.766	0.736	0.745	103.5	124.2
	4	1.290	6	1	1.273	1.340	1.301	168.0	216.8
	5	1.610	6	1	1.561	1.533	1.541	159.5	256.8
	6	2.090	6	1	1.752	1.761	1.751	139.6	291.8
	7	3.850	2	1	0.525	0.583	0.548	71.2	274.0

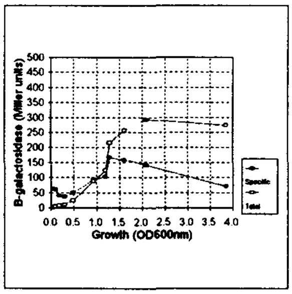

HS1002	0	0.052	6	2	0.054	0.054	0.048	76.9	4.0
[01E04]	0.5	0.082	6	2	0.070	0.075	0.067	67.6	5.5
	1	0.163	6	2	0.095	0.094	0.089	45.2	7.4
	1.5	0.279	6	2	0.125	0.122	0.118	35.1	9.8
	2	0.431	6	2	0.225	0.349	0.281	54.3	23.4
	2.5	0.820	6	1	0.522	0.539	0.525	106.6	87.4
	3	0.930	6	1	0.863	0.830	0.841	150.6	140.1
	4	1.320	6	1	1.372	1.260	1.310	165.4	218.3
	5	1.460	6	1	1.655	1.642	1.643	187.5	273.8
	6	1.740	6	1	1.811	1.667	1.733	166.0	288.8
	7	3.960	2	1	0.585	0.551	0.562	71.0	281.0

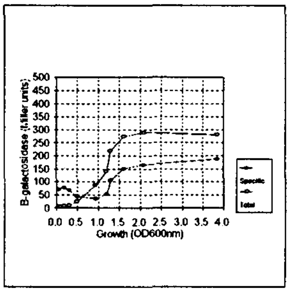

HS1003	0	0.063	6.5	2	0.049	0.047	0.042	51.3	3.2
[01H01]	0.5	0.092	6.5	2	0.048	0.046	0.041	34.3	3.2
	1	0.192	6.5	2	0.054	0.054	0.048	19.2	3.7
	1.5	0.323	6.5	2	0.069	0.070	0.064	15.1	4.9
	2	0.472	6.5	2	0.300	0.251	0.270	43.9	20.7
	2.5	0.760	6.5	1	0.347	0.358	0.347	70.1	53.3
	3	0.950	6.5	1	0.412	0.379	0.390	63.1	59.9
	4	1.310	6.5	1	0.513	0.509	0.505	59.3	77.7
	5	1.630	6.5	1	0.572	0.744	0.652	61.5	100.3
	6	2.110	6.5	1	0.766	0.630	0.692	50.5	106.5
	7	3.720	3	1	0.733	0.778	0.750	67.2	249.8

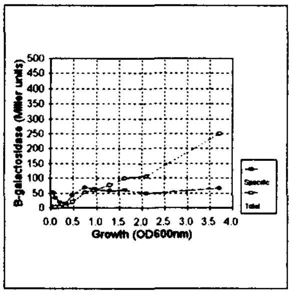

HS1004	0	0.065	7	2	0.052	0.053	0.047	51.1	3.3
[02C08]	0.5	0.106	7	2	0.054	0.053	0.048	32.0	3.4
	1	0.199	7	2	0.065	0.069	0.061	21.9	4.4
	1.5	0.348	7	2	0.080	0.080	0.074	15.2	5.3
	2	0.598	7	2	0.225	0.224	0.219	26.1	15.6
	2.5	0.830	7	1	0.373	0.364	0.363	62.4	51.8
	3	0.930	7	1	0.341	0.346	0.338	51.8	48.2
	4	1.170	7	1	0.414	0.374	0.388	47.4	55.4
	5	1.510	7	1	0.447	0.478	0.457	43.2	65.2
	6	1.820	7	1	0.543	0.527	0.529	41.5	75.6
	7	3.560	3	1	0.619	0.557	0.582	54.5	194.0

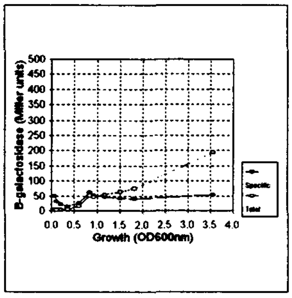

HS1005	0	0.050	7	2	0.051	0.049	0.044	62.9	3.1
[02D11]	0.5	0.072	7	2	0.057	0.052	0.049	48.1	3.5
	1	0.161	7	2	0.055	0.055	0.049	21.7	3.5
	1.5	0.275	7	2	0.069	0.058	0.058	14.9	4.1
	2	0.409	7	2	0.118	0.119	0.113	19.6	8.0
	2.5	0.790	7	1	0.218	0.203	0.205	37.0	29.2
	3	1.000	7	1	0.314	0.304	0.303	43.3	43.3
	4	1.230	7	1	0.631	0.600	0.610	70.8	87.1
	5	1.630	7	1	1.088	1.071	1.074	94.1	153.4
	6	2.200	7	1	1.410	1.508	1.453	94.4	207.6
	7	4.150	2	1	0.819	0.875	0.841	101.3	420.5

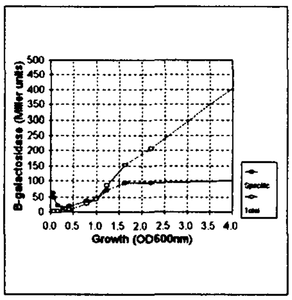

Strain	Time [h]	OD600 [nm]	Rxn Time [min]	Cell Vol [ml]	OD420 [nm] sample1	OD420 [nm] sample2	Avg.	Specific Activity [Miller U]	Total Activity [Miller U]
HS1006	0	0.043	1339	2	0.242	0.246	0.238	2.1	0.1
[02E11]	0.5	0.063	1339	2	0.314	0.305	0.304	1.8	0.1
	1	0.129	1339	2	0.383	0.389	0.380	1.1	0.1
	1.5	0.256	1339	2	0.547	0.571	0.553	0.8	0.2
	2	0.361	215	2	0.349	0.377	0.357	2.3	0.8
	2.5	0.690	211	1	0.595	0.630	0.607	4.2	2.9
	3	0.920	19	1	0.795	0.843	0.813	46.5	42.8
	4	1.440	3	1	0.568	0.520	0.538	124.5	179.3
	5	1.870	3	1	0.884	0.919	0.896	159.6	298.5
	6	2.350	3	1	1.285	1.249	1.261	178.9	420.3
	7	4.020	2	1	0.930	0.991	0.955	118.7	477.3
HS1007	0	0.047	1339	2	0.288	0.294	0.285	2.3	0.1
[02E12]	0.5	0.077	1339	2	0.415	0.375	0.389	1.9	0.1
	1	0.159	1339	2	0.485	0.492	0.483	1.1	0.2
	1.5	0.290	1339	2	0.651	0.752	0.696	0.9	0.3
	2	0.417	215	2	0.521	0.522	0.516	2.9	1.2
	2.5	0.700	24	1	0.544	0.424	0.478	28.5	19.9
	3	0.850	10	1	0.535	0.873	0.698	82.1	69.8
	4	1.210	2.5	1	0.357	0.287	0.316	104.5	126.4
	5	1.630	2.5	1	0.450	0.482	0.460	112.9	184.0
	6	2.390	2.5	1	0.677	0.651	0.658	110.1	263.2
	7	3.890	2	1	0.729	0.817	0.767	98.6	383.5
HS1008	0	0.063	1311	2	0.405	0.396	0.395	2.4	0.2
[02H06]	0.5	0.098	1311	2	0.429	0.437	0.427	1.7	0.2
	1	0.207	1311	2	0.480	0.503	0.486	0.9	0.2
	1.5	0.342	1311	2	0.746	0.762	0.748	0.8	0.3
	2	0.519	187	2	0.596	0.572	0.578	3.0	1.5
	2.5	0.950	4	1	0.282	0.231	0.251	65.9	62.6
	3	1.080	3	1	0.356	0.400	0.372	114.8	124.0
	4	1.340	3	1	0.277	0.281	0.273	67.9	91.0
	5	1.750	3	1	0.376	0.453	0.409	77.8	136.2
	6	2.550	3	1	0.485	0.586	0.530	69.2	176.5
	7	3.960	2	1	1.097	1.201	1.143	144.3	571.5
HS1009	0	0.062	1311	2	1.187	1.190	1.183	7.3	0.5
[03C06]	0.5	0.105	1311	2	0.431	0.431	0.425	1.5	0.2
	1	0.188	298	2	0.592	0.561	0.571	5.1	1.0
	1.5	0.321	298	2	0.835	0.807	0.815	4.3	1.4
	2	0.491	120	2	1.199	1.301	1.244	10.6	5.2
	2.5	0.890	3	1	0.199	0.209	0.198	74.2	66.0
	3	1.040	2	1	0.474	0.305	0.384	184.4	191.8
	4	1.380	2	1	0.557	0.576	0.561	203.1	280.3
	5	1.700	2	1	0.699	0.634	0.661	194.3	330.2
	6	2.080	2	1	0.903	0.614	0.753	180.9	376.3
	7	4.120	2	1	0.690	0.802	0.740	89.8	370.0
HS1010	0	0.059	1311	2	0.343	0.369	0.350	2.3	0.1
[03F05]	0.5	0.092	1311	2	0.408	0.385	0.391	1.6	0.1
	1	0.187	1311	2	0.506	0.502	0.498	1.0	0.2
	1.5	0.310	1311	2	0.798	0.727	0.757	0.9	0.3
	2	0.480	187	2	0.509	0.533	0.515	2.9	1.4
	2.5	0.840	2	1	0.335	0.352	0.338	200.9	168.8
	3	1.230	2	1	0.663	0.662	0.657	266.9	328.3
	4	1.340	2	1	1.070	1.051	1.055	393.5	527.3
	5	1.780	2	1	1.201	1.215	1.202	337.6	601.0
	6	2.080	2	1	1.380	1.143	1.256	301.8	627.8
	7	3.890	2	1	0.931	0.865	0.892	114.7	446.0

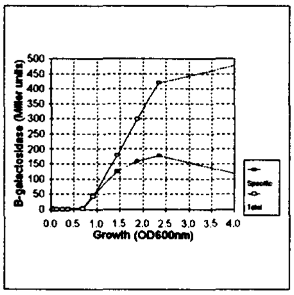

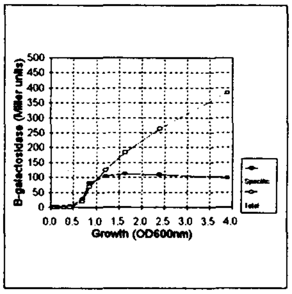

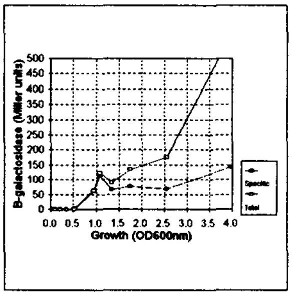

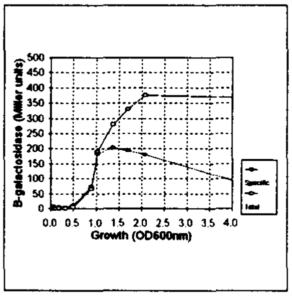

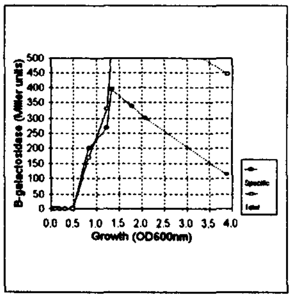

Strain	Time [h]	OD600 [nm]	Rxn Time [min]	Cell Vol [ml]	OD420 [nm] sample1	OD420 [nm] sample2	Avg.	Specific Activity [Miller U]	Total Activity [Miller U]	
HS1011	0	0.060	146	2	0.436	0.432	0.428	24.4	1.5	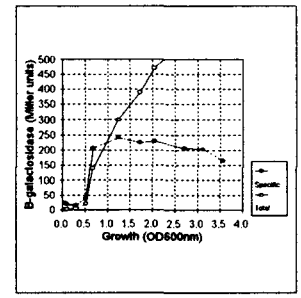
[04C7-d]	0.5	0.111	125	2	0.597	0.489	0.537	19.4	2.1	
	1	0.300	63	2	0.626	0.588	0.601	15.9	4.8	
	1.5	0.523	22	2	0.919	0.889	0.898	39.0	20.4	
	2	0.679	2	2	0.565	0.573	0.563	207.3	140.7	
	2.5	1.240	2	1	0.517	0.695	0.600	241.9	300.0	
	3	1.720	2	1	0.753	0.818	0.780	226.6	389.8	
	4	2.040	2	1	0.941	0.955	0.942	230.9	471.0	
	5	2.700	2	1	1.143	1.106	1.119	207.1	559.3	
	6	3.110	2	1	1.346	1.195	1.265	203.3	632.3	
	7	3.560	2	1	0.876	1.503	1.184	166.2	591.8	
HS1012	0	0.056	510	2	0.364	0.395	0.374	6.5	0.4	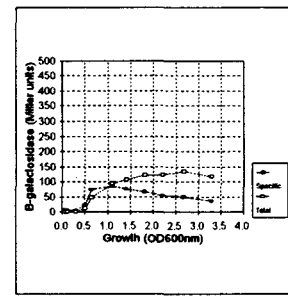
[04D09]	0.5	0.116	510	2	0.591	0.515	0.547	4.6	0.5	
	1	0.304	146	2	0.410	0.390	0.394	4.4	1.3	
	1.5	0.506	38	2	0.869	0.957	0.907	23.6	11.9	
	2	0.650	6	2	0.599	0.571	0.579	74.2	48.3	
	2.5	1.100	6	1	0.601	0.540	0.565	85.5	94.1	
	3	1.410	6	1	0.667	0.644	0.650	76.8	108.3	
	4	1.820	6	1	0.711	0.769	0.734	67.2	122.3	
	5	2.210	6	1	0.759	0.716	0.732	55.2	121.9	
	6	2.670	6	1	0.814	0.812	0.807	50.4	134.5	
	7	3.290	4	1	0.515	0.443	0.473	35.9	118.3	
HS1013	0	0.048	1390	2	0.168	0.197	0.177	1.3	0.1	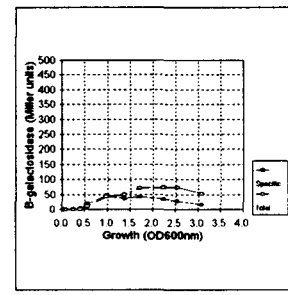
[04F8-d]	0.5	0.088	1390	2	0.311	0.238	0.269	1.1	0.1	
	1	0.248	510	2	0.306	0.351	0.323	1.3	0.3	
	1.5	0.413	146	2	0.330	0.365	0.342	2.8	1.2	
	2	0.563	38	2	0.894	0.873	0.878	20.5	11.5	
	2.5	0.960	8	1	0.369	0.343	0.350	45.6	43.8	
	3	1.370	8	1	0.417	0.399	0.402	36.7	50.3	
	4	1.700	8	1	0.571	0.601	0.580	42.6	72.5	
	5	2.230	8	1	0.645	0.580	0.607	34.0	75.8	
	6	2.540	8	1	0.591	0.612	0.596	29.3	74.4	
	7	3.070	10	1	0.519	0.557	0.532	17.3	53.2	
HS1014	0	0.047	1390	2	0.384	0.365	0.369	2.8	0.1	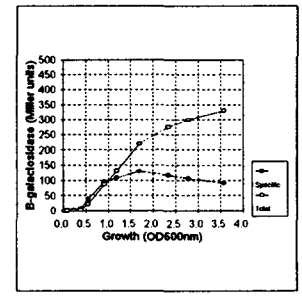
[05A10]	0.5	0.089	1390	2	0.555	0.551	0.547	2.2	0.2	
	1	0.230	510	2	0.464	0.422	0.437	1.9	0.4	
	1.5	0.391	125	2	0.603	0.612	0.602	6.2	2.4	
	2	0.554	22	2	0.941	0.911	0.920	37.7	20.9	
	2.5	0.920	4	1	0.423	0.293	0.352	95.7	88.0	
	3	1.190	4	1	0.564	0.492	0.522	109.7	130.5	
	4	1.690	4	1	0.883	0.886	0.879	130.0	219.6	
	5	2.340	4	1	1.024	1.198	1.105	118.1	276.3	
	6	2.780	4	1	1.218	1.184	1.195	107.5	298.8	
	7	3.580	3	1	1.083	0.910	0.991	92.2	330.2	
HS1015	0	0.056	1390	2	0.172	0.182	0.171	1.1	0.1	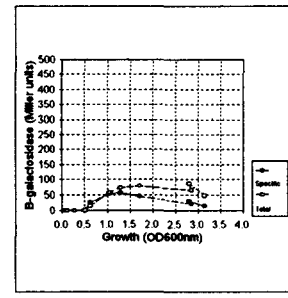
[05C08]	0.5	0.110	1390	2	0.255	0.243	0.243	0.8	0.1	
	1	0.275	1390	2	0.606	0.388	0.491	0.6	0.2	
	1.5	0.504	126	2	0.336	0.351	0.338	2.7	1.3	
	2	0.620	22	2	0.775	0.699	0.731	26.8	16.6	
	2.5	1.050	7	1	0.419	0.397	0.402	54.7	57.4	
	3	1.290	7	1	0.521	0.506	0.508	56.2	72.5	
	4	1.710	7	1	0.588	0.526	0.551	46.0	78.7	
	5	2.850	7	1	0.601	0.324	0.457	22.9	65.2	
	6	2.800	7	1	0.630	0.598	0.608	31.0	86.9	
	7	3.140	10	1	0.496	0.482	0.483	15.4	48.3	

Strain	Time [h]	OD600 [nm]	Rxn Time [min]	Cell Vol [ml]	OD420 [nm] sample1	OD420 [nm] sample2	OD420 [nm] Avg.	Specific Activity [Miller U]	Total Activity [Miller U]	
HS1016	0	0.041	108	2	0.342	0.304	0.317	35.8	1.5	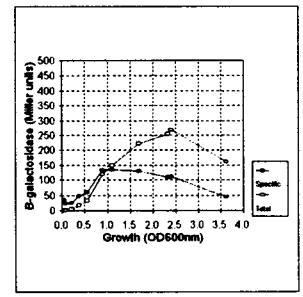
[06A12]	0.5	0.076	108	2	0.375	0.393	0.378	23.0	1.8	
	1	0.206	46	2	0.491	0.474	0.477	25.1	5.2	
	1.5	0.372	21	2	0.779	0.750	0.759	48.5	18.1	
	2	0.555	18	2	1.212	1.206	1.203	60.2	33.4	
	2.5	0.890	4	1	0.495	0.473	0.478	134.3	119.5	
	3	1.110	4	1	0.593	0.618	0.600	135.0	149.9	
	4	1.690	4	1	0.881	0.907	0.888	131.4	222.0	
	5	2.330	4	1	1.015	1.035	1.019	109.3	254.7	
	6	2.400	4	1	1.193	0.966	1.074	111.8	268.4	
	7	3.620	4	1	0.655	0.651	0.647	44.7	161.8	
HS1017	0	0.052	109	2	0.431	0.432	0.426	37.5	2.0	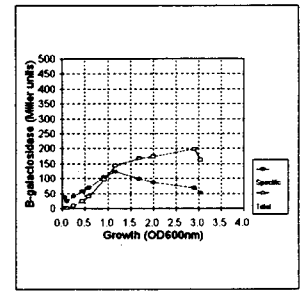
[06C03-d]	0.5	0.100	108	2	0.550	0.493	0.516	23.9	2.4	
	1	0.245	27	2	0.542	0.538	0.534	40.4	9.9	
	1.5	0.434	18	2	0.958	0.859	0.903	57.8	25.1	
	2	0.583	18	2	1.441	1.469	1.449	69.0	40.3	
	2.5	0.920	4	1	0.409	0.373	0.385	104.6	96.3	
	3	1.160	4	1	0.514	0.643	0.573	123.4	143.1	
	4	1.690	4	1	0.757	0.600	0.673	99.5	168.1	
	5	2.000	4	1	0.740	0.668	0.698	87.3	174.5	
	6	2.900	4	1	0.870	0.729	0.794	68.4	198.4	
	7	3.040	4	1	0.702	0.614	0.652	53.6	163.0	
HS1018	0	0.064	493	2	0.588	0.567	0.572	9.1	0.6	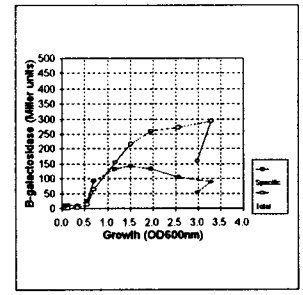
[06E01-d]	0.5	0.124	109	2	0.320	0.328	0.318	11.8	1.5	
	1	0.339	93	2	0.578	0.590	0.578	9.2	3.1	
	1.5	0.547	27	2	0.719	0.801	0.754	25.5	14.0	
	2	0.692	8	2	1.031	1.040	1.030	93.0	64.3	
	2.5	1.170	4	1	0.669	0.586	0.622	132.8	155.4	
	3	1.510	4	1	0.802	0.944	0.867	143.5	216.7	
	4	1.960	4	1	1.027	1.067	1.041	132.8	260.3	
	5	2.560	4	1	1.134	1.046	1.084	105.9	271.0	
	6	3.290	4	1	1.314	1.046	1.174	89.2	293.5	
	7	2.980	4	1	0.609	0.682	0.640	53.6	159.9	
HS1019	0	0.058	493	2	0.447	0.561	0.498	8.7	0.5	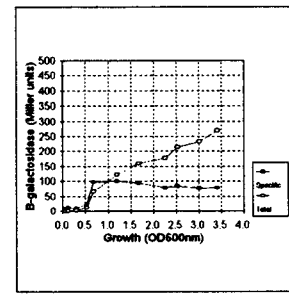
[06E01-l]	0.5	0.114	109	2	0.274	0.295	0.279	11.2	1.3	
	1	0.299	93	2	0.526	0.489	0.502	9.0	2.7	
	1.5	0.525	27	2	0.725	0.669	0.691	24.4	12.8	
	2	0.675	8	2	1.048	1.084	1.060	98.1	66.3	
	2.5	1.200	4	1	0.504	0.485	0.489	101.8	122.1	
	3	1.680	4	1	0.638	0.653	0.640	95.2	159.9	
	4	2.260	4	1	0.760	0.679	0.714	78.9	178.4	
	5	2.530	4	1	0.913	0.811	0.856	84.6	214.0	
	6	3.010	4	1	0.965	0.919	0.936	77.7	234.0	
	7	3.410	3	1	0.751	0.879	0.809	79.1	269.7	
HS1020	0	0.061	93	2	0.407	0.400	0.398	35.0	2.1	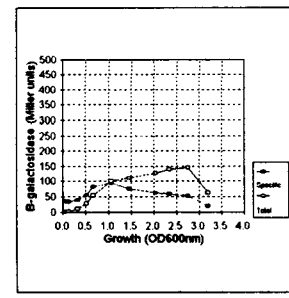
[07A08]	0.5	0.124	46	2	0.370	0.379	0.369	32.3	4.0	
	1	0.317	27	2	0.659	0.658	0.653	38.1	12.1	
	1.5	0.515	18	2	1.028	1.047	1.032	55.6	28.7	
	2	0.660	8	2	0.884	0.863	0.868	82.1	54.2	
	2.5	1.060	5	1	0.554	0.464	0.503	94.9	100.6	
	3	1.460	5	1	0.537	0.586	0.556	76.1	111.1	
	4	2.040	5	1	0.591	0.686	0.633	62.0	126.5	
	5	2.350	5	1	0.675	0.726	0.695	59.1	138.9	
	6	2.750	5	1	0.747	0.721	0.728	52.9	145.6	
	7	3.200	10	1	0.643	0.621	0.626	19.6	62.6	

Strain	Time [h]	OD600 [nm]	Rxn Time [min]	Cell Vol [ml]	OD420 [nm] sample1	OD420 [nm] sample2	OD420 [nm] Avg.	Specific Activity [Miller U]	Total Activity [Miller U]
HS1022	0	0.035	1512	2	0.080	0.091	0.071	0.7	0.0
[07B09]	0.5	0.072	1512	2	0.211	0.215	0.198	0.9	0.1
	1	0.172	1512	2	0.442	0.450	0.431	0.8	0.1
	1.5	0.357	97	2	0.224	0.234	0.214	3.1	1.1
	2	0.593	33	2	0.402	0.417	0.395	10.1	6.0
	2.5	1.070	7	1	0.394	0.345	0.355	47.3	50.6
	3	1.450	7	1	0.431	0.514	0.458	45.1	65.4
	4	2.220	7	1	0.601	0.680	0.626	40.3	89.4
	5	2.620	7	1	0.617	0.767	0.677	36.9	96.7
	6	2.870	7	1	0.560	0.599	0.565	28.1	80.6
	7	3.570	8.5	1	0.423	0.404	0.399	13.1	46.9
HS1023	0	0.047	90	2	0.310	0.332	0.306	36.2	1.7
[07D07-d]	0.5	0.107	62	2	0.456	0.470	0.448	33.8	3.6
	1	0.250	30	2	0.646	0.646	0.631	42.1	10.5
	1.5	0.486	3	2	0.319	0.364	0.327	112.0	54.4
	2	0.718	3	2	0.684	0.657	0.656	152.2	109.3
	2.5	1.270	3	1	0.528	0.442	0.470	123.4	156.7
	3	1.620	3	1	0.555	0.571	0.548	112.8	182.7
	4	2.180	3	1	0.615	0.580	0.583	89.1	194.2
	5	2.680	3	1	0.480	0.546	0.498	61.9	166.0
	6	2.810	3	1	0.709	0.704	0.692	82.0	230.5
	7	3.610	5.5	1	0.487	0.450	0.454	22.8	82.5
HS1024	0	0.038	1331	2	0.175	0.172	0.159	1.6	0.1
[07E04]	0.5	0.090	1331	2	0.226	0.273	0.235	1.0	0.1
	1	0.211	1331	2	0.384	0.361	0.358	0.6	0.1
	1.5	0.411	110.5	2	0.283	0.321	0.287	3.2	1.3
	2	0.657	4	2	0.430	0.408	0.404	76.9	50.5
	2.5	1.280	4	1	0.426	0.577	0.487	95.0	121.6
	3	1.570	4	1	0.626	0.441	0.519	82.6	129.6
	4	2.110	4	1	0.912	0.616	0.749	88.7	187.3
	5	2.620	4	1	0.679	**0.414**	0.532	50.7	132.9
	6	2.790	4	1	0.672	0.786	0.714	64.0	178.5
	7	3.430	5	1	0.715	0.730	0.708	41.3	141.5
HS1025	0	0.046	171	2	0.256	0.301	0.264	16.7	0.8
[07F09]	0.5	0.103	103	2	0.261	0.270	0.251	11.8	1.2
	1	0.229	75	2	0.366	0.344	0.340	9.9	2.3
	1.5	0.441	13	2	0.372	0.329	0.336	29.3	12.9
	2	0.663	1	2	0.393	0.410	0.387	291.5	193.3
	2.5	1.290	1	1	0.355	0.262	0.294	227.5	293.5
	3	1.530	1	1	0.452	0.351	0.387	252.6	386.5
	4	2.100	1	1	0.759	0.688	0.709	337.4	708.5
	5	3.030	1	1	0.930	0.743	0.822	271.1	821.5
	6	3.400	1	1	1.024	0.913	0.954	280.4	953.5
	7	3.730	1.5	1	1.237	1.301	1.254	224.1	836.0
HS1026	0	0.039	174.5	2	0.257	0.236	0.232	17.0	0.7
[07F10]	0.5	0.085	90	2	0.244	0.256	0.235	15.4	1.3
	1	0.206	75	2	0.319	0.340	0.315	10.2	2.1
	1.5	0.389	11.5	2	0.373	0.375	0.359	40.1	15.6
	2	0.632	1	2	0.489	0.399	0.429	339.4	214.5
	2.5	1.190	1	1	0.409	0.434	0.407	341.6	406.5
	3	1.430	1	1	0.512	0.520	0.501	350.3	501.0
	4	1.990	1	1	0.851	0.762	0.792	397.7	791.5
	5	2.620	1	1	1.016	1.111	1.049	400.2	1048.5
	6	2.860	1	1	**0.564**	1.050	0.792	276.9	792.0
	7	3.790	2	1	1.010	0.959	0.970	127.9	484.8

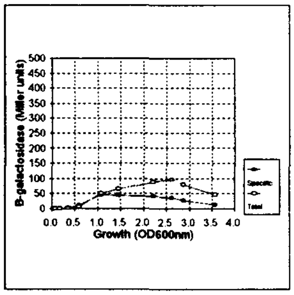

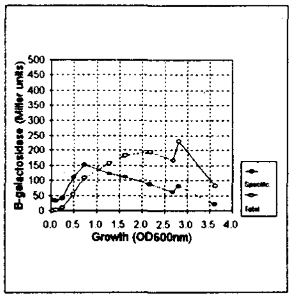

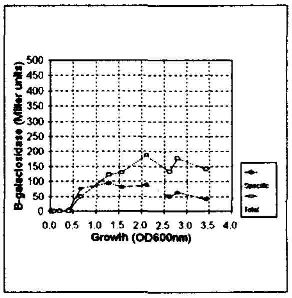

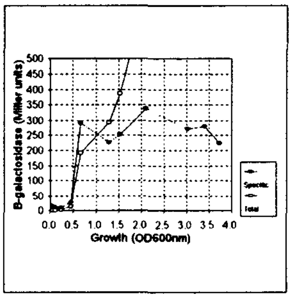

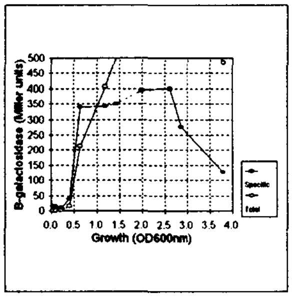

Strain	Time [h]	OD600 [nm]	Rxn Time [min]	Cell Vol [ml]	OD420 [nm] sample1	OD420 [nm] sample2	Avg.	Specific Activity [Miller U]	Total Activity [Miller U]
HS1027	0	0.037	171	2	0.316	0.300	0.293	23.2	0.9
[07F11]	0.5	0.078	103	2	0.271	0.258	0.250	15.5	1.2
	1	0.175	93	2	0.420	0.422	0.406	12.5	2.2
	1.5	0.373	17	2	0.400	0.387	0.379	29.8	11.1
	2	0.623	2	2	0.611	0.621	0.601	241.2	150.3
	2.5	1.180	2	1	0.521	**0.441**	0.466	197.5	233.0
	3	1.440	2	1	0.608	0.608	0.593	205.9	296.5
	4	2.030	2	1	0.776	0.864	0.805	198.3	402.5
	5	2.620	2	1	1.038	0.985	0.997	190.2	498.3
	6	2.980	2	1	0.919	1.188	1.039	174.2	519.3
	7	3.590	2	1	1.445	1.105	1.260	175.5	630.0
HS1028	0	0.046	483	2	0.379	0.348	0.349	7.8	0.4
[08H08]	0.5	0.098	150	2	0.240	0.246	0.228	7.8	0.8
	1	0.240	93	2	0.318	0.349	0.319	7.1	1.7
	1.5	0.422	12	2	0.354	0.389	0.357	35.2	14.9
	2	0.683	4.5	2	0.527	0.555	0.526	85.6	58.4
	2.5	1.200	4.5	1	0.469	0.429	0.434	80.4	96.4
	3	1.580	4.5	1	0.528	0.596	0.547	76.9	121.6
	4	2.040	4.5	1	0.553	0.492	0.508	55.3	112.8
	5	2.660	4.5	1	0.595	0.656	0.611	51.0	135.7
	6	2.830	4.5	1	0.596	0.730	0.648	50.9	144.0
	7	3.500	3.5	1	0.629	0.680	0.640	52.2	182.7
HS1029	0	0.040	1513	2	0.281	0.275	0.263	2.2	0.1
[09B11]	0.5	0.088	1513	2	0.366	0.367	0.352	1.3	0.1
	1	0.204	483	2	0.253	0.263	0.243	1.2	0.3
	1.5	0.413	103	2	0.269	0.317	0.278	3.3	1.3
	2	0.647	3	2	0.406	0.420	0.398	102.5	66.3
	2.5	1.120	3	1	0.313	0.272	0.278	82.6	92.5
	3	1.640	2	1	0.326	0.298	0.297	90.5	148.5
	4	2.020	2	1	0.485	0.444	0.450	111.3	224.8
	5	2.560	2	1	0.595	0.655	0.610	119.1	305.0
	6	2.760	2	1	**0.583**	**0.859**	0.706	127.9	353.0
	7	3.140	2	1	1.174	0.843	0.994	158.2	496.8
HS1030	0	0.052	483	2	0.427	0.401	0.399	7.9	0.4
[09C07]	0.5	0.103	150	2	0.209	0.201	0.190	6.1	0.6
	1	0.247	139	2	0.217	0.287	0.237	3.5	0.9
	1.5	0.478	8.5	2	0.401	0.414	0.393	48.3	23.1
	2	0.698	3	2	0.492	0.501	0.482	115.0	80.3
	2.5	1.240	3	1	0.342	0.335	0.324	87.0	107.8
	3	1.560	3	1	0.467	0.416	0.427	91.1	142.2
	4	2.150	3	1	0.510	0.552	0.516	80.0	172.0
	5	2.660	3	1	0.666	0.747	0.692	86.7	230.5
	6	2.860	3	1	0.737	0.823	0.765	89.2	255.0
	7	3.330	2	1	**1.182**	0.675	0.914	137.2	456.8
HS1031	0	0.039	1512	2	0.310	0.280	0.280	2.4	0.1
[09E10]	0.5	0.090	1512	2	0.398	0.410	0.389	1.4	0.1
	1	0.199	1512	2	0.674	0.671	0.658	1.1	0.2
	1.5	0.389	24	2	0.271	0.298	0.270	14.4	5.6
	2	0.637	2	2	0.286	0.305	0.281	110.1	70.1
	2.5	1.140	2	1	0.290	0.375	0.318	139.3	158.8
	3	1.430	2	1	0.439	0.532	0.471	164.5	235.3
	4	2.000	2	1	0.758	0.636	0.682	170.5	341.0
	5	2.770	2	1	0.646	0.852	0.734	132.5	367.0
	6	2.880	2	1	0.527	0.937	0.717	124.5	358.5
	7	3.450	3.5	1	0.917	0.879	0.883	73.1	252.3

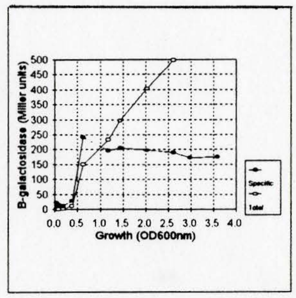

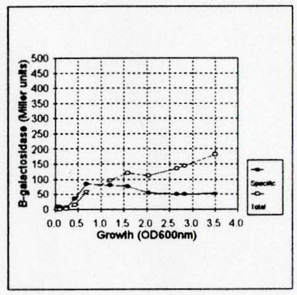

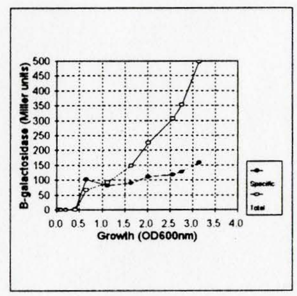

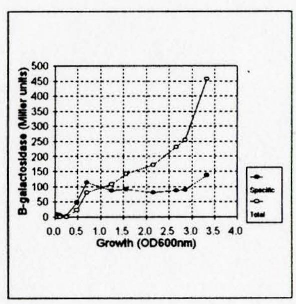

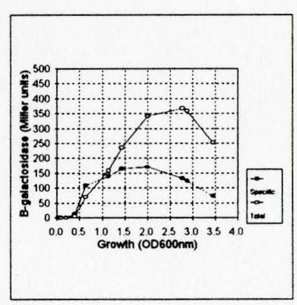

Strain	Time [h]	OD600 [nm]	Rxn Time [min]	Cell Vol [ml]	OD420 [nm] sample1	OD420 [nm] sample2	Avg.	Specific Activity [Miller U]	Total Activity [Miller U]
HS1032	0	0.040	158	2	0.246	0.228	0.222	17.6	0.7
[09H12]	0.5	0.092	103	2	0.257	0.255	0.241	12.7	1.2
	1	0.234	75	2	0.320	0.320	0.305	8.7	2.0
	1.5	0.435	18	2	0.379	0.379	0.364	23.2	10.1
	2	0.646	3	2	0.557	0.558	0.543	140.0	90.4
	2.5	1.240	3	1	0.462	0.471	0.452	121.4	150.5
	3	1.450	3	1	0.513	0.489	0.486	111.7	162.0
	4	2.080	3	1	0.498	0.497	0.483	77.3	160.8
	5	2.620	3	1	0.580	0.630	0.590	75.1	196.7
	6	2.870	3	1	0.696	0.663	0.665	77.2	221.5
	7	3.070	4	1	0.749	0.805	0.762	62.1	190.5
HS1033	0	0.041	1512	2	0.244	0.268	0.241	1.9	0.1
[12A10]	0.5	0.087	1512	2	0.397	0.352	0.360	1.4	0.1
	1	0.198	1512	2	0.487	0.545	0.501	0.8	0.2
	1.5	0.375	86	2	0.273	0.302	0.273	4.2	1.6
	2	0.611	5.5	2	0.252	0.261	0.242	35.9	22.0
	2.5	1.130	5.5	1	0.310	0.320	0.300	48.3	54.5
	3	1.470	5.5	1	0.365	0.393	0.364	45.0	66.2
	4	2.060	5.5	1	0.433	0.457	0.430	38.0	78.2
	5	2.470	5.5	1	0.419	0.486	0.438	32.2	79.5
	6	2.750	5.5	1	0.436	0.535	0.471	31.1	85.5
	7	3.150	6	1	0.425	0.374	0.385	20.3	64.1
HS1034	0	0.045	1513	2	0.442	0.439	0.426	3.1	0.1
[12C09]	0.5	0.093	1513	2	0.464	0.483	0.459	1.6	0.2
	1	0.214	483	2	0.316	0.349	0.318	1.5	0.3
	1.5	0.407	40.5	2	0.363	0.360	0.347	10.5	4.3
	2	0.626	3	2	0.291	0.294	0.278	73.9	46.2
	2.5	1.140	3	1	0.244	0.275	0.245	71.5	81.5
	3	1.470	3	1	0.333	0.303	0.303	68.7	101.0
	4	1.950	3	1	0.343	0.330	0.322	55.0	107.2
	5	2.370	3	1	0.370	0.338	0.339	47.7	113.0
	6	2.610	3	1	0.347	0.317	0.317	40.5	105.7
	7	3.110	6	1	0.525	0.632	0.564	30.2	93.9
HS1035	0	0.032	1513	2	0.145	0.164	0.140	1.4	0.0
[13B08]	0.5	0.057	1513	2	0.205	0.205	0.190	1.1	0.1
	1	0.130	1513	2	0.284	0.289	0.272	0.7	0.1
	1.5	0.258	152.5	2	0.351	0.327	0.324	4.1	1.1
	2	0.454	27	2	0.342	0.327	0.320	13.0	5.9
	2.5	0.800	7	1	0.464	0.416	0.425	75.9	60.7
	3	1.010	2.5	1	0.273	0.282	0.263	104.0	105.0
	4	1.360	2.5	1	0.431	0.387	0.394	115.9	157.6
	5	1.720	2.5	1	0.534	0.541	0.523	121.5	209.0
	6	1.890	2.5	1	0.530	0.597	0.549	116.1	219.4
	7	3.030	4	1	0.667	0.554	0.596	49.1	148.9
HS1036	0	0.041	1512	2	0.533	0.516	0.510	4.1	0.2
[13C08]	0.5	0.082	1512	2	0.710	0.826	0.753	3.0	0.2
	1	0.192	150	2	0.208	0.210	0.194	3.4	0.6
	1.5	0.390	53	2	0.513	0.472	0.478	11.6	4.5
	2	0.630	3.5	2	0.257	0.271	0.249	56.5	35.6
	2.5	1.150	3.5	1	0.333	0.350	0.327	81.1	93.3
	3	1.480	3.5	1	0.507	0.488	0.483	93.1	137.9
	4	1.970	3.5	1	0.573	0.633	0.588	85.3	168.0
	5	2.650	3.5	1	0.537	0.647	0.577	62.2	164.9
	6	2.650	3.5	1	0.861	0.570	0.701	75.5	200.1
	7	3.520	4	1	0.756	0.612	0.669	47.5	167.3

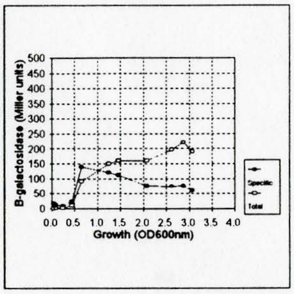

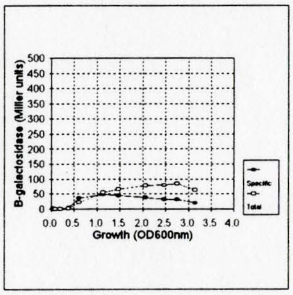

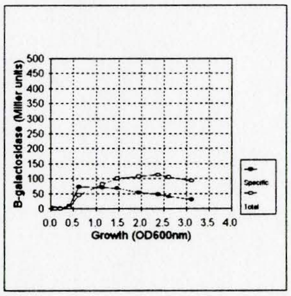

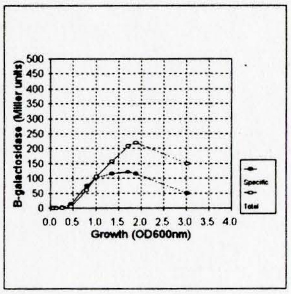

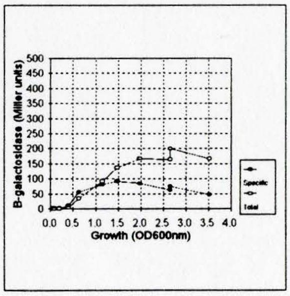

Strain	Time [h]	OD600 [nm]	Rxn Time [min]	Cell Vol [ml]	OD420 [nm] sample1	OD420 [nm] sample2	Avg.	Specific Activity [Miller U]	Total Activity [Miller U]
HS1037	0	0.044	1512	2	0.158	0.138	0.133	1.0	0.0
[14C03]	0.5	0.086	1512	2	**0.081**	**0.173**	0.112	0.4	0.0
	1	0.217	1512	2	0.239	0.237	0.223	0.3	0.1
	1.5	0.424	174	2	0.295	0.275	0.270	1.8	0.8
	2	0.640	6.5	2	0.342	0.356	0.334	40.1	25.7
	2.5	1.190	6.5	1	0.452	0.433	0.428	55.3	65.8
	3	1.440	6.5	1	0.600	0.633	0.602	64.3	92.5
	4	2.070	6.5	1	0.669	0.561	0.600	44.6	92.3
	5	3.190	6.5	1	0.706	0.581	0.629	30.3	96.7
	6	2.850	6.5	1	0.607	0.625	0.601	32.4	92.5
	7	3.390	6	1	0.382	0.471	0.412	20.2	68.6

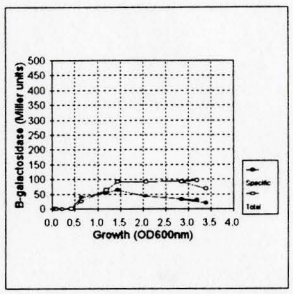

HS1038	0	0.044	1511	2	0.130	0.138	0.119	0.9	0.0
[14D08]	0.5	0.085	1511	2	0.175	0.140	0.143	0.6	0.0
	1	0.201	1511	2	0.209	0.222	0.201	0.3	0.1
	1.5	0.409	174	2	0.259	0.270	0.250	1.8	0.7
	2	0.634	6	2	0.376	0.393	0.370	48.6	30.8
	2.5	1.150	6	1	0.393	0.471	0.417	60.4	69.5
	3	1.450	6	1	0.564	0.591	0.563	64.7	93.8
	4	1.980	6	1	0.736	0.582	0.644	54.2	107.3
	5	2.950	6	1	0.621	0.500	0.546	30.8	90.9
	6	2.950	6	1	0.604	0.558	0.566	32.0	94.3
	7	3.210	6	1	0.350	0.482	0.401	20.8	66.8

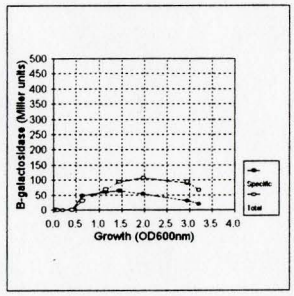

HS1039	0	0.048	483	2	0.377	0.343	0.345	7.4	0.4
[15G03]	0.5	0.100	483	2	0.434	0.446	0.425	4.4	0.4
	1	0.231	483	2	0.693	0.748	0.706	3.2	0.7
	1.5	0.432	37.5	2	0.420	0.397	0.394	12.1	5.2
	2	0.631	4	2	0.378	0.395	0.372	73.6	46.4
	2.5	1.110	4	1	0.400	0.420	0.395	89.0	98.8
	3	1.370	4	1	0.590	0.411	0.486	88.6	121.4
	4	1.910	4	1	0.528	0.419	0.459	60.0	114.6
	5	2.920	4	1	0.628	0.625	0.612	52.4	152.9
	6	3.100	4	1	0.557	0.569	0.548	44.2	137.0
	7	3.150	4	1	0.670	0.680	0.660	52.4	165.0

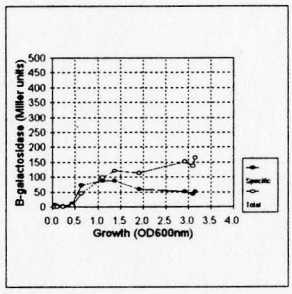

HS1040	0	0.038	1511	2	0.212	0.208	0.195	1.7	0.1
[16E03]	0.5	0.072	483	2	0.127	0.140	0.119	1.7	0.1
	1	0.158	1511	2	0.355	0.315	0.320	0.7	0.1
	1.5	0.305	76	2	0.394	0.347	0.356	7.7	2.3
	2	0.498	27.5	2	0.598	0.558	0.563	20.6	10.2
	2.5	0.880	4	1	0.328	0.357	0.328	93.0	81.9
	3	0.980	4	1	0.426	0.431	0.414	105.5	103.4
	4	1.280	4	1	0.702	0.628	0.650	127.0	162.5
	5	2.080	4	1	0.782	0.717	0.735	88.3	183.6
	6	2.320	4	1	0.693	0.736	0.700	75.4	174.9
	7	3.110	4	1	0.577	0.617	0.582	46.8	145.5

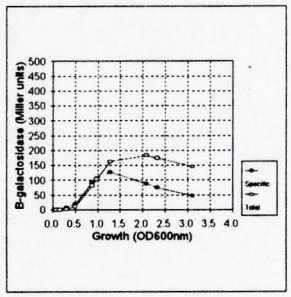

HS1041	0	0.046	1513	2	0.404	0.446	0.410	2.9	0.1
[16F07]	0.5	0.087	483	2	0.221	0.236	0.214	2.5	0.2
	1	0.196	483	2	0.321	0.350	0.321	1.7	0.3
	1.5	0.403	55	2	0.433	0.405	0.404	9.1	3.7
	2	0.617	3.5	2	0.410	0.399	0.390	90.2	55.6
	2.5	1.100	3.5	1	0.415	0.468	0.427	110.8	121.9
	3	1.490	3.5	1	0.546	0.477	0.497	95.2	141.9
	4	2.070	3.5	1	0.648	0.545	0.582	80.3	166.1
	5	2.740	3.5	1	0.579	0.690	0.620	64.6	177.0
	6	2.890	3.5	1	0.539	0.664	0.587	58.0	167.6
	7	3.450	4	1	0.448	0.496	0.457	33.1	114.3

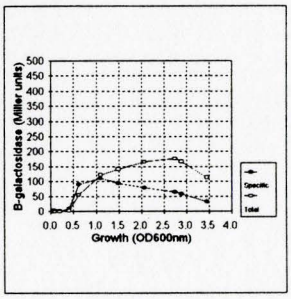

Strain	Time [h]	OD600 [nm]	Rxn Time [min]	Cell Vol [ml]	OD420 [nm] sample1	OD420 [nm] sample2	Avg.	Specific Activity [Miller U]	Total Activity [Miller U]
HS1042	0	0.043	1239	2	0.284	0.217	0.245	2.3	0.1
[21B04]	0.5	0.091	1239	2	0.566	0.537	0.546	2.4	0.2
	1	0.214	171	2	0.216	0.199	0.202	2.8	0.6
	1.5	0.374	80.5	2	0.402	0.429	0.410	6.8	2.5
	2	0.592	5.5	2	0.283	0.291	0.281	43.2	25.5
	2.5	1.040	5.5	1	0.335	0.367	0.345	60.3	62.7
	3	1.420	5.5	1	0.377	0.318	0.342	43.7	62.1
	4	1.790	5.5	1	0.388	0.374	0.375	38.1	68.2
	5	2.360	5.5	1	0.446	0.436	0.435	33.5	79.1
	6	2.690	5.35	1	0.486	0.511	0.493	34.2	92.1
	7	3.010	3	1	0.961	0.965	0.957	106.0	319.0
HS1043	0	0.051	1239	2	0.157	0.157	0.151	1.2	0.1
[21F08]	0.5	0.103	1239	2	0.227	0.224	0.220	0.9	0.1
	1	0.226	271	2	0.120	0.127	0.118	1.0	0.2
	1.5	0.439	130.5	2	0.274	0.287	0.275	2.4	1.1
	2	0.638	5.5	2	0.191	0.219	0.199	28.4	18.1
	2.5	1.350	5.5	1	0.199	0.210	0.199	26.7	36.1
	3	1.440	5.5	1	0.322	0.298	0.304	38.4	55.3
	4	1.860	5.5	1	0.391	0.424	0.402	39.2	73.0
	5	2.400	5.5	1	0.588	0.634	0.605	45.8	110.0
	6	2.820	5.5	1	0.780	0.721	0.745	48.0	135.4
	7	2.700	3	1	0.497	0.486	0.486	59.9	161.8
HS1044	0	0.049	171	2	0.174	0.192	0.177	10.6	0.5
[22E03]	0.5	0.095	103.5	2	0.254	0.275	0.259	13.1	1.2
	1	0.231	48	2	0.322	0.295	0.303	13.6	3.2
	1.5	0.428	73	2	0.289	0.286	0.282	4.5	1.9
	2	0.646	5	2	0.429	0.494	0.456	70.5	45.6
	2.5	1.010	5	1	0.435	0.450	0.437	86.4	87.3
	3	1.460	5	1	0.533	0.489	0.505	69.2	101.0
	4	1.960	5	1	0.732	0.684	0.702	71.6	140.4
	5	2.620	5	1	0.805	0.772	0.783	59.7	156.5
	6	2.920	5	1	0.705	0.634	0.664	45.4	132.7
	7	3.420	3	1	0.706	0.716	0.705	68.7	235.0
HS1045	0	0.055	209	2	0.220	0.202	0.205	8.9	0.5
[22F08]	0.5	0.102	103.5	2	0.284	0.288	0.280	13.3	1.4
	1	0.243	48	2	0.308	0.324	0.310	13.3	3.2
	1.5	0.458	13	2	0.314	0.312	0.307	25.8	11.8
	2	0.661	5	2	0.579	0.555	0.561	84.9	56.1
	2.5	1.350	5	1	0.461	0.478	0.464	68.7	92.7
	3	1.360	5	1	0.584	0.634	0.603	88.7	120.6
	4	2.130	5	1	0.701	0.704	0.697	65.4	139.3
	5	2.330	5	1	0.698	0.725	0.706	60.6	141.1
	6	2.710	5	1	0.593	0.626	0.604	44.5	120.7
	7	2.970	12.5	1	0.682	0.632	0.651	17.5	52.1
HS1046	0	0.049	171	2	0.207	0.230	0.213	12.7	0.6
[22F09]	0.5	0.102	103	2	0.222	0.246	0.228	10.9	1.1
	1	0.235	80.5	2	0.301	0.288	0.289	7.6	1.8
	1.5	0.448	13	2	0.237	0.234	0.230	19.7	8.8
	2	0.645	3	2	0.631	0.711	0.665	171.8	110.8
	2.5	1.460	3	1	0.525	0.499	0.506	115.5	168.7
	3	1.430	3	1	0.575	0.650	0.607	141.4	202.2
	4	1.920	3	1	0.668	0.759	0.708	122.8	235.8
	5	2.300	3	1	0.771	0.742	0.751	108.8	250.2
	6	2.770	3	1	0.778	0.728	0.747	89.9	249.0
	7	2.840	3	1	0.570	0.481	0.520	61.0	173.2

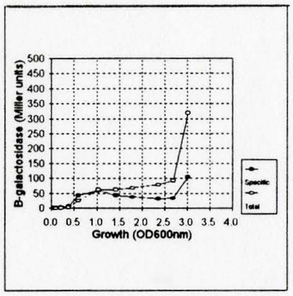

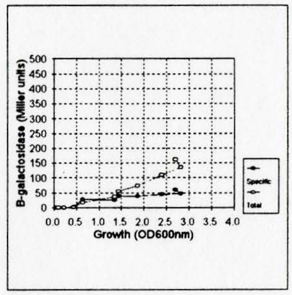

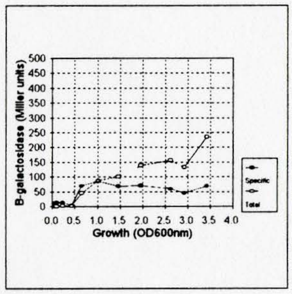

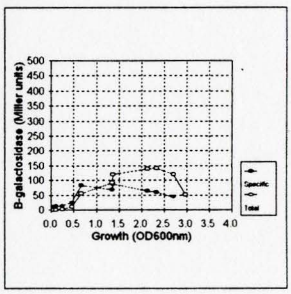

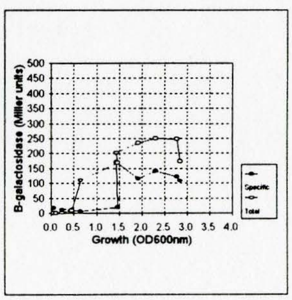

Strain	Time [h]	OD600 [nm]	Rxn Time [min]	Cell Vol [ml]	OD420 [nm] sample1	OD420 [nm] sample2	Avg.	Specific Activity [Miller U]	Total Activity [Miller U]	
HS1047	0	0.060	1239	2	0.215	0.220	0.212	1.4	0.1	
[22G10]	0.5	0.112	1239	2	0.391	0.388	0.384	1.4	0.2	
	1	0.219	271	2	0.179	0.185	0.176	1.5	0.3	
	1.5	0.442	80.5	2	0.316	0.301	0.303	4.3	1.9	
	2	0.659	12	2	0.509	0.511	0.504	31.9	21.0	
	2.5	1.130	12	1	0.514	0.551	0.527	38.8	43.9	
	3	1.470	12	1	0.845	0.823	0.828	46.9	69.0	
	4	1.930	12	1	0.988	0.972	0.974	42.1	81.2	
	5	2.390	12	1	1.181	1.119	1.144	39.9	95.3	
	6	2.850	12	1	1.329	1.219	1.268	37.1	105.7	
	7	2.840	3	1	0.545	0.511	0.522	61.3	174.0	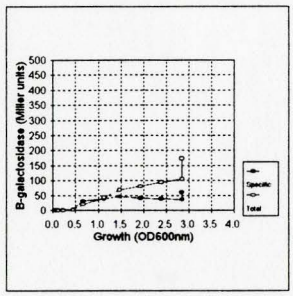
HS1048	0	0.053	271	2	0.162	0.148	0.149	5.2	0.3	
[23E01]	0.5	0.103	171	2	0.174	0.170	0.166	4.7	0.5	
	1	0.238	171	2	0.219	0.224	0.216	2.6	0.6	
	1.5	0.438	48	2	0.372	0.398	0.379	9.0	3.9	
	2	0.665	6	2	0.448	0.463	0.450	56.3	37.5	
	2.5	1.210	6	1	0.497	0.486	0.486	66.9	80.9	
	3	1.660	6	1	0.678	0.675	0.671	67.3	111.8	
	4	1.860	6	1	0.862	0.932	0.891	79.8	148.5	
	5	2.560	6	1	1.057	1.032	1.039	67.6	173.1	
	6	2.970	6	1	0.945	0.967	0.950	53.3	158.3	
	7	3.160	3	1	0.221	0.247	0.228	24.1	76.0	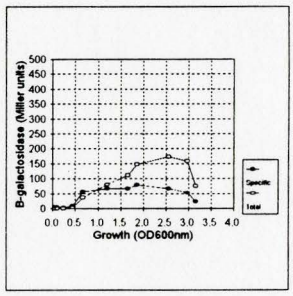
HS1049	0	0.042	271	2	0.173	0.161	0.161	7.1	0.3	
[24B12]	0.5	0.091	171	2	0.162	0.168	0.159	5.1	0.5	
	1	0.226	171	2	0.198	0.182	0.184	2.4	0.5	
	1.5	0.407	48	2	0.395	0.360	0.372	9.5	3.9	
	2	0.622	6	2	0.421	0.395	0.402	53.9	33.5	
	2.5	1.070	6	1	0.471	0.440	0.450	70.0	74.9	
	3	1.140	6	1	0.598	0.612	0.599	87.6	99.8	
	4	1.910	6	1	0.828	0.890	0.853	74.4	142.2	
	5	2.540	6	1	0.862	0.971	0.911	59.7	151.8	
	6	2.890	6	1	0.821	0.896	0.853	49.2	142.1	
	7	3.620	3	1	0.687	0.908	0.792	72.9	263.8	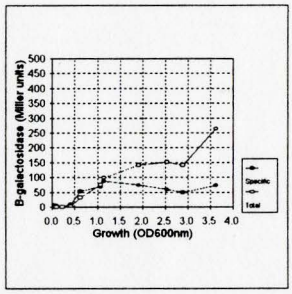
HS1050	0	0.047	271	2	0.214	0.197	0.200	7.8	0.4	
[24C07]	0.5	0.094	171	2	0.252	0.247	0.244	7.6	0.7	
	1	0.228	162.5	2	0.286	0.278	0.276	3.7	0.8	
	1.5	0.398	80.5	2	0.753	0.930	0.836	13.0	5.2	
	2	0.636	11.5	2	0.477	0.475	0.470	32.1	20.4	
	2.5	1.100	11.5	1	0.434	0.415	0.419	33.1	36.4	
	3	1.600	11.5	1	0.476	0.546	0.505	27.4	43.9	
	4	1.890	11.5	1	0.625	0.630	0.622	28.6	54.0	
	5	2.460	11.5	1	0.651	0.642	0.641	22.6	55.7	
	6	2.780	11.5	1	0.536	0.705	0.615	19.2	53.4	
	7	3.430	3	1	0.389	0.398	0.388	37.7	129.2	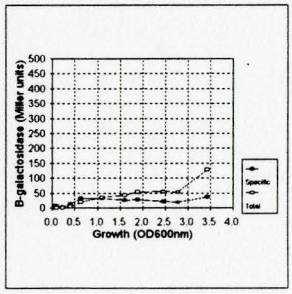
HS1051	0	0.040	1239	2	0.268	0.222	0.239	2.4	0.1	
[25A11]	0.5	0.070	271	2	0.200	0.211	0.200	5.3	0.4	
	1	0.155	171	2	0.284	0.244	0.258	4.9	0.8	
	1.5	0.300	80.5	2	0.471	0.367	0.413	8.6	2.6	
	2	0.488	16.5	2	0.290	0.316	0.297	18.4	9.0	
	2.5	0.920	5	1	0.337	0.359	0.342	74.3	68.4	
	3	1.140	5	1	0.567	0.536	0.546	95.7	109.1	
	4	1.540	5	1	0.680	0.690	0.679	88.2	135.8	
	5	1.830	5	1	0.828	0.853	0.835	91.2	166.9	
	6	2.350	5	1	1.136	1.136	1.130	96.2	226.0	
	7	2.400	3	1	0.390	0.390	0.384	53.3	128.0	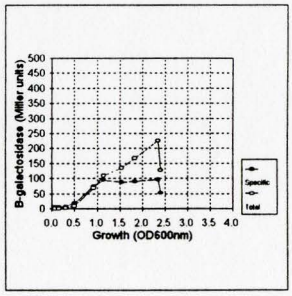

Strain	Time [h]	OD600 [nm]	Rxn Time [min]	Cell Vol [ml]	OD420 [nm] sample1	OD420 [nm] sample2	OD420 [nm] Avg.	Specific Activity [Miller U]	Total Activity [Miller U]
HS1052	0	0.042	1231	2	0.354	0.362	0.352	3.4	0.1
[25B04]	0.5	0.093	271	2	0.182	0.188	0.179	3.6	0.3
	1	0.222	171	2	0.225	0.230	0.222	2.9	0.6
	1.5	0.423	80.5	2	0.457	0.465	0.455	6.7	2.8
	2	0.642	3	2	0.255	0.269	0.256	66.5	42.7
	2.5	1.130	3	1	0.346	0.360	0.347	102.4	115.7
	3	1.440	3	1	0.499	0.406	0.447	103.4	148.8
	4	1.950	3	1	0.587	0.533	0.554	94.7	184.7
	5	2.700	3	1	0.591	0.597	0.588	72.6	196.0
	6	2.790	3	1	0.651	0.662	0.651	77.7	216.8
	7	2.800	7.5	1	0.978	1.135	1.051	50.0	140.1
HS1053	0	0.042	2131	2	0.326	0.299	0.307	1.7	0.1
[26A06]	0.5	0.090	2131	2	0.396	0.398	0.391	1.0	0.1
	1	0.206	271	2	0.194	0.189	0.186	1.7	0.3
	1.5	0.388	80.5	2	0.258	0.267	0.257	4.1	1.6
	2	0.628	3	2	0.134	0.140	0.131	34.8	21.8
	2.5	1.070	3	1	0.198	0.185	0.186	57.8	61.8
	3	1.340	3	1	0.291	0.313	0.296	73.6	98.7
	4	1.980	3	1	0.489	0.467	0.472	79.5	157.3
	5	2.360	3	1	0.601	0.516	0.553	78.0	184.2
	6	2.790	3	1	0.709	0.619	0.658	78.6	219.3
	7	2.980	7.5	1	0.712	0.753	0.727	32.5	96.9
HS1054	0	0.043	105	2	0.250	0.253	0.246	27.2	1.2
[26E05]	0.5	0.095	95.5	2	0.331	0.409	0.364	20.1	1.9
	1	0.222	72.5	2	0.368	0.374	0.365	11.3	2.5
	1.5	0.445	16	2	0.513	0.489	0.495	34.8	15.5
	2	0.631	2	2	0.575	0.581	0.572	226.6	143.0
	2.5	1.110	2	1	0.587	0.563	0.569	256.3	284.5
	3	1.320	2	1	0.661	0.773	0.711	269.3	355.5
	4	1.840	2	1	0.882	0.790	0.830	225.5	415.0
	5	2.280	2	1	1.075	1.063	1.063	233.1	531.5
	6	2.530	2	1	0.920	1.042	0.975	192.7	487.5
	7	2.550	1.5	1	1.150	1.197	1.168	305.2	778.3
HS1055	0	0.042	105	2	0.250	0.307	0.273	30.9	1.3
[28F07]	0.5	0.093	95.5	2	0.402	0.412	0.401	22.6	2.1
	1	0.234	72.5	2	0.502	0.475	0.483	14.2	3.3
	1.5	0.421	16	2	0.579	0.587	0.577	42.8	18.0
	2	0.630	2	2	0.644	0.647	0.640	253.8	159.9
	2.5	1.320	2	1	0.580	0.624	0.596	225.8	298.0
	3	1.470	2	1	0.578	0.771	0.669	227.4	334.3
	4	2.070	2	1	0.770	0.965	0.862	208.1	430.8
	5	2.460	2	1	0.983	1.038	1.005	204.2	502.2
	6	2.690	2	1	0.839	0.850	0.839	155.9	419.3
	7	2.740	1.5	1	1.744	1.589	1.661	404.0	1107.0
HS1056	0	0.041	263	2	0.290	0.268	0.273	12.7	0.5
[29G11]	0.5	0.090	237	2	0.247	0.272	0.254	5.9	0.5
	1	0.220	171	2	0.278	0.288	0.277	3.7	0.8
	1.5	0.415	40	2	0.607	0.583	0.589	17.7	7.4
	2	0.641	1.5	2	0.363	0.438	0.395	205.1	131.5
	2.5	1.150	1.5	1	0.394	0.368	0.375	217.4	250.0
	3	1.540	1.5	1	0.525	0.486	0.500	216.2	333.0
	4	2.000	1.5	1	0.586	0.594	0.584	194.7	389.3
	5	2.440	1.5	1	0.760	0.765	0.757	206.7	504.3
	6	2.900	1.5	1	0.679	0.583	0.625	143.7	416.7
	7	2.720	1.5	1	0.568	0.969	0.763	186.9	508.3

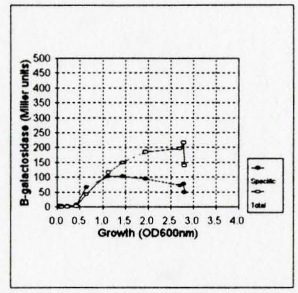

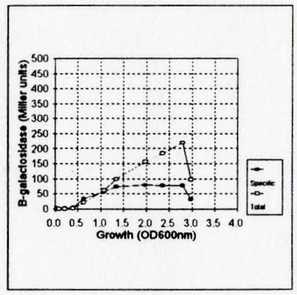

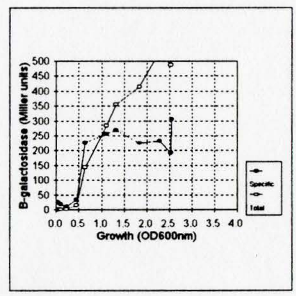

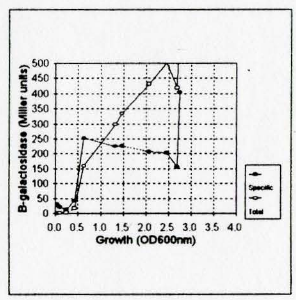

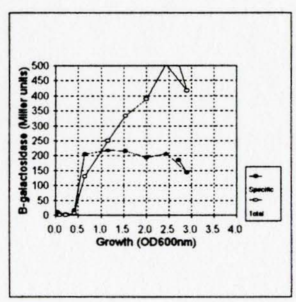

Strain	Time [h]	OD600 [nm]	Rxn Time [min]	Cell Vol [ml]	OD420 [nm] sample1	sample2	Avg.	Specific Activity [Miller U]	Total Activity [Miller U]
HS1057	0	0.044	237	2	0.204	0.202	0.197	9.4	0.4
[31B04]	0.5	0.091	171	2	0.204	0.210	0.201	6.5	0.6
	1	0.234	105	2	0.225	0.213	0.213	4.3	1.0
	1.5	0.408	40	2	0.489	0.520	0.499	15.3	6.2
	2	0.628	1.5	2	0.613	0.564	0.583	309.2	194.2
	2.5	1.090	1.5	1	0.481	0.468	0.469	286.5	312.3
	3	1.450	1.5	1	0.781	0.692	0.731	335.9	487.0
	4	1.860	1.5	1	0.931	0.897	0.908	325.4	605.3
	5	2.610	1.5	1	0.871	0.921	0.890	227.3	593.3
	6	2.790	1.5	1	1.031	1.097	1.058	252.8	705.3
	7	2.690	1.5	1	1.418	1.411	1.409	349.1	939.0
HS1058	0	0.045	237	2	0.238	0.212	0.219	10.3	0.5
[31B09]	0.5	0.096	171	2	0.219	0.231	0.219	6.7	0.6
	1	0.232	105	2	0.231	0.226	0.223	4.6	1.1
	1.5	0.429	40	2	0.382	0.407	0.389	11.3	4.9
	2	0.646	1	2	0.369	0.386	0.372	287.5	185.7
	2.5	1.130	1	1	0.406	0.403	0.399	352.7	398.5
	3	1.490	1	1	0.704	0.722	0.707	474.5	707.0
	4	2.140	1	1	1.069	1.031	1.044	487.9	1044.0
	5	2.880	1	1	1.260	1.156	1.202	417.4	1202.0
	6	3.310	1	1	1.372	1.180	1.270	383.7	1270.0
	7	2.720	1.5	1	1.847	1.701	1.768	433.3	1178.7
HS1059	0	0.048	237	2	0.288	0.277	0.277	12.2	0.6
[31D07-d]	0.5	0.094	171	2	0.269	0.277	0.267	8.3	0.8
	1	0.222	105	2	0.253	0.234	0.238	5.1	1.1
	1.5	0.419	40	2	0.581	0.584	0.577	17.2	7.2
	2	0.631	2.5	2	0.309	0.301	0.299	94.8	59.8
	2.5	1.180	2.5	1	0.388	0.329	0.353	119.5	141.0
	3	1.400	2.5	1	0.412	0.475	0.438	125.0	175.0
	4	1.850	2.5	1	0.675	0.603	0.633	136.9	253.2
	5	2.350	2.5	1	0.580	0.581	0.575	97.8	229.8
	6	2.760	2.5	1	0.610	0.562	0.580	84.1	232.0
	7	2.640	1.5	1	0.631	0.675	0.647	163.4	431.3
HS1060	0	0.051	171	2	0.284	0.281	0.277	15.9	0.8
[31D07-l]	0.5	0.112	105	2	0.242	0.240	0.235	10.0	1.1
	1	0.261	95.5	2	0.290	0.286	0.282	5.7	1.5
	1.5	0.466	40	2	0.642	0.716	0.673	18.1	8.4
	2	0.677	4	2	0.616	0.602	0.603	111.3	75.4
	2.5	1.250	4	1	0.629	0.656	0.637	127.3	159.1
	3	1.500	4	1	0.700	0.666	0.677	112.8	169.3
	4	1.970	4	1	0.774	0.761	0.762	96.6	190.4
	5	2.630	4	1	0.810	0.815	0.807	76.7	201.6
	6	2.900	4	1	1.010	1.101	1.050	90.5	262.4
	7	2.660	1.5	1	0.494	0.433	0.458	114.7	305.0
HS1061	0	0.046	2131	2	0.332	0.329	0.325	1.7	0.1
[31F08-n]	0.5	0.098	2131	2	0.399	0.411	0.399	1.0	0.1
	1	0.225	263	2	0.189	0.188	0.183	1.5	0.3
	1.5	0.459	72.5	2	0.266	0.266	0.260	3.9	1.8
	2	0.638	4	2	0.263	0.276	0.264	51.6	32.9
	2.5	1.100	4	1	0.332	0.299	0.310	70.3	77.4
	3	1.380	4	1	0.496	0.516	0.500	90.6	125.0
	4	1.880	4	1	0.716	0.645	0.675	89.7	168.6
	5	2.330	4	1	0.622	0.689	0.650	69.7	162.4
	6	2.690	4	1	0.599	0.768	0.678	63.0	169.4
	7	3.000	1.5	1	0.666	0.630	0.642	142.7	428.0

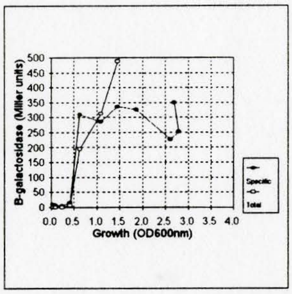

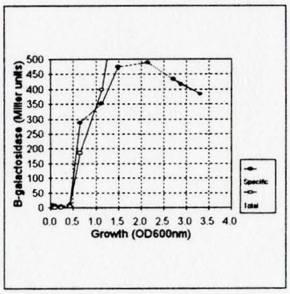

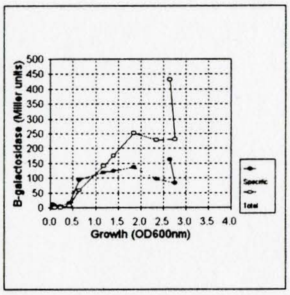

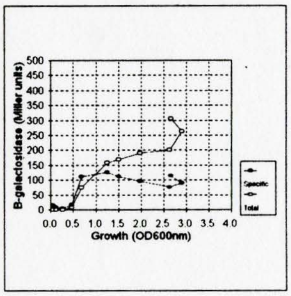

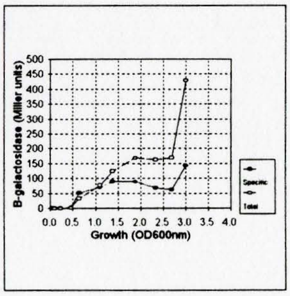

Strain	Time [h]	OD600 [nm]	Rxn Time [min]	Cell Vol [ml]	OD420 [nm] sample1	sample2	Avg.	Specific Activity [Miller U]	Total Activity [Miller U]
HS1062	0	0.033	1179	2	0.078	0.079	0.057	0.7	0.0
[31F09]	0.5	0.072	1179	2	0.233	0.254	0.221	1.3	0.1
	1	0.178	1179	2	0.328	0.369	0.327	0.8	0.1
	1.5	0.336	71	2	2.350	0.218	1.262	26.5	8.9
	2	0.593	8	2	0.272	0.296	0.262	27.6	16.4
	2.5	1.220	3.5	1	0.258	0.252	0.233	54.6	66.6
	3	1.290	3.5	1	0.415	0.409	0.390	86.4	111.4
	4	1.840	3.5	1	0.534	0.513	0.502	77.9	143.3
	5	2.320	3.5	1	0.528	0.592	0.538	66.3	153.7
	6	2.710	3.5	1	0.837	0.899	0.846	89.2	241.7
	7	2.860	5	1	0.770	0.718	0.722	50.5	144.4
HS1063	0	0.032	1179	2	0.148	0.133	0.119	1.6	0.1
[32D07]	0.5	0.078	1179	2	0.242	0.236	0.217	1.2	0.1
	1	0.191	419	2	0.231	0.227	0.207	1.3	0.2
	1.5	0.383	71	2	0.316	0.305	0.289	5.3	2.0
	2	0.627	7	2	0.348	0.356	0.330	37.6	23.6
	2.5	1.130	7	1	0.282	0.342	0.290	36.7	41.4
	3	1.330	7	1	0.375	0.374	0.353	37.9	50.4
	4	1.800	7	1	0.427	0.523	0.453	36.0	64.7
	5	2.310	7	1	0.480	0.529	0.483	29.8	68.9
	6	2.710	7	1	0.459	0.541	0.478	25.2	68.3
	7	2.780	5	1	0.335	0.293	0.292	21.0	58.4
HS1064	0	0.037	419	2	0.307	0.282	0.273	8.8	0.3
[32D11]	0.5	0.084	145	2	0.298	0.296	0.275	11.3	0.9
	1	0.213	71	2	0.327	0.328	0.306	10.1	2.2
	1.5	0.389	24	2	0.451	0.467	0.437	23.4	9.1
	2	0.608	6.5	2	0.541	0.520	0.509	64.3	39.1
	2.5	1.110	6.5	1	0.446	0.490	0.446	61.8	68.6
	3	1.400	6.5	1	0.548	0.568	0.536	58.9	82.5
	4	1.850	6.5	1	0.636	0.794	0.693	57.6	106.6
	5	2.390	6.5	1	0.589	0.532	0.539	34.7	82.8
	6	2.620	6.5	1	0.659	0.697	0.656	38.5	100.9
	7	2.860	5	1	0.396	0.448	0.400	28.0	80.0
HS1065	0	0.038	1179	2	0.300	0.257	0.257	2.9	0.1
[33B07]	0.5	0.091	145	2	0.199	0.207	0.181	6.9	0.6
	1	0.227	71	2	0.271	0.281	0.254	7.9	1.8
	1.5	0.396	24	2	0.279	0.282	0.259	13.6	5.4
	2	0.624	11.5	2	0.262	0.271	0.245	17.0	10.6
	2.5	1.090	11.5	1	0.247	0.237	0.220	17.6	19.1
	3	1.320	11.5	1	0.275	0.299	0.265	17.5	23.0
	4	1.820	11.5	1	0.349	0.318	0.312	14.9	27.1
	5	2.320	11.5	1	0.367	0.360	0.342	12.8	29.7
	6	2.660	11.5	1	0.400	0.449	0.403	13.2	35.0
	7	2.820	5	1	0.162	0.173	0.146	10.3	29.1
HS1066	0	0.039	419	2	0.379	0.399	0.367	11.2	0.4
[33C09]	0.5	0.086	71	2	0.198	0.206	0.180	14.7	1.3
	1	0.239	55	2	0.375	0.394	0.363	13.8	3.3
	1.5	0.415	11.5	2	0.308	0.300	0.282	29.5	12.3
	2	0.669	5	2	0.415	0.418	0.395	59.0	39.5
	2.5	1.330	5	1	0.352	0.317	0.313	47.0	62.5
	3	1.500	5	1	0.339	0.388	0.342	45.5	68.3
	4	2.130	5	1	0.495	0.380	0.416	39.0	83.1
	5	2.720	5	1	0.403	0.377	0.368	27.1	73.6
	6	3.200	5	1	0.580	0.436	0.486	30.4	97.2
	7	3.090	5	1	0.341	0.323	0.310	20.1	62.0

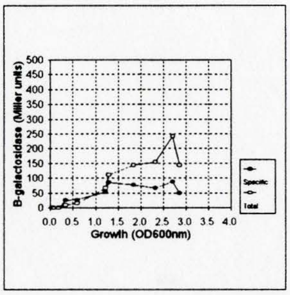

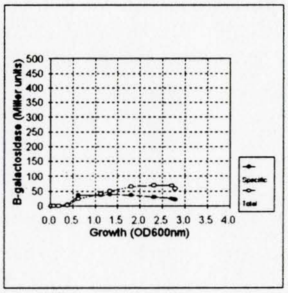

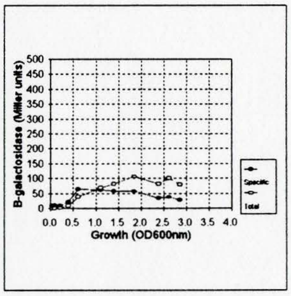

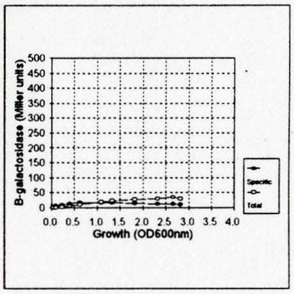

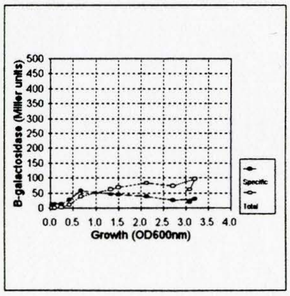

Strain	Time [h]	OD600 [nm]	Rxn Time [min]	Cell Vol [ml]	OD420 [nm] sample1	OD420 [nm] sample2	Avg.	Specific Activity [Miller U]	Total Activity [Miller U]
HS1067	0	0.037	1179	2	0.175	0.165	0.148	1.7	0.1
[34C08-n]	0.5	0.080	1179	2	0.322	0.301	0.290	1.5	0.1
	1	0.210	419	2	0.261	0.266	0.242	1.4	0.3
	1.5	0.375	71	2	0.259	0.258	0.237	4.4	1.7
	2	0.626	5	2	0.211	0.215	0.191	30.5	19.1
	2.5	1.100	5	1	0.181	0.190	0.164	29.7	32.7
	3	1.460	5	1	0.280	0.342	0.289	39.6	57.8
	4	1.990	5	1	0.439	0.442	0.419	42.1	83.7
	5	2.660	5	1	0.475	0.593	0.512	38.5	102.4
	6	3.240	5	1	0.456	0.459	0.436	26.9	87.1
	7	3.460	5	1	0.326	0.274	0.278	16.1	55.6
HS1068	0	0.034	1179	2	0.106	0.096	0.079	1.0	0.0
[34C08-m]	0.5	0.073	1179	2	0.230	0.245	0.216	1.3	0.1
	1	0.179	1179	2	0.456	0.481	0.447	1.1	0.2
	1.5	0.353	71	2	0.197	0.203	0.178	3.6	1.3
	2	0.584	7	2	0.138	0.164	0.129	15.8	9.2
	2.5	0.900	7	1	0.229	0.196	0.191	30.2	27.2
	3	1.160	7	1	0.400	0.228	0.292	36.0	41.7
	4	1.670	7	1	0.366	0.337	0.330	28.2	47.1
	5	2.160	7	1	0.360	0.306	0.311	20.6	44.4
	6	2.430	7	1	0.417	0.441	0.407	23.9	58.1
	7	3.160	5	1	0.222	0.234	0.206	13.0	41.2
HS1069	0	0.027	419	2	0.238	0.228	0.211	9.3	0.3
[34E11]	0.5	0.064	219	2	0.236	0.247	0.220	7.8	0.5
	1	0.174	71	2	0.171	0.173	0.150	6.1	1.1
	1.5	0.353	34	2	0.285	0.285	0.263	11.0	3.9
	2	0.574	0.5	2	0.100	0.120	0.088	153.3	88.0
	2.5	0.790	0.5	1	0.166	0.148	0.135	341.8	270.0
	3	1.020	0.5	1	0.241	0.200	0.199	389.2	397.0
	4	1.500	0.5	1	0.296	0.204	0.228	304.0	456.0
	5	2.030	0.5	1	0.406	0.373	0.368	362.1	735.0
	6	2.500	0.5	1	0.547	0.503	0.503	402.4	1006.0
	7	2.950	2.5	1	1.140	1.166	1.131	153.4	452.4
HS1070	0	0.033	419	2	0.226	0.190	0.186	6.7	0.2
[35B06]	0.5	0.074	219	2	0.270	0.266	0.246	7.6	0.6
	1	0.194	71	2	0.253	0.277	0.243	8.8	1.7
	1.5	0.362	34	2	0.287	0.297	0.270	11.0	4.0
	2	0.572	6.5	2	0.308	0.311	0.288	38.7	22.1
	2.5	0.910	6.5	1	0.370	0.321	0.324	54.7	49.8
	3	1.230	6.5	1	0.382	0.403	0.371	46.3	57.0
	4	1.660	6.5	1	0.436	0.457	0.425	39.3	65.3
	5	2.190	6.5	1	0.510	0.481	0.474	33.3	72.8
	6	2.570	6.5	1	0.359	0.531	0.423	25.3	65.1
	7	2.810	5	1	0.352	0.322	0.315	22.4	63.0
HS1071	0	0.043	419	2	0.222	0.207	0.193	5.3	0.2
[35B09]	0.5	0.080	219	2	0.084	0.290	0.165	4.7	0.4
	1	0.188	71	2	0.211	0.203	0.185	6.9	1.3
	1.5	0.345	34	2	0.376	0.364	0.348	14.8	5.1
	2	0.564	4	2	0.228	0.261	0.223	49.3	27.8
	2.5	0.910	4	1	0.313	0.280	0.275	75.4	68.6
	3	1.170	4	1	0.421	0.399	0.388	82.9	97.0
	4	1.720	4	1	0.431	0.377	0.382	55.5	95.5
	5	1.810	4	1	0.667	0.785	0.704	97.2	176.0
	6	2.510	4	1	0.645	0.722	0.662	65.9	165.4
	7	2.950	2.5	1	0.713	0.747	0.708	96.0	283.2

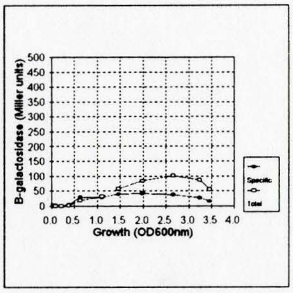

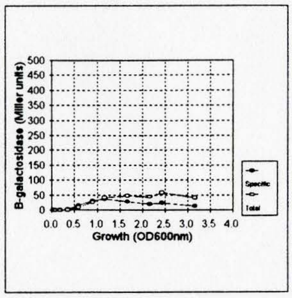

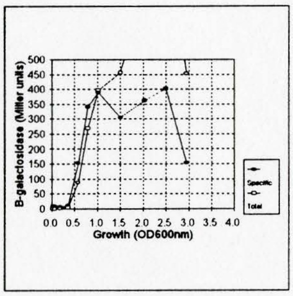

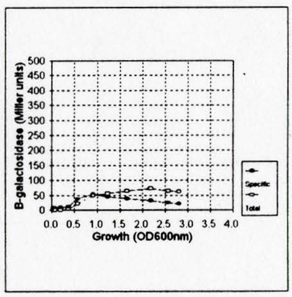

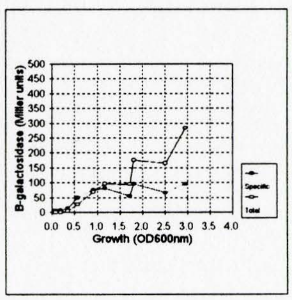

Strain	Time [h]	OD600 [nm]	Rxn Time [min]	Cell Vol [ml]	OD420 [nm] sample1	OD420 [nm] sample2	Avg.	Specific Activity [Miller U]	Total Activity [Miller U]	
HS1072	0	0.039	137	2	0.291	0.289	0.268	25.1	1.0	
[35C12]	0.5	0.087	63	2	0.249	0.234	0.220	20.0	1.7	
	1	0.171	47	2	0.410	0.420	0.393	24.4	4.2	
	1.5	0.357	16	2	0.348	0.362	0.333	29.1	10.4	
	2	0.574	3.5	2	0.232	0.238	0.213	53.0	30.4	
	2.5	1.140	3.5	1	0.261	0.276	0.247	61.8	70.4	
	3	1.460	3.5	1	0.315	0.267	0.269	52.6	76.9	
	4	2.060	3.5	1	0.348	0.434	0.369	51.2	105.4	
	5	2.690	3.5	1	0.356	0.397	0.355	37.7	101.3	
	6	3.120	3.5	1	0.322	0.296	0.287	26.3	82.0	
	7	3.210	2.5	1	0.394	0.418	0.384	47.9	153.6	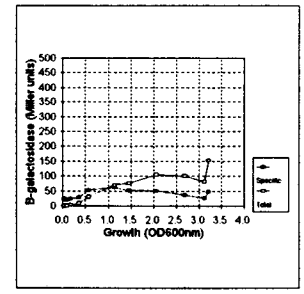
HS1073	0	0.038	1171	2	0.130	0.130	0.108	1.2	0.0	
[35F12]	0.5	0.076	1171	2	0.247	0.244	0.224	1.3	0.1	
	1	0.149	411	2	0.244	0.250	0.225	1.8	0.3	
	1.5	0.308	63	2	0.190	0.194	0.170	4.4	1.3	
	2	0.533	16.5	2	0.261	0.265	0.241	13.7	7.3	
	2.5	0.820	5	1	0.262	0.248	0.233	56.8	46.6	
	3	1.190	5	1	0.370	0.364	0.345	58.0	69.0	
	4	1.750	5	1	0.406	0.467	0.415	47.4	82.9	
	5	2.160	5	1	0.427	0.479	0.431	39.9	86.2	
	6	2.480	5	1	0.422	0.499	0.439	35.4	87.7	
	7	2.890	2.5	1	0.338	0.367	0.331	45.7	132.2	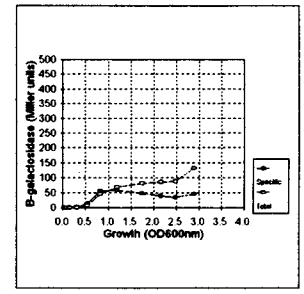
HS1074	0	0.033	1171	2	0.206	0.206	0.184	2.4	0.1	
[35G05]	0.5	0.068	1171	2	0.469	0.484	0.455	2.9	0.2	
	1	0.122	211	2	0.305	0.280	0.271	5.3	0.6	
	1.5	0.268	63	2	0.188	0.194	0.169	5.0	1.3	
	2	0.491	12.5	2	0.187	0.169	0.156	12.7	6.2	
	2.5	0.870	4.5	1	0.282	0.274	0.256	65.4	56.9	
	3	1.150	4.5	1	0.349	0.367	0.336	64.9	74.7	
	4	1.730	4.5	1	0.440	0.451	0.424	54.4	94.1	
	5	2.340	4.5	1	0.458	0.472	0.443	42.1	98.4	
	6	2.700	4.5	1	0.479	0.455	0.445	36.6	98.9	
	7	2.850	2.5	1	0.495	0.531	0.491	68.9	196.4	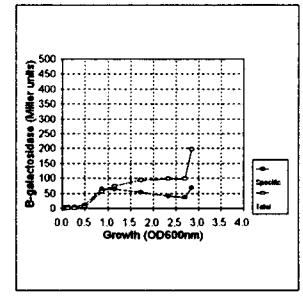
HS1075	0	0.037	1171	2	0.336	0.352	0.322	3.7	0.1	
[35G11]	0.5	0.078	1171	2	0.453	0.453	0.431	2.4	0.2	
	1	0.152	411	2	0.313	0.316	0.293	2.3	0.4	
	1.5	0.330	63	2	0.235	0.237	0.214	5.1	1.7	
	2	0.543	4.5	2	0.232	0.228	0.208	42.6	23.1	
	2.5	0.990	4.5	1	0.305	0.302	0.282	63.2	62.6	
	3	1.300	4.5	1	0.387	0.412	0.378	64.5	83.9	
	4	1.880	4.5	1	0.460	0.466	0.441	52.1	98.0	
	5	2.450	4.5	1	0.370	0.399	0.363	32.9	80.6	
	6	2.880	4.5	1	0.455	0.366	0.389	30.0	86.3	
	7	3.250	2.5	1	0.310	0.282	0.274	33.7	109.6	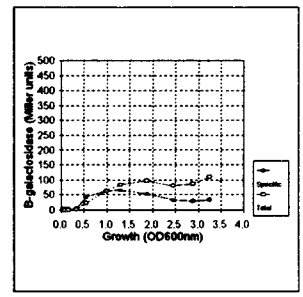
HS1076	0	0.038	1171	2	0.227	0.250	0.217	2.4	0.1	
[35G12]	0.5	0.074	1171	2	0.333	0.358	0.324	1.9	0.1	
	1	0.153	411	2	0.271	0.276	0.252	2.0	0.3	
	1.5	0.316	63	2	0.185	0.185	0.163	4.1	1.3	
	2	0.515	1	2	0.073	0.072	0.051	49.0	25.2	
	2.5	0.880	1	1	0.157	0.144	0.129	146.0	128.5	
	3	1.120	1	1	0.189	0.172	0.159	141.5	158.5	
	4	1.640	1	1	0.198	0.215	0.185	112.5	184.5	
	5	2.150	1	1	0.247	0.269	0.236	109.8	236.0	
	6	2.430	1	1	0.315	0.260	0.266	109.3	265.5	
	7	3.190	2.5	1	0.349	0.364	0.335	41.9	133.8	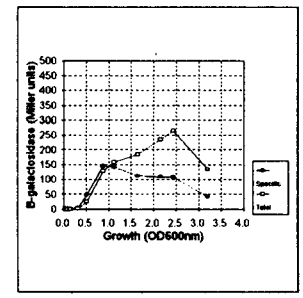

Strain	Time [h]	OD600 [nm]	Rxn Time [min]	Cell Vol [ml]	OD420 [nm] sample1	OD420 [nm] sample2	Avg.	Specific Activity [Miller U]	Total Activity [Miller U]	
HS1077	0	0.060	1171	2	0.175	0.171	0.151	1.1	0.1	
[36A05]	0.5	0.087	1171	2	0.223	0.241	0.210	1.0	0.1	
	1	0.153	137	2	0.242	0.237	0.218	5.2	0.8	
	1.5	0.318	63	2	0.199	0.198	0.177	4.4	1.4	
	2	0.523	1	2	0.040	0.042	0.019	18.2	9.5	
	2.5	0.840	1	1	0.157	0.164	0.139	164.9	138.5	
	3	1.060	1	1	0.349	0.412	0.359	338.2	358.5	
	4	1.550	1	1	0.393	0.443	0.396	255.5	396.0	
	5	2.130	1	1	0.701	0.596	0.627	294.1	626.5	
	6	2.470	1	1	0.485	0.538	0.490	198.2	489.5	
	7	3.080	2.5	1	0.810	0.786	0.776	100.8	310.4	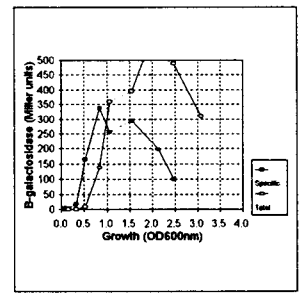
HS1078	0	0.041	411	2	0.345	0.351	0.326	9.7	0.4	
[36A11]	0.5	0.087	211	2	0.346	0.318	0.310	8.4	0.7	
	1	0.161	63	2	0.247	0.268	0.236	11.6	1.9	
	1.5	0.347	47	2	0.478	0.471	0.453	13.9	4.8	
	2	0.558	2.5	2	0.181	0.193	0.165	59.1	33.0	
	2.5	0.980	2.5	1	0.229	0.224	0.205	83.5	81.8	
	3	1.270	2.5	1	0.193	0.260	0.205	64.4	81.8	
	4	1.810	2.5	1	0.347	0.372	0.338	74.6	135.0	
	5	2.370	2.5	1	0.334	0.341	0.316	53.2	126.2	
	6	2.800	2.5	1	0.407	0.449	0.406	58.0	162.4	
	7	2.870	2.5	1	0.609	0.723	0.644	89.8	257.6	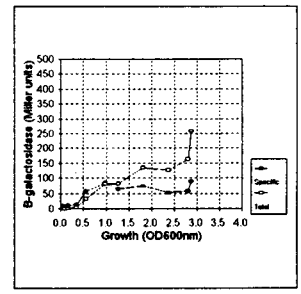
HS1079	0	0.062	411	2	0.270	0.269	0.248	4.9	0.3	
[36B03]	0.5	0.098	211	2	0.295	0.285	0.268	6.5	0.6	
	1	0.161	137	2	0.359	0.370	0.343	7.8	1.3	
	1.5	0.333	47	2	0.385	0.370	0.356	11.4	3.8	
	2	0.531	4	2	0.201	0.218	0.188	44.1	23.4	
	2.5	0.930	4	1	0.294	0.267	0.259	69.5	64.6	
	3	1.230	4	1	0.351	0.342	0.325	66.0	81.1	
	4	1.830	4	1	0.422	0.378	0.378	51.6	94.5	
	5	2.350	4	1	0.447	0.429	0.416	44.3	104.0	
	6	2.660	4	1	0.344	0.397	0.349	32.8	87.1	
	7	3.320	2.5	1	0.442	0.396	0.397	47.8	158.8	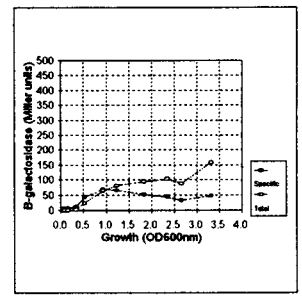
HS1080	0	0.063	1171	2	0.238	0.233	0.214	1.4	0.1	
[36B07]	0.5	0.107	1171	2	0.452	0.437	0.423	1.7	0.2	
	1	0.190	137	2	0.322	0.322	0.300	5.8	1.1	
	1.5	0.375	47	2	0.465	0.463	0.442	12.5	4.7	
	2	0.575	6.5	2	0.201	0.177	0.167	22.3	12.8	
	2.5	0.960	6.5	1	0.308	0.342	0.303	48.6	46.6	
	3	1.270	6.5	1	0.295	0.368	0.310	37.5	47.6	
	4	1.820	3	1	0.240	0.235	0.216	39.5	71.8	
	5	2.400	3	1	0.311	0.312	0.290	40.2	96.5	
	6	2.560	3	1	0.416	0.412	0.392	51.0	130.7	
	7	2.860	2.5	1	0.436	0.484	0.438	61.3	175.2	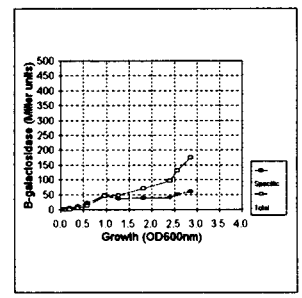
HS1081	0	0.035	1171	2	0.238	0.252	0.223	2.7	0.1	
[36G06]	0.5	0.078	1171	2	0.240	0.300	0.248	1.4	0.1	
	1	0.154	137	2	0.301	0.301	0.279	6.6	1.0	
	1.5	0.319	63	2	0.249	0.243	0.224	5.6	1.8	
	2	0.549	1.5	2	0.046	0.038	0.020	12.1	6.7	
	2.5	0.960	1.5	1	0.126	0.111	0.097	67.0	64.3	
	3	1.280	1.5	1	0.242	0.226	0.212	110.4	141.3	
	4	1.760	1.5	1	0.284	0.276	0.258	97.7	172.0	
	5	2.250	1.5	1	0.282	0.267	0.253	74.8	168.3	
	6	2.380	1.5	1	0.353	0.363	0.336	94.1	224.0	
	7	2.760	2.5	1	0.730	0.727	0.707	102.4	282.6	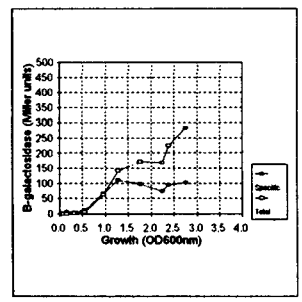

Strain	Time [h]	OD600 [nm]	Rxn Time [min]	Cell Vol [ml]	OD420 [nm] sample1	OD420 [nm] sample2	Avg.	Specific Activity [Miller U]	Total Activity [Miller U]	
HS1082	0	0.037	1414	2	0.347	0.274	0.309	2.9	0.1	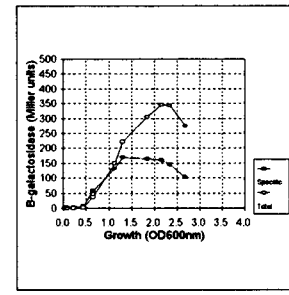
[39C08]	0.5	0.090	1414	2	0.620	0.651	0.634	2.5	0.2	
	1	0.225	209	2	0.247	0.257	0.250	2.7	0.6	
	1.5	0.438	61.5	2	0.412	0.401	0.405	7.5	3.3	
	2	0.651	2	2	0.155	0.152	0.152	58.2	37.9	
	2.5	1.130	2	1	0.299	0.303	0.299	132.3	149.5	
	3	1.310	2	1	0.444	0.451	0.446	170.0	222.8	
	4	1.850	2	1	0.540	0.683	0.610	164.7	304.8	
	5	2.160	2	1	0.667	0.719	0.691	160.0	345.5	
	6	2.340	2	1	0.667	0.709	0.686	146.6	343.0	
	7	2.680	2	1	0.593	0.510	0.550	102.5	274.8	
HS1083	0	0.041	146	2	0.299	0.280	0.288	24.0	1.0	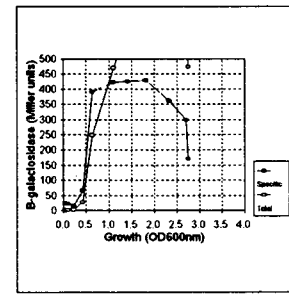
[39E02]	0.5	0.091	91	2	0.383	0.395	0.387	23.4	2.1	
	1	0.226	61.5	2	0.432	0.496	0.462	16.6	3.8	
	1.5	0.418	10	2	0.536	0.582	0.557	66.6	27.9	
	2	0.638	1.5	2	0.746	0.751	0.747	390.0	248.8	
	2.5	1.110	1.5	1	0.738	0.675	0.705	423.1	469.7	
	3	1.420	1.5	1	0.823	0.989	0.904	424.4	602.7	
	4	1.820	1.5	1	1.184	1.163	1.172	429.1	781.0	
	5	2.330	1.5	1	1.256	1.271	1.262	360.9	841.0	
	6	2.700	1.5	1	1.201	1.221	1.209	298.5	806.0	
	7	2.750	2	1	0.995	0.901	0.946	172.0	473.0	
HS1084	0	0.030	1414	2	0.123	0.168	0.144	1.7	0.1	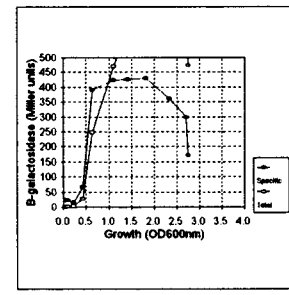
[39E12]	0.5	0.069	1414	2	0.678	0.618	0.646	3.3	0.2	
	1	0.191	146	2	0.224	0.226	0.223	4.0	0.8	
	1.5	0.379	35	2	0.433	0.403	0.416	15.7	5.9	
	2	0.626	4	2	0.324	0.297	0.309	61.6	38.6	
	2.5	1.020	4	1	0.444	0.443	0.442	108.2	110.4	
	3	1.310	4	1	0.519	0.480	0.498	94.9	124.4	
	4	1.800	4	1	0.576	0.620	0.596	82.8	149.0	
	5	2.330	4	1	0.679	0.709	0.692	74.2	173.0	
	6	2.670	4	1	0.673	0.615	0.642	60.1	160.5	
	7	2.840	2.5	1	0.452	0.501	0.475	66.8	189.8	
HS1085	0	0.023	1414	2	0.147	0.210	0.177	2.7	0.1	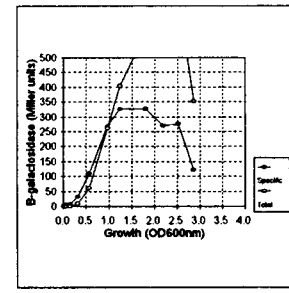
[39F11]	0.5	0.058	1414	2	0.836	0.892	0.862	5.3	0.3	
	1	0.143	129.5	2	0.282	0.280	0.279	7.5	1.1	
	1.5	0.314	18	2	0.344	0.378	0.359	31.8	10.0	
	2	0.562	1.5	2	0.214	**0.160**	0.185	109.7	61.7	
	2.5	0.970	1.5	1	0.417	0.368	0.391	268.4	260.3	
	3	1.240	1.5	1	0.611	0.606	0.607	326.1	404.3	
	4	1.800	1.5	1	0.845	0.921	0.881	326.3	587.3	
	5	2.190	1.5	1	0.886	0.891	0.887	269.9	591.0	
	6	2.520	1.5	1	1.037	1.053	1.043	275.9	695.3	
	7	2.860	2	1	0.732	0.677	0.703	122.8	351.3	
HS1086	0	0.030	1414	2	0.145	0.152	0.147	1.7	0.1	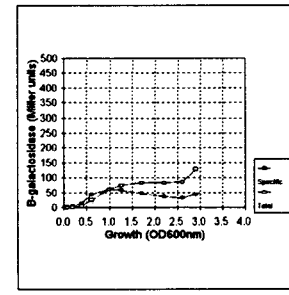
[39H08]	0.5	0.072	1414	2	0.536	0.511	0.522	2.6	0.2	
	1	0.186	129.5	2	0.310	0.281	0.294	6.1	1.1	
	1.5	0.387	35	2	0.385	0.390	0.386	14.2	5.5	
	2	0.607	7.5	2	0.394	0.424	0.407	44.7	27.1	
	2.5	1.000	7.5	1	0.478	0.452	0.463	61.7	61.7	
	3	1.260	7.5	1	0.550	0.575	0.561	59.3	74.7	
	4	1.710	7.5	1	0.647	0.604	0.624	48.6	83.1	
	5	2.210	7.5	1	0.586	0.666	0.624	37.6	83.2	
	6	2.610	7.5	1	0.665	0.615	0.638	32.6	85.1	
	7	2.900	2.5	1	0.346	0.306	0.324	44.7	129.6	

Strain	Time [h]	OD600 [nm]	Rxn Time [min]	Cell Vol [ml]	OD420 [nm] sample1	OD420 [nm] sample2	OD420 [nm] Avg.	Specific Activity [Miller U]	Total Activity [Miller U]	
HS1087	0	0.031	1414	2	0.116	0.135	0.124	1.4	0.0	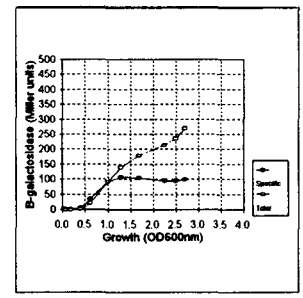
[41F10]	0.5	0.069	1414	2	0.272	0.302	0.285	1.5	0.1	
	1	0.182	1414	2	0.706	0.677	0.690	1.3	0.2	
	1.5	0.396	91	2	0.356	0.377	0.365	5.1	2.0	
	2	0.607	7.5	2	0.312	0.324	0.316	34.7	21.1	
	2.5	1.000	4	1	0.347	0.388	0.366	91.4	91.4	
	3	1.290	4	1	0.539	0.579	0.557	107.9	139.3	
	4	1.690	4	1	0.729	0.705	0.715	105.8	178.8	
	5	2.250	4	1	0.838	0.870	0.852	94.7	213.0	
	6	2.500	4	1	0.942	0.947	0.943	94.3	235.6	
	7	2.700	2.5	1	0.696	0.654	0.673	99.7	269.2	
HS1088	0	0.030	1414	2	0.086	0.085	0.084	1.0	0.0	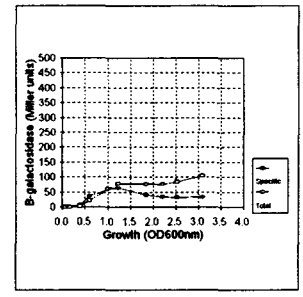
[42B07]	0.5	0.069	1414	2	0.283	0.300	0.290	1.5	0.1	
	1	0.169	1414	2	0.845	0.856	0.849	1.8	0.3	
	1.5	0.389	61.5	2	0.385	0.388	0.385	8.0	3.1	
	2	0.597	6	2	0.277	0.256	0.265	36.9	22.0	
	2.5	1.000	6	1	0.344	0.396	0.368	61.3	61.3	
	3	1.230	6	1	0.465	0.483	0.472	64.0	78.7	
	4	1.850	6	1	0.490	0.437	0.462	41.6	76.9	
	5	2.210	6	1	0.461	0.462	0.460	34.7	76.6	
	6	2.530	6	1	0.499	0.513	0.504	33.2	84.0	
	7	3.090	2.5	1	0.263	0.269	0.264	34.2	105.6	
HS1089	0	0.030	1414	2	0.250	0.247	0.247	2.9	0.1	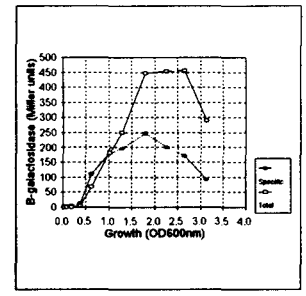
[42H10]	0.5	0.077	1414	2	0.501	0.520	0.509	2.3	0.2	
	1	0.185	146	2	0.219	0.184	0.200	3.7	0.7	
	1.5	0.385	35	2	0.384	0.368	0.374	13.9	5.3	
	2	0.620	3	2	0.408	0.415	0.410	110.1	68.3	
	2.5	1.010	3	1	0.541	0.557	0.547	180.5	182.3	
	3	1.280	3	1	0.781	0.728	0.753	196.0	250.8	
	4	1.800	3	1	1.346	1.339	1.341	248.2	446.8	
	5	2.260	3	1	1.411	1.313	1.360	200.6	453.3	
	6	2.650	3	1	1.371	1.367	1.367	171.9	455.7	
	7	3.130	2	1	0.609	0.554	0.580	92.6	289.8	
HS1090	0	0.035	1414	2	0.807	0.791	0.797	8.1	0.3	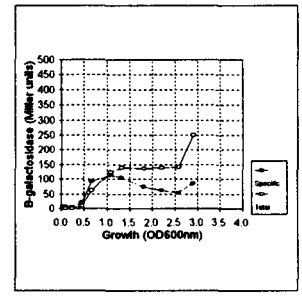
[43E02]	0.5	0.087	146	2	0.221	0.208	0.213	8.4	0.7	
	1	0.232	129.5	2	0.359	0.347	0.351	5.8	1.4	
	1.5	0.455	18	2	0.364	0.394	0.377	23.0	10.5	
	2	0.665	5.5	2	0.712	0.657	0.683	93.3	62.0	
	2.5	1.090	5.5	1	0.693	0.689	0.689	114.9	125.3	
	3	1.320	5.5	1	0.772	0.769	0.769	105.9	139.7	
	4	1.810	5.5	1	0.754	0.754	0.752	75.5	136.7	
	5	2.200	5.5	1	0.766	0.775	0.769	63.5	139.7	
	6	2.580	5.5	1	0.761	0.810	0.784	55.2	142.5	
	7	2.900	2.5	1	0.658	0.601	0.628	86.6	251.0	
HS1091	0	0.032	1414	2	0.809	0.800	0.803	8.9	0.3	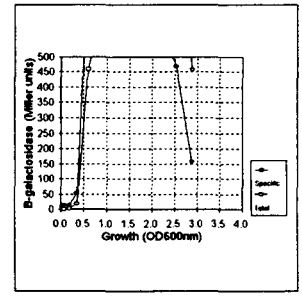
[43G05-d]	0.5	0.071	129.5	2	0.288	0.270	0.277	15.1	1.1	
	1	0.184	61.5	2	0.343	0.319	0.329	14.5	2.7	
	1.5	0.353	10	2	0.383	0.392	0.386	54.6	19.3	
	2	0.592	1	2	0.924	0.917	0.919	775.8	459.3	
	2.5	0.980	1	1	0.751	0.749	0.748	763.3	748.0	
	3	1.200	1	1	0.870	0.917	0.892	742.9	891.5	
	4	1.770	1	1	0.916	0.973	0.943	532.5	942.5	
	5	2.330	1	1	1.298	1.265	1.280	549.1	1279.5	
	6	2.530	1	1	1.198	1.178	1.186	468.8	1186.0	
	7	2.880	2	1	0.896	0.941	0.917	159.1	458.3	

Strain	Time [h]	OD600 [nm]	Rxn Time [min]	Cell Vol [ml]	OD420 [nm] sample1	OD420 [nm] sample2	Avg.	Specific Activity [Miller U]	Total Activity [Miller U]
HS1092	0	0.027	1392	2	0.069	0.058	0.062	0.8	0.0
[43G05-I]	0.5	0.061	1392	2	0.127	0.154	0.139	0.8	0.0
	1	0.157	1392	2	0.364	0.346	0.353	0.8	0.1
	1.5	0.340	69	2	0.381	0.362	0.370	7.9	2.7
	2	0.579	11	2	0.389	0.383	0.384	30.1	17.5
	2.5	0.950	4	1	0.337	0.341	0.337	88.7	84.3
	3	1.150	4	1	0.380	0.346	0.361	78.5	90.3
	4	1.820	4	1	0.776	0.752	0.762	104.7	190.5
	5	2.360	4	1	0.904	0.927	0.914	96.8	228.4
	6	3.010	4	1	0.805	1.089	0.945	78.5	236.3
	7	3.120	2.5	1	0.496	0.483	0.488	62.5	195.0
HS1093	0	0.030	1392	2	0.280	0.266	0.271	3.2	0.1
[43G11]	0.5	0.074	1392	2	0.480	0.425	0.451	2.2	0.2
	1	0.202	187	2	0.199	0.217	0.206	2.7	0.6
	1.5	0.400	39.5	2	0.379	0.399	0.387	12.2	4.9
	2	0.611	4	2	0.463	0.433	0.446	91.2	55.8
	2.5	1.100	4	1	0.552	0.537	0.543	123.3	135.6
	3	1.250	4	1	0.506	0.571	0.537	107.3	134.1
	4	1.760	4	1	0.685	0.631	0.656	93.2	164.0
	5	2.280	4	1	0.689	0.731	0.708	77.6	177.0
	6	2.730	4	1	0.719	0.757	0.736	67.4	184.0
	7	2.680	2.5	1	0.418	0.432	0.423	63.1	169.2
HS1094	0	0.031	1392	2	0.225	0.268	0.245	2.8	0.1
[44A08]	0.5	0.057	1392	2	0.477	0.514	0.494	3.1	0.2
	1	0.148	187	2	0.239	0.229	0.232	4.2	0.6
	1.5	0.352	39.5	2	0.492	0.485	0.487	17.5	6.2
	2	0.599	4	2	0.368	0.354	0.359	74.9	44.9
	2.5	1.020	4	1	0.605	0.677	0.639	156.6	159.8
	3	1.150	4	1	0.893	0.871	0.880	191.3	220.0
	4	1.720	4	1	1.248	1.223	1.234	179.3	308.4
	5	2.240	4	1	1.303	1.317	1.308	146.0	327.0
	6	2.470	4	1	1.406	1.443	1.423	144.0	355.6
	7	2.890	2.5	1	0.777	0.805	0.789	109.2	315.6
HS1095	0	0.031	187	2	0.311	0.288	0.298	25.7	0.8
[44C09]	0.5	0.072	124	2	0.356	0.344	0.348	19.5	1.4
	1	0.193	39.5	2	0.342	0.330	0.334	21.9	4.2
	1.5	0.398	13	2	0.413	0.385	0.397	38.4	15.3
	2	0.629	4	2	0.647	0.768	0.706	140.2	88.2
	2.5	1.020	4	1	0.781	0.770	0.774	189.6	193.4
	3	1.160	4	1	0.928	0.995	0.960	206.8	239.9
	4	1.720	4	1	1.133	1.143	1.136	165.1	284.0
	5	2.230	4	1	1.287	1.277	1.280	143.5	320.0
	6	2.470	4	1	1.579	1.577	1.576	159.5	394.0
	7	2.980	2.5	1	0.478	0.512	0.493	66.2	197.2
HS1096	0	0.031	1392	2	1.071	0.995	1.031	11.9	0.4
[45B11]	0.5	0.068	124	2	0.289	0.247	0.266	15.8	1.1
	1	0.204	69	2	0.350	0.298	0.322	11.4	2.3
	1.5	0.388	13	2	0.495	0.535	0.513	50.9	19.7
	2	0.639	1.5	2	0.643	0.610	0.625	325.8	208.2
	2.5	1.040	1.5	1	0.683	0.642	0.661	423.4	440.3
	3	1.230	1.5	1	0.711	0.717	0.712	385.9	474.7
	4	1.680	1.5	1	0.877	0.884	0.879	348.6	585.7
	5	2.130	1.5	1	0.871	0.860	0.864	270.3	575.7
	6	2.480	1.5	1	0.863	0.846	0.853	229.2	568.3
	7	2.720	2.5	1	0.883	0.831	0.855	125.7	342.0

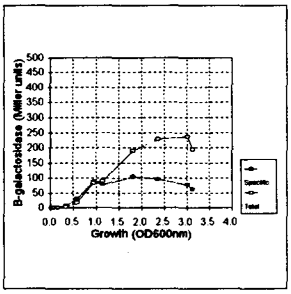

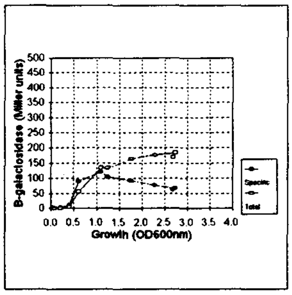

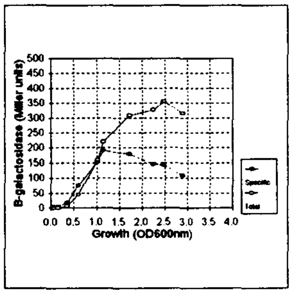

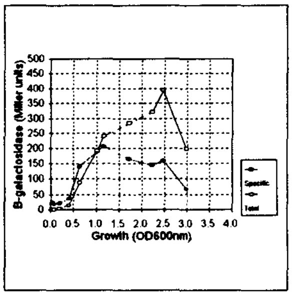

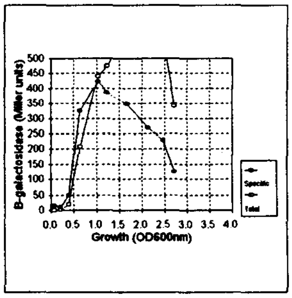

Strain	Time [h]	OD600 [nm]	Rxn Time [min]	Cell Vol [ml]	OD420 [nm] sample1	OD420 [nm] sample2	Avg.	Specific Activity [Miller U]	Total Activity [Miller U]	
HS1098	0	0.029	1392	2	0.404	0.401	0.401	5.0	0.1	
[46A08]	0.5	0.073	1392	2	0.673	0.697	0.683	3.4	0.2	
	1	0.191	187	2	0.402	0.322	0.360	5.0	1.0	
	1.5	0.383	39.5	2	0.495	0.488	0.490	16.2	6.2	
	2	0.628	3	2	0.406	0.429	0.416	110.3	69.3	
	2.5	0.980	3	1	0.755	0.773	0.762	259.2	254.0	
	3	1.180	3	1	0.471	0.543	0.505	142.7	168.3	
	4	1.750	3	1	1.081	1.073	1.075	204.8	358.3	
	5	2.230	3	1	1.145	1.150	1.146	171.2	381.8	
	6	2.520	3	1	1.083	1.093	1.086	143.7	362.0	
	7	3.190	2.5	1	0.692	0.712	0.700	87.8	280.0	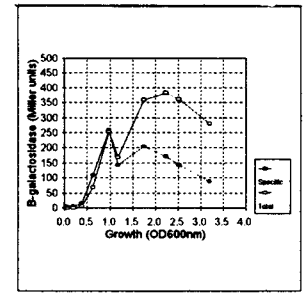
HS1099	0	0.031	124	2	0.340	0.284	0.310	40.3	1.3	
[46D12]	0.5	0.078	107.5	2	0.494	0.416	0.453	27.0	2.1	
	1	0.197	69	2	0.795	0.805	0.798	29.4	5.8	
	1.5	0.397	13	2	0.823	0.770	0.795	77.0	30.6	
	2	0.604	3	2	0.535	0.527	0.529	146.0	88.2	
	2.5	0.910	3	1	0.498	0.504	0.499	182.8	166.3	
	3	1.070	3	1	0.767	0.753	0.758	236.1	252.7	
	4	1.510	3	1	0.557	0.631	0.592	130.7	197.3	
	5	1.950	3	1	0.824	0.872	0.846	144.6	282.0	
	6	2.300	3	1	0.866	0.885	0.874	126.6	291.2	
	7	2.700	2.5	1	0.361	0.403	0.380	56.3	152.0	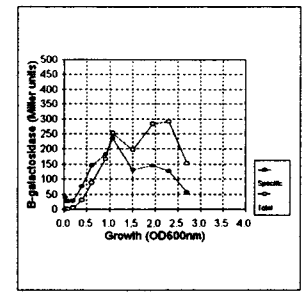
HS1100	0	0.041	1392	2	0.922	0.898	0.908	8.0	0.3	
[47B12]	0.5	0.096	124	2	0.243	0.245	0.242	10.2	1.0	
	1	0.243	69	2	0.325	0.328	0.325	9.7	2.4	
	1.5	0.442	13	2	0.328	0.335	0.330	28.7	12.7	
	2	0.654	6.5	2	0.701	0.638	0.668	78.5	51.3	
	2.5	1.100	6.5	1	0.497	0.501	0.497	69.5	76.5	
	3	1.260	6.5	1	0.622	0.665	0.642	78.3	98.7	
	4	1.890	6.5	1	0.851	0.847	0.847	68.9	130.3	
	5	2.600	6.5	1	0.777	1.033	0.903	53.4	138.9	
	6	2.740	6.5	1	0.917	0.839	0.876	49.2	134.8	
	7	3.140	2.5	1	0.366	0.374	0.368	46.9	147.2	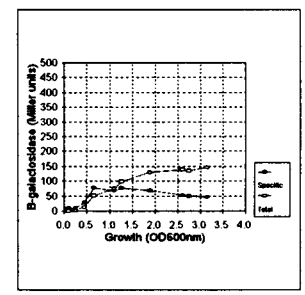
HS1101	0	0.037	1392	2	0.520	0.516	0.516	5.0	0.2	
[47D08]	0.5	0.081	1392	2	0.713	0.748	0.729	3.2	0.3	
	1	0.184	187	2	0.251	0.254	0.251	3.6	0.7	
	1.5	0.377	39.5	2	0.391	0.409	0.398	13.4	5.0	
	2	0.619	6.5	2	0.599	0.589	0.592	73.6	45.5	
	2.5	0.910	6.5	1	0.554	0.670	0.610	103.1	93.8	
	3	0.980	6.5	1	0.689	0.782	0.734	115.1	112.8	
	4	1.470	6.5	1	0.859	0.886	0.871	91.1	133.9	
	5	1.860	6.5	1	0.709	0.633	0.669	55.3	102.9	
	6	2.220	6.5	1	0.745	0.706	0.724	50.1	111.3	
	7	2.840	2.5	1	0.413	0.462	0.436	61.3	174.2	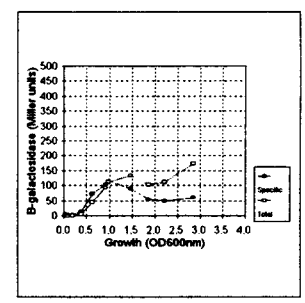
HS1103	0	0.029	1319	2	0.340	0.398	0.338	4.4	0.1	
[48B01-m]	0.5	0.058	406	2	0.350	0.341	0.315	6.7	0.4	
	1	0.152	176	2	0.417	0.425	0.390	7.3	1.1	
	1.5	0.305	20.5	2	0.254	0.237	0.215	17.2	5.2	
	2	0.536	11.5	2	0.630	0.616	0.592	48.0	25.7	
	2.5	1.080	5.5	1	0.367	0.379	0.342	57.6	62.2	
	3	1.420	5.5	1	0.439	0.466	0.422	54.0	76.6	
	4	2.000	5.5	1	0.641	0.629	0.604	54.9	109.8	
	5	2.570	5.5	1	0.717	0.664	0.660	46.7	119.9	
	6	3.020	5.5	1	0.532	0.572	0.521	31.4	94.7	
	7	3.660	2.4	1	0.306	0.331	0.288	32.7	119.8	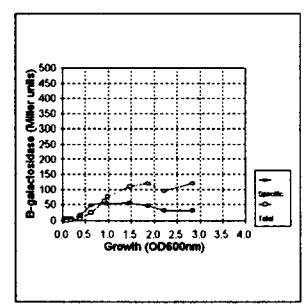

Strain	Time [h]	OD600 [nm]	Rxn Time [min]	Cell Vol [ml]	OD420 [nm] sample1	OD420 [nm] sample2	Avg.	Specific Activity [Miller U]	Total Activity [Miller U]
HS1104	0	0.038	179	2	0.270	0.258	0.233	17.1	0.7
[48E04]	0.5	0.067	59	2	0.281	0.274	0.247	31.2	2.1
	1	0.167	20.5	2	0.253	0.252	0.222	32.3	5.4
	1.5	0.329	9	2	0.404	0.412	0.377	63.7	20.9
	2	0.531	1.5	2	0.404	0.446	0.394	247.3	131.3
	2.5	1.110	1.5	1	0.654	0.644	0.618	371.2	412.0
	3	1.410	1.5	1	0.996	0.938	0.936	442.6	624.0
	4	2.050	1.5	1	0.733	0.904	0.788	256.1	525.0
	5	2.710	1.5	1	0.731	0.712	0.691	169.9	460.3
	6	3.050	1.5	1	0.891	0.650	0.740	161.6	493.0
	7	3.660	1.1	1	0.808	0.557	0.652	161.8	592.3
HS1105	0	0.031	1319	2	0.378	0.392	0.354	4.3	0.1
[49F03]	0.5	0.063	406	2	0.371	0.379	0.344	6.7	0.4
	1	0.161	176	2	0.411	0.385	0.367	6.5	1.0
	1.5	0.318	15	2	0.274	0.272	0.242	25.4	8.1
	2	0.556	8.5	2	0.703	0.697	0.669	70.8	39.4
	2.5	1.120	1.5	1	0.359	0.294	0.296	175.9	197.0
	3	1.380	1.5	1	0.450	0.443	0.416	200.7	277.0
	4	2.090	1.5	1	0.364	0.550	0.426	135.9	284.0
	5	2.700	1.5	1	0.404	0.397	0.370	91.2	246.3
	6	3.060	1.5	1	0.681	0.352	0.486	105.8	323.7
	7	3.400	1.9	1	0.475	0.470	0.442	68.3	232.4

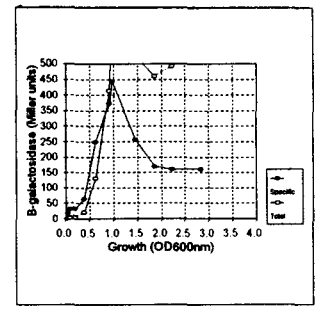

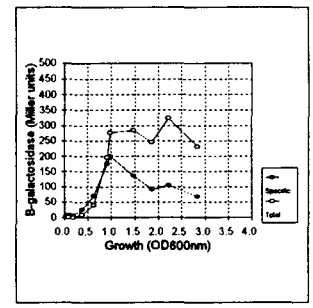

Appendix B. Summary of characteristics of σ^s-dependent *lacZ* fusion mutants. (a) Status of complementation results are of strains in MC4100 background. (b) From the categories in Table 3, complementation results of 28 strains have not been obtained for strains which exhibited two transconjugant phenotypes and for those in the "status unknown" category. (c) Transduction of *lacZ* fusions into a new GC4468 background resulted in some strains having two transductant phenotypes. d & l are abbreviations representing dark and light colonies formed from perhaps two different strains originating from the same well. Many were probably the result of two strains containing independent *lacZ* fusions that were inoculated into a single well during the storage procedure or by cross-contamination. n and m represent mutants exhibiting normal colony phenotype and mucoid phenotype. A common trend was the loss of the mucoid phenotype upon transduction into the GC4468 background. Levels of β-galactosidase activity for recipients and transconjugants depicted by the "+" signs are not to the same scale. "Two morphologies over time" represent strains showing a difference in β-galactosidase expression only after several days.

STRAIN	[Location]	(a) COMMENTS / COMPLEMENTATION RESULTS (of strains in MC4100 background)	(b) COMPLEMENTATION RESULTS UNKNOWN	(c) TRANSDUCTION 2 PHENOTYPES
HS1001	01D04	complemented		
HS1002	01E04	complemented		
HS1003	01H01	complemented		
HS1004	02C08-d	complemented		
HS1005	02D11	complemented		y
HS1006	02E11	suspected katE mutant // complemented wrt B-gal		
HS1007	02E12	suspected katE mutant // complemented wrt B-gal		
HS1008	02H06	complemented		
HS1009	03C06	complemented		
HS1010	03F05-l	TCJ 2 morphologies	x	
HS1011	04C07-d	complemented		
HS1012	04D09	TCJ 2 morphologies	x	y
HS1013	04F08-d	complemented		y
HS1014	05A10	suspected katE mutant // compemented wrt B-gal		
HS1015	05C08-l	complemented wrt B-gal		y
HS1016	06A12-d	complemented		
HS1017	06C03	complemented		
HS1018	06E01-d		x	
HS1019	06E01-l		x	
HS1020	07A08	TCJ 2 morphologies	x	
HS1021	07B07	TCJ 2 morphologies // not complemented wrt B-gal	x	
HS1022	07B09		x	y
HS1023	07D07-d	not complemented wrt B-gal		
HS1024	07E04	TCJ 2 morphologies	x	
HS1025	07F09	not complemented wrt catalase		
HS1026	07F10	complemented		
HS1027	07F11	complemented		
HS1028	08H08	complemented		
HS1029	09B11	complemented		

STRAIN	[Location]	RECIPIENTS (GC4468 BKGRD)	B-gal	cat	TRANSCONJUGANTS (GC4468 BKGRD)	B-gal	cat	COMMENTS
HS1001	01D04		+	+		+	-	
HS1002	01E04		+	+		-	-	
HS1003	01H01		+	+	dark partial colonies appear over time	-	-	
HS1004	02C08-d		+	+		+	-	
HS1005	02D11		+	+	2 morphologies over time	++	-	
HS1006	02E11		+	-		-	-	suspected katE mutant
HS1007	02E12		+	-		-	-	suspected katE mutant
HS1008	02H06		+	+	2 morphologies over time	++	-	not highly RpoS-dependent
HS1009	03C06		+	+		-	-	
HS1010	03F05-l		+	+		+	-	not highly RpoS-dependent
HS1011	04C07-d		++	+		++++	-	not highly RpoS-dependent
HS1012	04D09		+	+		++	-	
HS1013	04F08-d		+	+		-	-	
HS1014	05A10		++	-	small white colonies appear over time	-	-	suspected katE mutant
HS1015	05C08-l		+	+		-	-	
HS1016	06A12-d		+	+		++++	-	not highly RpoS-dependent
HS1017	06C03		+	+		++++	-	not highly RpoS-dependent
HS1018	06E01-d	d&l appear same	+	+	d&l appear same	+++	-	
HS1019	06E01-l	d&l appear same	+	+	d&l appear same	++	-	same as 6E01-d // may omit from studies
HS1020	07A08		+	+		++++	-	not highly RpoS-dependent
HS1021	07B07		+	+	small white colonies appear over time	-	-	
HS1022	07B09		+	+		-	-	
HS1023	07D07-d		+	+		++++	-	not highly RpoS-dependent
HS1024	07E04		+	+		++	-	
HS1025	07F09		+	+	2 morphologies // problem strain	+++	-	
HS1026	07F10		+	+	2 morphologies // problem strain	+++	-	
HS1027	07F11		+	+	2 morphologies // problem strain	+++	-	
HS1028	08H08		-	+		+++	-	not highly RpoS-dependent
HS1029	09B11		+	+	2 morphologies over time	+	-	

STRAIN	[Location]	(a) COMMENTS / COMPLEMENTATION RESULTS (of strains in MC4100 background)	(b) COMPLEMENTATION RESULTS UNKNOWN	(c) TRANSDUCTION 2 PHENOTYPES
HS1030	09C07	not complemented wrt B-gal		
HS1031	09E10	TCJ 2 morphologies	x	
HS1032	09H12	complemented		
HS1033	12A10-l	complemented		
HS1034	12C09	complemented		
HS1035	13B08-l	complemented		
HS1036	13C08	complemented		
HS1037	14C03-l	TCJ 2 morphologies	x	y
HS1038	14D08	complemented		
HS1039	15G03	TCJ 2 morphologies	x	
HS1040	16E03-d	complemented		
HS1041	16F07	complemented		
HS1042	21B04-l	complemented		
HS1043	21F08	complemented		
HS1044	22E03	complemented		
HS1045	22F08-l	complemented		
HS1046	22F09-d	complemented		
HS1047	22G10	complemented		
HS1048	23E01		x	
HS1049	24B12	complemented		
HS1050	24C07	complemented		
HS1051	25A11-d	complemented		
HS1052	25B04	complemented		
HS1053	26A06	complemented		
HS1054	26E05	complemented		
HS1055	28F07	complemented		
HS1056	29G11	complemented		y
HS1057	31B04	complemented		
HS1058	31B09	complemented		

STRAIN	[Location]	RECIPIENTS (GC4468 BKGRD)	B-gal	cat	TRANSCONJUGANTS (GC4468 BKGRD)	B-gal	cat	COMMENTS
HS1030	09C07		+	+		-	-	
HS1031	09E10		+	+		+	-	
HS1032	09H12		+	+		+++	-	
HS1033	12A10-l		+	+	problem strain	-	-	
HS1034	12C09		+	+	problem strain	+	-	
HS1035	13B08-l		+++	+		-	-	
HS1036	13C08		+	+	problem strain	+	-	
HS1037	14C03-l		-	+		-	-	
HS1038	14D08		++	+		++	-	
HS1039	15G03		+	+		+	-	
HS1040	16E03-d		+	+		+	-	
HS1041	16F07		++	+	problem strain	++	-	
HS1042	21B04-l		+	+		+	-	
HS1043	21F08		+	+	2 morphologies over time	-	-	
HS1044	22E03		+	+	problem strain	++++	-	
HS1045	22F08-l		+	+		++++	-	
HS1046	22F09-d		+	+		+++	-	
HS1047	22G10		+	+		-	-	
HS1048	23E01		+	+		-	-	
HS1049	24B12		+	+		-	-	
HS1050	24C07		-	+	2 morphologies when 1 colony restreaked	+	-	
HS1051	25A11-d		+	+		++	-	
HS1052	25B04		+	+		+++	-	
HS1053	26A06		+	+	problem strain	+++	-	not highly RpoS-dependent
HS1054	26E05		+	+		+	-	
HS1055	28F07		+	+	problem strain	++++	-	
HS1056	29G11		+	+		++	-	
HS1057	31B04		+	+		+++	-	not highly RpoS-dependent
HS1058	31B09		+	+		+++	-	not highly RpoS-dependent

STRAIN	[Location]	(a) COMMENTS / COMPLEMENTATION RESULTS (of strains in MC4100 background)	(b) COMPLEMENTATION RESULTS UNKNOWN	(c) TRANSDUCTION 2 PHENOTYPES
HS1059	31D07-d		x	
HS1060	31D07-l		x	
HS1061	31F08-n		x	
HS1062	31F09	suspected katE mutant // complemented wrt B-gal		y
HS1063	32D07	TCJ 2 morphologies	x	y
HS1064	32D11	complemented		
HS1065	33B07	TCJ 2 morphologies	x	
HS1066	33C09	complemented		
HS1067	34C08-n		x	
HS1068	34C08-m		x	
HS1069	34E11	not complemented wrt B-gal		y
HS1070	35B06	not complemented wrt B-gal		y
HS1071	35B09	complemented		y
HS1072	35C12-l		x	
HS1073	35F12	complemented		
HS1074	35G05	complemented		
HS1075	35G11	complemented		
HS1076	35G12	complemented		
HS1077	36A05-l	complemented		
HS1078	36A11-l		x	
HS1079	36B03	complemented		
HS1080	36B07-l		x	
HS1081	36G06	complemented		
HS1082	39C08	complemented		
HS1083	39E02-l	complemented		
HS1084	39E12	complemented		y
HS1085	39F11	complemented		
HS1086	39H08-l	complemented		
HS1087	41F10-d	complemented		

STRAIN	[Location]	RECIPIENTS (GC4468 BKGRD)	B-gal	cat	TRANSCONJUGANTS (GC4468 BKGRD)	B-gal	cat	COMMENTS
HS1059	31D07-d	d&l appear same	+	+	d&l appear same	++	-	
HS1060	31D07-l	d&l appear same	+	+	d& l appear same	++	-	same as 31D07-d // may omit from studies
HS1061	31F08-n		+	+	2 morphologies over time	++	-	
HS1062	31F09		+	-	few partial dark colonies	++	-	suspected katE mutant
HS1063	32D07		+	+	2 morphologies over time	-	-	
HS1064	32D11		+	+		+++	-	not highly RpoS-dependent
HS1065	33B07		+	+		++++	-	Jan 5/96 // not RpoS-dependent // omit
HS1066	33C09		+	+		++++	-	not highly RpoS-dependent
HS1067	34C08-n		+	+		-	-	
HS1068	34C08-m	no longer mucoid	+	+	no longer mucoid	-	-	same as 34C08-n // may omit from studies
HS1069	34E11		++	+		-	-	
HS1070	35B06		+	+		++	-	not highly RpoS-dependent
HS1071	35B09		+	+	problem strain	++	-	
HS1072	35C12-l		+	+		+++	-	not highly RpoS-dependent // can't grow on minimal
HS1073	35F12		+	+	problem strain	-	-	
HS1074	35G05		+	+		-	-	
HS1075	35G11		+	+		++	-	not highly RpoS-dependent
HS1076	35G12		+	+		-	-	
HS1077	36A05-l		+	+		+	-	
HS1078	36A11-l		+	+	problem strain	++	-	
HS1079	36B03		+	+	few dark partial colonies	+++	-	not highly RpoS-dependent
HS1080	36B07-l		+	+	problem strain	++	-	
HS1081	36G06		+	+	problem strain	-	-	
HS1082	39C08		+	+		-	-	
HS1083	39E02-l		+++	+	problem strain	+++	-	
HS1084	39E12		++	+		+	-	
HS1085	39F11		+++	+		++	-	
HS1086	39H08-l		+	+		++	-	
HS1087	41F10-d		+	+		-	-	

STRAIN	[Location]	(a) COMMENTS / COMPLEMENTATION RESULTS (of strains in MC4100 background)	(b) COMPLEMENTATION RESULTS UNKNOWN	(c) TRANSDUCTION 2 PHENOTYPES
HS1088	42B07	complemented		
HS1089	42H10	complemented		
HS1090	43E02	TCJ 2 morphologies	x	
HS1091	43G05-d	complemented		y
HS1092	43G05-l	complemented		
HS1093	43G11	complemented		
HS1094	44A08	complemented		y
HS1095	44C09	complemented		
HS1096	45B11	complemented		y
HS1097	45F04-d	complemented		
HS1098	46A08-n		x	
HS1099	46D12-l	complemented		
HS1100	47B12	complemented	x	
HS1101	47D08		x	
HS1102	48B01-n	complemented	x	
HS1103	48B01-m	complemented	x	
HS1104	48E04	complemented		y
HS1105	49F03	complemented		

STRAIN	[Location]	RECIPIENTS (GC4468 BKGRD)	B-gal	cat	TRANSCONJUGANTS (GC4468 BKGRD)	B-gal	cat	COMMENTS
HS1088	42B07		+++	+		-	-	
HS1089	42H10		+	+		-	-	
HS1090	43E02		+	+		-	-	
HS1091	43G05-d	d&l appear same	+++	+	darker than 43G05-l // problem strain	++	-	
HS1092	43G05-l	d&l appear same	+	+	lighter than 43G05-d // problem strain	-	-	
HS1093	43G11		+	+		-	-	
HS1094	44A08		+	+	problem strain	+++	-	
HS1095	44C09		+	+		++	-	
HS1096	45B11		+	+	problem strain	++	-	
HS1097	45F04-d		++	+	problem strain	++	-	
HS1098	46A08-n		+	+	problem strain	++	-	
HS1099	46D12-l		+	+		++++	-	not highly RpoS-dependent
HS1100	47B12		+	+	problem strain	++++	-	not highly RpoS-dependent
HS1101	47D08		+	+		-	-	
HS1102	48B01-n		+	+		-	-	
HS1103	48B01-m	no longer mucoid	+	+	no longer mucoid	-	-	same as 48B01-n // may omit from studies
HS1104	48E04		+	+		++++	-	
HS1105	49F03		+	+	2 morphologies over time	++++	-	

Appendix C. Raw data of the growth-phase-dependent expression of *rpoS*$^-$ transconjugants. Twelve of fifteen *rpoS*$^-$ strains with an induction ratio greater than 5.0 were reassayed with the entire range of time points used for the *rpoS*$^+$ recipients in Appendix A. Data was plotted two different ways, the first row of graphs on a time scale and the second. Time 7 h represents an overnight sample.

Calculation of Specific Activity:

[1000 x OD(420 nm)] / [Rxn Time (min) x Volume Assayed (ml) x OD(600 nm)]

Strain	Time (h)	OD600 (nm)	OD420 (nm) sample 1	sample 2	avg	Rxn Time (min)	Vol (ml)	Specific Activity (Miller U)		
HS1008t	0.0	0.077	0.046	0.058	0.052	475	2	0.7	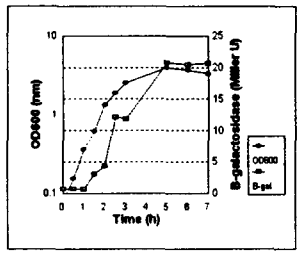	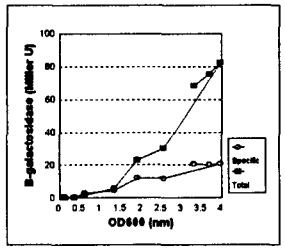
[02H06t]	0.5	0.154	0.067	0.073	0.070	312	2	0.7		
	1.0	0.362	0.100	0.116	0.108	225	2	0.7		
	1.5	0.620	0.229	0.235	0.232	62	2	3.0		
	2.0	1.340	0.266	0.268	0.267	23	2	4.3		
	2.5	1.900	0.232	0.229	0.231	10	1	12.1		
	3.0	2.550	0.293	0.311	0.302	10	1	11.8		
	5.0	3.970	0.435	0.391	0.413	5	1	20.8		
	6.0	3.700	0.404	0.352	0.378	5	1	20.4		
	7.0	3.310	0.350	0.334	0.342	5	1	20.7		
HS1010t	0.0	0.114	0.084	0.069	0.077	475	2	0.7	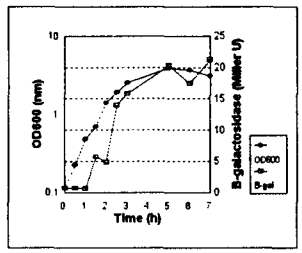	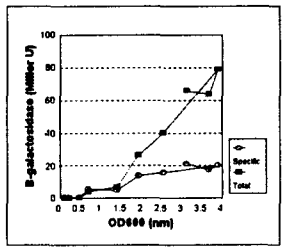
[03F05t]	0.5	0.227	0.100	0.098	0.099	312	2	0.7		
	1.0	0.484	0.153	0.144	0.149	225	2	0.7		
	1.5	0.700	0.511	0.485	0.498	62	2	5.7		
	2.0	1.400	0.315	0.313	0.314	23	2	4.9		
	2.5	1.920	0.270	0.267	0.269	10	1	14.0		
	3.0	2.540	0.399	0.406	0.403	10	1	15.8		
	5.0	3.900	0.402	0.390	0.396	5	1	20.3		
	6.0	3.670	0.285	0.355	0.320	5	1	17.4		
	7.0	3.110		0.331	0.330	5	1	21.2		
HS1024t	0.0	0.073	0.031	0.034	0.033	475	2	0.5	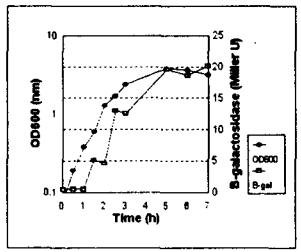	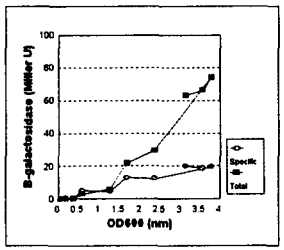
[07E04t]	0.5	0.190	0.063	0.072	0.068	312	2	0.6		
	1.0	0.378	0.093	0.098	0.096	225	2	0.6		
	1.5	0.590	0.371	0.377	0.374	62	2	5.1		
	2.0	1.280	0.266	0.278	0.272	23	2	4.6		
	2.5	1.680	0.224	0.213	0.219	10	1	13.0		
	3.0	2.360	0.308	0.285	0.297	10	1	12.6		
	5.0	3.790	0.355	0.387	0.371	5	1	19.6		
	6.0	3.570	0.394	0.270	0.332	5	1	18.6		
	7.0	3.140	0.317	0.315	0.316	5	1	20.1		
HS1031t	0.0	0.069	0.065	0.048	0.057	475	2	0.9	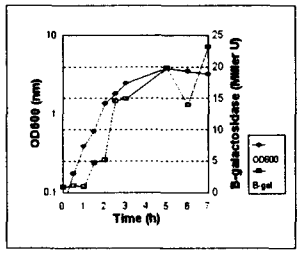	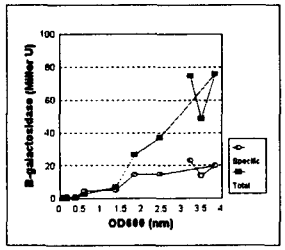
[09E10t]	0.5	0.174	0.118	0.124	0.121	312	2	1.1		
	1.0	0.390	0.169	0.161	0.165	225	2	0.9		
	1.5	0.600	0.345	0.365	0.355	62	2	4.8		
	2.0	1.360	0.330	0.318	0.324	23	2	5.2		
	2.5	1.820	0.270	0.262	0.266	10	1	14.6		
	3.0	2.460	0.389	0.346	0.368	10	1	14.9		
	5.0	3.840	0.416	0.344	0.380	5	1	19.8		
	6.0	3.490	0.409	0.077	0.243	5	1	13.9		
	7.0	3.220	0.369	0.377	0.373	5	1	23.2		

Strain	Time (h)	OD600 (nm)	OD420 (nm) sample 1	OD420 (nm) sample 2	OD420 (nm) avg	Rxn Time (min)	Vol (ml)	Specific Activity (Miller U)
HS1034t	0.0	0.111	0.165	0.169	0.167	475	2	1.6
[12C09t]	0.5	0.262	0.199	0.199	0.199	312	2	1.2
	1.0	0.543	0.245	0.203	0.224	90	2	2.3
	1.5	0.940	0.596	0.620	0.608	62	2	5.2
	2.0	1.670	0.394	0.397	0.396	23	2	5.1
	2.5	2.250	0.272	0.271	0.272	10	1	12.1
	3.0	2.580	0.329	0.345	0.337	10	1	13.1
	5.0	3.880	0.264	0.292	0.278	5	1	14.3
	6.0	3.960	0.175	0.210	0.193	5	1	9.7
	7.0	3.070	0.196	0.207	0.202	5	1	13.1
HS1037t	0.0	0.094	0.028	0.013	0.021	475	2	0.2
[14C03t]	0.5	0.191	0.054	0.047	0.051	312	2	0.4
	1.0	0.415	0.086	0.071	0.079	225	2	0.4
	1.5	0.560	0.208	0.186	0.197	62	2	2.8
	2.0	1.340	0.270	0.241	0.256	38	2	2.5
	2.5	1.790	0.154	0.143	0.149	10	1	8.3
	3.0	2.460	0.191	0.181	0.186	10	1	7.6
	5.0	4.040	0.195	0.183	0.189	5	1	9.4
	6.0	3.680	0.188	0.151	0.170	5	1	9.2
	7.0	3.200	0.120	0.144	0.132	5	1	8.3
HS1043t	0.0	0.071	0.015	0.033	0.024	230	2	0.7
[21F08t]	0.5	0.170	0.029	0.039	0.034	225	2	0.4
	1.0	0.405	0.069	0.080	0.075	175	2	0.5
	1.5	0.760	0.233	0.208	0.221	120	2	1.2
	2.0	1.260	0.274	0.272	0.273	20	2	5.4
	3.0	2.240	0.290	0.292	0.291	30	1	4.3
	4.0	3.080	0.177	0.173	0.175	15	1	7.6
	5.0	3.550	0.199	0.185	0.192	18	1	6.0
	6.0	3.870	0.141	0.132	0.137	15	1	4.7
	7.0	3.400	0.102	0.114	0.108	15	1	4.2
HS1057t	0.0	0.077	0.054	0.051	0.053	230	2	1.5
[31B04t]	0.5	0.161	0.096	0.101	0.099	225	2	1.4
	1.0	0.382	0.224	0.208	0.216	175	2	1.6
	1.5	0.740	0.576	0.586	0.581	50	2	7.9
	2.0	1.190	0.621	0.620	0.621	20	2	13.0
	3.0	2.030	0.569	0.599	0.584	10	1	28.8
	4.0	3.920	0.327	0.347	0.337	4	1	43.0
	5.0	3.580	0.580	0.633	0.607	7	1	48.4
	6.0	3.890	0.321	0.342	0.332	3	1	56.8
	7.0	3.220	0.220	0.210	0.215	3	1	44.5

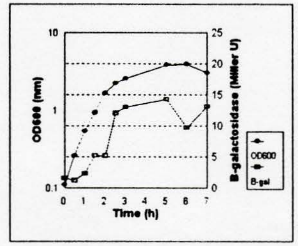

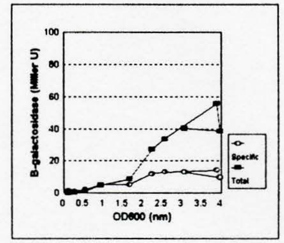

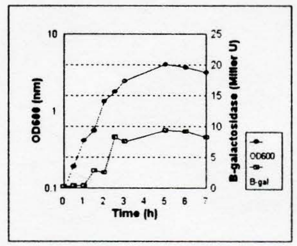

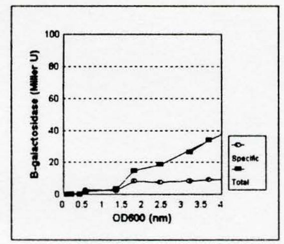

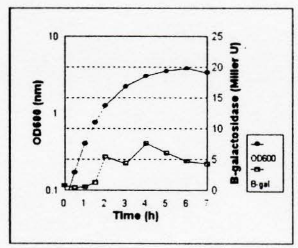

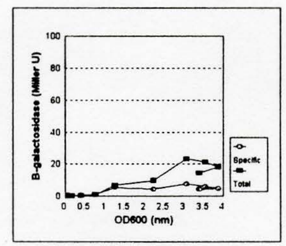

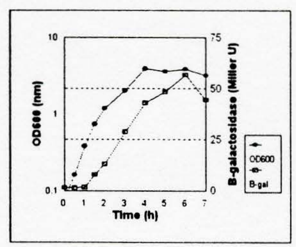

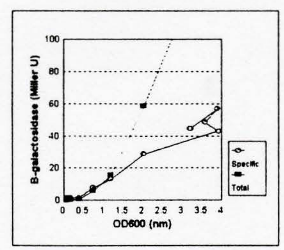

Strain	Time (h)	OD600 (nm)	OD420 (nm) sample 1	OD420 (nm) sample 2	OD420 (nm) avg	Rxn Time (min)	Vol (ml)	Specific Activity (Miller U)
HS1058t	0.0	0.079	0.139	0.113	0.126	425	2	1.9
[31B09t]	0.5	0.142	0.179	0.169	0.174	425	2	1.4
	1.0	0.332	0.345	0.358	0.352	390	2	1.4
	1.5	0.740	0.210	0.206	0.208	25	2	5.6
	2.0	1.180	0.350	0.357	0.354	10	2	15.0
	2.5	1.500	0.267	0.279	0.273	10	1	18.2
	3.0	1.900	0.406	0.399	0.403	10	1	21.2
	4.0	2.660	0.401	0.403	0.402	5	1	30.2
	5.0	3.240	0.632	0.625	0.629	3	1	64.7
	6.0	3.700	0.776	0.780	0.778	8	1	52.6
	7.0	4.020	0.405	0.395	0.400	5	1	39.8
HS1061t	0.0	0.070	0.030	0.040	0.035	230	2	1.1
[31F08t]	0.5	0.146	0.046	0.052	0.049	225	2	0.7
	1.0	0.357	0.073	0.070	0.072	175	2	0.6
	1.5	0.780	0.292	0.314	0.303	120	2	1.6
	2.0	1.160	0.141	0.153	0.147	40	2	1.6
	3.0	2.200	0.265	0.276	0.271	10	1	12.3
	4.0	2.960	0.354	0.362	0.358	15	1	16.1
	5.0	3.380	0.260	0.236	0.248	7	1	21.0
	6.0	3.760	0.297	0.314	0.306	15	1	10.8
	7.0	3.120	0.284	0.283	0.284	15	1	12.1
HS1063t	0.0	0.080	0.024	0.044	0.034	230	2	0.9
[32D07t]	0.5	0.176	0.057	0.066	0.062	225	2	0.8
	1.0	0.413	0.119	0.120	0.120	175	2	0.8
	1.5	0.750	0.329	0.287	0.308	50	2	4.1
	2.0	1.280	0.188	0.200	0.194	40	2	1.9
	3.0	2.260	0.236	0.226	0.231	10	1	10.2
	4.0	3.140	0.281	0.290	0.286	15	1	12.1
	5.0	3.650	0.183	0.157	0.170	7	1	13.3
	6.0	3.970	0.196	0.205	0.201	15	1	6.7
	7.0	3.200	0.188	0.180	0.184	15	1	7.7
HS1075t	0.0	0.078	0.096	0.100	0.098	425	2	1.5
[35G11t]	0.5	0.150	0.123	0.145	0.134	425	2	1.1
	1.0	0.323	0.335	0.335	0.335	390	2	1.3
	1.5	0.770	0.202	0.228	0.215	25	2	5.6
	2.0	1.160	0.255	0.274	0.265	10	2	11.4
	2.5	1.650	0.232	0.237	0.235	10	1	14.2
	3.0	2.070	0.323	0.309	0.316	10	1	15.3
	4.0	2.810	0.248	0.250	0.249	5	1	17.7
	5.0	3.360	0.329	-----	0.329	3	1	32.6
	6.0	3.710	0.392	0.395	0.394	8	1	26.5
	7.0	4.010	0.466	0.467	0.467	15	1	15.5

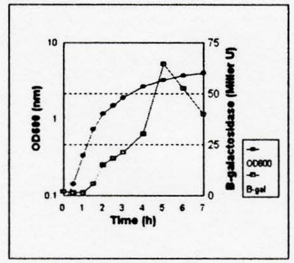

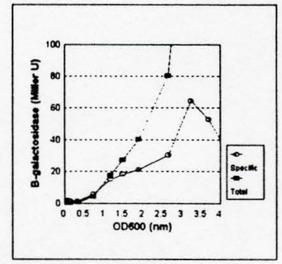

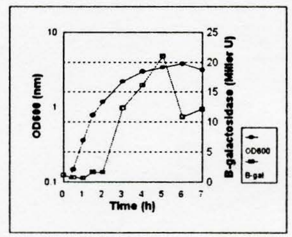

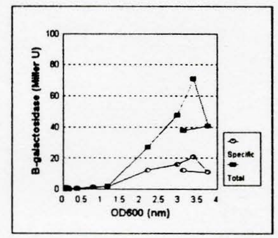

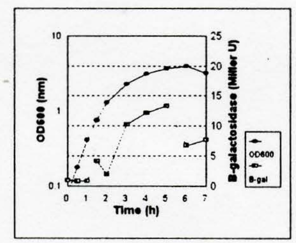

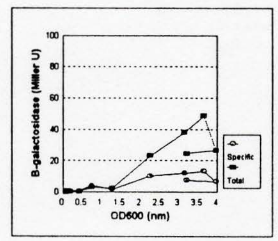

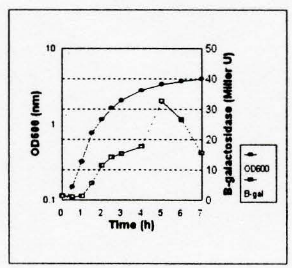

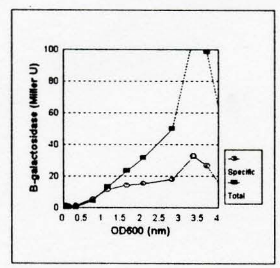

Appendix D. Comparisons of two sets of growth-phase induction of *rpoS*$^+$ recipients assayed independently. β-galactosidase activity is plotted against growth at OD(600 nm). The data set on the left was the reassayed results and on the right is the original assay done by Suzana Gligorijevic. The overnight sample is represented by 7 h.

Calculation for Specific Activity:

[1000 x OD(420 nm)] / [Rxn Time (min) x Volume Assayed (ml) x OD(600 nm)]

Calculation for Total Activity:

[Specific Activity x OD(600 nm)]

Reassayed							
Strain	Time (h)	OD600 (nm)	OD420 (nm) avg	Rxn Time (min)	Vol (ml)	Specific Activity (Miller U)	Total Activity (Miller U)
HS1008	0	0.0	0.2	475	2	7.4	0.3
[02H06]	0.5	0.1	0.2	305	2	2.9	0.4
	1	0.3	0.1	80	2	2.7	0.8
	1.5	0.4	0.4	20	2	25.6	10.5
	2	1.1	0.6	5	2	59.4	64.2
	2.5	1.4	0.9	7	1	89.7	125.6
	3	1.8	1.1	6	1	106.5	187.5
	5	2.9	1.4	5	1	94.6	274.4
	6	3.0	0.6	2	1	107.7	323.0
	7	2.7	0.6	1	1	218.2	593.5
HS1010	0	0.1	0.2	475	2	2.8	0.2
[03F05]	0.5	0.2	0.2	305	2	1.5	0.3
	1	0.4	0.1	80	2	2.2	0.8
	1.5	0.5	1.1	20	2	60.0	28.2
	2	1.2	1.1	5	2	93.9	108.0
	2.5	1.4	0.8	7	1	85.7	120.0
	3	1.8	1.4	6	1	130.0	230.2
	5	3.0	1.4	5	1	92.7	274.3
	6	3.2	0.6	2	1	95.5	302.8
	7	3.4	0.3	1	1	97.3	330.0
HS1024	0	0.1	0.1	475	2	2.4	0.1
[07E04]	0.5	0.2	0.1	305	2	1.3	0.2
	1	0.4	0.1	80	2	1.5	0.6
	1.5	0.5	0.9	20	2	40.5	21.9
	2	1.2	1.0	5	2	79.2	98.2
	2.5	1.5	0.9	7	1	80.8	123.6
	3	1.9	0.9	6	1	77.2	146.0
	5	3.0	0.8	5	1	54.6	162.7
	6	3.1	0.3	2	1	54.5	166.3
	7	3.5	0.2	1	1	61.7	214.0

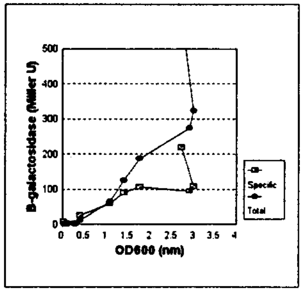

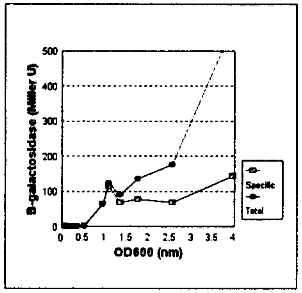

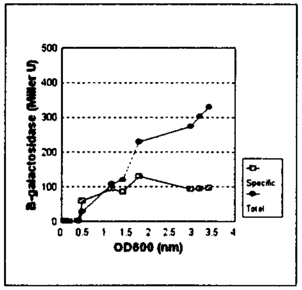

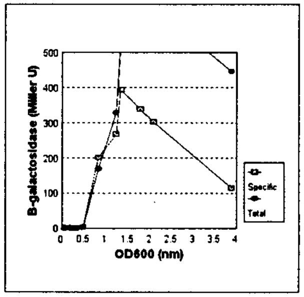

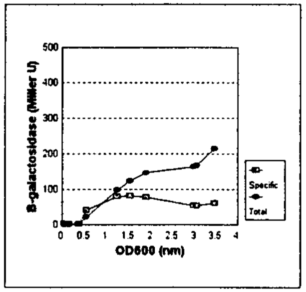

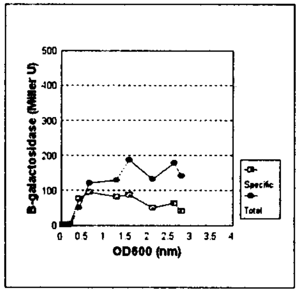

Original Data Otained						
Time (h)	OD600 (nm)	OD420 (nm) avg	Rxn Time (min)	Vol (ml)	Specific Activity (Miller U)	Total Activity (Miller U)
0	0.1	0.4	1311	2	2.4	0.2
0.5	0.1	0.4	1311	2	1.7	0.2
1	0.2	0.5	1311	2	0.9	0.2
1.5	0.3	0.7	1311	2	0.8	0.3
2	0.5	0.6	187	2	3.0	1.5
2.5	1.0	0.3	4	1	65.9	62.6
3	1.1	0.4	3	1	114.8	124.0
4	1.3	0.3	3	1	67.9	91.0
5	1.8	0.4	3	1	77.8	136.2
6	2.6	0.5	3	1	69.2	176.5
7	4.0	1.1	2	1	144.3	571.5
0	0.1	0.4	1311	2	2.3	0.1
0.5	0.1	0.4	1311	2	1.6	0.1
1	0.2	0.5	1311	2	1.0	0.2
1.5	0.3	0.8	1311	2	0.9	0.3
2	0.5	0.5	187	2	2.9	1.4
2.5	0.8	0.3	2	1	200.9	168.8
3	1.2	0.7	2	1	266.9	328.3
4	1.3	1.1	2	1	393.5	527.3
5	1.8	1.2	2	1	337.6	601.0
6	2.1	1.3	2	1	301.8	627.8
7	3.9	0.9	2	1	114.7	446.0
0	0.0	0.2	1331	2	1.6	0.1
0.5	0.1	0.2	1331	2	1.0	0.1
1	0.2	0.4	1331	2	0.6	0.1
1.5	0.4	0.3	110.5	2	3.2	1.3
2	0.7	0.4	4	2	76.9	50.5
2.5	1.3	0.5	4	1	95.0	121.6
3	1.6	0.5	4	1	82.6	129.6
4	2.1	0.7	4	1	88.7	187.3
5	2.6	0.5	4	1	50.7	132.9
6	2.8	0.7	4	1	64.0	178.5
7	3.4	0.7	5	1	41.3	141.5

Reassayed

Strain	Time (h)	OD600 (nm)	OD420 (nm) avg	Rxn Time (min)	Vol (ml)	Specific Activity (Miller U)	Total Activity (Miller U)
HS1031 [09E10]	0	0.1	0.2	475	2	3.5	0.2
	0.5	0.1	0.2	305	2	2.1	0.3
	1	0.3	0.1	80	2	2.1	0.7
	1.5	0.5	0.4	20	2	23.6	11.1
	2	1.1	1.3	5	2	111.8	126.3
	2.5	1.4	1.4	7	1	144.4	205.0
	3	1.8	1.3	6	1	125.0	218.8
	5	3.0	1.2	5	1	80.7	240.4
	6	3.0	0.6	2	1	102.9	306.5
	7	3.3	0.3	1	1	93.1	302.5
HS1034 [12C09]	0	0.1	0.1	475	2	2.2	0.1
	0.5	0.1	0.1	305	2	1.4	0.2
	1	0.3	0.1	80	2	2.7	0.9
	1.5	0.4	0.3	20	2	17.2	7.1
	2		0.7	5	2	ERR	ERR
	2.5	1.4	0.6	7	1	59.4	83.7
	3	1.8	0.5	6	1	51.6	91.3
	5	2.9	0.5	5	1	34.6	101.6
	6	3.0	0.2	2	1	37.0	110.8
	7	3.7	0.1	1	1	36.4	133.5
HS1037 [14C03]	0	0.0	0.0	475	2	0.7	0.0
	0.5	0.2	0.1	305	2	0.4	0.1
	1	0.4	0.1	80	2	1.1	0.4
	1.5	0.5	0.2	20	2	8.3	4.0
	2	1.2	0.5	5	2	37.2	45.0
	2.5	1.5	0.5	7	1	43.6	65.9
	3	1.9	0.4	6	1	37.5	71.2
	5	3.1	0.5	5	1	29.0	90.7
	6	3.2	0.2	2	1	29.5	93.5
	7	3.1	0.1	1	1	33.6	104.5

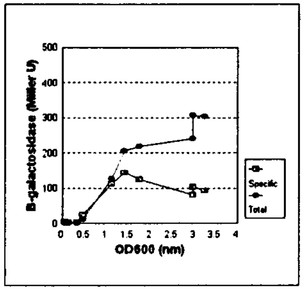

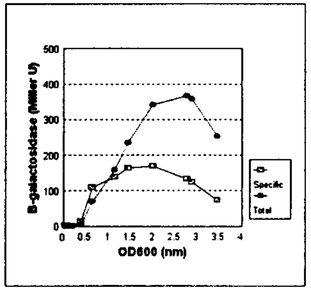

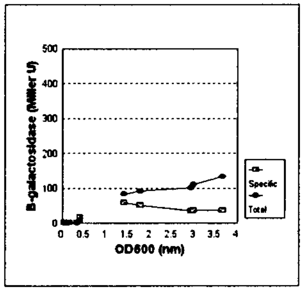

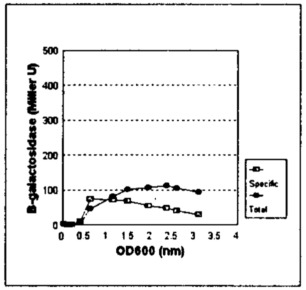

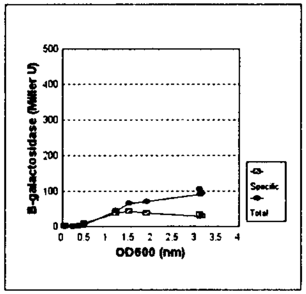

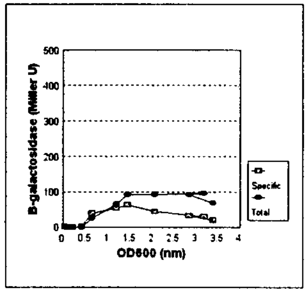

Original Data Otained

Strain	Time (h)	OD600 (nm)	OD420 (nm) avg	Rxn Time (min)	Vol (ml)	Specific Activity (Miller U)	Total Activity (Miller U)
HS1031 [09E10]	0	0.0	0.3	1512	2	2.4	0.1
	0.5	0.1	0.4	1512	2	1.4	0.1
	1	0.2	0.7	1512	2	1.1	0.2
	1.5	0.4	0.3	24	2	14.4	5.6
	2	0.6	0.3	2	2	110.1	70.1
	2.5	1.1	0.3	2	1	139.3	158.8
	3	1.4	0.5	2	1	164.5	235.3
	4	2.0	0.7	2	1	170.5	341.0
	5	2.8	0.7	2	1	132.5	367.0
	6	2.9	0.7	2	1	124.5	358.5
	7	3.5	0.9	3.5	1	73.1	252.3
HS1034 [12C09]	0	0.0	0.4	1513	2	3.1	0.1
	0.5	0.1	0.5	1513	2	1.6	0.2
	1	0.2	0.3	483	2	1.5	0.3
	1.5	0.4	0.3	40.5	2	10.5	4.3
	2	0.6	0.3	3	2	73.9	46.2
	2.5	1.1	0.2	3	1	71.5	81.5
	3	1.5	0.3	3	1	68.7	101.0
	4	2.0	0.3	3	1	55.0	107.2
	5	2.4	0.3	3	1	47.7	113.0
	6	2.6	0.3	3	1	40.5	105.7
	7	3.1	0.6	6	1	30.2	93.9
HS1037 [14C03]	0	0.0	0.1	1512	2	1.0	0.0
	0.5	0.1	0.1	1512	2	0.4	0.0
	1	0.2	0.2	1512	2	0.3	0.1
	1.5	0.4	0.3	174	2	1.8	0.8
	2	0.6	0.3	6.5	2	40.1	25.7
	2.5	1.2	0.4	6.5	1	55.3	65.8
	3	1.4	0.6	6.5	1	64.3	92.5
	4	2.1	0.6	6.5	1	44.6	92.3
	5	3.2	0.6	6.5	1	30.3	96.7
	6	2.9	0.6	6.5	1	32.4	92.5
	7	3.4	0.4	6	1	20.2	68.6

Reassayed

Strain	Time (h)	OD600 (nm)	OD420 (nm) avg	Rxn Time (min)	Vol (ml)	Specific Activity (Miller U)	Total Activity (Miller U)
HS1043	0	0.1	0.0	230	2	1.4	0.1
[21F08]	0.5	0.1	0.1	225	2	1.1	0.1
	1	0.3	0.1	175	2	1.0	0.4
	1.5	0.7	0.5	50	2	7.3	5.0
	2	1.1	0.2	5	0.5	68.4	75.2
	3	1.8	0.3	5	0.5	75.0	135.0
	4	2.6	0.3	3	0.5	89.6	229.3
	5	3.1	0.3	3	0.5	65.0	198.3
	6	3.4	0.3	3	0.5	58.4	200.3
	7	4.3	0.2	3	0.5	29.2	124.3
HS1057	0	0.1	0.1	230	2	4.5	0.2
[31B04]	0.5	0.1	0.2	225	2	3.1	0.3
	1	0.3	0.2	148	2	2.6	0.7
	1.5	0.7	0.7	50	2	10.7	7.3
	2	1.1	0.8	5	0.5	294.2	326.6
	3	1.8	1.2	4	0.5	344.3	619.8
	4	2.5	0.6	1	0.5	485.2	1213.0
	5	3.1	0.5	1	0.5	339.9	1057.0
	6	3.5	0.5	1	0.5	309.6	1096.0
	7	4.1	0.3	1	0.5	154.5	632.0
HS1058	0	0.1	0.4	430	2	7.2	0.5
[31B09]	0.5	0.1	0.4	425	2	5.0	0.5
	1	0.2	0.2	135	2	3.3	0.7
	1.5	0.6	0.1	25	2	3.5	1.9
	2	0.9	0.4	10	0.5	94.1	88.5
	2.5	1.4	0.7	10	0.5	107.9	146.8
	3	1.7	1.4	10	0.5	161.7	274.9
	4	2.3	1.3	5	0.5	229.0	535.8
	5	3.2	0.7	1	0.5	422.5	1369.0
	6	3.7	0.9	1	0.5	463.0	1727.0
	7	4.8	0.8	2	0.5	176.2	842.0

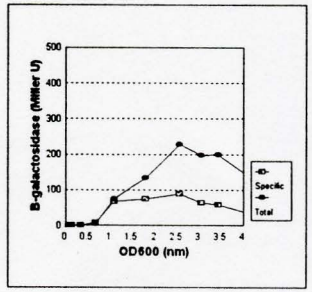

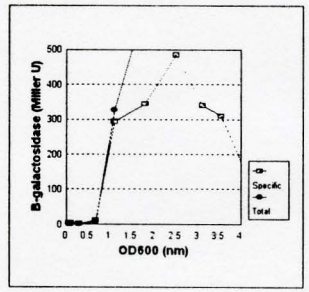

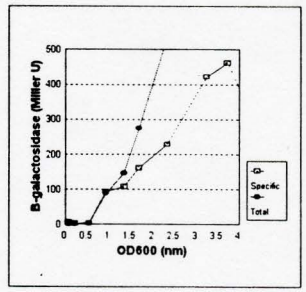

Original Data Otained

Time (h)	OD600 (nm)	OD420 (nm) avg	Rxn Time (min)	Vol (ml)	Specific Activity (Miller U)	Total Activity (Miller U)
0	0.1	0.2	1239	2	1.2	0.1
0.5	0.1	0.2	1239	2	0.9	0.1
1	0.2	0.1	271	2	1.0	0.2
1.5	0.4	0.3	130.5	2	2.4	1.1
2	0.6	0.2	5.5	2	28.4	18.1
2.5	1.4	0.2	5.5	1	26.7	36.1
3	1.4	0.3	5.5	1	38.4	55.3
4	1.9	0.4	5.5	1	39.2	73.0
5	2.4	0.6	5.5	1	45.8	110.0
6	2.8	0.7	5.5	1	48.0	135.4
7	2.7	0.5	3	1	59.9	161.8
0	0.0	0.2	237	2	9.4	0.4
0.5	0.1	0.2	171	2	6.5	0.6
1	0.2	0.2	105	2	4.3	1.0
1.5	0.4	0.5	40	2	15.3	6.2
2	0.6	0.6	1.5	2	309.2	194.2
2.5	1.1	0.5	1.5	1	286.5	312.3
3	1.5	0.7	1.5	1	335.9	487.0
4	1.9	0.9	1.5	1	325.4	605.3
5	2.6	0.9	1.5	1	227.3	593.3
6	2.8	1.1	1.5	1	252.8	705.3
7	2.7	1.4	1.5	1	349.1	939.0
0	0.0	0.2	237	2	10.3	0.5
0.5	0.1	0.2	171	2	6.7	0.6
1	0.2	0.2	105	2	4.6	1.1
1.5	0.4	0.4	40	2	11.3	4.9
2	0.6	0.4	1	2	287.5	185.7
2.5	1.1	0.4	1	1	352.7	398.5
3	1.5	0.7	1	1	474.5	707.0
4	2.1	1.0	1	1	487.9	1044.0
5	2.9	1.2	1	1	417.4	1202.0
6	3.3	1.3	1	1	383.7	1270.0
7	2.7	1.8	1.5	1	433.3	1178.7

Reassayed

Strain	Time (h)	OD600 (nm)	OD420 (nm) avg	Rxn Time (min)	Vol (ml)	Specific Activity (Miller U)	Total Activity (Miller U)
[31F08]	0.5	0.2	0.1	225	2	1.4	0.2
	1	0.4	0.2	175	2	1.4	0.6
	1.5	0.9	0.8	50	2	9.9	8.4
	2	1.2	0.2	5	0.5	72.3	89.6
	3	1.9	0.6	5	0.5	120.0	230.4
	4	2.7	0.6	3	0.5	157.4	425.0
	5	3.2	0.6	3	0.5	121.8	389.7
	6	3.5	0.6	3	0.5	113.4	392.3
	7	4.1	0.4	3	0.5	70.9	288.7
HS1063	0	0.1	0.0	230	2	1.4	0.1
[32D07]	0.5	0.1	0.1	225	2	0.9	0.1
	1	0.4	0.2	175	2	1.7	0.6
	1.5	0.7	1.1	50	2	14.6	10.5
	2	1.1	0.2	5	0.5	57.6	63.4
	3	1.8	0.3	5	0.5	60.4	110.0
	4	2.7	0.3	3	0.5	68.7	182.7
	5	3.3	0.2	3	0.5	49.4	161.0
	6	3.5	0.2	3	0.5	44.0	152.3
	7	4.1	0.1	3	0.5	23.2	95.7
HS1075	0	0.1	0.2	430	2	2.9	0.2
[35G11]	0.5	0.1	0.3	425	2	2.4	0.3
	1	0.3	0.2	135	2	2.1	0.7
	1.5	0.8	0.5	25	2	13.4	10.2
	2	1.1	0.3	10	0.5	49.8	53.3
	2.5	1.5	0.3	10	0.5	47.2	69.8
	3	1.7	0.4	10	0.5	45.2	77.7
	4	2.1	0.3	5	0.5	49.1	100.6
	5	2.7	0.2	2	0.5	57.1	153.0
	6	3.1	0.2	1	0.5	136.1	422.0
	7	4.9	0.1	5	0.5	9.8	47.6

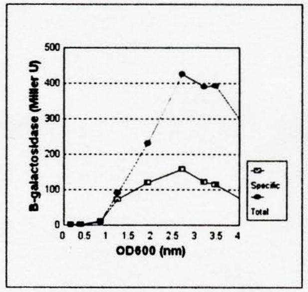

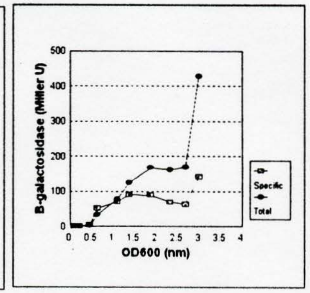

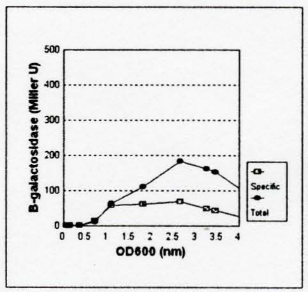

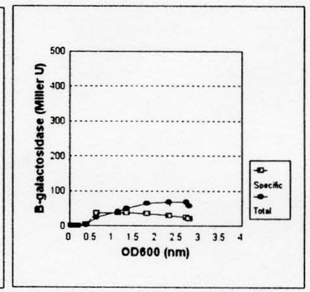

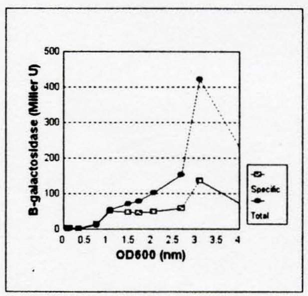

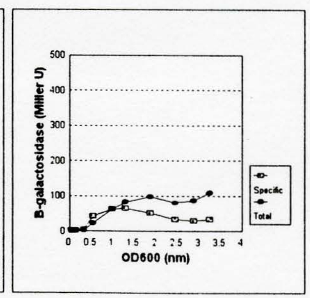

Original Data Otained

Time (h)	OD600 (nm)	OD420 (nm) avg	Rxn Time (min)	Vol (ml)	Specific Activity (Miller U)	Total Activity (Miller U)
0.5	0.1	0.4	2131	2	1.0	0.1
1	0.2	0.2	263	2	1.5	0.3
1.5	0.5	0.3	72.5	2	3.9	1.8
2	0.6	0.3	4	2	51.6	32.9
2.5	1.1	0.3	4	1	70.3	77.4
3	1.4	0.5	4	1	90.6	125.0
4	1.9	0.7	4	1	89.7	168.6
5	2.3	0.6	4	1	69.7	162.4
6	2.7	0.7	4	1	63.0	169.4
7	3.0	0.6	1.5	1	142.7	428.0
0	0.0	0.1	1179	2	1.6	0.1
0.5	0.1	0.2	1179	2	1.2	0.1
1	0.2	0.2	419	2	1.3	0.2
1.5	0.4	0.3	71	2	5.3	2.0
2	0.6	0.3	7	2	37.6	23.6
2.5	1.1	0.3	7	1	36.7	41.4
3	1.3	0.4	7	1	37.9	50.4
4	1.8	0.5	7	1	36.0	64.7
5	2.3	0.5	7	1	29.8	68.9
6	2.7	0.5	7	1	25.2	68.3
7	2.8	0.3	5	1	21.0	58.4
0	0.0	0.3	1171	2	3.7	0.1
0.5	0.1	0.4	1171	2	2.4	0.2
1	0.2	0.3	411	2	2.3	0.4
1.5	0.3	0.2	63	2	5.1	1.7
2	0.5	0.2	4.5	2	42.6	23.1
2.5	1.0	0.3	4.5	1	63.2	62.6
3	1.3	0.4	4.5	1	64.5	83.9
4	1.9	0.4	4.5	1	52.1	98.0
5	2.5	0.4	4.5	1	32.9	80.6
6	2.9	0.4	4.5	1	30.0	86.3
7	3.3	0.3	2.5	1	33.7	109.6

Appendix E. Nucleotide sequences of selected fusion junctions and alignment results from Blastn searches. Ten sequences were submitted for nucleotide search of the databases (Genbank, NCBI Blastn). Sequences in lower case letters represent the confirmed 5' end of the Mu c vector region. Submitted sequences are represented by upper case letters starting from the first nucleotide of the fusion junction for all except HS1038 (14D08) where the beginning of the submitted sequence is represented by an asterick. Strains HS1001 (01D04), HS1028 (08H08) and HS1038 (14D08) were sequenced by automatic sequencer and the remainder manually. All were submitted to the Genbank database in January 26, 1996.

```
HS1001 (01D04)
88 letters
5' -- aataca
GGNATCAGTTTACTGGTCAGGNGACAGAGCAATGGGGAANGCTNNACGGNGNTCATNTGAGGACNATGGTAGNTAACNGNA
ATCA -- 3'
```

Sequences producing High-scoring Segment Pairs:	High Score	Smallest Sum Probability P(N)	N
gb|L02362|ECOLEXDIN Escherichia coli repressor protein (l...	188	6.9e-08	1
gb|U00006|ECOUW89 E. coli chromosomal region from 89.2 ...	188	7.2e-08	1

```
>gb|L02362|ECOLEXDIN Escherichia coli repressor protein (lexA) gene 3' end;
            DNA-damage-inducible protein (dinF) gene, complete cds.
            Length = 2201

  Plus Strand HSPs:

 Score = 188 (51.9 bits), Expect = 6.9e-08, P = 6.9e-08
 Identities = 56/85 (65%), Positives = 56/85 (65%), Strand = Plus / Plus

Query:     1 GGNATCAGTTTACTGGTCAGGNGACAGAGCAATGGGGAANGCTNNACGGNGNTCATNTGA 60
             || | |||||||  ||| | | || ||||||||||||| |  ||   ||  | | || |||
Sbjct:  1571 GGAAACAGTTTAAAGGTAAAGTGAAAGAGCAATGGGGCAAACTGACCGATGATGATATGA 1630

Query:    61 GGACNATGGTAGNTAACNGNAATCA 85
              ||  || | || |||  |  ||||
Sbjct:  1631 CGATCATTGAAGGTAAACGTGATCA 1655


>gb|U00006|ECOUW89 E. coli chromosomal region from 89.2 to 92.8 minutes.
            Length = 176,195

  Plus Strand HSPs:

 Score = 188 (51.9 bits), Expect = 7.2e-08, P = 7.2e-08
 Identities = 56/85 (65%), Positives = 56/85 (65%), Strand = Plus / Plus

Query:       1 GGNATCAGTTTACTGGTCAGGNGACAGAGCAATGGGGAANGCTNNACGGNGNTCATNTGA 60
               || | |||||||  ||| | | || ||||||||||||| |  ||   ||  | | || |||
Sbjct:  124507 GGAAACAGTTTAAAGGTAAAGTGAAAGAGCAATGGGGCAAACTGACCGATGATGATATGA
124566

Query:      61 GGACNATGGTAGNTAACNGNAATCA 85
                ||  || | || |||  |  ||||
Sbjct:  124567 CGATCATTGAAGGTAAACGTGATCA 124591
```

```
HS1002 (01E04)
88 letters
5' -- aataca
AATAAAGATGAAGCCGGCGGTAACTGGAAACAGTTTAAAGGTAANGTGAAAGAGCATNGGGCANCTGACCGTGTGTATGCG
TCATTGN -- 3'

                                                                    Smallest
                                                                      Sum
                                                             High  Probability
Sequences producing High-scoring Segment Pairs:              Score  P(N)       N

gb|L02362|ECOLEXDIN Escherichia coli repressor protein (l...   282  1.0e-15    1
gb|U00006|ECOUW89   E. coli chromosomal region from 89.2 ...   282  1.1e-15    1

>gb|L02362|ECOLEXDIN Escherichia coli repressor protein (lexA) gene 3' end;
            DNA-damage-inducible protein (dinF) gene, complete cds.
            Length = 2201

  Plus Strand HSPs:

 Score = 282 (77.9 bits), Expect = 1.0e-15, P = 1.0e-15
 Identities = 58/61 (95%), Positives = 58/61 (95%), Strand = Plus / Plus

Query:      1 AATAAAGATGAAGCCGGCGGTAACTGGAAACAGTTTAAAGGTAANGTGAAAGAGCATNGG 60
              |||||||||||||||||||||||||||||||||||||||||||| ||||||||||  ||
Sbjct:  1546 AATAAAGATGAAGCCGGCGGTAACTGGAAACAGTTTAAAGGTAAAGTGAAAGAGCAATGG 1605

Query:     61 G 61
              |
Sbjct:  1606 G 1606


>gb|U00006|ECOUW89 E. coli chromosomal region from 89.2 to 92.8 minutes.
            Length = 176,195

  Plus Strand HSPs:

 Score = 282 (77.9 bits), Expect = 1.1e-15, P = 1.1e-15
 Identities = 58/61 (95%), Positives = 58/61 (95%), Strand = Plus / Plus

Query:        1 AATAAAGATGAAGCCGGCGGTAACTGGAAACAGTTTAAAGGTAANGTGAAAGAGCATNGG 60
              |||||||||||||||||||||||||||||||||||||||||||| ||||||||||  ||
Sbjct:  124482 AATAAAGATGAAGCCGGCGGTAACTGGAAACAGTTTAAAGGTAAAGTGAAAGAGCAATGG
124541

Query:       61 G 61
              |
Sbjct:  124542 G 124542


>gb|M96622|DDIRASB Dictyostelium discoideum rasB mRNA, complete cds.
            Length = 672

  Plus Strand HSPs:

 Score = 111 (30.7 bits), Expect = 4.1, P = 0.98
 Identities = 31/42 (73%), Positives = 31/42 (73%), Strand = Plus / Plus

Query:      1 AATAAAGATGAAGCCGGCGGTAACTGGAAACAGTTTAAAGGT 42
              || |||||| ||   || |||| |   ||| ||||||||||
Sbjct:    576 AAGAAAGATAAAAAAGGTGGTATCCTTAAAAAGTTTAAAGGT 617
```

```
HS1004 (02C08)
99 letters
5' -- aataca
GAGTGTTCATGACGCCACATCAGGCATGGCAACGACAAATTTAAAGGCGAAGTAGAAACCATTGCAGCTGGNNCAACTGGT
CGGTAGAGTATCGNCAAT -- 3'
```

Sequences producing High-scoring Segment Pairs:	High Score	Smallest Sum Probability P(N)	N
emb|Z50870|ECMESJORF E.coli orfs and mesJ gene	188	1.2e-15	2
dbj|D49445|ECODNAE Escherichia coli dnaE gene for DnaE,...	188	3.5e-15	2

```
>emb|Z50870|ECMESJORF E.coli orfs and mesJ gene
            Length = 3007

  Plus Strand HSPs:

 Score = 188 (51.9 bits), Expect = 1.2e-15, Sum P(2) = 1.2e-15
 Identities = 40/43 (93%), Positives = 40/43 (93%), Strand = Plus / Plus

Query:     4 TGTTCATGACGCCACATCAGGCATGGCAACGACAAATTTAAAG 46
             || |||||||||||||||||||||||||||||||||| || |
Sbjct:   185 TGATCATGACGCCACATCAGGCATGGCAACGACAAATTAAAGG 227

 Score = 139 (38.4 bits), Expect = 1.2e-15, Sum P(2) = 1.2e-15
 Identities = 29/32 (90%), Positives = 29/32 (90%), Strand = Plus / Plus

Query:    67 GCTGGNNCAACTGGTCGGTAGAGTATCGNCAA 98
             |||||  |||||||||||||||||||| |||
Sbjct:   246 GCTGGAACAACTGGTCGGTAGAGTATCGGCAA 277

 Score = 131 (36.2 bits), Expect = 5.3e-11, Sum P(2) = 5.3e-11
 Identities = 27/28 (96%), Positives = 27/28 (96%), Strand = Plus / Plus

Query:    38 AATTTAAAGGCGAAGTAGAAACCATTGC 65
             || ||||||||||||||||||||||||||
Sbjct:   218 AAATTAAAGGCGAAGTAGAAACCATTGC 245


>dbj|D49445|ECODNAE Escherichia coli dnaE gene for DnaE, DNA polymerase III
            holoenzyme catalytic subunit, AccA, alpha subunit of acetyl-coA
            carboxylase, LdcC, probably constitutive lysine decarboxylase,
            YaeR, YaeN, YaeO, YaeP, YaeQ, YaeJ, NlpE, lipoprotein, YaeF, ProS.
            Length = 8550

  Plus Strand HSPs:

 Score = 188 (51.9 bits), Expect = 3.5e-15, Sum P(2) = 3.5e-15
 Identities = 40/43 (93%), Positives = 40/43 (93%), Strand = Plus / Plus

Query:     4 TGTTCATGACGCCACATCAGGCATGGCAACGACAAATTTAAAG 46
             || |||||||||||||||||||||||||||||||||| || |
Sbjct:  2989 TGATCATGACGCCACATCAGGCATGGCAACGACAAATTAAAGG 3031

 Score = 139 (38.4 bits), Expect = 3.5e-15, Sum P(2) = 3.5e-15
 Identities = 29/32 (90%), Positives = 29/32 (90%), Strand = Plus / Plus

Query:    67 GCTGGNNCAACTGGTCGGTAGAGTATCGNCAA 98
             |||||  |||||||||||||||||||| |||
Sbjct:  3050 GCTGGAACAACTGGTCGGTAGAGTATCGGCAA 3081

 Score = 131 (36.2 bits), Expect = 1.5e-10, Sum P(2) = 1.5e-10
 Identities = 27/28 (96%), Positives = 27/28 (96%), Strand = Plus / Plus
```

```
Query:    38 AATTTAAAGGCGAAGTAGAAACCATTGC 65
             || ||||||||||||||||||||||||||
Sbjct:  3022 AAATTAAAGGCGAAGTAGAAACCATTGC 3049
```

HS1009 (03C06)
131 letters
5' -- aataca
GTGGACTTGTATCAGCAACAAGGCGTTGAGAAATCACGCATTCTGATCAAGCTGGCTTCGACCTGGGAAGGAATTCGCGCG
GCAGAAGAGCTGGAAANAGAAGGTATTAACTGCAACCTGACGCTGCTGTN -- 3'

Sequences producing High-scoring Segment Pairs:	High Score	Smallest Sum Probability P(N)	N
dbj|D10483|ECO110K E.coli K12 genome, 0-2.4min. region...	331	6.4e-20	1

>dbj|D10483|ECO110K E.coli K12 genome, 0-2.4min. region. >emb|D10483|ECAPAH02
E.coli K12 genome, 0-2.4min. region.
Length = 111,401

Plus Strand HSPs:

Score = 331 (92.0 bits), Expect = 6.4e-20, P = 6.4e-20
Identities = 78/94 (82%), Positives = 78/94 (82%), Strand = Plus / Plus

```
Query:    37 CGCATTCTGATCAAGCTGGCTTCGACCTGGGAAGGAATTCGCGCGGCAGAAGAGCTGGAA 96
             || |||||||||||| |||||||| |||||| | || || || || |||||| ||||||||
Sbjct:  8280 CGTATTCTGATCAAACTGGCTTCTACCTGGCAGGGTATCCGTGCTGCAGAACAGCTGGAA 8339

Query:    97 ANABAAGGTATTAACTGCAACCTGACGCTGCTGT 130
             | | |||| || ||||| |||||||| |||||||
Sbjct:  8340 AAAGAAGGCATCAACTGTAACCTGACCCTGCTGT 8373
```

HS1011 (04C07)
108 letters
5' -- aataca
ACCGTTAAGTCTGGCGCACTCTGAGTGCCATTTCCAAACAGGTCTACGGTAACGCTAATCTGTACAATAAAATCTTCGAAG
CGAATAAACCGATGCTAAAMASCCCGG -- 3'

Sequences producing High-scoring Segment Pairs:	High Score	Smallest Sum Probability P(N)	N

*** NONE ***

HS1028 (08H08)
493 letters
5' -- aataca
GGCGGGAAGAAAGATGGTGTGTGCAAACAATGGCCAAAGCGCCGNTCGCCAAGTGACGAATCAGATTGTACGCGGGATGTT
GGGGAGTTTGCGGGGGGGGAGAAGAAGGTAAGTCAGGCGAGATTTGNCTTTGCCTGATGCGACGCTGGCGCGTCTNATCAT
GCCCACCCCACTGCAATATATNGAATTTTAATTATTTTCCAGGAATGAACGANGCACACTTTGCTAACAATAATAAAGGGA
GCTTTCGTTCCCTNNATTCGTTCANTCGGTTANGATTTNCCATTNCCAGCCACAGGCTNNTTANGAAGAAGNTGNCGCTTG
GTATCAGTGCGCCNATGATCGCCGGTATNNCATNTNTCCANCGTCACNNGTCCCCNTCGNTCTTGNTCCANTACNTTAGNN
CNANAACAACCCCNANNTTNTTTACTCNGNNGAACCACNACCNAATNCCCATCCNNTCNCGTTTCCGCNNGCGTNNCCCNT
ATCNTTG -- 3'

Sequences producing High-scoring Segment Pairs:		High Score	Smallest Sum Probability P(N)	N
gb|U14003|ECOUW93	Escherichia coli K-12 chromosomal re...	1145	1.2e-108	4
gb|K02498|ECOALKA	E. coli alkA gene encoding 3-methyla...	182	7.9e-05	1
gb|U00008|ECOHU49	centisome 49 region of E.coli K12 BH...	182	8.3e-05	1
gb|J01706|ECOTHR	E.coli threonine operon with thrA, t...	155	9.4e-05	2

>gb|U14003|ECOUW93 Escherichia coli K-12 chromosomal region from 92.8 to 00.1 minutes.
Length = 338,534

Minus Strand HSPs:

Score = 1145 (316.4 bits), Expect = 1.2e-108, Sum P(4) = 1.2e-108
Identities = 237/252 (94%), Positives = 237/252 (94%), Strand = Minus / Plus

```
Query:     305 GNAAATCNTAACCGANTGAACGAATNNAGGGAACGAAAGCTCCCTTTATTATTGTTAGCA 246
               | ||||| ||||||| ||||||||| ||||| ||||||||||||||||||||||||||
Sbjct:  179225 GAAAATCGTAACCGAATGAACGAATAAAGGGAGCGAAAGCTCCCTTTATTATTGTTAGCA
179284

Query:     245 AAGTGTGCNTCGTTCATTCCTGGAAAATAATTAAAATTCNATATATTGCAGTGGGGTGGG 186
               |||||||| |||||||||||| |||||||||||||||| ||||||||||||||||||||
Sbjct:  179285 AAGTGTGCTTCGTTCATTCCTGAAAAATAATTAAAATTCAATATATTGCAGTGGGGTGGG
179344

Query:     185 CATGATNAGACGCGCCAGCGTCGCATCAGGCAAAGNCAAATCTCGCCTGACTTACCTTCT 126
               |||||| |||||||||||||||||||||||| |||||||||||||||||||||||||||
Sbjct:  179345 CATGATAAGACGCGCCAGCGTCGCATCAGGCAAAGACAAATCTCGCCTGACTTACCTTCT
179404

Query:     125 TCTCCCCCCCCCGCAAACTCCCCAACATCCCGCGTACAATCTGATTCGTCACTTGGCGANC 66
               |||||||||| ||||||||||||||||||||||||||||||||||||||||||||| |
Sbjct:  179405 TCTCCCCCCCCAGCAAACTCCCCAACATCCCGCGTACAATCTGATTCGTCACTTGGCGAGC
179464

Query:      65 GGCGCTTTGGCC 54
               |||||||| | |
Sbjct:  179465 GGCGCTTTTGGC 179476
```

Score = 271 (74.9 bits), Expect = 1.2e-108, Sum P(4) = 1.2e-108
Identities = 63/79 (79%), Positives = 63/79 (79%), Strand = Minus / Plus

```
Query:     379 ATGNNATACCGGCGATCATNGGCGCACTGATACCAAGCGNCANCTTCTTCNTAANNAGCC 320
               |||  || ||| ||||||| ||||||||| | ||||||| || ||||||| |||  ||||
Sbjct:  179150 ATGGCATCCCGCCGATCATCGGCGCACTGTTGCCAAGCGCCAGCTTCTTCTTAATCAGCC
179209

Query:     319 TGTGGCTGGNAATGGNAAA 301
               |||||||| |||| |||
Sbjct:  179210 TGTGGCTGTTAATGAGAAA 179228
```

```
 Score = 162 (44.8 bits), Expect = 1.5e-17, Sum P(2) = 1.5e-17
 Identities = 36/41 (87%), Positives = 36/41 (87%), Strand = Minus / Plus

Query:     195 GTGGGGTGGGCATGATNAGACGCGCCAGCGTCGCATCAGGC 155
               ||  ||| ||||||||| ||||||| ||||||||||||||
Sbjct:  324023 GTTTGGTAGGCATGATAAGACGCGGCAGCGTCGCATCAGGC 324063

 Score = 159 (43.9 bits), Expect = 2.7e-17, Sum P(2) = 2.7e-17
 Identities = 50/75 (66%), Positives = 51/75 (68%), Strand = Minus / Plus

Query:     190 GTGGGCATGATNAGACGCGCCAGCGTCGCATCAGGCAAAGNCAAATCTCGCCTGACTTAC 131
               || |||  ||| ||||||| |||||||||||| |||| |  |||| | | | |  ||
Sbjct:  240616 GTAGGCCAGATAAGACGCGTCAGCGTCGCATCTGGCATAAACAAAGCGCACTTTGCTGGT
240675

Query:     130 CTTCTTCTCCCCCCC 116
               ||  + | | | |||
Sbjct:  240676 CTGTYCCCCTCACCC 240690

 Score = 151 (41.7 bits), Expect = 0.0018, Sum P(3) = 0.0018
 Identities = 33/37 (89%), Positives = 33/37 (89%), Strand = Minus / Plus

Query:     190 GTGGGCATGATNAGACGCGCCAGCGTCGCATCAGGCA 154
               || ||| |||| |||||||| ||||||||||||||
Sbjct:  16830 GTAGGCCTGATAAGACGCGCAAGCGTCGCATCAGGCA 16866

 Score = 151 (41.7 bits), Expect = 0.0018, Sum P(3) = 0.0018
 Identities = 33/37 (89%), Positives = 33/37 (89%), Strand = Minus / Plus

Query:     190 GTGGGCATGATNAGACGCGCCAGCGTCGCATCAGGCA 154
               || ||| |||| |||||||| ||||||||||||||
Sbjct:  16930 GTAGGCCTGATAAGACGCGCAAGCGTCGCATCAGGCA 16966

 Score = 151 (41.7 bits), Expect = 0.0018, Sum P(3) = 0.0018
 Identities = 33/37 (89%), Positives = 33/37 (89%), Strand = Minus / Plus

Query:     190 GTGGGCATGATNAGACGCGCCAGCGTCGCATCAGGCA 154
               || ||| |||| |||||||| ||||||||||||||
Sbjct:  17030 GTAGGCCTGATAAGACGCGCAAGCGTCGCATCAGGCA 17066

 Score = 151 (41.7 bits), Expect = 0.0018, Sum P(3) = 0.0018
 Identities = 33/37 (89%), Positives = 33/37 (89%), Strand = Minus / Plus

Query:     190 GTGGGCATGATNAGACGCGCCAGCGTCGCATCAGGCA 154
               || ||| |||| |||||||| ||||||||||||||
Sbjct:  17130 GTAGGCCTGATAAGACGCGCAAGCGTCGCATCAGGCA 17166

 Score = 147 (40.6 bits), Expect = 0.0037, Sum P(3) = 0.0037
 Identities = 39/52 (75%), Positives = 39/52 (75%), Strand = Minus / Plus

Query:     187 GGCATGATNAGACGCGCCAGCGTCGCATCAGGCAAAGNCAAATCTCGCCTGA 136
               ||| |||| |||||||| ||||||||||||||||      | | | ||| ||
Sbjct:  16733 GGCCTGATAAGACGCGCGAGCGTCGCATCAGGCAGTCGGCACTGTTGCCGGA 16784

 Score = 105 (29.0 bits), Expect = 1.2e-108, Sum P(4) = 1.2e-108
 Identities = 21/21 (100%), Positives = 21/21 (100%), Strand = Minus / Plus

Query:      43 CACACCATCTTTCTTCCCGCC 23
               |||||||||||||||||||||
Sbjct:  179489 CACACCATCTTTCTTCCCGCC 179509

 Score = 96 (26.5 bits), Expect = 0.0032, Sum P(2) = 0.0032
 Identities = 26/35 (74%), Positives = 26/35 (74%), Strand = Minus / Plus
```

```
Query:     227 CCTGGAAAATAATTAAAATTCNATATATTGCAGTG 193
               |||  | ||| |   |||||| |||||||||||  |
Sbjct:  100010 CCTACATAATCACGCAAATTCAATATATTGCAGAG 100044

 Score = 90 (24.9 bits), Expect = 1.2e-108, Sum P(4) = 1.2e-108
 Identities = 18/18 (100%), Positives = 18/18 (100%), Strand = Minus / Plus

Query:      60 TTTGGCCATTGTTTGCAC 43
               ||||||||||||||||||
Sbjct:  179471 TTTGGCCATTGTTTGCAC 179488

 Score = 85 (23.5 bits), Expect = 4.6, Sum P(4) = 0.99
 Identities = 19/22 (86%), Positives = 19/22 (86%), Strand = Minus / Plus

Query:     167 CGTCGCATCAGGCAAAGNCAAA 146
               || |||||||||| || ||||
Sbjct:  132309 CGCCGCATCAGGCATAGACAAA 132330
```

HS1038 (14D08)
535 letters
5' -- aataca

```
NTNNTANAGAGCTNGTATGGCTACGTGGTNGTCNCAGCGCAGANNTCACCAATGTCTAGCGCANGGCATCATGNCGACTGG
CTCTATNTTTGAAAGCTNA*GNTATATATGGTNGACAGGGGNNTCANCNGAATGGANAAGGCGGCTNCCACTCCATCATNA
AATAATTGAAGCTCACCGCCGCGGTCATTNAAACTCGNCGCACTTTNTGNCGGNCNTNGGGGGCGCTNTTCAGACTCNNAC
CCNNAGTNTATACNTCGCAGATGNNCTGAAAGGCCNNNCTNTGGTGGCNGNTTTCANCTACACCNTNANCGCTCTTATGGN
NATNCTGGNCNNGCAGNTGCTGAAGGGGACTCCAACANCNACNGCGACCGNATCATACTCATTCTGCTATGTGGNNNANTC
GGCCGTNCCCNCCAGNACGATNTTGGGGTCNAACTCNGAAATTATTTCANNCTCCNCTCCACGGGNGTNCTCCTGANANNG
TTGGNTNCACCCNAATTCCNCAATTNTCNGCCCCNCCCGNAAANACTCN -- 3'
```

Sequences producing High-scoring Segment Pairs:	High Score	Smallest Sum Probability P(N)	N
gb|L10328|ECOUW82 E. coli; the region from 81.5 to 84.5 m...	148	4.6e-06	2

>gb|L10328|ECOUW82 E. coli; the region from 81.5 to 84.5 minutes.
Length = 136,254

Plus Strand HSPs:

Score = 148 (40.9 bits), Expect = 4.6e-06, Sum P(2) = 4.6e-06
Identities = 42/62 (67%), Positives = 42/62 (67%), Strand = Plus / Plus

```
Query:      1 GNTATATATGGTNGACAGGGGNNTCANCNGAATGGANAAGGCGGCTNCCACTCCATCATN 60
              | ||||| |  | | | || |  |||   ||||| | ||  ||||| ||||||||||||
Sbjct:  26314 GTTATATTTTTTCGCCCGGTGATTCAGAAGAATGCAAAAAACGGCTACCACTCCATCAAA 26373

Query:     61 AA 62
              ||
Sbjct:  26374 AA 26375
```

Score = 137 (37.9 bits), Expect = 4.6e-06, Sum P(2) = 4.6e-06
Identities = 41/62 (66%), Positives = 41/62 (66%), Strand = Plus / Plus

```
Query:    245 GAAGGGGACTCCAACANCNACNGCGACCGNATCATACTCATTCTGCTATGTGGNNNANTC 304
              | | || ||||| | |   |  ||||||| |   |||| ||||||||||||| |   | |
Sbjct:  26555 GCAAGGCACTCCGATAAACAAGGCGACCGTAAATTACTGATTCTGCTATGTTGCTTATTT 26614

Query:    305 GG 306
              ||
Sbjct:  26615 GG 26616
```

```
HS1042 (21B04)
102 letters
5' -- aataca
CCCGGACTTTCCACAGAGCGTTACACCTGGVTAGTCATCATGAACCTGATTACNACGTTATTBTSTCGACGATTCAAAGTA
GCCAAAGGCGCTGGGACTGG -- 3'
```

Sequences producing High-scoring Segment Pairs:	High Score	Smallest Sum Probability P(N)	N
gb|U00039|ECOUW76 E. coli chromosomal region from 76.0 to...	159	6.7e-15	3

```
>gb|U00039|ECOUW76 E. coli chromosomal region from 76.0 to 81.5 minutes.
           Length = 225,419

  Minus Strand HSPs:

 Score = 159 (45.7 bits), Expect = 6.7e-15, Sum P(3) = 6.7e-15
 Identities = 33/40 (82%), Positives = 36/40 (90%), Strand = Minus / Plus

Query:       68 CGASAVAATANCGTNGTAATCAGGTTSATGATSACTAVCC 29
                |||+| |||| ||| ||||||||||+|||||+|||| ||
Sbjct:  126998 CGACAAAATATCGTTGTAATCAGGTTGATGATCACTATCC 127037

 Score = 135 (38.8 bits), Expect = 6.7e-15, Sum P(3) = 6.7e-15
 Identities = 27/30 (90%), Positives = 29/30 (96%), Strand = Minus / Plus

Query:       30 CCAGGTGTAASGSTCTGTGGAAAGNCCGGG 1
                ||||||||||+|+|||||||||||  |||||
Sbjct:  127037 CCAGGTGTAACGCTCTGTGGAAAGTCCGGG 127066

 Score = 90 (25.9 bits), Expect = 6.7e-15, Sum P(3) = 6.7e-15
 Identities = 18/18 (100%), Positives = 18/18 (100%), Strand = Minus / Plus

Query:       89 CCTTTGGCTACTTTGAAT 72
                ||||||||||||||||||
Sbjct:  126974 CCTTTGGCTACTTTGAAT 126991

 Score = 77 (22.1 bits), Expect = 8.0e-14, Sum P(3) = 8.0e-14
 Identities = 17/19 (89%), Positives = 17/19 (89%), Strand = Minus / Plus

Query:      101 CCAGTCCCAGCGCCTTTGG 83
                ||||||||||||||  || |
Sbjct:  126961 CCAGTCCCAGCGCCCTTTG 126979
```

HS1073 (35F12)
120 letters
5' -- aataca
CAGTGACAGAAGATGGCCGTMAAAYAACGGACAGAGGGCAGCGAATTGBTSATGTTCTCACTGGACCCGACGGTYATYYMT
MCGKKGCACCGACGAGCTCCAGTGGGGAATTCACTTAAA -- 3'

Sequences producing High-scoring Segment Pairs:	High Score	Smallest Sum Probability P(N)	N
*** NONE ***			

```
HS1077 (36A5)
134 letters
5' -- aataca
CTGATGTACATGTCTTGAACCAGTGATGCGGCGGGCAATGCTCTATCACTCTGACCTTCGAGACTGGGACATCTCTGATAT
CGCACAGGTTCAGTGCAAATAAACTGCAACTCGCATGCTTGATTACTGAGCAG -- 3'

                                                                    Smallest
                                                                      Sum
                                                          High     Probability
Sequences producing High-scoring Segment Pairs:          Score     P(N)        N

gb|U00039|ECOUW76 E. coli chromosomal region from 76.0 to...   196   3.6e-23    4


>gb|U00039|ECOUW76 E. coli chromosomal region from 76.0 to 81.5 minutes.
           Length = 225,419

  Plus Strand HSPs:

 Score = 196 (54.2 bits), Expect = 3.6e-23, Sum P(4) = 3.6e-23
 Identities = 40/41 (97%), Positives = 40/41 (97%), Strand = Plus / Plus

Query:       1 CTGATGTACATGTCTTGAACCAGTGATGCGGCGGGCAATGC 41
               ||||||||||||||| |||||||||||||||||||||||||
Sbjct:   74895 CTGATGTACATGTCTTCAACCAGTGATGCGGCGGGCAATGC 74935

 Score = 175 (48.4 bits), Expect = 3.6e-23, Sum P(4) = 3.6e-23
 Identities = 35/35 (100%), Positives = 35/35 (100%), Strand = Plus / Plus

Query:      41 CTCTATCACTCTGACCTTCGAGACTGGGACATCTC 75
               |||||||||||||||||||||||||||||||||||
Sbjct:   74936 CTCTATCACTCTGACCTTCGAGACTGGGACATCTC 74970

 Score = 95 (26.3 bits), Expect = 3.6e-23, Sum P(4) = 3.6e-23
 Identities = 19/19 (100%), Positives = 19/19 (100%), Strand = Plus / Plus

Query:      75 CTGATATCGCACAGGTTCA 93
               ||||||||||||||||||
Sbjct:   74971 CTGATATCGCACAGGTTCA 74989

 Score = 90 (24.9 bits), Expect = 3.6e-23, Sum P(4) = 3.6e-23
 Identities = 18/18 (100%), Positives = 18/18 (100%), Strand = Plus / Plus

Query:      98 AAATAAACTGCAACTCGC 115
               ||||||||||||||||||
Sbjct:   74996 AAATAAACTGCAACTCGC 75013

 Score = 74 (20.4 bits), Expect = 6.7e-22, Sum P(4) = 6.7e-22
 Identities = 18/22 (81%), Positives = 18/22 (81%), Strand = Plus / Plus

Query:     102 AAACTGCAACTCGCATGCTTGA 123
               | ||||||||||||  |  ||||
Sbjct:   79427 ATACTGCAACTCGCTTAATTGA 79448
```

REFERENCES

Aldea, M., T. Garrido, C. Hernandez-Chico, M. Vicente, and S. R. Kushner. 1989. Induction of a growth-phase-dependent promoter triggers transcription of *bolA*, an *Escherichia coli* morphogene. EMBO J. **8**:3923-3931.

Aldea, M., T. Garrido, J. Pla, and M. Vicente. 1990. Division genes in *Escherichia coli* are expressed coordinately to cell septum requirements by gearbox promoters. EMBO J. **9**:3787-3794.

Aldea, M., C. Hernandez-Chico, A. G. de la Campa, S. R. Kushner, and M. Vicente. 1988. Identification, cloning, and expression of *bolA*, an *ftsZ*-dependent morphogene of *Escherichia coli*. J. Bacteriol. **170**:5169-5176.

Almiron, M., A. J. Link, D. Furlong, and R. Kolter. 1992. A novel DNA-binding protein with regulatory and protective roles in starved *Escherichia coli*. Genes & Dev. **6**:2646-2654.

Altuvia S., M. Almiron, G. Huisman, R. Kolter, and G. Storz. 1994. The *dps* promoter is activated by OxyR during growth and by IHF and σ^s in stationary phase. Mol. Microbiol. **13**:265-272.

Ananthaswamy, H. N., and A. Eisenstark. 1976. Near-UV-induced breaks in phage DNA: sensitization by H_2O_2 (a tryptophan photoproduct). Photochem. Photobiol. **24**:439-442.

Arber, W., L. Enquist, B. Hohn, N. E. Murray and K. Murray. 1983. Experimental methods for use with lambda. In: Lambda II, p. 433-466. (Hendrix, R. W., J. W. Roberts, F. W. Stahl, R. A. Weisberg, eds.) Cold Spring Harbor Laboratory, N. Y., USA.

Arnqvist A., A. Olsen, and S. Normark. 1994. σ^s-dependent growth-phase induction of the *csgBA* promoter in *Escherichia coli* can be achieved *in vivo* by σ^{70} in the absence of the nucleiod-associated protein H-NS. Mol. Microbiol. **13**:1021-1032.

Atlung, T., A. Nielsen, and F. G. Hansen. 1989. Isolation, characterization and nucleotide sequence of *appY*, a regulatory gene for growth-phase-dependent gene expression in *Escherichia coli*. J. Bacteriol. **171**:1683-1691.

Aviv M., H. Giladi, G. Schreiber, A. B. Oppenheim, and G. Glaser. 1994. Expression of the genes coding for the *Escherichia coli* integration host factor are controlled by growth phase, *rpoS*, ppGpp and by autoregulation. Mol. Microbiol. **14**:1021-1031.

Back, J. F., D. Oakenfull, and M. B. Smith. 1979. Increased thermal stability of proteins in the presence of sugars and polyols. Biochemistry **18**:5191-5196.

Badger, J. L., and V. L. Miller. 1995. Role of RpoS in survival of *Yersinia enterocolitica* to a variety of environmental stresses. J. Bacteriol. **177**:5370-5373.

Blattner, F. R., V. Burland, G. Plunkett III, H. J. Sofia, and D. L. Daniels. 1993. Analysis of the *Escherichia coli* genome. IV. DNA sequence of the region from 89.2 to 92.8 minutes. Nucleic Acids Res. **21**:5408-5417.

Boeker, E. A., and E. E. Snell. 1972. Amino acid decarboxylases. In: The Enzymes, 3rd ed., vol. 6, p. 217-253. Boyer (ed). Academic Press, N. Y.

Bohringer, J., D. Fischer, G. Mosler, and R. Hengge-Aronis. 1995. UDP-glucose is a potential intracellular signal molecule in the control of expression of σ^s and σ^s-dependent genes in *Escherichia coli.* J. Bacteriol. **177**:413-422.

Boos, W., U. Ehmann, E. Bremer, A. Middendorf, and P. Postma. 1987. Trehalase of *Escherichia coli.* J. Biol. Chem. **262**:13212-13218.

Bremer, E., T. J. Silhavy, and G. M. Weinstock. 1985. Transposable λ p*lac*Mu bacteriophages for creating *lacZ* operon fusions and kanamycin resistance insertions in *Escherichia coli.* J. Bacteriol. **162**:1092-1099.

Bremer, E., T. J. Silhavy, J. M. Weisemann, and G. M. Weinstock. 1984. λ p*lac*Mu: a transposable derivative of bacteriophage lambda for creating *lacZ* protein fusions in a single step. J. Bacteriol. **158**:1084-1093.

Buchanan, C. E., and M. O. Sowell. 1982. Synthesis of penicillin-binding protein 6 by stationary phase *Escherichia coli.* J. Bacteriol. **151**:491-494.

Burland, V., G. Plunkett III, D. L. Daniels, and F. R. Blattner. 1993. DNA sequence and analysis of 136 kilobases of the *Escherichia coli* genome: organizational symmetry around the origin of replication. Genomics **16**:551-561.

Burland, V., G. Plunkett III, H. J. Sofia, D. L. Daniels, and F. R. Blattner. 1995. Analysis of the *Escherichia coli* genome VI: DNA sequence of the region from 92.8 through 100 minutes. Nucleic Acids Res. **23**:2105-2119.

Casadaban, M. J., and J. Chou. 1984. *In vivo* formation of gene fusions encoding hybrid β-galactosidase proteins in one step with a transposable Mu-*lac* transducing phage. Proc. Natl. Acad. Sci. U.S.A. **81**:535-539.

Cashel, M., and K. E. Rudd. 1987. The Stringent Response. In: *Escherichia coli* and *Salmonella typhimurium*, cellular and molecular biology, vol 2, p. 1410-1438. (F. C. Neidhardt, J. L. Ingraham, B. Magasanik, K. B. Low, M. Schaechter, H. E. Umbarger, eds.). American Society for Microbiology, Washington, DC.

Chang, Y-Y, A-Y Wang, and J. E. Cronan, Jr. 1994. Expression of *Escherichia coli* pyruvate oxidase (PoxB) depends on the sigma factor encoded by the *rpoS* (*katF*) gene. Mol. Microbiol. **11**:1019-1028.

Chen, C-Y., N. A. Buchmeier, S. Libby, F. C. Fang, M. Krause, and D. G. Guiney. 1995. Central regulatory role for the RpoS sigma factor in expression of *Salmonella dublin* plasmid virulence genes. J. Bacteriol. **177**:5303-5309.

Christman, M. F., R. W. Morgan, F. S. Jacobson, and B. N. Ames. 1985. Positive control of a regulon for defenses against oxidative stress and some heat-shock proteins in *Salmonella typhimurium*. Cell **41**:753-762.

Christman, M. F., G. Storz, and B. N. Ames. 1989. OxyR, a positive regulator of hydrogen peroxide- inducible genes in *Escherichia coli* and *Salmonella typhimurium*, is homologous to a family of bacterial regulatory proteins. Proc. Natl. Acad. Sci. **86**:3484-3488.

Chung, C. T., S. L. Niemela, and R. H. Miller. 1989. One-step preparation of competent *Escherichia coli*: transformation and storage of bacterial cells in the same solution. Proc. Nat. Acad. Sci. USA **86**:2172-2175.

Clairborne, A., and I. Fridovich. 1979. Purification of the o-dianisidine peroxidase from *Escherichia coli* B. J. Biol. Chem. **254**:4245-4252.

Csonka, L. N. 1989. Physiological and genetic responses of bacteria to osmotic stress. Microbiol. Rev. **53**:121-147.

Dassa, J., H. Fsihi, C. Marck, M. Dion, M. Kieffer-Bontemps, and P. L. Boquet. 1991. A new oxygen-regulated operon in *Escherichia coli* comprises the genes for a putative third cytochrome oxidase and for pH 2.5 acid phosphatase (*appA*). Mol. Gen. Genet. **229**:341-352.

Demple, B., J. Halbrook, and S. Linn. 1983. *Escherichia coli xthA* mutants are hypersensitive to hydrogen peroxide. J. Bacteriol. **153**:1079-1082.

Diaz-Guerra, L., F. Moreno, and J. L. San Millan. 1989. *appR* gene product activates transcription of microcin C7 plasmid genes. J. Bacteriol. **171**:2906-2908.

Dougherty, T. J., and M. J. Pucci. 1994. Penicillin-binding proteins are regulated by *rpoS* during transitions in growth states of *Escherichia coli*. Antimicrobial Agents and Chem. **38**:205-210.

Errington, J. 1993. *Bacillus subtilis* sporulation: regulation of gene expression and control of morphogenesis. Microbiol. Rev. **57**:1-33.

Espinosa-Urgel, M., and A. Tormo. 1993. σ^s-dependent promoters in *Escherichia coli* are located in DNA regions with intrinsic curvature. Nuc. Acids Res. **21**:3667-3670.

Fang, F. C., S. J. Libby, N. A. Buchmeier, P. C. Loewen, J. Switala, J. Harwood, and D. G. Guiney. 1992. The alternative σ factor KatF (RpoS) regulates *Salmonella* virulence. Proc. Natl. Acad. Sci. USA **89**:11978-11982.

Finkle, S. E., and R. C. Johnson. 1992. The Fis protein: it's not just for DNA inversion anymore. Mol. Microbiol. **6**:3257-3265.

Friedman, D. I. 1988. Integration host factor: a protein for all reasons. Cell **55**:545-554.

Furth, M. E., S. H. Wickner. 1983. Lambda DNA replication. In: Lambda II, p. 145-173. (Hendrix, R. W., J. W. Roberts, F. W. Stahl, R. A. Weisberg, eds.) Cold Spring Harbor Laboratory, N. Y., USA.

Garcia-Bustos, J. F., N. Pezzi, and E. Mendez. 1985. Structure and mode of action of microcin C7, an antibacterial peptide produced by *Escherichia coli*. Antimicrob. Agents Chemother. **27**:791-797.

Gennis, R. B., and L. P. Hager. 1976. Pyruvate oxidase. In: The Enzymes of Biological Membranes, vol 2, p. 493-504. (A. Martonosis, ed.). N. Y.: Plenum.

Gentry, D. R., V. J. Hernandez, L. H. Nguyen, D. B. Jensen, and M. Cashel. 1993. Synthesis of the stationary-phase sigma factor σ^s is positively regulated by ppGpp. J. Bacteriol. **175**:7982-7989.

Giaever, H. M., O. B. Stryvold, I. Kaasen, and A. R. Strom. 1988. Biochemical and genetic characterization of osmoregulatory trehalose synthesis in *Escherichia coli*. J. Bacteriol. **170**:2841-2849.

Goldemberg, S. H. 1980. Lysine decarboxylase mutants of *Escherichia coli*: Evidence for two enzyme forms. J. Bacteriol. **141**:1428-1431.

Groat, R. G., J. E. Schultz, E. Zychlinsky, A. Bockman, and A Matin. 1986. Starvation proteins in Escherichia coli: kinetics of synthesis and role in starvation survival. J. Bacteriol. **168**:486-493.

Grossberger, D. 1987. Minipreps of DNA from bacteriophage lambda. Nucleic Acids Res. **15**:6737.

Heimberger, A., and A. Eisenstark. 1988. Compartmentalization of catalases in *Escherichia coli*. Biochemical and Biophysical Res. Comm. **154**:392:397.

Heinkoff, S., G. W. Haughn, J. M. Calvo, and J. C. Wallace. 1988. A large family of bacterial activator proteins. Proc. Natl., Acad. Sci. USA **85**:6602-6606.

Hendrix, R. W. 1983. Progress Since 1970. In Lambda II, p. 13-20. (Hendrix, R. W., J. W. Roberts, F. W. Stahl, R. A. Weisberg, eds.) Cold Spring Harbor Laboratory, N. Y., USA.

Hengge-Aronis, R. 1993 (a). The role of *rpoS* in early stationary-phase gene regulation in *Escherichia coli* K12. In: Starvation in Bacteria, p. 171-200. (S. Kjelleberg, ed.). Plenum Press, N. Y., USA.

Hengge-Aronis, R. 1993 (b). Survival of hunger and stress: the role of *rpoS* in early stationary phase gene regulation in *E. coli*. Cell **71**:165-168.

Hengge-Aronis, R., and D. Fischer. 1992. Identification and molecular analysis of *glgS*, a novel growth-phase-regulated and *rpoS*-dependent gene involved in glycogen synthesis in *Escherichia coli*. Mol. Microbiol. **6**:1877-1886.

Hengge-Aronis, R., W. Klein, R. Lange, M. Rimmele, and W. Boos. 1991. Trehalose synthesis genes are controlled by the putative sigma factor encoded by *rpoS* and are involved in stationary-phase thermotolerance in *Escherichia coli*. J. Bacteriol. **173**:7918-7924.

Hengge-Aronis, R., R. Lange, N. Henneberg, and D. Fischer. 1993. Osmotic regulation of *rpoS*-dependent genes in *Escherichia coli*. J. Bacteriol. **175**:259-265.

Horecker, B. L., and P. Z. Smyrniotis. 1955. Purification and properties of yeast transaldolase. J. Biol. Chem. **212**:811-825.

Huisman, G. W., and R. Kolter. 1994. Sensing starvation: a homoserine lactone-dependent signalling pathway in *Escherichia coli*. Science **265**:537-539.

Huisman, G. W., and R. Kolter. 1994. Regulation of gene expression at the onset of stationary phase in *Escherichia coli*. In: Regulation of Bacterial Differentiation , p. 21-40, (P. Piggot, C. P. Moran, Jr., P. Youngman, eds.). American Society for Microbiology, Washington, D. C., USA

Ichikawa, J. K., C. Li, J. Fu, and S. Clarke. 1994. A gene at 59 minutes on the *Escherichia coli* chromosome encodes a lipoprotein with unusual amino acid repeat sequences. J. Bacteriol. **176**:1630-1638.

Iuchi, S., A. Aristarkhov, J. M. Dong, J. S. Taylor, and E. C. C. Lin. 1994. Effects of nitrate respiration on expression of the Arc-controlled operons encoding succinate dehydrogenase and flavin-linked L-lactate dehydrogenase. J. Bacteriol. **176**:1695-1701.

Ivanova, A., C. Miller, G. Glinsky, and A. Eisenstark. 1994. Role of *rpoS* (*katF*) in *oxyR*-independent regulation of hydroperoxidase I in *Escherichia coli*. Mol. Microbiol. **12**:571-578.

Ivanova, A., M. Renshaw, R. V. Guntaka, and A. Eisenstark. 1992. DNA base sequence variability in *katF* (putative sigma factor) gene of *Escherichia coli*. Nucleic Acids Res. **20**:5479-5480.

Jenkins, D. E., J. E. Schultz, and A. Matin. 1988. Starvation-induced cross-protection against heat or H_2O_2 challenge in *Escherichia coli*. J. Bacteriol. **170**:3910-3914.

Jenkins, D. E., S. A. Chaisson, and A. Matin. 1990. Starvation-induced cross-protection against osmotic challenge in *Escherichia coli*. J. Bacteriol. **172**:2779-2781.

Jung, J. U., C. Gutierrez, F. Martin, M. Ardourel, and M. Villarejo. 1990. Transcription of *osmB*, a gene encoding an *Escherichia coli* lipoprotein, is regulated by dual signals. J. Biol. Chem. **265**:10574-10581.

Kaasen, I., P. Falkenberg, O. B. Styrvold, and A. R. Strom. 1992. Molecular cloning and physical mapping of the *otsBA* genes, which encode the osmoregulatory trehalose pathway of *Escherichia coli*: evidence that transcription is activated by KatF (AppR). J. Bacteriol. **174**:889-898.

Kawamukai, M., H. Matsuda, W. Fujii, R. Utsumi and T. Komano. 1989. Nucleotide sequences of *fic* and *fic-1* genes involved in cell filamentation induced by cAMP in *Escherichia coli*. J. Bacteriol. **171**:4525-4529.

Kolter, R., D. A. Siegele, and A. Tormo. 1993. The stationary phase of the bacterial life cycle. Annu. Rev. Microbiol. **47**:855-874.

Komano, T., R. Utsumi, and M. Kawamukai. 1991. Functional analysis of the *fic* gene involved in regulation of cell division. Res. Microbiol. **142**:269-277.

Krause, M., F. C. Fang, and D. G. Guiney. 1992. Regulation of plasmid virulence gene expression in *Salmonella dublin* involves an unusual operon structure. J. Bacteriol. **174**:4482-4489.

Krause, M., C. Roudier, J. Fierer, J. Hawood, and D. G. Guiney. 1991. Molecular analysis of the virulence locus of the *Salmonella dublin* plasmid pSDL2. Mol. Microbiol. **5**:307-316.

Landini, P., L. I. Hajec. And M. R. Volkert. 1994. Structure and transcriptional regulation of the *Escherichia coli* adaptive response gene *aidB*. J. Bacteriol. **176**:6583-6589.

Lange, R., M. Barth, and R. Hengge-Aronis. 1993. Complex transcriptional control of the σ^s-dependent stationary-phase-induced and osmotically regulated *osmY* (*csi-5*) gene suggests novel roles for Lrp, Cyclic AMP (cAMP) receptor protein-cAMP complex, and integration host factor in the stationary-phase response of *Escherichia coli*. J. Bacteriol. **175**:7910-7917.

Lange, R., D. Fischer, and R. Hengge-Aronis. 1995. Identification of transcriptional start sites and the role of ppGpp in the expression of *rpoS*, the structural gene for the σ^s subunit of RNA polymerase in *Escherichia coli*. J. Bacteriol. **177**:4676-4680.

Lange, R., and R. Hengge-Aronis. 1991 (a). Identification of a central regulator of stationary-phase gene expression in *Escherichia coli*. Mol. Microbiol. **5**:49-59.

Lange, R., and R. Hengge-Aronis. 1991 (b). Growth phase-regulated expression of *bolA* and morphology of stationary-phase *Escherichia coli* cells are controlled by the novel sigma factor σ^s. J. Bacteriol. **173**:4474-4481.

Lange, R., and R. Hengge-Aronis. 1994 (a). The cellular concentration of the σ^s subunit of RNA polymerase in *Escherichia coli* is controlled at the levels of transcription, translation, and protein stability. Genes & Dev. **8**:1600-1612.

Lange, R., and R. Hengge-Aronis. 1994 (b). The *nlpD* gene is located in an operon with *rpoS* on the *Escherichia coli* chromosome and encodes a novel lipoprotein with a potential function in a cell wall formation. Mol. Microbiol. **13**:733-743.

Leathers, T. D., J. Noti, and H. E. Umbarger. 1979. Physical characterization of *ilv-lac* fusions. J. Bacteriol. **140**:251-260.

Li, S-J., and J. E. Cronan, Jr. 1993. Growth rate regulation of *Escherichia coli* acetyl coenzyme A carboxylase, which catalyses the first committed step of lipid biosynthesis. J. Bacteriol. **175**:332-340.

Loewen, P. C. 1984. Isolation of catalase-deficient *Escherichia coli* mutants and genetic mapping of *katE*, a locus that affects catalase activity. J. Bacteriol. **157**:622-626.

Loewen, P. C., and R. Hengge-Aronis. 1994. The role of the sigma factor σ^s (KatF) in bacterial global regulation. Annu. Rev. Microbiol. **48**:53-80.

Loewen, P. C., J. Switala, and B. L. Triggs-Raine. 1985 (a). Catalases HPI and HPII in *Escherichia coli* are induced independently. Archives of Biochemistry and Biophysics **243**:144-149.

Loewen, P. C., and B. L. Triggs. 1984. Genetic mapping of *katF*, a locus that with *katE* affects the synthesis of a second catalase species in *Escherichia coli*. J. Bacteriol. **160**:668-675.

Loewen, P. C., B. L. Triggs, C. S. George, and B. E. Hrabarchuk. 1985 (b). Genetic mapping of *katG*, a locus that affects synthesis of the bifunctional catalase-peroxidase hydroperoxidase I in *Escherichia coli*. J. Bacteriol. **162**:661-667.

Loewen, P. C., I. von Ossowski, J. Switala, and M. R. Mulvey. 1993. KatF (σ^s) synthesis in *Escherichia coli* is subject to post-transcriptional regulation. J. Bacteriol. **175**:2150-2153.

Lomovskaya, O. L., J. P. Kidwell, and A. Matin. 1994. Characterization of the σ^{38}-dependent expression of a core *Escherichia coli* starvation gene, *pexB*. J. Bacteriol. **176**:3928-3935.

Lonetto, M., M. Gribskov, and C. A. Gross. 1992. The σ^{70} family: sequence conservation and evolutionary relationships. J. Bacteriol. **174**:3843-3849.

Ma, M., and J. W. Eaton. 1992. Multicellular oxidant defence in unicellular organisms. Proc. Natl. Acad. Sci. USA **89**:7924-7928.

Matin, A. 1991. The molecular basis of carbon-starvation-induced general resistance in *Escherichia coli*. Mol. Microbiol. **5**:3-10.

McCann, M. P., J. P. Kidwell, and A. Matin. 1991. The Putative σ factor KatF has a central role in development of starvation-mediated general resistance in *Escherichia coli*. J. Bacteriol. **173**:4188-4194.

McCann, M. P., C. D. Fraley, and A. Matin. 1993. The putative σ factor KatF is regulated post-transcriptionally during carbon starvation. J. Bacteriol. **175**:2143-2149.

McCormick, J. P., J. R. Fisher, J. P Pachlatko, and A. Eisenstark. 1976. Characterization of a cell-lethal tryptophan photo-oxidation product: Hydrogen peroxide. Science **191**:468-469.

Meng, S-Y, and G. N. Bennett. 1992 (a). Nucleotide sequence of the *Escherichia coli cad* operon: a system for neutralization of low extracellular pH. J. Bacteriol. **174**:2659-2669.

Meng, S-Y, and G. N. Bennett. 1992 (b). Regulation of the *Escherichia coli cad* operon: location of a site required for acid induction. J. Bacteriol. **174**:2670-2678.

Miller, J. H. 1992. A Short Course in Bacterial Genetics: a laboratory manual and handbook for *Escherichia coli* and related bacteria. Cold Spring Harbor Laboratory Press, USA.

Morgan, R. W., M. F. Christman, F. S. Jocobson, G. Storz, and B. N. Ames. 1986. Hydrogen peroxide-inducible proteins in *Salmonella typhimurium* overlaps with heat shock and other stress proteins. Proc. Natl. Acad. Sci. **83**:8059.

Mukhopadhyay, S., and H. E. Schellhorn. 1994. Induction of *Escherichia coli* hydroperoxidase I by acetate and other weak acids. J. Bacteriol. **176**:2300-2307.

Mulvey, M. R., and P. C. Loewen. 1989. Nucleotide sequence of *katF* of *Escherichia coli* suggests KatF protein is a novel σ transcription factor. Nucleic Acids Res. **17**:9979-9991.

Mulvey, M. R., P. A. Sorby, B. L. Triggs-Raine, and P. C. Loewen. 1988. Cloning and physical characterization of *katE* and *katF* required for catalase HPII expression in *Escherichia coli*. Gene **73**:337-345.

Mulvey, M. R., J. Switala, A. Borys, and P. C. Loewen. 1990. Regulation of transcription of *katE* and *katF* in *Escherichia coli*. J. Bacteriol. **172**:6713-6720.

Nagasawa, S., S. Tokishita, H. Aiba, and T. Mizuno. 1992. A novel sensor-regulator protein that belongs to the homologous family of signal-transduction proteins involved in adaptive responses in *Escherichia coli*. Mol. Microbiol. **6**:799-807.

Nguyen, L. H., D. B. Jensen, N. E. Thompson, D. R. Gentry, and R. R. Burgess. 1993. *In vitro* functional characterization of overproduced *Escherichia coli katF/rpoS* gene product. Biochemistry **32**:11112-11117.

Nimmo, H. G. 1987. The tricarboxylic acid cycle and anaplerotic reactions. In: *Escherichia coli* and *Salmonella typhimurium*, cellular and molecular biology, vol 1, p. 156-169. (F. C. Neidhardt, J. L. Ingraham, B. Magasanik, K. B. Low, M. Schaechter, H. E. Umbarger, eds.). American Society for Microbiology, Washington, DC.

Norel, F., V. Robbe-Saule, M. Y. Popoff and C. Coynault. 1992. The putative sigma factor KatF(RpoS) is required for the transcription of the *Salmonella typhimurium* virulence gene *spvB* in *Escherichia coli*. FEMS Microbiol. Letters **99**:271-276.

Novoa, M. A., L. Diaz-Guerra, J. L. San Millan, and F. Moreno. 1986. Cloning and mapping of the genetic determinants for microcin C7 production and immunity. J. Bacteriol. **168**:1384-1391.

Olsen, A., A. Arnqvist, M. Hammar, S. Sukupolvi, and S. Normark. 1993. The RpoS sigma factor relieves H-NS-mediated transcriptional repression of *csgA*, the subunit gene of fibronectin-binding curli in *Escherichia coli*. Mol. Microbiol. **7**:523-536.

Olsen, A., A. Jonsson, and S. Normark. 1989. Fibronectin binding mediated by a novel class of surface organelles on *Escherichia coli*. Nature **338**:652-655.

O'Neal, C. R., W. M. Gabriel, A. K. Turk, S. J. Libby, F. C. Fang, and M. P. Spector. 1994. RpoS is necessary for both the positive and negative regulation of starvation survival genes during phosphate, carbon, and nitrogen starvation in *Salmonella typhimurium*. J. Bacteriol. **176**:4610-4616.

von Ossowski, I., M. R. Mulvey, P. A. Leco, A. Borys, and P. C. Loewen. 1991. Nucleotide sequence of *Escherichia coli katE*, which encodes catalase HPII. J. Bacteriol. **173**:514-520.

Ozaki, M., A. Wada, N. Fujita, and A. Ishihama. 1991. Growth phase-dependent modification of RNA polymerase in *Escherichia coli*. Mol. Gen. Genet. **230**:17-23.

Ozaki, M., N. Fujita, A. Wada, and A. Ishihama. 1992. Promoter selectivity of the stationary-phase forms of *Escherichia coli* RNA polymerase and conversion *in vitro* of the S1 form enzyme into a log-phase enzyme-like form. Nucleic Acids Res. **2**:257-261.

Raina, S., D. Missiakas, L. Baird, S. Kumar, and C. Georgopoulos. 1993. Identification and transcriptional analysis of the *Escherichia coli htrE* operon which is homologous to pap and related pilin operons. J. Bacteriol. **175**:5009-5021.

Roy, R., S. Mukhopadhyay, L. I. C. Wei, and H. E. Schellhorn. 1995. Isolation and sequencing of gene fusions carried by λp*lac*Mu specialized transducing phage. Nucleic Acids Res. **23**:3076-3078.

Sak, B. D., A. Eisenstark, and D. Touati. 1989. Exonuclease III and the catalase hydroperoxidase II in *Escherichia coli* are both regulated by the *katF* gene product. Proc. Natl. Acad. Sci. USA **86**:3271-3275.

Sambrook, J., E. F. Fritsch, T. Maniatis. 1989. Molecular cloning: a laboratory manual, 2nd ed. Cold Spring Harbor Laboratory Press, USA.

Sammartano, L. J., R. W. Tuveson, and R. Davenport. 1986. Control of sensitivity to inactivation by H_2O_2 and broad-spectrum near-UV radiation by *Escherichia coli katF* locus. J. Bacteriol. **168**:13-21.

Saporito, S. M., B. J. Smith-White, R. P. Cunningham. 1988. Nucleotide sequence of the *xthA* gene of *Escherichia coli* K12. J. Bacteriol. **170**:4542-4547.

Schellhorn, H. E., and H. M. Hassan. 1988. Transcriptional regulation of *katE* in *Escherichia coli* K-12. J. Bacteriol. **170**:4286-4292.

Schellhorn, H. E., and V. L. Stones. 1992. Regulation of *katF* and *katE* in *Escherichia coli* K-12 by weak acids. J. Bacteriol. **174**:4769-4776.

Siegele, D. A., and R. Kolter. 1992. Life after log. J. Bacteriol. **174**:345-348.

Silhavy, T. J., M. L. Berman. L. W. Enquist. 1984. Experiments with gene fusions. Cold Spring Harbor Laboratory Press, USA.

Slonczewski J. L., T. N. Gonzalez, F. M. Bartholomew, N. J. Holt. 1987. Mu d-directed *lacZ* fusions regulated by low pH in *Escherichia coli*. J. Bacteriol. **169**:3001-3006.

Small, P., D. Blankenhorn, D. Welty, E. Zinser, and J. L. Slonczewski. 1994. Acid and base resistance in *Escherichia coli* and *Shigella flexneri*: role of *rpoS* and growth pH. J. Bacteriol. **176**:1729-1737.

Sofia, H. J., V. Burland, D. L. Daniels, G. Plunkett III and F. R. Blattner. 1994. Analysis of the Escherichia coli genome. V. DNA sequence of the region from 76.0 to 81.5 minutes. Nucleic Acids Res. **22**:2576-2586.

Sorensen, M. A., K. F. Jensen, and S. Pedersen. 1994. High concentrations of ppGpp decrease the RNA chain growth rate: Implications for protein synthesis and translational fidelity during amino acid starvation in *Escherichia coli*. J. Mol. Biol. **236**:441-454.

Spector, M. P., and C. L. Cubitt. 1992. Starvation-inducible loci of *Salmonella typhimurium*: regulation and roles in starvation-survival. Mol. Microbiol. **6**:1467-1476.

Sprenger, G. A., U. Schorken, G. Sprenger, and H. Sahm. 1995. Transaldolase B of *Escherichia coli* K-12: cloning of its gene. *talB*, and characterization of the enzyme from recombinant strains. J. Bacteriol. **177**:5930-5936.

Storz, G., L. A. Tartaglia, S. B. Farr, B. N. Ames. 1990. Bacterial defences against oxidative stress. Trends Genet. **6**:363-368.

Takayama, M., T. Ohyama, K. Igarashi, and H. Kobayashi. 1994. *Escherichia coli cad* operon functions as a supplier of carbon dioxide. Molec. Microbiol. **11**:913-918.

Takayanagi, Y., K. Tanaka, and H. Takahashi. 1994. Structure of the 5' upstream region and the regulation of the *rpoS* gene of *Escherichia coli*. Mol. Gen. Genet. **243**:525-531.

Tanaka, K., S. Kusano, N. Fujita, A. Ishihama, and H. Takahashi. 1995. Promoter determinants for *Escherichia coli* RNA polymerase holoenzyme containing σ^{38} (the *rpoS* gene product). Nuc. Acids Res. **23**:827-834.

Tanaka, K., Y. Takayanagi, N. Fujita, A. Ishihama, and H. Takahashi. 1993. Heterogeneity of the principal σ factor in *Escherichia coli*: the *rpoS* gene product, σ^{38}, is a second principal σ factor of RNA polymerase in stationary-phase *Escherichia coli*. Proc. Natl. Acad. Sci. USA **90**:3511-3515.

Tempest, D. W., O. M. Neijssel. 1987. Growth yield and energy distribution. In: *Escherichia coli* and *Salmonella typhimurium*, cellular and molecular biology, vol 2, p. 797-806. (F. C. Neidhardt, J. L. Ingraham, B. Magasanik, K. B. Low, M. Schaechter, H. E. Umbarger, eds.). American Society for Microbiology, Washington, DC., USA.

Tormo, A., M. Almiron, and R. Kolter. 1990. *surA*, an *Escherichia coli* gene essential for survival in stationary phase. J. Bacteriol. **172**:4339-4347.

Touati, E., E. Dassa, and P. L. Boquet. 1986. Pleiotropic mutations in *appR* reduce pH 2.5 acid phosphatase expression and restore succinate utilisation in CRP-deficient strains of *Escherichia coli*. Mol. Gen. Genet. **202**:257-264.

Touati, E., E. Dassa, J. Dassa, and P. L. Boquet. 1987. Acid Phosphatase (pH 2.5) of *Escherichia coli*: Regulatory Characteristics. In: Phosphate Metabolism and Cellular Regulation in Microorganisms, p. 31-40. (A. Torriani-Gorini, F. G. Rothman, S. Silver, A. Wright, E. Yagil, eds.) Washington DC: American Society for Microbiology.

Touati, E., E. Dassa, J. Dassa P. L. Boquet, and D. Touati. 1991. Are *appR* and *katF* the same *Escherichia coli* gene encoding a new sigma transcription initiation factor? Res. Microbiol. **142**:29-36.

Toussaint, A., and A. Resibois. 1983. Phage Mu: transposition as a life style. In: Mobile genetic elements, p. 105-158. (J. A. Shapiro ed.) Academic Press Inc., N. Y., USA.

Tuveson, R. W., R. B. Jonas. 1979. Genetic control of near-UV (300-400 nm) sensitivity independent of the *recA* gene in strains of *Escherichia coli* K-12. Photochem. Photobiol. **30**:667-676.

Ueguchi, C., and T. Mizuno. 1993. The *Escherichia coli* nucleiod protein H-NS functions directly as a transcriptional repressor. EMBO J. **12**:1039-1046.

Ueguchi, C., M. Kakeda, H. Yamada, and T. Mizuno. 1994. An analogue of the DnaJ molecular chaperone in *Escherichia coli*. Proc. Natl. Acad. Sci. USA **91**:1054-1058.

Utsumi, R., S. Kusafuka, T. Nakayama, K. Tanaka, Y. Takayanagi, H. Takahashi, M. Noda, M. Kawamukai. 1993. Stationary phase-specific expression of the *fic* gene in *Escherichia coli* K-12 is controlled by the *rpoS* gene product (σ^{38}). FEMS Microbiol. Letters **113**:273-278.

Volkert, M. R., L. I. Hajec, Z. Matijasevic, F. C. Fang, and R. Prince. 1994. Induction of the *Escherichia coli aidB* gene under oxygen-limiting conditions requires a functional *rpoS* (*katF*) gene. J. Bacteriol. **176**:7638-7645.

Wada, A., Y. Yamazaki, N. Fujita, and A. Ishihama. 1990. Structure and probable genetic location of a "ribosome modulation factor" associated with 100S ribosomes in stationary-phase *Escherichia coli* cells. Proc. Natl. Acad. Sci. USA **87**:2657-2661.

Wang, A-Y, and J. E. Cronan, Jr. 1994. The growth phase-dependent synthesis of cyclopropane fatty acids in *Escherichia coli* is the result of an RpoS (KatF)-dependent promoter plus enzyme instability. Mol. Microbiol. **11**:1009-1017.

Weichart, D., R. Lange, N. Henneberg, and R. Hengge-Aronis. 1993. Identification and characterization of stationary phase-inducible genes in *Escherichia coli*. Mol. Microbiol. **10**:407-420.

White, D. 1995. Central metabolic pathways. In: The Physiology and Biochemistry of Prokaryotes, p. 155-182. Indiana University, Oxford University Press, N. Y., USA

Willetts, N., and R. Skurray. 1987. Structure and function of the F factor and mechanism of conjugation. In: *Escherichia coli* and *Salmonella typhimurium*, cellular and molecular biology, vol 2. p. 1110-1133. (F. C. Neidhardt, J. L. Ingraham, B. Magasanik, K. B. Low, M. Schaechter, H. E. Umbarger, eds.). American Society for Microbiology, Washington, DC., USA.

Xu, J., and R. C. Johnson. 1995 (a). Identification of genes negatively regulated by Fis: Fis and RpoS comodulate growth-phase-dependent gene expression in *Escherichia coli.* J. Bacteriol. **177**:938-947.

Xu, J., and R. C. Johnson. 1995 (b). Fis activates the RpoS-dependent stationary-phase expression of *proP* in *Escherichia coli.* J. Bacteriol. **177**:5222-5231.

Xu, J., and R. C. Johnson. 1995 (c). *aldB*, an RpoS-dependent gene in *Escherichia coli* encoding an aldehyde dehydrogenase that is repressed by Fis and activated by Crp. J. Bacteriol. **177**:3166-3175.

Yamashino, T., M. Kakeda, C. Ueguchi, and T. Mizuno. 1994. An analogue of the DnaJ molecular chaperone whose expression is controlled by σ^s during the stationary phase and phosphate starvation in *Escherichia coli.* Mol. Microbiol. **13**:475-483.

Yamashino, T., C. Ueguchi, and T. Mizuno. 1995. Quantitative control of the stationary phase-specific sigma factor, σ^s, in *Escherichia coli*: involvement of the nucleiod protein H-NS. EMBO J. **14**:594-602.

Yim, H. H., and M. Villarejo. 1992. *osmY*, a new hyperosmotically inducible gene, encodes a periplasmic protein in *Escherichia coli.* J. Bacteriol. **174**:3637-3644.

Yim, H. H., R. L. Brems, and M. Villarejo. 1994. Molecular characterization of the promoter of *osmY*, an *rpoS*-dependent gene. J. Bacteriol. **176**:100-107.

Yoshida, T., C. Ueguchi, and T. Mizuno. 1993. Physical map location of a set of *Escherichia coli* genes (*hde*) whose expression is affected by the nucleiod protein H-NS. J. Bacteriol. **175**:7747-7748.

Yura T., H. Mori, H. Nagai, T. Nagata, A. Ishihama, N. Fujita, K. Isono, K. Mizobuchi, and A. Nakata. 1992. Systematic sequencing of the *Escherichia coli* genome: analysis of the 0-2.4 min region. Nucleic Acids Res. **20**:3305-3308.

Zambrano, M. M., D. A. Siegele, M. Almiron, A. Tormo, R. Kolter. 1993. Microbial competition: *Escherichia coli* mutants that take over stationary phase cultures. Science **259**:1757-1760.